2008

Permeation of hydrocarbons through polyvinyl chloride (PVC) and polyethylene (PE) pipes and pipe gaskets

Feng Mao
Iowa State University

Permeation of hydrocarbons through polyvinyl chloride (PVC) and polyethylene (PE) pipes and pipe gaskets

by

Feng Mao

A dissertation submitted to the graduate faculty

in partial fulfillment of the requirements for the degree of

DOCTOR OF PHILOSOPHY

Major: Civil Engineering (Environmental Engineering)

Program of Study Committee:
Say Kee Ong, Major Professor
Timothy Ellis
Roy Gu
Robert Horton
Thomas B. Moorman

Iowa State University

Ames, Iowa

2008

TABLE OF CONTENTS

LIST OF TABLES

LIST OF FIGURES

ACKNOWLEDGEMENTS

First, I am deeply indebted to my advisor Professor Say Kee Ong for his motivation, guidance, support, and encouragement throughout the course of this research. He has been and will continue to be my best source of inspiration and support. I would like to extend my gratitude to Professor Roy Gu, Professor Timothy Ellis, Professor Robert Horton and Professor Thomas B. Moorman for serving on my Ph.D. committee as well as providing invaluable discussions and insights.

I am extremely grateful for the invaluable assistance and advice I received from Mr. James Gaunt throughout the course of this research. I would like to thank Dr. Warren Straszheim for training me in the use of microscopes and Dr. Robert Ewing for teaching me *scilab* programming. Special thanks go to Mr. David Schoeller for his tremendous work in volatile organic compound sample analysis.

I would like to acknowledge the following organizations and individuals for their contributions of expertise and materials to this research: Endot Industries, Inc.; Cresline Plastic Pipe Co., Inc.; Chevron Phillips Chemical Company LP; Griffin Pipe; Hultec S&B Technical Products; Iplex Pipelines Australia Pty Ltd; Specified Fittings; and Uni-Bell PVC Pipe Association.

This research was financially supported by Awwa Research Foundation through the grant of # 2946. I would like to thank Ms. Maureen Hodgins, Dr. Jian Zhang, Dr. Glen R. Boyd, Mr. Stewart Burn, and Mr. Wayne Miller for their comments on part of the research work.

Lastly but most importantly, I want to thank my wife and my parents who have stood by me all these years. Without them, this dissertation would not be possible.

ABSTRACT

Plastic pipes have been used increasingly as a means for the conveyance of drinking water in water distribution systems. Although there are research and case studies documenting the permeation of organic compounds through plastic pipes, there is still a lack of understanding on the performance of PE and PVC pipe materials in hydrocarbon-contaminated soils commonly encountered under field conditions.

A microscopic visualization technique was developed to investigate the permeation of organic solvents through PVC pipes by observing the formation and propagation of organic fronts in pipe materials with a light microscope. The threshold concentrations of toluene where a moving front was formed were 25% (v/v) of toluene in polyethylene glycol and 40% (v/v) of toluene in NIST reference fuel. For a combination of BTEX compounds in NIST reference fuel, a BTEX concentration of 40% (v/v) or higher was required to initiate a moving front and potentially cause permeation. This implies that new PVC pipe materials are an effective barrier to resist the permeation of typical commercial gasoline.

Permeation of benzene, toluene and trichloroethylene (TCE) through 1-inch diameter PVC pipes from vapor and aqueous phases was further investigated by using pipe-bottle tests, gravimetric sorption tests and microscopic visualization tests. Saturated organic vapors penetrated through 1-inch PVC pipes within 30 days. Organic compounds in saturated aqueous solutions also permeated through PVC pipes but the breakthrough times were significantly delayed. The breakthrough times of saturated aqueous solutions of TCE and benzene were found to range from 60 days to 240 days, depending on the experimental mixing conditions. Insignificant sorption and no moving front were detected when exposed to the organic vapors that were in equilibrium with ≤ 40% (v/v) benzene or toluene in NIST

reference fuel. Insignificant sorption and no moving front were detected when exposed to water that is ≤ 60% of the aqueous solubility of benzene and toluene. Based on the experiments conducted, new PVC pipe materials are an effective barrier against the permeation of BTEX in either gasoline vapors or gasoline-contaminated groundwater.

Permeation of petroleum-based hydrocarbons through PVC pipes equipped with Rieber gasket systems was examined by conducting pipe-drum tests as well as model simulation. Under premium gasoline-exposure conditions, the steady-state permeation rates of benzene were estimated to be 0.73±0.29 mg/joint/day and 0.19±0.18 mg/joint/day for 2-inch SBR and NBR gaskets, respectively. The corresponding diffusion coefficients of benzene in SBR and NBR gaskets were determined to be 1.1×10^{-7} cm^2/s and $6.0\times10^{-8}cm^2/s$, respectively. The results of model simulations demonstrated that small size gasketed pipes were more vulnerable to permeation than large size gasketed pipes, and pressurized pipes joint systems potentially posed much higher permeation risk than non-pressurized joint systems.

Permeation of BTEX compounds through 1-inch diameter SIDR 9 high density polyethylene (PE) pipe was investigated under simulated field conditions of subsurface gasoline spills, gasoline-contaminated groundwater and unsaturated soil with varied levels of contamination. Using the time-lag method, the concentration-dependent diffusion coefficients of BTEX compounds in PE pipe were estimated to be in the order of 10^{-8} cm^2/s when exposed to free product gasoline and in the order of 10^{-9} cm^2/s when exposed to gasoline-contaminated water solutions or unsaturated contaminated soil. This study demonstrated that small size pipes were more vulnerable to permeation than large size pipes, and pipes with water stagnation periods posed a much higher risk of exceeding the MCL of

benzene than pipes with continuous water flow. Under otherwise identical conditions, a PE pipe buried in soil of high organic matter was found to permeate to a lesser extent than a pipe buried in a soil of low organic matter.

Permeation parameters of benzene in 1-inch SIDR 9 PE pipes were estimated by fitting the measured data to a permeation model based on a combination of equilibrium partitioning and Fick's diffusion. For bulk concentrations between 6.0 to 67.5 mg/L in soil pore water, the concentration-dependent diffusion coefficients of benzene were found to range from 2.0×10^{-9} cm^2/s to 2.8×10^{-9} cm^2/s while the solubility parameter was determined to be 23.7. PE pipes exposed to an instantaneous plume exhibit distinguishable permeation characteristics from those exposed to a continuous source with a constant input. The properties of aquifer such as dispersion coefficients (D_L) also influence the permeation behavior of organic contaminants through PE pipes.

CHAPTER 1. INTROUDCTION

1.1 Background

Over the past several decades, plastic pipes have been used increasingly as a means for the conveyance of drinking water in water distribution systems. In comparison with cast iron and cement or cement-lined pipes, plastic pipes are easy to install and handle due to their lighter weight. Plastic pipes also exhibit an excellent resistance to corrosion which is one of the problems associated with metal or cement-lined pipes. Plastic materials commonly used for the distribution of drinking water include polyvinyl chloride (PVC), polyethylene (PE), and polybutylene (PB).

However, there is strong literature and field evidence to suggest that organic contaminants can permeate through plastic pipes and adversely affect the quality of drinking water in water distribution systems. According to a recent survey completed by Iowa State University, more than 50 incidents of drinking water contamination resulting from permeation have been reported in the United States (Ong et al., 2007). The majority of the reported permeation incidents were due to gross soil contamination in the area surrounding the pipe and the contaminants of interest include highly volatile hydrocarbons and chlorinated organic solvents.

Since the permeation information obtained from the survey was sparse, qualitative, and incomplete, it is necessary to conduct laboratory experiments under controlled conditions to study the permeation of organic contaminants through plastic pipes. PB pipe, the most permeable of the three plastic pipes listed above, has been extensively studied and documented (Park et al., 1991; Holsen et al., 1991a). PE behaves similarly to PB, except

that it is less permeable (Vonk, 1985). PVC pipe is generally thought to be essentially impermeable to environmental organic contaminants but permeation cannot be excluded in heavily contaminated situations (Vonk, 1985; Berens, 1985).

Due to fundamental differences in the polymer structures, PE and PVC exhibit different permeation behavior. PE is characterized as a semi-crystalline polymer, i.e., having both crystalline and amorphous regions. The crystalline zones act as impermeable barriers for sorption and diffusion, while the non-crystalline matrix is readily permeable. In contrast, PVC is an amorphous glassy polymer with very limited flexibility of the polymer chains. At high concentrations of pollutants, such as in a gross spillage situation, swelling of PVC by solvents may cause rapid penetration through the PVC pipe wall.

Besides the structural characteristics of polymer, the chemical activity and the molecular characteristics of the organic contaminant may influence the permeation of organic compounds through polymeric materials. It has been shown that in most polymer-penetrant system, both diffusion and permeation coefficient exhibit a general increase when there are similarity in molecular structures between the penetrant molecules and the polymer materials (Sangam and Rowe, 2001). Moreover, the diffusion coefficient decreases with increasing penetrant weight, size (molecular volume) and cross sectional area of the penetrant (Berens and Hopfenberg, 1982; Saleem et al, 1989; Park and Nibras, 1993; Park and Bontoux, 1993; Aminabhavi and Nail, 1998).

Under actual field conditions, environmental factors may also have a potential impact on permeation. Pipe materials may suffer degradation or deterioration due to UV exposure, temperatures extremes, abrasion, stress variation, and even biological attack (Uni-Bell, 2001). Such degradation or deterioration may result in the loss in structural integrity and the pipes

become more susceptible to the process of permeation. On the other hand, from the perspective of organic contaminants, environmental conditions (such as temperature, soil characteristics, microbiological activity, etc.) significantly influence the distribution of the chemical contaminant among aqueous, solid, gas and immiscible (non-aqueous-liquid) phases, which implicitly determines the effective availability of those compounds for permeation through pipe materials.

1.2 Motivations

Previous studies have greatly improved the level of understanding of pipe permeation risks. However, there are some significant issues that remain unresolved.

1.2.1 Rapid predictive test to predict the susceptibility of PVC pipe to permeation

Despite great interests in the susceptibility of PVC pipe to permeation, permeation studies for PVC pipes are few and the quantitative data is extremely sparse. This is usually attributed to a lack of an effective and rapid technique for permeation testing. The pipe-bottle exposure test is one of conventional techniques for permeation testing. It involves placement of a pipe into the exposure media with periodic analysis of target compound in the pipe water. This method has been successfully used for testing PB and PE pipes (Vonk, 1985; Park et al., 1991; Holsen et al., 1991b). To estimate the breakthrough time, long-term sampling and analysis of the organic compounds must be carried out which is time consuming and expensive.

In addtion, the prediction of the susceptibility of the pipe to permeation using the pipe-bottle test is based on information after permeation has occurred. To accurately predict permeation, the concentration profile in the pipe material itself must be measured. As such,

there is a need for a rapid test method which can investigate the permeation of organic compounds through PVC pipe and provide information on the spatial distribution of penetrant in the polymer.

1.2.2 Simulated environmental contamination conditions

Field contamination conditions are generally characterized by complex mixtures of organic chemicals distributed among aqueous, solid, and gas phases and non-aqueous phase liquids (NAPL), which implicitly determine the effective availability of these compounds for permeation through pipe materials. Up till now significantly less effort has been devoted to simulate field contamination conditions and thus there are few data that can be applied to predict the permeation of organic contaminants through PVC and PE pipes in the real world. Previous PVC studies generally focused on the sorption or permeation characteristics of organic solvents (Berens, 1985; Vonk, 1985) while very little is known about the permeation of organic contaminants through PVC pipes from either the aqueous or the vapor phase. Furthermore, none of the studies undertake to date has systemically examined the permeation susceptibility of PVC and PE pipes to gasoline (including free product gasoline, gasoline vapor and gasoline contaminated groundwater), although gasoline-range organics are involved in most of the reported permeation incidents (Holsen, 1991b; Ong et al., 2007).

1.2.3 Permeation of organic contaminants through gasketed PVC pipes

There is significant concern in water utilities about the permeation of organic contaminants through gasketed PVC pipes because the gasket material used to join and seal the pipe is more susceptible to permeation than the PVC pipe material itself (Olson et al., 1987). The most widely used method for joining PVC pipes is the Rieber joint system.

However, little is known about the performance of the Rieber joint system to resist permeation of organic contaminants. It remains unknown whether the maximum contaminant level (MCL) of contaminants in pipe water will be exceeded because the gaskets only account for a very small percentage of the total area of piping systems and the gasketed PVC pipes are primarily used in water mains with high rates of flow and little stagnation. To answer the question, it is necessary to conduct experimental studies to determine the permeation rates of contaminates under typical field conditions.

1.2.4 Model simulation of organic permeation through pipes and gaskets

Modeling the process of organic permeation through pipes and gaskets, although critical, has received little attention so far. Model simulation studies are greatly useful in exploring permeation mechanisms, determining permeation parameters and predicting the permeation behavior for pipes and gaskets with different dimensions (sizes) under different exposure conditions. Fickian diffusion and Case II diffusion were proposed as the dominant mechanisms for the permeation of organic chemicals through PE pipe and PVC pipe, respectively (Vonk, 1985; Berens, 1985). To support or refute the proposed mechanisms, it is important to evaluate whether the observed data follow the corresponding model predictions.

1.3 Thesis Overview

This thesis is organized as follows.

In Chapter 2, we introduced the fundamentals of the polymer permeability and the mathematics of diffusion, and conducted a comprehensive review of previous research on the permeation of organic contaminants through plastic pipes.

In Chapter 3, we developed a microscopic visualization technique to test the

permeation of organic solvents through PVC pipes by observing the formation and propagation of the organic moving front, one of the key characteristics of organic penetration in PVC pipe samples. We conducted both modeling and lab studies to explore the principles of this technique, particularly the physical implications of the moving front and its correlation to the permeation data obtained from the pipe-bottle tests. We applied the microscopic visualization technique to compare the relative susceptibility of different PVC pipes to permeation, and to predict the threshold contamination level of benzene, toluene, ethylbenzene, and xylene (BTEX) compounds at which a moving front would be formed. The estimated threshold contamination levels allowed us to evaluate the susceptibility of PVC pipes to the permeation of free product gasoline.

In Chapter 4, we investigated the permeation of organic contaminants through PVC pipes from the vapor and aqueous phases by using the microscopic visualization tests, pipe-bottle tests, and gravimetric sorption tests. We attempted to determine the threshold contamination levels of BTEX compounds at which PVC pipes would be susceptible to permeation under organic vapor or aqueous solution exposure conditions. The estimated contamination levels served a base to evaluate the susceptibility of PVC pipes to the permeation of gasoline vapors and gasoline-contaminated groundwater. Combining the results obtained from the vapor and aqueous experiments with the previous solvent data in Chapter 3, we further examined the similarities and differences of the permeation behavior of organic contaminants through PVC pipes from the solvent, vapor and aqueous phases.

In Chapter 5, we extended our research to address the permeation of organic contaminants through the gasket of PVC pipe with a Rieber gasket system. We investigated the permeation of BTEX compounds through styrene-butadiene rubber (SBR) and

acrylonitrile-butadiene rubber (NBR) gaskets of 2-inch PVC pipe under simulated subsurface gasoline spill and gasoline-contaminated groundwater conditions. With the software package of Multiphysics (COMSOL), we performed model simulation studies to determine the diffusion coefficients of contaminants under experiemntal conditions, to estimate the steady-state permeation rates of contaminants into larger size gaskets, and to predict the permeation behavior of contaminants in pressurized Rieber joint systems.

In chapter 6, we switched our focus from PVC pipes to PE pipes. We investigated the permeation of BTEX compounds through 1-inch SIDR 9 PE pipe under simulated field conditions, including gasoline leaks and spills, gasoline-contaminated groundwater, and gasoline-contaminated soil with various levels of contamination. We determined the diffusion coefficients of BTEX under experimental conditions with the time-lag method. We established some empirical equations to correlate the steady state permeation rates of benzene and toluene to their bulk concentrations. These equations allowed us to predict the concentration of benzene and toluene in pipe water and evaluate whether their MCLs are exceeded under the water stagnation and continuous water flow conditions. We further examined the impacts of soil organic matter on the permeation of PE pipes by BTEX compounds.

In Chapter 7, we studied the permeation process of benzene through PE pips by using a numerical modeling method. With the numerical computational package of Scilab (ENPC, France), we estimated the permeation parameters of benzene in 1-inch SIDR 9 PE pipes by fitting the measured data in Chapter 6 to a permeation model based on a combination of equilibrium partitioning and Fick's diffusion. We evaluated the permeation risks of benzene

for SIDR 9 and SIDR 7 series of PE pipes. We also examined how time-dependent boundary conditions affect the permeation behaviors of benzene through PE pipes.

We concluded the thesis in Chapter 8 with the conclusions and directions for future work.

References

Aminabhavi, T.M. and H.G. Naik. 1998. Chemical compatibility testing of geomembranes-Sorption/desorption, diffusion and swelling phenomena. *Geomembranes and Geotextiles*, 16(6): 333-354.

Berens, A.R. 1985. Prediction of organic chemical permeation through PVC pipe. *Journal AWWA*, 77(11): 57-64.

Berens, A.R. and H.B. Hopfenberg. 1982. Diffusion of organic vapors at low concentration in glassy PVC, polystyrene and PMMA. *Journal of Membrane Science*, 10(2-3): 283-303.

Holsen, T.M., J.K. Park, L. Bontoux, D. Jenkins, and R.E. Selleck. 1991a. The effect of soils on the permeation of plastic pipes by organic chemicals. *Journal AWWA*, 83(11): 85-91.

Holsen, T.M., J.K. Park, D. Jenkins, and R.E. Selleck. 1991b. Contamination of potable water by permeation of plastic pipe. *Journal AWWA*, 83(8): 53-56.

Olson, A.J., D.Goodman, and J.P. Pfau. 1987. Evaluation of permeation of organic solvents through PVC, asbestos/cement, and ductile iron pipes. *Journal of Vinyl and Additive Technology*, 9(3): 114-118**.**

Ong, S.K., J.A.Gaunt, F.Mao, C.L.Cheng, L.E.Agelet, and C.R.Hurburgh. 2007. Impact of petroleum-based hydrocarbons on PE/PVC pipes and pipe gaskets. AwwaRF, Denver, CO.

Park, J.K. and M. Nibras. 1993. Mass flux of organic chemicals through polyethylene geomembranes. *Water Environmental Research*, 65 (3): 227-237.

Park, J.K. and L. Bontoux. 1993. Thermodynamic modeling of the sorption of organic chemicals in thermoplastics and elastomers. *Journal of applied polymer science*, 47(5): 771-780.

Park, J.K., L. Bontoux, D. Jenkins, and R.E. Selleck. 1991. Permeation of polybutylene pipe and gasket material by organic chemicals. *Journal AWWA*, 83(10): 71-78.

Saleem, M., A.A. Asfour, D. De Kee, and B. Harison. 1989. Diffusion of organic penetrant through lowdensity polyethylene (LDPE) films: effect of size and shape of the penetrant molecules. *Journal of Applied Polymer Science*, 37(3): 617- 625.

Sangam, H.P. and R.K. Rowe. 2001. Migration of dilute aqueous organic pollutants through HDPE geomembranes. *Geotextiles and Geomembranes*, 19(6): 329-357.

Uni-Bell. 2001. Handbook of PVC pipe design and construction. Uni-Bell PVC Pipe Assocaition, Dallas, TX.

Vonk, M.W. 1985. Permeation of organic compounds through pipe materials, Pub. No. 85. KIWA, Neuwegein, Netherlands.

CHAPTER 2. LITERATURE REVIEW

This chapter starts by introducing the fundamentals of the polymer permeability and the mathematics of diffusion, followed by a comprehensive review of previous research on the permeation of organic contaminants through the plastic pipes.

2.1 Polymer Permeability and Mathematics of Diffusion

The permeation of small molecules within a polymer is of fundamental interest to polymer scientists and has received considerable attention over the past several decades (Crank and Park, 1968; Crank, 1975; Comyn, 1985; Neogi, 1996). This mass transport process can occur in polymers because most of polymers are an essentially porous medium. The intrinsic porosity of the polymer matrix results from random nature of the polymer networks formed and the vibration of the molecular chains leaving sites into which small molecules can adsorb. Polymers can be manufactured deliberately as porous materials such as foams or membranes but even nominally solid, homogeneous polymers are likely to be porous to some degree owing to defects, inclusions and different phases, which leave pores, voids and cracks capable of accommodating penetrant molecules.

The permeation of small molecules within a polymer involves three key stages:

- Sorption consisting of the penetrant molecules removal from the exposed medium and its dispersion on or into the polymeric matrix;
- Diffusion of the sorbed penetrant through the polymer material;
- Desorption of the penetrant from the polymer material to the receiving medium.

2.1.1 Sorption

In the initiation of the permeation process, the sorption process may involve

adsorption, absorption, incorporation into micro-voids, cluster formation, solvation-shell formation and other modes of mixing (Rogers, 1985). The penetrant molecules may experience more than one concurrent or sequential mode of sorption in a given polymeric material. For example, two-mode models have been proposed for gas sorption in glassy amorphous polymers consisting of absorption into the polymer matrix and additional incorporation into micro-voids or fillers in the material (Crank and Park, 1968). The distribution of the penetrant between different modes of sorption may change with sorbed concentration, temperature, time of sorption to equilibrium, and swelling of matrix due to the interaction between the polymer and the penetrant. The extent to which penetrant molecules are sorbed and their mode of sorption in a polymer depend upon the activity of the penetrant within the polymer at equilibrium.

If the penetrant is inert to the polymer, i.e., there is no solvency or swelling effects, the penetrant partition into the polymeric matrix may proceed according to Henry's law:

$$C_{p1} = S_1 C_e \qquad \text{(Eq. 2.1)}$$

where C_{p1} is the concentration of penetrant on the polymer surface in contact with the exposed medium; C_e is the concentration of penetrant in the exposed medium; and S_1 is the partitioning coefficient (solubility parameter) and is a constant for the given penetrant, exposed medium, polymer and temperature of interest.

2.1.2 Diffusion

Diffusion in the polymer material is the net passage of penetrant molecules within the polymeric matrix. It can be passive if the driving force is purely a Brownian molecular motion, or be activated by external effects such as electrical, osmotic or convective forces.

The fundamental of diffusion can be described by Fick's laws where the macroscopic transport of molecules is a function of the concentration gradient. In some cases, however, penetrant causes significant swelling of the polymer, leading to a modification of the behavior predicted by Fick's equations. Alfrey et al. (1966) proposed a classification for diffusion behavior based on the relative rates of diffusion and polymer relaxation. Three diffusion types are classified:

- Case I or Fickian diffusion in which the rate of diffusion is much less than that of relaxation;
- Case II diffusion, the other extreme in which the rate of diffusion is very rapid compared with that of relaxation;
- Non-Fickian or anomalous diffusion which occurs when the diffusion and relaxation rates are comparable.

Fickian law of diffusion

Fick's adaptation of Fourier's heat transfer equations has led to the renowned Fick's first law:

$$F = -D\frac{\partial C}{\partial x} \qquad \text{(Eq. 2.2)}$$

Fick's first law is based on the hypothesis that the rate of transfer of diffusing substance through unit area of a section (F) is proportional to the concentration gradient measured normal to the section $\frac{\partial C}{\partial x}$, x is the space coordinate normal to the reference plan and D is the diffusion coefficient. The first law can only be directly applied to diffusion in the steady state, that is, where concentration is not varying with time.

By considering the mass-balance of an element of volume and assuming one dimensional diffusion (along the x-axis), it is easy to show that the fundamental differential equation of diffusion takes the form

$$\frac{\partial C}{\partial t} = \frac{\partial}{\partial x}(D\frac{\partial C}{\partial x}) \qquad \text{(Eq. 2.3)}$$

If the diffusion coefficient is a constant, the equation becomes the Fick's second law

$$\frac{\partial C}{\partial t} = D\frac{\partial^2 C}{\partial x^2} \qquad \text{(Eq. 2.4)}$$

For the diffusion in a cylinder (such as plastic pipes), the governing equation is

$$\frac{\partial C}{\partial t} = \frac{1}{r}\frac{\partial}{\partial r}(rD\frac{\partial C}{\partial r}) \qquad \text{(Eq. 2.5)}$$

If the medium is a hollow cylinder whose inner and outer radii are a and b, respectively, and if the diffusion coefficient is constant, the equation describing the steady-state condition is

$$\frac{d}{dr}(r\frac{dC}{dr}) = 0\,,\ a<r<b \qquad \text{(Eq. 2.6)}$$

Given the boundary conditions of $C=C_1$ at $r=a$ and $C=C_2$ at $r=b$, the general solution of this is

$$C = \frac{C_1 \ln(b/r) + C_2 \ln(r/a)}{\ln(b/a)} \qquad \text{(Eq. 2.7)}$$

The rate of mass transferred per unit length F, of the cylinder is

$$F = -2\pi rD\frac{\partial C}{\partial r} = \frac{2\pi D(C_2 - C_1)}{\ln(b/a)} \qquad \text{(Eq. 2.8)}$$

For many penetrant-polymer systems, D is not a constant but rather is a function of the sorbed penetrant concentration, $D(C)$. The concentration–dependence is a reflection of

the plasticizing action of sorbed penetrant (Rogers, 1985). In this case, the governing equation becomes

$$\frac{\partial C}{\partial t} = \frac{\partial}{\partial x}(D(C)\frac{\partial C}{\partial x}) \qquad \text{(Eq. 2.9)}$$

There are relatively few rigorous solutions of the diffusion equation for a concentration-dependent *D*. The usual method to estimate *D(C)* is to utilize solution for a constant *D* and then extract a value of *D(C)* from those data. One procedure is to transform equation 2.9 into

$$\frac{\partial C}{\partial t} = D(C)\frac{\partial^2 C}{\partial x^2} + \frac{\partial D(C)}{\partial C}(\frac{\partial C}{\partial x})^2 \qquad \text{(Eq. 2.10)}$$

Experiments are then performed over sufficiently small internals of *C* such that $\frac{\partial D(C)}{\partial C}$ is small compared with *D(C)* so that the second term may be neglected. This gives a mean or integral value of the diffusion coefficient $\overline{D}$, over the concentration range C_1 to C_2 and is defined as

$$\overline{D} = \frac{1}{C2 - C1}\int_{C1}^{C2} D(C)dC \qquad \text{(Eq. 2.11)}$$

$\overline{D}$ may be determined over several ranges of concentration to obtain an estimate of *D(C)*.

Case II diffusion

Characteristics of Case II diffusion. The phenomenon of Case II diffusion has the following characteristics: when a polymer sheet is exposed to an organic vapor or liquid (penetrant), the weight of the polymer increases linearly with exposure time due to the sorption of this penetrant. Optical microscopic analysis (Thomas and windle, 1982) and Ruthford backscatting spectrometry experiments (Mills et al., 1986) revealed the presence of a sharp diffusion front. Behind the front the concentration gradient of the penetrant is

negligible. The formation of the front is preceded by the induction period, during which the penetrant concentration is observed to be a smoothly decreasing function of distance into the sheet. Immediately after the induction time, a sharp front is formed which advances at a constant velocity. The concentration of the penetrant behind the front increases with time until its equilibrium concentration is reached. For sufficiently low partial pressure or low concentration of penetrant outside the polymer sheet, experiments have indicated that front formation was inhibited (Hui et al., 1987a).

Overall, the essential features of Case-II diffusion are as follows: (i) a sharp diffusion front; (ii) linear weight gain with time (linear kinetics); (iii) essentially no concentration gradient behind the front; and (iv) the existence of an induction time.

Models of Case II diffusion. To explain the Case II behavior, Frisch et al. (1969) introduced an additional corrective term (which is linear with time) into Fickian-type relation of penetration depth. This term, however, was not based on any clear physical principle, although the authors did recognize the significance of the stress gradient which exists across the moving boundary. Another earlier explanation of Case II behavior was proposed by Peterlin (1969). He suggested that the sharp diffusion front, characteristic of Case II diffusion, was preceded by a region of penetrant at low concentration which forms a precursor to the front. He also recognized that the velocity of the front must be controlled by some independent materials property, and suggested time dependent rupture and disentanglement of molecular chains as possible processes. Based on the assumption of a sharp penetrant front which moves at a constant velocity, Peterlin further developed equations to predict the profile of concentration, which showed a discomtinuity (the sharp front). This treatment, however, did not pay attention to the control of front velocity and

thereby could not handle situations in which the front either decelerated with time (Thomas and Windle, 1978) or accelerated (Jacques et al., 1974). Similarly, Astarita and Sarti (1978) demonstrated that if arbitrary assumptions were made concerning the front velocity, namely that it was zero until a critical concentration was reached and then increased according to some power of the additional concentration, it was indeed possible to model Case II behavior.

Of the various models proposed to explain Case II diffusion, the model of Thomas and Windle (TW) (1982), appeared to be most successful. According to TW model, the diffusive process is strongly coupled to the mechanical response of the polymer, in the sense that the rate at which the penetrant is absorbed must be compatible with the swelling rate controlled by the creep deformation of the surrounding polymer. The creep deformation is dependent on both the osmotic pressure (which is the driving force of the swelling) and the viscosity of the polymer. The viscosity and diffusivity of the polymer are extremely sensitive to the concentration of the penetrant. The plasticization caused by sorption of the penetrant results in a large decrease in viscosity and increase in diffusivity within a very narrow range of concentration. These changes reduce the polymer segmental relaxation times from a very large (glassy behavior) to a very short (rubbery behavior). The strong dependence of viscosity and diffusivity on penetrant concentration produces the characteristic of Case II diffusion, the propagation of a sharp front.

Hui et al. (1987a, 1987b) investigated the ability of the TW model to predict the swelling kinetics for a very thin film with negligible diffusion resistance. These predictions were then compared to the sorption kinetics of iodohexane at the surface of polystyrene using Rutherford backscattering spectrometry. Their results verified the existence of various essential features of Case II transport as predicted by the TW model, especially the Fickian

precursor penetrating ahead of the sharp front and the induction period before establishing a constant rate of front movement. The model, however, underestimated the swelling rate at short time or low volume fraction and overestimated the swelling rate when the surface penetrant volume fraction approached its equilibrium value. Hui et al. also obtained the solutions to the TW model by assuming that the swelling interface has obtained a steady-state velocity and that the diffusion resistance in the swollen region is negligible.

Rossi and coworkers (1995, 1997) provided some new insights of Case II diffusion with a phenomenological model that incorporated diffusion into the glassy core. Two important time scales associated with the establishment of a diffusing front and the crossover from Case II to Fickian diffusion behavior were predicted. In their approach, the plasticization-imposed constraint was used for the solvent flux across the glass-swollen interface. As a result, the front velocity became independent of the solvent concentration immediately behind the advancing front. This approximation was not consistent with the rate-control mechanism in the TW model and was not entirely in accord with the experimental observations.

More recently, Qian and Taylor (2000) developed a phenomenological model that took into account the diffusion in both the glassy core and the swollen gel. The model included the rate-controlled motion of the front separating these two regions, and the expression of the front velocity was constructed using the rate-control mechanism of the TW model. According to the phenomenological model, the boundary separating the glassy core from the swollen gel moves at a nearly constant velocity in the early stage. As the diffusion proceeds, the front velocity decreases. The shape of the Fickian tail ahead of the boundary can be determined, and a slowly varying Fickian precursor can also be explicitly obtained.

Effects of geometry on solvent front penetration. Most of experimental observations in Case II diffusion used sheet specimens and the Case II swelling were characterized by either linear weight-gain kinetics or a constant penetrating front velocity. Lee and Kim (1992) examined the fundamental issue whether a penetrating solvent front would maintain a constant rate throughout a radially symmetric polymer sample, such as a sphere or a cylinder, under conditions where the front penetrating behavior in a sheet sample of identical polymer composition and comparable dimension was Case II diffusion. Both of their experimental and theoretical results revealed that the initial stage of the solvent penetration in radially symmetric geometries exhibited the same transport characteristics as in sheet samples. This was followed by an intermediate transition region with an apparent linear front movement prior to an accelerated front penetration towards the core.

2.1.3 Desorption

This process is the opposite of sorption. Generally, the net desorption occurs if the concentration of the penetrant in the receiving medium is lower than the concentration required for maintaining the partition equilibrium with the polymer. Similar to the sorption process, Henry's law can be used to express the relationship between the concentrations in the two phases

$$C_{p2} = S_2 C_r \qquad \text{(Eq. 2.12)}$$

where C_{p2} is the concentration of penetrant on the polymer surface in contact with the receiving medium; C_r is the concentration of penetrant in the receiving medium; and S_2 is the partitioning coefficient (solubility parameter) and is a constant for given penetrant, receiving medium, polymer and temperature of interest. In the simplest case whether the receiving

medium is identical to the exposed medium, S_2 may be assumed to be equal to S_1 in equation 2.1.

However, it should be noted that desorption is not simply the inverted process of sorption. If penentrant molecules are strongly bound in the polymer, the desorption of the penetrant may exhibit significant hysteresis.

2.1.4 Permeability

As described above, the permeation of small molecules through the polymer material involves sorption, diffusion and desorption processes. It is interesting to combine the three processes and estimate the steady-state flux of the penetrant across the polymer material into the receiving medium. For a polymer with a fixed thickness l, if the concentrations at the two surfaces are C_{p1} and C_{p2}, respectively, the flux from the polymer to the receiving medium is given by

$$F = D\frac{C_{p1} - C_{p2}}{l} \qquad \text{(Eq. 2.13)}$$

Substituting equation 2.1 and equation 2.12 into equation 2.13, and assuming the exposed medium and the receiving medium share the same solubility parameter S, equation 2.12 becomes

$$F = D\frac{S_1C_e - S_2C_r}{l} = DS\frac{C_e - C_r}{l} = P\frac{C_e - C_r}{l} \qquad \text{(Eq. 2.14)}$$

where P is defined as the permeability or permeation coefficient. Essentially, P is a mass transfer coefficient that takes account the sorption, diffusion and desorption processes.

2.1.5 Measurement, calculation and estimation of permeation parameters

Gravimetric sorption method

The gravimetric sorption method measures the rate at which a penetrant is absorbed or desorbed from a polymer sample. In the gravimetric sorption test, the samples are immersed in a container filled with the penetrant of interest and the mass uptake of penentrant by polymer sample is periodically measured. The mass uptake is plotted versus time according to equation:

$$M_t / M_\infty = kt^n \qquad \text{(Eq. 2.15)}$$

where M_t is defined as the mass of penetrant uptake at time t, and M_∞ is the mass of penetrant uptake as time approaches infinity. If the exponent n is 0.5 (for planar system), the diffusion is Fickian. Case II diffusion is observed for n=1.0.

For Fickian diffusion in a thin slab of polymer with a thickness of l, the equation describing sorption and desorption is

$$\frac{M_t}{M_\infty} = 1 - \frac{8}{\pi^2}\sum_{n=0}^{\infty}\frac{1}{(2n+1)^2}\exp\left[-\frac{D(2n+1)^2\pi^2 t}{l^2}\right] \qquad \text{(Eq. 2.16)}$$

The value of t/l^2 for which $M_t / M_\infty = 1/2$, conveniently written as $(t/l^2)_{1/2}$, is given by

$$\left(\frac{t}{l^2}\right)_{1/2} = -\frac{1}{\pi^2 D}\ln\left[\frac{\pi^2}{16} - \frac{1}{9}\left(\frac{\pi^2}{16}\right)^9\right] \qquad \text{(Eq. 2.17)}$$

Approximately, ignoring the term of $1/9(\pi^2/16)^9$ (the error is about 0.001 percent) produces

$$D = \frac{0.04919}{(t/l^2)_{1/2}} \qquad \text{(Eq. 2.18)}$$

So, if the half time of a sorption or desorption process is observed experimentally, the value of the diffusion coefficient can be determined.

For one-dimensional radial Fickian diffusion in a cylinder with radius *a*, the equation describing sorption and desorption is

$$\frac{M_t}{M_\infty} = 1 - \sum_{n=1}^{\infty} \frac{4}{a^2 a_n^{\ 2}} \exp(-D a_n^{\ 2} t) \qquad \text{(Eq. 2.19)}$$

where the a_n are the positive roots of

$$J_0(a a_n) = 0 \qquad \text{(Eq. 2.20)}$$

J_0 is the Bessel function of the first kind of order zero and aa_n are the zeros of that function. An alternative solution useful for interpretation of short time behavior is given as

$$\frac{M_t}{M_\infty} = 4\left(\frac{Dt}{\pi a^2}\right)^{1/2} - \pi\left(\frac{Dt}{\pi a^2}\right) - \frac{\pi}{3}\left(\frac{Dt}{\pi a^2}\right)^{3/2} + \cdots \qquad \text{(Eq. 2.21)}$$

The empirical prediction using $\frac{M_t}{M_\infty} = 4\left(\frac{Dt}{\pi a^2}\right)^{1/2}$ is only valid for the first 15 to 20% of the total sorption process.

In the Case II diffusion, the sorption kinetics is assumed to be controlled by rate-limiting relaxation phenomenon positioned at the advanced front (Ensore et al., 1978, 1980). The sorption/desorption process may be described by

$$\frac{M_t}{M_\infty} = 1 - \left(1 - \frac{k_0}{C_{sw} a'} t\right)^N \qquad \text{(Eq. 2.22)}$$

Here, k_0 is defined as the Case II relaxation constant; C_{sw} is the equilibrium concentration of penetrant in the swollen region; a' is the sample radius for cylindrical and spherical samples and the film half –thickness *l/2* for planar samples. The exponent *N* is determined by sample

geometry and has values of 1 for films, 2 for cylinders, and 3 for spheres. For s cylinder of radius *a*, Case II diffusion is defined by equation 2.22 with *N*=2

$$\frac{M_t}{M_\infty} = 1 - (1 - \frac{k_0}{C_{sw}a}t)^2 = \frac{2k_0}{C_{sw}a}t - (\frac{k_0}{C_{sw}a}t)^2 \qquad \text{(Eq. 2.23)}$$

Time lag method

The time lag method measures the rate at which a migrating substance, or penetrant, come through a sheet film of the plastic rubber being tested. This method is generally used to measure gas transport through packaging films. It may also be useful for measuring solvent transport through soft and rubbery polymers.

The basis of the time lag method is that the permeation rate of a substance that is brought into contact with a polymer sample becomes constant with time. This means that the concentration of the penetrant in a closed (detection) chamber on the desorption side, after a certain transition period, will become linearly increasing. Consider diffusion through a flat sheet with a thickness of *l*, whose exposure surface (*x=0*) is maintained at a constant concentration C_e. If the diffusion coefficient is constant, the penetrant is continually removed from the low concentration side (C_r=*0*), the amount of diffusant *Q(t)* which passes through the sheet in time *t* is given by

$$Q(t) = lC_e\left\{\frac{Dt}{l^2} - \frac{1}{6} - \frac{2}{\pi^2}\sum_{n=1}^{\infty}\frac{(-1)^n}{n^2}\exp\left(\frac{-Dn^2\pi^2 t}{l^2}\right)\right\} \qquad \text{(Eq. 2.24)}$$

As $t \rightarrow \infty$, the steady state is approached and the exponential terms become negligibly small, so that the graph of *Q(t)* against *t* tends to the line

$$Q_t = \frac{DC_e}{l}\left(t - \frac{l^2}{6D}\right) \qquad \text{(Eq. 2.25)}$$

which has an intercept, L, on the t-axis given by

$$T_L = \frac{l^2}{6D} \qquad \text{(Eq. 2.26)}$$

The time lag for the hollow cylinder $a \le r \le b$ is given by

$$T_L = \frac{b^2 - a^2 + (b^2 + a^2)\ln(a/b)}{4D\ln(a/b)} \qquad \text{(Eq. 2.27)}$$

So, if the time lag is observed experimentally, the value of the diffusion coefficient can be determined.

Light microscopy and spectrometry method

In order to establish which diffusion mechanism is applied for a given polymeric matrix/penetrant system, the concentration profile and the rate of diffusion must be measured. Both the gravimetric sorption method and the time-lag method are therefore less valuable as it does not provide any information about the spatial distribution of penetrant in the polymer nor the structural features of polymer materials.

Light microscopy has been used to measure the distance of penetration for diffusion in glass polymers since a sharp front, separating the swollen and rigid region, provides good contrast in the light microscope. In order to aid observation of the front as it penetrates the material, small amounts of iodine was added into the target solvent to give a charge complex with a characteristic color, providing enough contrast to make the advancing front readily visible (Thomas and Windle, 1978). In-situ dynamic observation of the progress of the moving front can also be achieved using a special cell, which allows the penetrant to come into contact with the edge of the polymer sample but not with the top or bottom surfaces (Morrissey and Vesely, 2000).

Rutherford backscattering spectrometry (RBS) has been applied by Hui et al. (1987a ,1987b) to determine the concentration profiles of iodohexane in polystyrene (PS). In RBS analysis, the sample is bombarded with high-energy ions (usually He^{2+}). These ions penetrate the sample and gradually slow down but eventually they collide with the atoms in the structure. In that instance they reflect backwards and emanate out of the sample. These reflected ions are collected by a detector which records their energy. The energy is a function of the depth of the collision and the mass of the target atom. Thus, from the measured energy the location of the collision and the mass (chemical identity) of the target atom can be deduced.

Magnetic resonance imaging (MRI) has been established as a method to monitor the diffusion of penetrants into polymers in a nondestructive and noninvasive manner. In MRI, the image contrast is governed by one of several nuclear magnetic resonance parameters and might reflect water mobility, chemical potential, self-diffusion coefficient, coherent flow or temperature, depending upon the exact form of the MRI measurement (McDonald and Newling, 1998). It allows spatial resolution down to a few micrometres in three dimensions (McDonald and Newling, 1998). Perry et al. (1994) first applied MRI to study liquid ingress into polymer. In their study, the acetone vapor ingress into poly(vinyl chloride) (PVC) was investigated and quantitative dynamical information about both the polymer and penetrant was obtained. Changes in the polymer chain dynamics were inferred, during a considerable period of time after the acetone had entered the polymer and achieved apparent concentration equilibrium. A similar work was conducted by Ercken et al. (1995) to investigate the diffusion of 1,4-dioxane in PVC and of acetone in polycarbonate (PC) using MRI. The results indicated that a diversity of diffusion behaviors can be observed, from Fickian

diffusion to Case II diffusion. More recently, with MRI technique, Lane and McDonald (1997) investigated the transition between Case II dynamics for the ingress of methanol into polymethyl methacrylate (PMMA). The transition was induced either by pre-swelling the polymer with small quantities of acetone or by temperature changes in the region of the polymer glass transition temperature. The experimental data were found to correlate well with the prediction from the theoretical model of Thomas and Windle (1982).

Estimation methods

Based on the free volume theory and the molecular theory, some macromolecular researchers have attempted to develop models to predict the transport of molecules through polymer materials. Of the various methods proposed to estimate the permeation coefficient for a specific penetrant/polymer system, the estimation based on n-octanol/water coefficient (k_{ow}) has obtained much interest.

The n-octanol/water coefficient, usually expressed as a logarithm, is a specific property of chemicals to describe their ability to partition between water and n-octanol (i.e. organic matter) in dilute solution. The coefficient k_{ow} is a constant for a given chemical at a given temperature. It reflects the lipophilicity of chemicals and can be used to estimate their polarity. The higher the numerical value, the stronger the tendency of the chemical to accumulate in organic matter. Since a polymer material is essentially an organic material, one may anticipate a relationship between n-octanol/water coefficient and the permeation parameters.

A strong correlation between the partition coefficient (log S_f) and n-octanol/water coefficient (log k_{ow}) has been obtained for various penetrant/polymer systems. A linear (Prasad et al., 1994) or a second order polynomial relationship (Park and Nibras, 1993) was

found between them. Sangam and Rowe (2001) correlated the values of log S_f reported for HDPE geomembranes in the literature with log k_{ow}, and an excellent correlation (r^2=0.97) was obtained, regardless of the test conditions. Such correlation substantiates the fact that the partition coefficient is mainly controlled by penetrant characteristics. As anticipated, as log k_{ow} increases, the chemical hydrophobia increases and hence the contaminant has a strong tendency to partition into the polymer phase.

Sangam and Rowe (2001) further grouped the penetrant into four main categories according to their molecule structures: aliphatic, aromatic, chlorinated and oxygenated. They found that the partitioning coefficient was dependent the chemical structure. This is attributed to the fact that the chemical structure affects their solubility in water and hence log k_{ow}. Consequently, aliphatic hydrocarbons with log k_{ow} > 3.5 have high partitioning coefficients followed by aromatic (2< log k_{ow} <3.5), chlorinated or halogenated (1<log k_{ow} <3) and finally oxygenated hydrocarbons which are highly soluble in water (log k_{ow} <0.5).

In addition, Sangam and Rowe (2001) plotted diffusion coefficient (log D) against log k_{ow} and found more scatter in the data than was the case for partition coefficient. The authors hypothesized that this scatter was due to a difference in the polymer material properties (such as crystallinity), which may have significant effect on the diffusion process. They also noted that there was a decrease in D at high log k_{ow} values and they suggested that this was likely due to the fact that chemicals with high k_{ow} are mostly relatively large molecules. The molecular diffusion process is highly dependent on the molecule size. When the molecule size of penetrant increases, high activation energy is required for diffusion to be completed. Similarly, the permeability (P) showed a relatively poor correlation with log k_{ow} but it was

still better than for diffusion coefficient because P is influenced by both the partitioning and diffusion coefficients.

In general, the estimation method based on k_{ow} provides a good basis for understanding the diffusion process. However, due to the complexity of diffusion, it has been seldom used in engineering field.

2.1.6 Factors affecting penetrant permeation through polymer

Similarity between the polymer and penetrant

In most polymer polymer-penetrant system, both diffusion and permeation coefficient exhibits a general increase with similarity between the components. For instance, strongly polar molecules have very low transport rates through polyethylene (PE), which is non-polar. In general, the permeation affinity for PE has the following order: alcohols < acids < ketones < esters <aromatic hydrocarbons < halogenated hydrocarbons (August and Taztky, 1984). This was further confirmed by Rowe et al. (1996). They studied the diffusion of organic pollutants through HDPE geomembranes and observed that some organic pollutants compounds (methyl ethyl ketone, acetic acid) migrated at much slower rates than the chlorinated solvents examined (dichloromethanes, 1,1-dichloroethane, and 1,2-dichloroethanes). Polar compound (methanol) was also found to be absorbed much less than nonpolar compounds (toluene, 1,2-dichlorobenzene, and 1,1,1-trichloroethane) in nonpolar thermoplastics such as polybutylene (PB) and PE (Park and Bontoux, 1992).

Bulk concentration of penetrant

In pure-Fickian diffusion within a polymer, the penetrant-polymer partition and diffusion coefficients are usually assumed as constants, independent of the bulk concentration of penetrant. However, this assumption is only valid when the bulk

concentration is low. In most of cases, the diffusion coefficient is strongly dependent on the bulk concentration of penetrant because the presence of permeant molecules with the polymer will weaken the interactions between adjacent polymer chains, which in turn leads to the commonly observed effects of plasticization. Volk (1985) reported that the diffusion coefficient of toluene in the softened PVC increased by several orders of magnitude in comparison with that in the original PVC. Muler et al. (1998) also found that the diffusion coefficients in PE geomembranes were approximately one order of magnitude lower for an aqueous solution than for a pure solvent. In the sorption study of organic chemicals in thermoplastics and elastomers, Park and Bontoux (1992) showed that the partition coefficient increased logarithmically with increasing of solvent activity for nonpolar compounds.

Molecular weight, size and shape of penetrant

The diffusion coefficient decreases with increasing permeant weight and size (molecular volume) (Saleem et al., 1989; Aminabhavi and Nail, 1998). For example, Saleem et al (1998) reported a decrease of diffusion coefficient with the increase of molar volume for some aliphatic aromatic and chlorinated penetrants through low-density polyethylene (LDPE). However, the magnitude of the decrease is higher for chlorinated chemicals than methyl substituted benzenes due to the bulky chlorine atom, which markedly reduces their mobility. The shape of penetrants has been reported to have a profound effect on the diffusion process (Berens and Hopfenberg, 1982; Saleem et al., 1989). Penetrants with linear, flexible and symmetrical molecules have higher mobility than rigid molecules. For instance, Saleem et al. (1989) showed that the diffusion coefficient for o-xylene is lower than for p-xylene. This is attributed to the symmetrical structure of p-xylene compared to the distorted shape of o-xylene with its two adjacent methyl groups. Berens and Hopfenberg (1982) have

shown that the diffusion of n-alkane and other elongated or flattened molecules are higher, by a factor of 10^3, than the diffusion of spherical molecules with similar molecular weight.

The effects of penetrant molecule size on Case II diffusion were also investigated (Gall et al., 1990). In this work, Rutherford back-scattering spectrometry was used to examine the detailed composition versus depth profile for polystyrene (PS) exposed to the vapor of a series of 1-iodo-n-alkanes ranging from iodopropane ($n=3$) to iodooctane ($n=8$), where n is the number of carbon atoms on the alkane chain. The results indicated that i) the velocity of the Case II front as well as the diffusion coefficient (D) in the PS decreased exponentially with n; ii) D decreased exponentially with molecular diameter for spherically symmetric solvent molecules; and iii) D for non-spherical molecules were as much as three orders of magnitude larger than that for spherical molecules with an equivalent molecular diameter.

Polymer properties

In regard to polymer properties, the diffusion of a contaminant is expected to decrease with increasing of density, chain rigidity, and degree of cross-linking. For example, PVC is an amorphous glassy polymer with very limited flexibility of the polymer chains while PE is a partially crystalline rubber-polymer having amorphous areas with high chain mobility. Small organic molecules permeate PVC through the small free volumes between the relatively immobile polymer chains, whereas permeation of PE occurs through the amorphous areas having relatively more mobile polymer chains. This structural difference accounts the different performance between PE and PVC to resist the permeation of organic chemicals. PVC is virtually impermeable at low solute activity while permeation may occur in PE (Vonk, 1985, 1986).

In the case of HDPE geomembranes (semi-crystalline polymers), the crystalline zones act as impermeable barriers to permeating molecules in two ways (Naylor, 1989). First, crystalline regions act as excluded volumes for the sorption process and as impermeable barriers for diffusion. Secondly, they act as giant cross-linking regions with respect to those chains, which enter and leave those regions from the surrounding non-crystalline matrix in which sorption and diffusion take place. The restraints of cross-linking on the segmental mobility of the polymer make the diffusion process more dependent on size, shape of concentration of the penetrant molecule (Naylor, 1989; Rogers, 1985).

Temperature

The permeation process is highly temperature dependent since energy is required to achieve this activated process. It has been established (Naylor, 1989; Chainey, 1990) that over small temperature ranges, temperature dependence of the diffusion, solubility and permeability coefficients can be described by the Arrhenius relationship

$$D = D_0 e^{(-\frac{E_d}{RT})} \qquad \text{(Eq. 2.28)}$$

$$P = P_0 e^{(-\frac{E_P}{RT})} \qquad \text{(Eq. 2.29)}$$

where E_d and E_p are the activation energies of diffusion and permeation, respectively. It is expected that for many polymer-penetrant systems, plots of log D vs. the reciprocal of the absolute temperature are linear over a limited temperature range (Saleem et al., 1989; Aminabhavi and Naik, 1998).

2.2 Permeation of Organic Contaminants through Thermoplastic Pipes

It has long been known that permeation of plastic pipes may result in the drinking water quality degradation (KIMA, 1961). The permeation of contaminants through a plastic pipe may involve three processes: (i) partition of the contaminant between outer surface of pipe and the medium containing the contaminant (sorption); (ii) diffusion of the permeant through the polymer materials of pipe; and (iii) partition between the inner surface of pipe and the water in the water (desorption). Since permeation can occur either from the vapor or aqueous phase, both water mains and fittings installed in the vadose and saturated zones are susceptible to contamination by permeation (DWI0441, 1992).

2.2.1 Survey studies

In 1980's, two surveys on the effect of organic chemicals on plastic pipe were completed in Netherlands (Vonk, 1985) and in the U.S. (Thompson and Jenkins, 1987). Recently, a national survey in the U.S. that took into consideration of the geographic, pipe types and size distribution of the utilities was conducted by Iowa State University under an Awwa Research Foundation contract (Ong et al., 2007). The main purposes of this survey were to document permeation incidents, to identify the major contaminants, and to estimate the frequency of permeation incidents for both service connections and water mains. Permeation incidents here refer to occurrences for which there was a customer complaint about taste, odor, or illness or for which laboratory data exceeded the U.S. EPA maximum contaminant levels (MCLs) that could be attributed to permeation of pipes or gaskets by hydrocarbons.

Most of the reported permeation incidents involved heavy contamination in the soil surrounding the pipe. The high risk areas for the occurrence of permeation incidents included industrial areas, former sites of fuel stations, and near underground storage tanks. Permeation incidents can also occur in low risk areas such residential areas, mainly due to the disposal and accidental leaking of gasoline, oil, and paint thinner products (Holsen et al., 1991a).

Three types of plastic pipe, polybutylene (PB), polyethylene (PE), and polyvinyl chloride (PVC), were involved in most of permeation incidents. PB was found to be the major material involved (43 percent of all U.S. incidents), followed by PE (39 percent) and PVC (15 percent) (Thompson and Jenkins, 1987). In a recent national survey (Ong et al., 2007), PB was found to be the dominant material involved, accounting for 72 percent of all U.S. incidents. Service lines were found to be more vulnerable to permeation incidents than mains, presumably because of stagnation periods (Ong et al., 2007).

Nearly all permeation incidents in the U.S. were related to petroleum products, mainly gasoline spills or leaks (Thompson and Jenkins, 1987; Ong et al., 2007). The aromatic compounds in gasoline, BTEX, permeated PB and PE pipes readily (much more readily than the aliphatics) and were the compounds of concern in permeation incidents. A small number of incidents involved chlorinated solvents (Holsen et al., 1991a; Ong et al., 2007). Plastic pipes showed an excellent resistance to the permeation by strongly polar pesticides (e.g., paraquat, malathion, and atrazine) and long-chained (high molecular weight) hydrocarbons (DWI0032, 1990; Vonk, 1985).

Holsen et al. (1991a) calculated the frequency of permeation incidents for both service connections and water mains. The frequency of permeation of service connections

for metal, polyethylene, polybutylene and polyvinyl chloride was 0, 3.6, 16.5, and 2.2 incidents per 10^6 connection-year. The frequency of permeation of water mains for metal, concrete, asbestos cement and polyvinyl chloride was 0.1, 0, 0.3, and 4.6 incidents per 10^5 mile-year.

2.2.2 Lab studies

Since information on pollutant permeation in actual service situations is sparse, qualitative, and incomplete, it is necessary to conduct laboratory experiments under controlled conditions. In the 1980's and early 1990's, some lab studies were conducted to investigate the permeation of organic contaminants through pipe materials.

In Berens's work (1985), PVC powders, films, and sheets were exposed to representative organic solvents at a wide range of concentrations and the possibility of organic pollutants permeating though PVC pipe were evaluated using gravimetric method. Berens noted that the solvent interaction parameter χ in the Flory-Huggins equation could be used as a measure of the solvent or swelling power of a particular organic solvents and, at ambient temperature, rigid PVC can be softened only by strong solvents ($\chi<0.5$) or swelling agents ($0.5<\chi<1$) at activities >0.5. He further found that at low activities (<0.25) solvent transport followed ideal Fickian diffusion kinetics and the calculated permeation through the wall of PVC pipes were virtually zero for many centuries. He concluded that except in case of a gross spill or leak of a strong swelling solvent, rigid PVC pipe was an effective barrier against permeation of environmental pollutants. However, one of criticisms of Berens's work is that the various test (activities) solution he used in his experiments were prepared by dissolving the organic solvents in polyethylene glycol and thus he never actually tested aqueous solutions of these organic solvents.

Vonk (1985) conducted a series of pipe-bottle aqueous exposure experiments to investigate the susceptibility of PVC and PE pipe to permeation of organic contaminants. PE pipe was found to be readily permeable while PVC pipe was much less permeable. Vonk suggested that the mechanism governing the permeation process for PVC pipe and PE pipe were different because of their different polymer structure. At room temperature PVC behaves as an amorphous glass polymer and its chains are rigid and immobile. In contrast, PE is a semi-crystalline rubber polymer and the chains of the amorphous areas have a high mobility. Vonk also proposed that the permeation through PE pipe followed the Fickian diffusion while Case II diffusion dominated in the permeation through PVC pipes, although his study did not involve any investigation of organic fronts, a typical characteristic of Case II diffusion.

Olson et al. (1987) tested several full-size commercially available water main PVC pipes and gasket joining materials exposed to pure organic solvents. The PVC pipes with gaskets showed faster permeation compared to the straight pipes. The authors concluded that the gasket material used to seal the pipes was more susceptible to permeation than the PVC pipe material.

Park et al. (1991) employed the pipe-bottle apparatus to determine the susceptibility of polybutylene (PB) pipe to permeation by a wide range of organic chemicals. The findings included that: (i) the permeability coefficient of all the organic chemicals tested commonly increased with the increasing of organic chemical concentration; (ii) long-straight-chain, high –molecular-weight, or highly branched organic chemicals appeared to have low permeability; (iii) chlorinated hydrocarbons tended to permeate pipe faster than unchlorinated hydrocarbons; (iv) there was no significant difference in the permeability of PB pipe

extruded by different manufacturers; and (v) organic chemicals that do not readily permeate PB pipe when present alone can have their permeability enhanced considerably when mixed with highly permeable organic chemicals. The last conclusion about the synergistic effect of organic mixture is important because most chemical spills and contamination events involve mixtures of similar components.

Holsen et al. (1991) examined the effect of soils on the permeation of plastic pipes by organic chemicals. In their work, PB pipes were buried in both water saturated and unsaturated soils contaminated with several organic chemicals at varying activities. Comparison of soil experiments with pipe-bottle experiment containing no soil indicated that the concentration of organic chemicals in the soil pore space controlled both the rate and extent of organic chemical permeation through buried plastic pipes. This study also revealed that under otherwise identical conditions, plastic pipes buried in soil of high organic carbon content would be permeated more slowly than a pipe buried in a soil of low organic carbon content.

Parker and Ranney (1994, 1995, 1996) did a series of exposure experiments to determine the ability of PVC to withstand long-term exposure to various organic contaminants in aqueous solution, although their concern was on the pipe material used in a groundwater monitoring well rather than the pipe for water conveyance. Interestingly, this study found that a solution containing a mixture of 18 good swelling agents of PVC, each at an activity of 0.05, was able to rapidly soften PVC. The authors concluded that a solution containing several organic solutes had a much greater ability to soften PVC than a solution containing any one of the solutes by itself.

2.2.3 Modeling studies

Selleck and Marinas (1991) developed and presented analytical solutions for the pure -Fickian diffusion of hydrophobic contaminants through plastic pipes. In their modeling work, the driving force for this diffusion process was the difference in the internal and external activity of organic compounds, and such process was controlled by the equilibrium partitioning of organic compounds between the pipe wall and the pipe water. The analytical solutions were used to calculate breakthrough times for ¾-inch polybutylene pipes exposed to a variety of organic contaminants. Two initial conditions of PB pipe were assumed, one was a new pipe installed in soil subject to gross contamination, and the other was previously contaminated pipe flushed with clean water.

The results of model simulation revealed that: (i) the breakthrough times for the previously contaminated pipe were on the order of minutes while the breakthrough times for the new pipe were on the order of weeks; (ii) a contamination incident cannot be corrected by simply flushing the line with clean water for a protracted period of time since the contaminated pipe will retain its status as a swollen, highly permeable medium; and (iii) the hydrostatic pressure within the pipeline provides negligible resistance to permeation at the pressure range commonly found in the distribution system.

Some cautions should be taken to apply the work of Selleck and Marinas for permeation prediction. One of the limitations in their mathematical evaluations was the assumption of pure-Fickian diffusion. Pure-Fickian diffusion within a polymer occurs only when the solute-polymer partition and diffusion coefficients are independent of solute activity. At activities in excess of 0.1, such assumption may become invalid. Especially, at a high activity, organic chemicals and solvents promote swelling of polymeric materials, which

in turn increases the rate of diffusion by several orders of magnitude (Vonk, 1985). Another pronounced deficiency is the assumption of just one permeating agent. Usually more than one contaminant is involved in actual permeation incidents. The diffusion coefficient for each organic compound in a multicomponent system may increase significantly in comparison with that in a single component system (Park et al., 1991).

2.3 Summary

Permeation of organic compounds through polymeric materials is strongly dependent on the structural characteristics of polymer, the chemical activity and the molecular characteristics of the organic contaminant. Under actual field conditions, environmental factors may also have a potential impact on permeation.

PE pipe is susceptible to permeation by organics at low levels of contamination. PVC pipe, for practical purposes, is resistant to permeation by organics except in conditions of gross environmental contamination but the gasket materials are highly permeable. Many of the laboratory studies conducted used pure solvents or gasoline which typically represents extreme or gross contamination conditions. Although there is a need to understand the risk of permeation at different concentration levels, there are very few studies available to assist in this assessment.

Reference

Alfrey, T.J., E.F. Gurnee, and W. G. Lloyd. 1966. Diffusion in glassy polymers. *Journal of Polymer Science*, Part C 12: 249-261.

Aminabhavi, T.M. and H.G. Naik. 1998. Chemical compatibility testing of geomembranes-sorption/desorption, diffusion and swelling phenomena. *Geomembranes and Geotextiles*, 16 (6): 333-354.

Astarita, G. and G.C. Sarti. 1978. A class of mathematical models for sorption of swelling solvents in glassy polymers. *Polymer Engineering Science*, 18 (5): 388-395.

Berens, A.R. 1985. Prediction of organic chemical permeation through PVC pipe. *Journal AWWA*, 77 (11): 57-64.

Berens, A.R. and H.B. Hopfenberg. 1982. Diffusion of organic vapors at low concentration in glassy PVC, polystyrene and PMMA. *Journal of Membrane Science*, 10(2-3): 283-303.

Comyn, J. 1985. Polymer Permeability. Elsevier Applied Science Publishers, Essex, UK.

Crank, J. 1975. The Mathematics of Diffusion. Clarendon Press, Oxford, UK.

Crank, J. and G.S Park. 1968. Diffusion in Polymers. Academic Press, London, UK.

DWI0441. 1992. Effects of organic chemicals in contaminated land on buried services. Foundation for Water Research (FWR), Malow, UK.

DWI0772. 1997. Permeation of Benzene, Trichloroethene and Tetrachloroethene through plastic pipe. Foundation for Water Research (FWR), Malow, UK.

Enscore, D.J., H.B. Hopfenberg and V. T. Stannett. 1977. Effect of particle size on the mechanism controlling n-hexane sorption in glassy polystyrene microspheres. *Polymer*, 18 (8): 793-800.

Enscore, D.J., H.B. Hopfenberg and V.T. Stannett. 1980. Diffusion, swelling, and consolidation in glassy polystyrene microspheres. *Polymer Engineering and Science,* 20(1): 102-107.

Ercken**,** M., P. Adriaensens, D.Vanderzandes, and J.Gelan. 1995. Study of solvent diffusion in polymeric materials using magnetic resonance imaging. *Macromolecules*, 28(26): 8541-8547.

Friedman, A. and G. Rossi. 1997. Phenomenological continuum equations to describe Case II diffusion in polymeric materials. *Macromolecules*, 30(1): 153-154.

Frisch, H.L., T.T. Wang, and T.K. Kwei. 1969. Diffusion in glassy polymers II. *Journal of Polymer Science Part A-2 Polymer Physics*, 7(20): 879-887.

Glaza, E.C. and J.K. Park. 1992. Permeation of organic contaminants through gasketed pipe joints. *Journal AWWA*, 84(7): 92-100.

Holsen, T.M., J. K. Park, L. Bontoux, D. Jenkins, and R.E. Selleck. 1991a. The effect of soils on the permeation of plastic pipes by organic chemicals. *Journal AWWA*, 83(11): 85-91.

Holsen, T. M., J. K Park, D. Jenkins, and R.E. Selleck. 1991b. Contamination of potable water by permeation of plastic pipe. *Journal AWWA*, 83(8): 53-56.

Hui, C.Y., K.C. Wu, R.C. Lasky, and E.J. Kramer. 1987a. Case-II diffusion in polymers. I. Transient swelling. *Journal of Applied Physics*, 61(11): 5129-5136.

Hui, C.Y., K.C. Wu, R.C. Lasky, and E.J. Kramer. 1987b. Case-II diffusion in polymers. II. Steady-state front motion. *Journal of Applied Physics*, 61(11): 5137-5149.

Lasky, R.C, K.C. Wu and C.Y. Hui. 1988. Initial stages of Case II diffusion at low penetrant activities. *Polymer*, 29: 673-679.

Lee, P.I. and C.J. Kim. 1992. Effect of Geometry on Solvent Front Penetration in Glassy Polymers. *Journal of Membrane Science*, 65(1-2): 77-93.

Mills, P.J., C.J. Palmstrom and E.J. Kramer. 1986. Concentration profiles of non-Fickian diffusants in glassy polymers by Rutherford backscattering spectrometry. *Journal of Materials Science*, 21(5): 1479-1486.

Morrissey, P. and D.Vesely. 2000. Accurate measurement of diffusion rates of small molecules through polymers. *Polymer*, 41(5):1865-1872.

Müler, W., I.Jakob, G.R. Tatzky, and H.August. 1998. Solubilities, diffusion and partitioning coefficients of organic pollutants in HDPE geomembranes: experimental results and calculations. In *Proc. of the Sixth International Conference on Geosynthetics*. Atlanta: Industrial Fabrics Association International.

Neogi, P. 1996. Diffusion in Polymers. Marcel Dekker Inc., New York.

Olson, A.J., D.Goodman and J.P. Pfau. 1987. Evaluation of permeation of organic solvents through PVC, asbestos/cement, and ductile iron pipes. *Journal of Vinyl and Additive Technology*, 9(3): 114-118**.**

Ong, S.K., J.A.Gaunt, F.Mao, C.L.Cheng, L.E.Agelet, and C.R.Hurburgh. 2007. Impact of petroleum-based hydrocarbons on PE/PVC pipes and pipe gaskets. AwwaRF, Denver, CO.

Park, J.K. and M. Nibras. 1993. Mass flux of organic chemicals through polyethylene geomembranes. *Water Environmental Research*, 65(3): 227-237.

Park, J.K., L. Bontoux, D. Jenkins and R.E. Selleck. 1991. Permeation of polybutylene pipe and gasket material by organic chemicals. *Journal AWWA*, 83(10): 71-78.

Parker, L.V. and T.A. Ranney. 1994. Softening of rigid PVC by aqueous solutions of organic solvents. U.S. Army Cold Regions Research and Engineering Laboratory, Special Report 94-27.

Parker, L.V. and T.A. Ranney. 1995. Additional studies on the softening of rigid PVC by aqueous solutions of organic solvents. U.S. Army Cold Regions Research and Engineering Laboratory, Special Report 95-8.

Parker, L.V. and T.A. Ranney. 1996. Further studies on the softening of rigid PVC by aqueous solutions of organic solvents. U.S. Army Cold Regions Research and Engineering Laboratory, Special Report 96-26.

Perry, K.L., P.J. McDonald, E. W. Randall and K. Zick. 1994. Stray field magnetic resonance imaging of the diffusion of acetone into poly(vinyl chloride). *Polymer*, 35 (13): 2744-2748.

Prasad, T.V., K.W. Brown, and J.C. Thomas. 1994. Diffusion coefficients of organics in high-density polyethylene (HDPE). *Waste Management and Research*, 12(1): 61-71.

Qian, T. and P.L, Taylor. 2000. From the Thomas-Windle model to a phenomenological description of Case-II diffusion in polymers. *Polymer*, 41(19): 7159-7163.

Rogers, C.E. 1985. Permeation of gases and vapors in polymers. In: Comyn, J. (Ed.), Polymer Permeability. Elsevier Applied Science Publishers, London, U.K.

Rossi, G., P.Pincus, and P.G de Gennes. 1995. A phenomenological description Case-II diffusion in polymeric materials. *Europhysics Letters*, 32(5): 391-396.

Saleem M., A.A. Asfour, D.De Kee and B. Harison. 1989. Diffusion of organic penetrant through low density polyethylene (LDPE) films: effect of size and shape of the penetrant molecules. *Journal of Applied Polymer Science*, 37(3): 617- 625.

Sangam, H.P. and R. K. Rowe. 2001. Migration of dilute aqueous organic pollutants through HDPE geomembranes. *Geotextiles and Geomembranes*, 19(6): 329-357.

Selleck, R.E. and B.J. Marinas. 1991. Analyzing the permeation of organic chemicals through plastic pipes. *Journal AWWA*, 83(7): 92-97.

Thomas, N.L. and A.H. Windle. 1978. Transport of methanol in poly(methyl methacrylate). *Polymer*, 19(3): 255-265.

Thomas, N.L. and A.H. Windle. 1982. Theory of case II diffusion. *Polymer*, 23(4): 529-42.

Vonk, M. W. 1985. Permeation of organic compounds through pipe materials, Pub. No. 85, KIWA, Neuwegein, Netherlands.

CHAPTER 3. A NEW MICROSCOPIC VISUALIZATION TECHNIQUE TO PREDICT THE PERMEATION OF ORGANIC SOLVENTS THROUGH PVC PIPES

A paper to be submitted to *Journal of American Water Works Association*

Feng Mao, James A. Gaunt, Say Kee Ong

Abstract

This study developed a microscopic visualization technique to investigate the permeation of organic solvents through PVC pipes by observing the formation and propagation of organic fronts in pipe materials with a light microscope. The microscopic visualization technique was able to predict the breakthrough time for the permeation of organic solvents through PVC pipes using the pipe-bottle experiments and assess the relative susceptibility of different PVC pipes to permeation. The threshold concentrations of toluene where a moving front was formed were 25% (v/v) of toluene in polyethylene glycol (PEG) and 40% (v/v) of toluene in NIST reference fuel. The impact on PVC pipe of the activities of the individual BTEX compounds in an exposure medium was found to be additive. For a combination of BTEX compounds in NIST reference fuel, a BTEX concentration of 40% (v/v) or higher was required to initiate a moving front and potentially cause permeation. This implies that new PVC pipe materials are an effective barrier to resist the permeation of typical commercial gasoline.

Keywords: PVC; Permeation; Moving Front; Microscopic

3.1 Introduction

Use of polyvinyl chloride (PVC) pipes in water distribution systems has increased dramatically within the past several decades, mainly due to their excellent resistance to abrasion, impact and corrosion (Uni-Bell, 2001). However, there are concerns with regard to the continued use and/or application of PVC pipes in contaminated soils or sites as organic contaminants external to the pipes may permeate through the porous, polymeric materials into the drinking water (US EPA, 2002). According to a survey completed in the 1980's, PVC pipes were involved in 15% of the total incidents of drinking water contamination from organic chemicals permeation (Thompson and Jenkins, 1987). In a recent national survey in the U.S., six permeation incidents were reported to be related to PVC water mains and service connections (Ong et al., 2007).

Despite the great interest in the susceptibility of PVC pipe to permeation, permeation studies on actual PVC pipes are few and quantitative data of permeation are extremely sparse (Vonk, 1985). This may be attributed to a lack of an effective and rapid technique for permeation testing. The pipe-bottle test is one of the conventional techniques for permeation testing, where a pipe is placed in the exposure media and the target compounds in the pipe water are periodically analyzed. This method has been successfully used for testing polyethylene (PE) and polybutylene (PB) (Vonk, 1985; Park et al., 1991). To estimate the breakthrough time, long-term sampling and analysis of the organic compounds must be carried out which is time consuming and expensive. For PVC pipe, the use of the pipe-bottle test would be a challenge since the permeation of organic molecules through PVC pipe is generally slow, especially for PVC pipe exposed to aqueous solutions of low contaminant concentrations.

Another technique is the gravimetric sorption test (Berens, 1985; Park and Bontoux, 1993). This method is based on the equilibrium sorption of a contaminant by pipe materials. The measurement of mass uptake in the sorption test is simple but it yields no direct information on the breakthrough time of a contaminant through the PVC pipe. Moreover, the sorption behavior may be strongly dependent on the geometry of polymeric materials and an appropriate equation taking into consideration the effect of geometry must be used to analyze the sorption data (Peppas and Peppas, 1994). To avoid such effect, researchers have used PVC sheets or films made of pure PVC (Berens, 1985) in sorption tests. However, the data obtained from pure PVC slab samples may not accurately reflect the permeation behavior of chemicals through PVC pipes since the presence of additives in the pipe can modify the state of the polymer at the molecular level and influence the transport properties of the material.

As such, the prediction of the susceptibility of the pipe to permeation using the pipe-bottle test is based on information after permeation has occurred. To accurately predict permeation, the concentration profile in the pipe material itself must be measured. The pipe-bottle tests provide the concentration of the penetrant in the receiving medium and do not provide information on the spatial distribution of penetrant in the polymer. In the field of macromolecule science, the polymeric matrix/penetrant systems have been examined by other techniques, such as light microscopy (Thomas and Windle, 1978; Morrissey and Vesely, 2000), Rutherford backscattering spectrometry (RBS) (Hui et al., 1987a, 1987b), and magnetic resonance imaging (MRI) (Perry et al., 1994; Ercken et al., 1995). To date, none of them has been applied to investigate the permeation of organic molecules through PVC pipes.

In this study, a rapid predictive technique using light microscopic visualization was developed. This technique is focused on visual examination of the formation and

propagation of the polymeric matrix/penetrant interface, defined here as the organic moving front. The validity of the technique was assessed by correlating the moving front data with the permeation data obtained from the pipe-bottle test. The light microscopic visualization technique was then employed to investigate the permeation behavior of benzene, toluene, ethylbenzene, and xylene (BTEX) in PVC pipes. Finally, this technique was used to compare the relative susceptibility to permeation of pipes obtained from different pipe manufacturers.

3.2 Principles of Microscopic Visualization Technique

It is well known that the penetration of a penetrant into glassy polymers generally results in swelling with the diffusion of the penetrant behaving as Fickian to Case II diffusion, depending on the relative magnitude of the relaxation rate of the polymer material to the diffusion rate of penetrant (Crank, 1975; Comyn, 1985). Fickian diffusion is observed when the rate of diffusion is much less than that of relaxation while Case II diffusion is the other extreme in which diffusion is very rapid compared with the relaxation rate (Alfrey et al., 1966). PVC is an amorphous glassy polymer with very limited flexibility of the polymer chains (Vonk, 1985). In the presence of high concentration of organic penetrants, such as in a gross spillage situation, interaction between the polymer and the penetrant results in the swelling of the PVC. Such swelling results in a sharp interface separating the inner glassy core from the outer swollen layer. This interface, the moving front (or diffusion front), is readily visible under a light microscope (Figure 3.1).

The presence of a moving front during permeation is one of essential features of Case II diffusion, where there is a negligible concentration gradient behind the moving front and a

concentration nearly equal to zero in front of the moving front (Thomas and Windle, 1982; Hui et al., 1987b). Case II diffusion was proposed as the dominant mechanism for the permeation of organic chemicals through PVC pipe (Vonk, 1985; Berens, 1985), although this conclusion has not been confirmed by any experiments. In contrast, it would be interesting to assess whether the sharp front can be predicted using Fickian diffusion equation.

In classic Fickian diffusion with a constant diffusion coefficient, the concentration profiles typically do not shown shape changes. In fact, any assumption of constant diffusion coefficient throughout the polymer is highly inappropriate for a swelling polymer system. When the polymer is exposed to a penetrant, the glassy polymer with a low diffusion coefficient is progressively converted to a rubbery polymer with a high diffusion coefficient. The diffusion coefficient for the rubbery polymer can be several orders of magnitude larger than that for the glassy polymer. For example, the diffusion coefficient of toluene in glassy PVC film was found to be about 10^{-14} cm^2/s while in swollen PVC film the diffusion coefficient was as high as 9×10^{-8} cm^2/s (Berens, 1985).

The moving front is typically found and reflects the sharp change in concentration profile of penetrants in the PVC matrix. Therefore, the penetration position of organic penetrants in PVC pipes can at least approximately estimated by observing propagation of a moving front due to the softening of the PVC by the solvent. Three assumptions were accordingly made in the present study: (i) permeation never occurs without the formation of the moving front; (ii) drinking water in the pipe would be contaminated only if the moving front propagates sufficiently and reaches the inner wall of pipes; and (iii) for a PVC pipe with

a known wall thickness, the breakthrough time of organic penetrants can be predicted by measuring the advancement rate (velocity) of the moving front.

3.3 Materials and Methods

3.3.1 Materials

A total of 58 PVC pipes from six manufacturers were purchased from local hardware stores. The pipe diameters ranged from ¾ inch to 2 inch. All the pipes were ASTM 1785D-certified, Schedule 40 and marked NSF-PW. Tests were not conducted on old, used, or compromised pipes since the age, exposure history, and conditions are typically not known. Five organic solvents, benzene, toluene, ethylbenzene, xylene (o-xylene, m-xylene and p-xyene) and trichloroethene (TCE), were selected on the basis of their occurrence in contaminated soil and purchased from Fisher Scientific (Chicago, IL).

To dilute a target organic solvent to a certain strength or activity level, inert solvents that do not interact with the PVC pipe material were used. Polyethylene glycol (PEG), an inert chemical that does not interact with the PVC pipe material was used by Berens (1985) to determine the chemical activity threshold at which significant sorption would occur. The National Institute of Standards & Technology (NIST) specifies a "reference fuel" to simulate free product gasoline, consisting of 91% (v/v) (91.09% w/w) 2,2,4-trimethylpentane (iso-octane) and 9% (v/v)(8.91 w/w) n-heptane. The reference fuel has been used to calibrate instruments for the determination of lead (NIST, 1988) and alcohols (National Bureau of Standards, 1986) in gasoline. This reference fuel may be a good surrogate for the alkanes in gasoline which are inert to pipe materials. Both PEG and the reference fuel were used in determining the chemical activity threshold before permeation occurs. PEG (Carbowax®

PEG400), 2,2,4,-trimehtylpentane, and n-heptane were purchased from Fisher Scientific (Chicago, IL).

3.3.2 Pipe-bottle test

The pipe-bottle test was used to evaluate the usefulness of the microscopic visualization technique in predicting the permeation of organic contaminants through PVC pipes. Experiments were conducted in a pipe-bottle apparatus consisting of a 1-L glass bottle with one PVC pipe mounted horizontally through holes drilled in the glass bottle (Figure 3.2). A chemically resistant sealant, Loctite® epoxy putty (Henkel Technologies, Rocky Hill, CT) was used to seal the gap between the glass bottle and the pipe. The ends of the pipes were sealed with Teflon® plugs. One of the Teflon® plugs had a small hole that was plugged with a removable threaded brass plug to allow filling and draining of the water inside the pipe with a glass syringe. The bottle was capped with a Teflon®-lined cap.

Three "mini" pipe-bottle apparatuses were set up with a 1-inch diameter PVC pipe directly exposed to pure benzene, toluene and TCE, respectively. Note that only one 1-inch pipe from a manufacturer was used in the experiments. In this test, the pipe was first filled with deionized water (pipe water) and the solvent was then added into the bottle until a visible liquid level of solvent appeared above the pipe. To minimize the amount of solvents added and thus reduce the amount of hazardous waste produced, the bottle space below the pipes was filled with glass beads. The pipe-water was sampled each day and analyzed for the presence of the target compounds. After each sampling event, the pipe was immediately flushed three times with deionized water before fresh deionized water was added and the pipe sealed with the threaded brass plug.

Benzene, toluene and TCE in water samples were determined using a gas chromatograph (Tracor 540, Tracor Instruments Austin, Inc., Austin TX) equipped with a packed column (1.8 m × 2 mm; 1% SP1000 on 60/80 mesh Carbopack B), a photoionization detector, and an automated purge and trap concentrator (Tekmar LSC2/ALS). The detection limits for benzene, toluene and TCE were 0.24 µg/L, 0.24 µg/L, and 1.2 µg/L, respectively.

3.3.3 Microscopic visualization test

Three types of experiments were conducted: (i) exposing 1-inch pipe specimens to three pure solvents (benzene, toluene and TCE) to correlate the moving front data to the permeation data obtained from the pipe-bottle tests; (ii) exposing 1-inch pipe specimens to toluene at various activity levels (pure solvent, 20-80% of solvent by volume in PEG/NIST reference fuel) to determine the threshold activity level that would result in the formation of the moving front; and (iii) exposing 58 pipes to pure toluene solvent to compare the relative susceptibility to permeation of different size pipes and pipe materials obtained from different pipe manufacturers. For test (i) and test (ii), only one-inch PVC pipe from a manufacturer was used.

In the first experiment, 1-inch diameter pipe specimens were cut to approximately 3.5 cm in length. One end of the pipe was sealed with a glass slide using Loctite® epoxy putty (Henkel Technologies, Rocky Hill, CT). The pipe was then filled with deionized water from the unsealed end. This end was then sealed with a glass slide using the same epoxy material. The pipe specimens were then immersed in 50 mL of test solvents (benzene, toluene and TCE) in a 120-mL glass jar with a Teflon®-lined lid. At different times, a pipe specimen was removed from the solvent, wiped dry, cut, and the progress of the moving front visualized.

As shown in Figure 3.1, three parameters can be measured: (i) the original pipe thickness (L_0), (ii) the thickness of the swollen layer at time t ($L_{s,t}$), and (iii) the thickness of the remaining glass core (or the distance of the sharp boundary to the inner wall, $L_{g,t}$). The penetration distance at time t was then calculated by:

$$\text{Penetration distance } (PD_t) = L_0 - L_{g,} \qquad \text{(Eq. 3.1)}$$

In this test, the distance of the moving front from the outside to the inside of the pipe (both of $L_{s,t}$ and $L_{g,t}$) was measured.

In the other two tests (ii and iii), pipes to be tested were cut across the longitudinal axis of the pipe, so as to form ring-like specimens of 1.5 cm in length. The pipe specimens were placed directly into the target solvents with both faces (outside and inside) exposed to the solvent. The specimens were removed from the solvent at specific times and dried using a paper towel of any external solvent. Each dried specimen was first cut parallel to the longitudinal axis and then cut across the longitudinal axis of the pipe specimen, so as to form an approximately 1/5 ring-like sample with a length of 0.5 cm. The sample cross section was observed directly under a reflected light microscope (Olympus BHM) and its image captured by a camera mounted on the microscope. Since in a typical contaminated site a solvent penetrates pipes from the outer wall to the inner wall, only the outer swollen layer ($L_{s,t}$) was measured for these experiments. With PC-Image (version 5.0) software package, the penetration distance of the moving front was precisely measured. All experiments were conducted at room temperature (23 $\pm$ 1.5^{o}C) for reasons of operational convenience and economy.

3.4 Results and Discussion

3.4.1 Pipe-bottle test

Significant permeation through PVC pipes occurred within 6.5 days for TCE, 16 days for toluene, and 20 days for benzene (Figure 3.3). No detectable permeation occurred through PVC pipes until a breakthrough point was reached. At that point, permeation occurred at a constant rate. The permeation curves for PVC pipes were consistent with those of Vonk (1985) who reported the permeation of a mixture of toluene and m-xylene through PVC pipes. At steady state permeation conditions, the concentrations of these compounds in the pipe-water were found to be close to their water solubilities at the end of the 1-day sampling intervals. Since permeation of organic solvents results in a rubbery phase and therefore loss in material strength, it is possible that the pipe may bust under pressure before the permeation is completely through the pipe wall thickness.

3.4.2 Microscopic visualization tests for PVC pipes exposed to pure solvents

In the microscopic visualization test, a sharp boundary (moving front) separating the inner glassy core from the outer swollen layer was distinctly observable as the solvent advanced into the PVC matrices. This provided an opportunity to carry out a dynamic observation of the progression of the moving front with time. Figure 3.4 shows the advancement of the moving front in a one-inch diameter PVC pipe exposed to pure toluene. The moving front reached the inner wall on the 16^{th} day, the day when the breakthrough of toluene was detected in the pipe-water of the pipe-bottle tests (Figure 3.3). The results indicated that no detectable permeation occurred until the moving front reached the inner wall of the PVC pipe. Similar moving fronts were observed for benzene and TCE (Figures not shown here). To the author's knowledge, this is the first experimental study directly

demonstrating the relationship between the moving front and permeation of solvents through PVC pipe.

The penetration distance versus the square root of penetration time for the 1-inch pipe in pure TCE, benzene and toluene are presented in Figure 3.5. The penetration distance for each compound was found to be linear with the square root of time with R^2>0.99. The linear equations are presented in Figure 3.5. TCE penetrated fastest in PVC pipe followed by toluene and benzene. The linear relationship of Figure 3.5 can be used to predict the breakthrough time of an organic solvent through the PVC pipe. Using the regression equations listed in Figure 3.5, the breakthrough times (t) for a pipe wall thickness of 3.61 ± 0.02 mm (1-inch diameter pipe) for the three solvents was predicted to be:

$$\text{For TCE: } t = \left(\frac{3.61 + 0.369}{1.523}\right)^2 = 6.8 \text{ days}$$

$$\text{For toluene: } t = \left(\frac{3.61 + 0.345}{1.031}\right)^2 = 14.7 \text{ days}$$

$$\text{For benzene: } t = \left(\frac{3.61 + 0.215}{0.879}\right)^2 = 18.9 \text{ days}$$

The pipe-bottle tests indicated that the actual breakthrough occurred at about 6.5 days for TCE, 16 days for toluene, and 20 days for benzene (Figure 3.3). The above calculations revealed that the breakthrough time of a solvent through PVC pipes can be predicted by using the penetration data from the microscopic visualization tests. The microscopic visualization test can be used as a rapid predictive test in lieu of a pipe-bottle test.

As shown in Figure 3.5, the penetrating front was found to be linearly dependent on the square-root time rather than on time. This observation deviated from a key feature of

Case II diffusion, where the moving front proceeds with a constant velocity meaning the penetration distance is linearly dependent on time (Thomas and Windle, 1982; Hui et al., 1987a, 1987b). This key feature of Case II diffusion is for a flat sheet sample. The question of whether the penetrating solvent would maintain a constant rate through a cylindrical polymer sample as in our experiments similar to a flat sheet sample as in a Case II diffusion was investigated by Lee and Kim (1992). Lee and Kim examined the effect of geometry on solvent penetration in glassy polymers, and found that solvent penetration in radially symmetric geometries exhibited the same transport characteristics as in sheet samples, except that at later stages, penetration of the solvent was observed to accelerate towards the core. Based on Lee and Kim's work, if the solvent penetration in PVC pipe conforms to Case II diffusion, then the moving front would advance at a constant velocity, i.e., penetration distance is proportional to penetration time at least in the initial stage. The results from this microscopic visualization test (Figure 3.5) clearly contradicts the Case II diffusion mechanism as proposed by Berens (1985) and Vonk (1985) for the permeation of solvents in PVC pipes.

A possible explanation for the square-root-time behavior observed in the experiments is the effect of sample thickness. Since Case II diffusion represents a shift in balance between the solvent diffusion and polymer relaxation processes with the latter being rate-controlling, increasing the sample thickness inevitably will result in a diffusion-limited situation, thereby shifting the linear kinetics to the familiar square-root-time Fickian behavior (Hopfenberg, 1978). This transition from Case II diffusion to apparent Fickian kinetics was observed in Berens's study (1985), which showed that the sorption kinetics of toluene in 0.6 mm PVC sheet was Case II (linear with time) while in 4.2 mm PVC sheet was Fickian (linear

with square root of time). The sorption or penetration kinetics for a polymer-penetrant pair can be Case II or Fickian, depending on the polymer sample thickness. The wall thickness of commercial PVC pipes (> 3 mm) is much thicker than those of thin sheet specimens (< 1 mm) used in the studies by others where Case II diffusion was found (Berens, 1985; Vonk, 1985). Because sample thickness significantly affects the sorption or penetration kinetics of penetrants, prediction of the permeation behavior of penetrant through PVC pipes from laboratory data on powders or thin films is not straightforward.

3.4.3 Microscopic visualization tests for PVC pipes exposed to solvents with PEG or NIST reference fuel

The thicknesses of the swollen layer ($L_{s,t}$) versus the square root of time for PVC samples exposed to toluene at five concentration levels (pure solvent, 80%, 60%, 40%, 35%, 30%, 25% and 20% (v/v) in PEG) are plotted in Figure 3.6. Consistent with the findings in pure solvents, the thickness of the swollen layer was found to be linearly related to the square root of time for mixtures of toluene and PEG. The rates at which the thickness of swollen layer grows decreased sharply with decreasing toluene concentration in PEG. When the volumetric percent was below 25%, there was no swollen layer meaning no moving front was formed for this contaminant level or lower.

The thicknesses of the swollen layer ($L_{s,t}$) versus the square root of time for PVC samples exposed to toluene at four concentration levels (pure solvent, 80%, 60%, 40%, and 20% (v/v) in NIST reference fuel) are plotted in Figure 3.7. In comparison to the results obtained from the PEG experiments, toluene penetrated into pipe samples at much slower rates for toluene in reference fuel than for toluene in PEG. For example, the growth rate of the thickness of swollen layer was found to be 0.445 mm/day$^{1/2}$ and 0.127 mm/day$^{1/2}$ for 80%

and 60% (v/v) of toluene in the reference fuel respectively while the corresponding rate was 0.830 mm/day$^{1/2}$ and 0.691 mm/day$^{1/2}$ for the same volume percentage of toluene in PEG. A significant penetration of toluene was observed for 40% of toluene in PEG while no moving front was detected for 40% of toluene in the reference fuel.

The difference in the penetration rates between PEG experiments and the reference fuel experiments may be due to the difference in the physicochemical properties between PEG and the reference fuel. Carbowax® PEG 400 is a hydrophilic polymer with an average molecular weight of 380-420 g/mole and a density of 1.1-1.2 g/cm^3. In contrast, isooctane, the major component of the reference fuel, is a hydrophobic solvent with a molecular weight of 114 g/mole and a density of 0.69 g/cm^3. Theoretically, the sorption process of toluene can be described by the partitioning between the inert chemical (PEG or the reference fuel) and the pipe material. Since the physicochemical properties of toluene are much closer to those of the reference fuel than PEG, toluene would have a greater tendency to partition into the reference fuel rather than the pipe material. In the mixtures of toluene and PEG, however, toluene is likely to escape from the force of attraction of PEG and partition into the pipe matrix. Compared to the reference fuel experiments, PEG experiments provided a conservative estimation of the threshold concentration at which permeation would not occur in PVC pipes. The 25%(v/v) toluene was found as the threshold concentration in PEG experiments while the reference fuel experiments revealed that the threshold value was as high as 40% (v/v) toluene.

Since the penetration behavior of the solvent is dependent on the other components in the mixture, the question is whether the penetration characteristics of a mixture of benzene, toluene, ethylbenzene and xylene (BTEX) as in free product gasoline will differ from the

penetration of a single compound such as benzene or toluene. More specifically, can the threshold value for a single compound be applied to mixtures of compounds?

Figure 3.8 presents the thicknesses of the swollen layer ($L_{s,t}$) versus the square root of time for PVC samples exposed to benzene, toluene, ethylbenzene, xylene solvents, and a mixture of BTEX with 25% (v/v) of each compound. As reported previously, no moving front was detected for a single compound with a concentration of 25% (v/v). However, the mixture of BTEX was sufficiently aggressive to produce a moving front that penetrated into the pipe matrix. The mixture of BTEX displayed a "compromised" aggressiveness since it was more aggressive than ethylbenzene and xylene but less aggressive than benzene and toluene (see Figure 3.8). As shown in Figure 3.8, the moving front data for BTEX at a specific exposure time can be modeled by multiplying the factor of 0.25 to the measured moving front data for each single compound and then adding them together. This result demonstrated that the penetration of an organic mixture through PVC pipes are additive in proportion to the percent volume of each component.

Further work was conducted to investigate the formation and propagation of the moving fronts in PVC samples exposed to the BTEX mixtures for five concentrations in the reference fuel. The concentrations included 100%BTEX and 25% of each BTEX compound (v/v), 80%BTEX and 20% NIST reference fuel (20% for each BTEX compound (v/v)), 60%BTEX and 40% NIST reference fuel (15% for each BTEX compound (v/v)), 40%BTEX and 60% NIST reference fuel (10% for each BTEX compound (v/v)). Similar to the observations for the mixtures of toluene and the reference fuel, no moving front was detected when the volumetric percent of the total BTEX was 40% (10% for each compound) or lower (Figure 3.9).

The results above provide information on the lingering uncertainties regarding permeation of PVC pipes by free product gasoline, as in a typical contaminated site or gasoline spill. The BTEX composition in gasoline varies depending on the source of the petroleum as well as the production method. For example, the fraction of aromatic compounds in straight-run gasoline is generally lower than 20% (v/v) while in catalytic reformed gasoline the fraction can be more than 50% (v/v) (Rittmann and MacCarty, 2001). In the United States, the aromatic fraction typically constitutes approximately 24-28% (v/v) of conventional gasoline and 19-23% (v/v) of reformulated gasoline, respectively (US EPA, 2007). The present study collected 11 premium gasoline samples from local gas stations at different seasons within two years and found that the volumetric fraction of BTEX in these gasoline samples was 23.8 ± 4.1%. Since the microscopic visualization tests revealed that a combination of BTEX compounds exceeding 40% (v/v) in NIST reference fuel is required to initiate swelling and to cause permeation of PVC pipe, it is concluded that the penetration of gasoline in PVC pipes would be extremely slow and PVC pipe should be an effective barrier against gasoline permeation.

3.4.4 Fifty-eight types of PVC pipes exposed to toluene

A 48-hour toluene exposure test was conducted for 58 types of PVC pipes from six manufacturers. The swollen layer thickness ($L_{s,t}$) for each pipe sample was measured for exposure times of 6, 12, 24, 30, 36, and 48 hours. The regression equation, $L_{s,t} = k\, t^{1/2}$, was found to be a good fit of the data with correlation (r^2) greater than 0.995. The slope of the regression line, *k*, is defined as the growth rate of the thickness of swollen layer and can be used as an index to evaluate the relative susceptibility to permeation.

The *k* value obtained for the 58 samples ranged from 0.185 to 0.234 mm/hour$^{1/2}$

(Figure 3.10). The mean and median values were 0.207 and 0.208 mm/hour$^{1/2}$, respectively, indicating a normal distribution. Although a difference in *k* values was detected, it was not clear whether the difference was due to measurement errors or the nature of pipe properties. To answer the question, three pipe samples (identified as Sample 8, Sample 10, and Sample 16) were selected and a 48-hour toluene exposure test was conducted. Quintuplicate was used for each sample. The results are shown in Figure 3.11. The measurement was very reproducible and the quintuplicate samples gave identical results. The differences in *k* values for the three samples (sample 8, sample 10 and sample 16) were statistically significant, although it remains unknown what factors have been responsible for such differences.

Efforts were also made to correlate the *k* values with pipe dimensions (Figure 3.12). It appeared that the pipe sizes did not significantly influence the *k* values. Therefore, the penetration data obtained from smaller size pipes may be used to predict the permeation behavior for large water mains by only considering the scale-up of the pipe wall thickness.

3.5 Conclusion

A rapid predictive microscopic visualization technique was developed to predict the permeation of organic solvents through PVC pipes by observing the formation and propagation of the organic moving front in the pipe materials. The microscopic visualization test demonstrated that no detectable permeation occurred until the moving front reached the inner wall of the PVC pipe. The breakthrough times of organic solvents in the pipe-bottle tests were predicted using the moving front advancement rate and the pipe wall thickness.

A series of microscopic visualization tests were conducted to predict the threshold contamination level of toluene and BTEX compounds where a moving front would be

formed and observed. The results suggested that (i) the threshold concentrations of toluene in PEG and in NIST reference fuel were 25%(v/v) and 40% (v/v), respectively; (ii) the impact on PVC pipe of the activities of the individual BTEX compounds in an exposure medium is additive, and (iii) a combination of BTEX compounds exceeding 40% (v/v) in NIST reference fuel is required to initiate swelling and to cause permeation of PVC pipe. As the sum of the volumetric fractions of BTEX compounds in free product gasoline is generally lower than 30%, PVC pipe should be an effective barrier against gasoline permeation.

The results of the experiments demonstrated that the microscopic visualization technique was rapid, accurate, and susceptible to detect the differences among PVC pipes in their susceptibility to organic permeation.

Acknowledgment

The authors thank the Awwa Research Fundation for its financial, technical and administrative assistance in funding and managing the project through which this information was discovered. The comments and views detailed herein may not necessarily reflect the views of the Awwa Research Fiundation, its officers, directors, affiliates, or agents.

Reference

Berens, A.R. 1985. Prediction of organic chemical permeation through PVC pipe. *Journal AWWA*, 77(11): 57-64

Comyn, J. 1985. Polymer Permeability. Elsevier Applied Science Publishers, Essex, UK.

Crank, J. 1975. The Mathematics of Diffusion. Clarendon Press, Oxford, UK.

Ercken, M., P. Adriaensens, D.Vanderzandes, and J.Gelan. 1995. Study of solvent diffusion in polymeric materials using magnetic resonance imaging. *Macromolecules*, 28(26): 8541-8547.

Hopfenberg, H.B.1978. The effect of film thickness and sample history on the parameters describing transport in glassy polymers. *Journal of membrane science*, 3(2):215-230.

Hui, C.Y., K.C. Wu, R.C. Lasky, and E.J. Kramer. 1987a. Case-II diffusion in polymers. I. Transient swelling. *Journal of Applied Physics*, 61(11): 5129-5136.

Hui, C.Y., K.C. Wu, R.C. Lasky, and E.J. Kramer. 1987b. Case-II diffusion in polymers. II. Steady-state front motion. *Journal of Applied Physics*, 61(11): 5137-5149.

Morrissey, P. and D.Vesely. 2000. Accurate measurement of diffusion rates of small molecules through polymers. *Polymer*, 41(5):1865-1872.

National Bureau of Standards, 1986. *Alcohols in Reference Fuel*. Standard Reference Material 1829. NBS (now NIST), Gaitbersburg, MD.

National Institute of Standards & Technology, 1988. *Lead in Reference Fuel*. Standard Reference Matherial 2712. NIST, Gaitbersburg, MD.

Ong, S.K., J.A.Gaunt, F.Mao, C.L.Cheng, L.E.Agelet, and C.R.Hurburgh. 2007. Impact of petroleum-based hydrocarbons on PE/PVC pipes and pipe gaskets. AwwaRF, Denver, CO.

Park, J.K. and L. Bontoux. 1993. Thermodynamic modeling of the sorption of organic chemicals in thermoplastics and elastomers. *Journal of applied polymer science*, 47(5): 771-780.

Park, J.K., L. Bontoux, D. Jenkins, and R.E. Selleck. 1991. Permeation of polybutylene pipe and gasket material by organic chemicals. *Journal AWWA*, 83(10): 71-78.

Peppas, N.A. and L.B. Peppas. 1994. Water diffusion and sorption in amorphous macromolecular systems and foods. *Journal of Food Engineering*, 22(1-4):189-210.

Perry, K.L., P.J. McDonald, E.W. Randall, and K. Zick. 1994. Stray field magnetic resonance imaging of the diffusion of acetone into poly(vinyl chloride). *Polymer*, 35(13): 2744-2748.

Lee, P.I. and C.J. Kim. 1992. Effect of geometry on solvent front penetration in glassy polymers. *Journal of Membrane Science.* 65(1-2):77-92.

Rittmann, B.E. and P.L.McCarty. 2001. Environmental Biotechnology: Principles and Applications. McGraw-Hill, New York.

Thomas, N.L. and A.H. Windle. 1978. Transport of methanol in poly(methyl methacrylate). *Polymer*, 19(3): 255-265.

Thomas, N.L. and A.H. Windle. 1982. Theory of case II diffusion. *Polymer*, 23(4): 529-42.

Thompson, C. and D. Jenkins. 1987. Review of water industry plastic pipe practices. AwwaRF, Denver, CO.

Uni-Bell. 2001. Handbook of PVC Pipe Design and Construction. Uni-Bell PVC Pipe Association, Dallas, TX.

US EPA. 2007. Conventional/reformulated gasoline parameters by reporting year (1997-2005)[Online]. <http://www.epa.gov/otaq/regs/fuels/rfg/properf/rfg-params.htm> <http://www.epa.gov/otaq/regs/fuels/rfg/properf/cg-params.htm>

US EPA. 2002. Permeation and leaching: technical information review [Online]. <http://www.epa.gov/safewater/disinfection/tcr/pdfs/whitepaper_tcr_permation-leaching.pdf>

Vonk, M.W. 1985. Permeation of organic compounds through pipe materials. Publication No. 85. KIWA, Neuwegein, Netherlands.

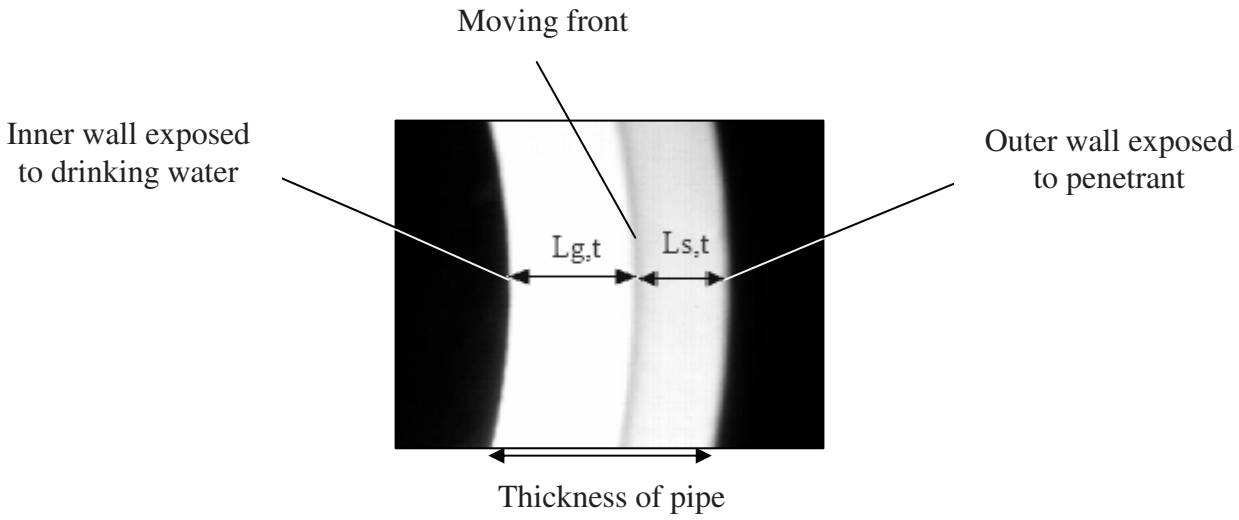

Figure 3.1 Crossing section of pipe showing moving front

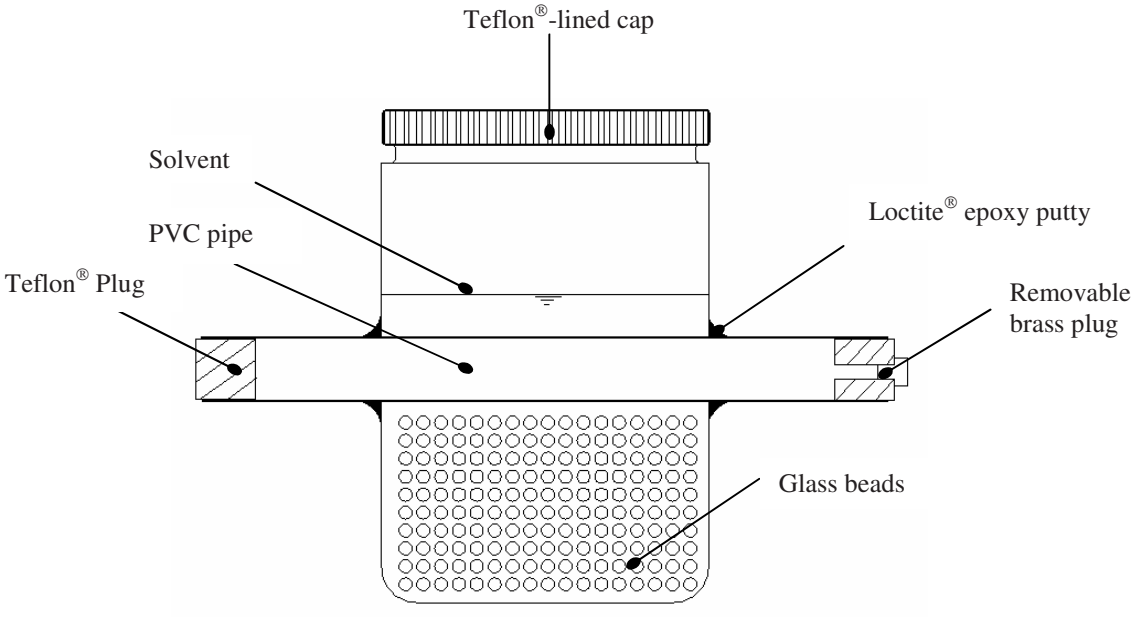

Figure 3.2 Pipe-bottle apparatus

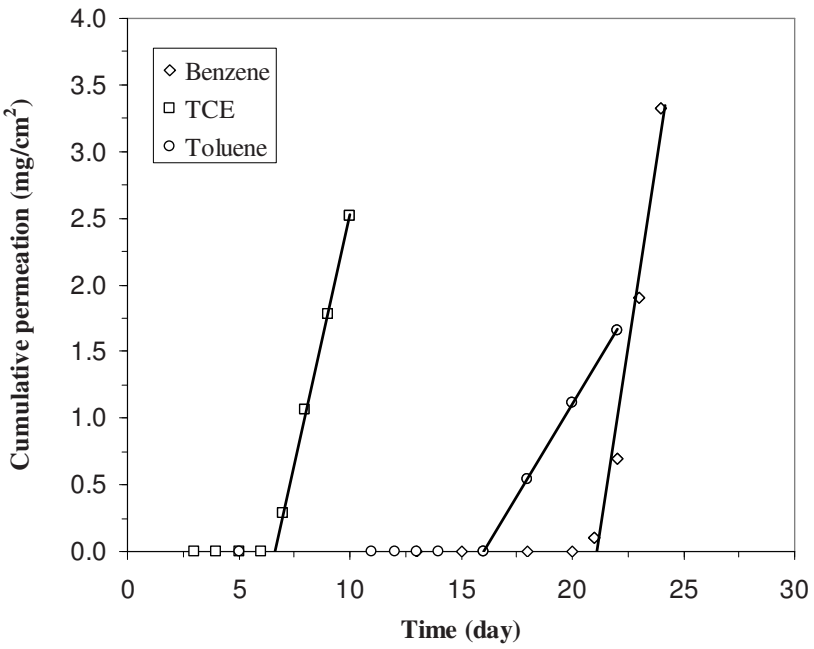

Figure 3.3 Cumulative mass permeated per unit area for PVC pipes exposed to solvents of benzene, toluene and trichloroethylene

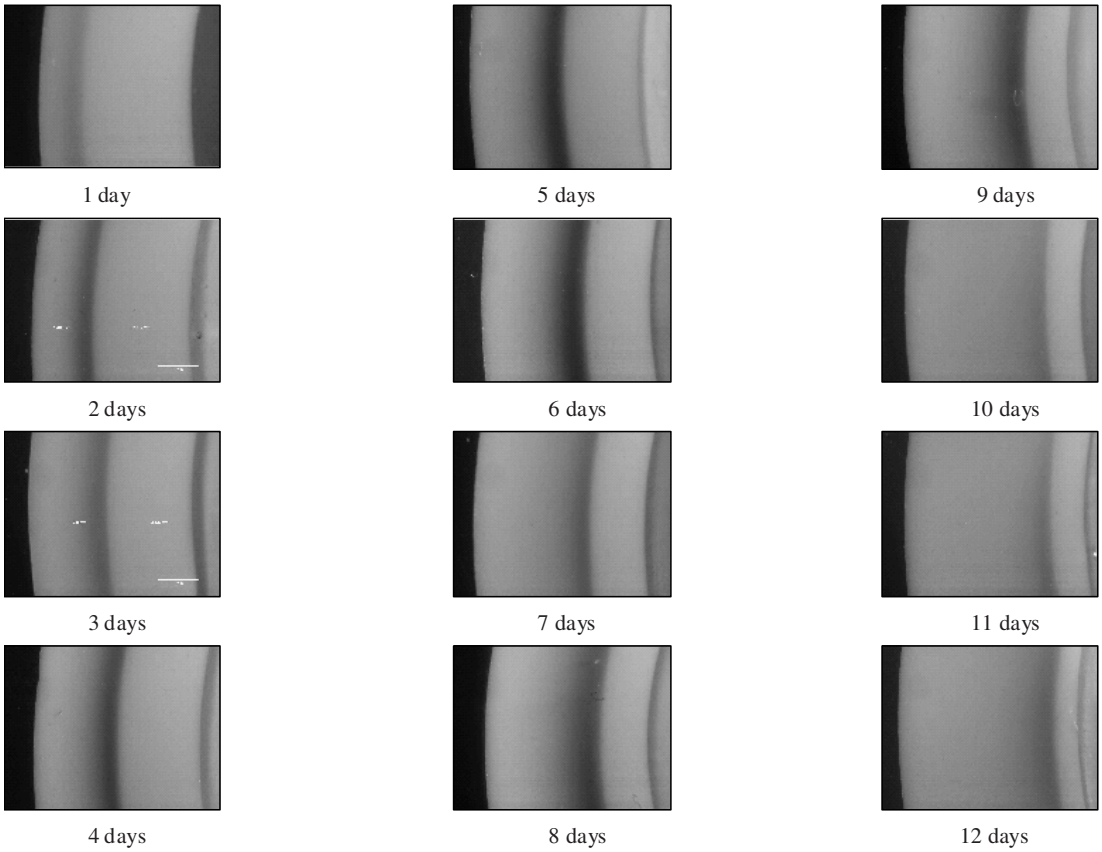

Figure 3.4 Advance of moving front with time in PVC pipe samples exposed to toluene solvent (left line: boundary of swollen outer wall; mid line: moving front; right line: boundary of inner wall)

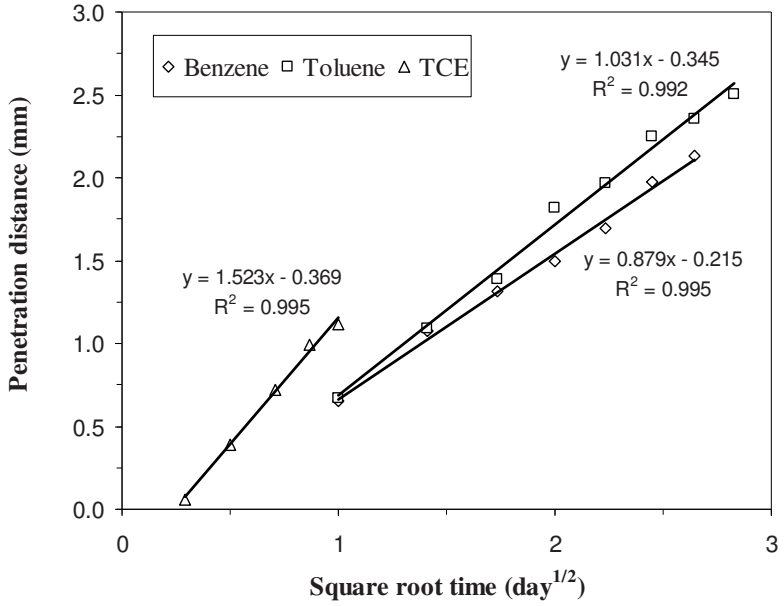

Figure 3.5 Penetration distance versus square root of time for PVC samples exposed to benzene, toluene and trichloroethylene (regression equation: y=penetration distance (mm), x=square root of time ($day^{1/2}$))

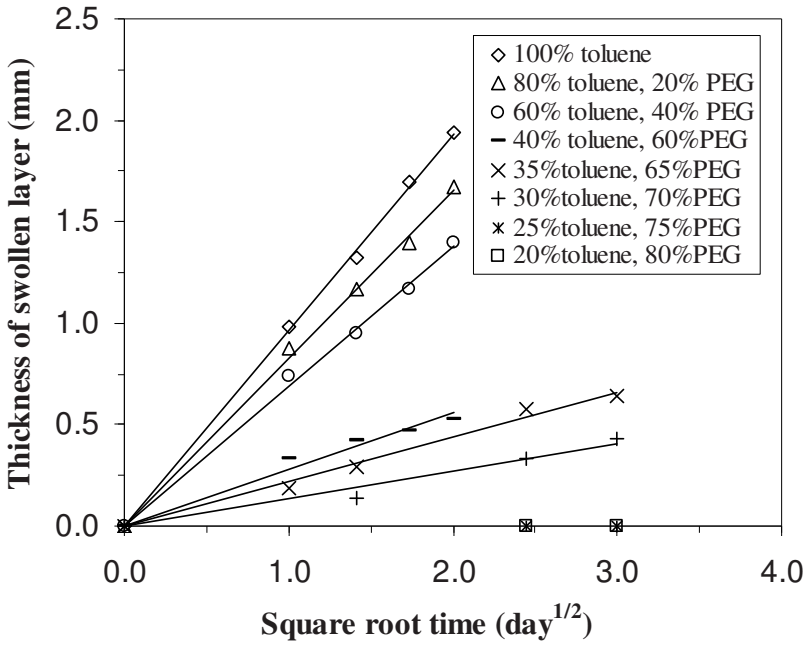

Figure 3.6 Thickness of swollen layer with time for PVC samples exposed to toluene in PEG

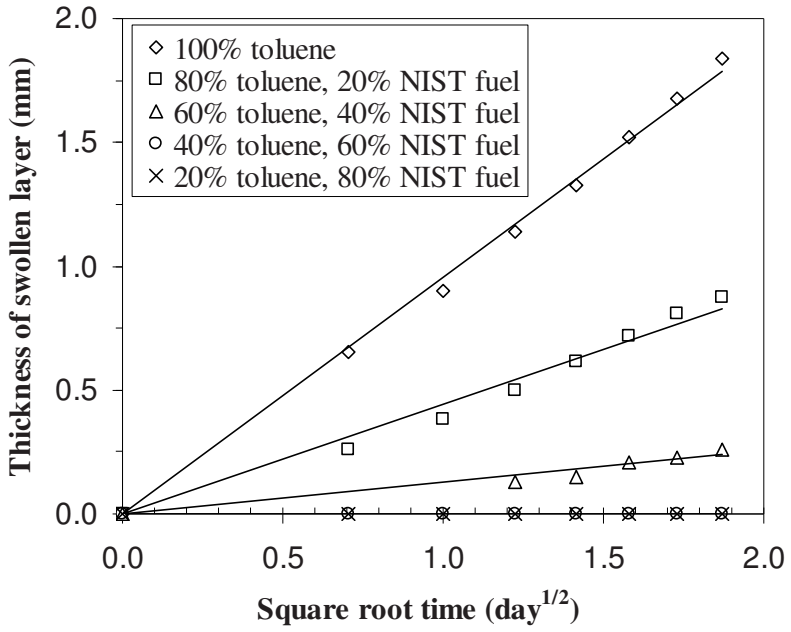

Figure 3.7 Thickness of swollen layer with time for PVC samples exposed to toluene in NIST reference fuel

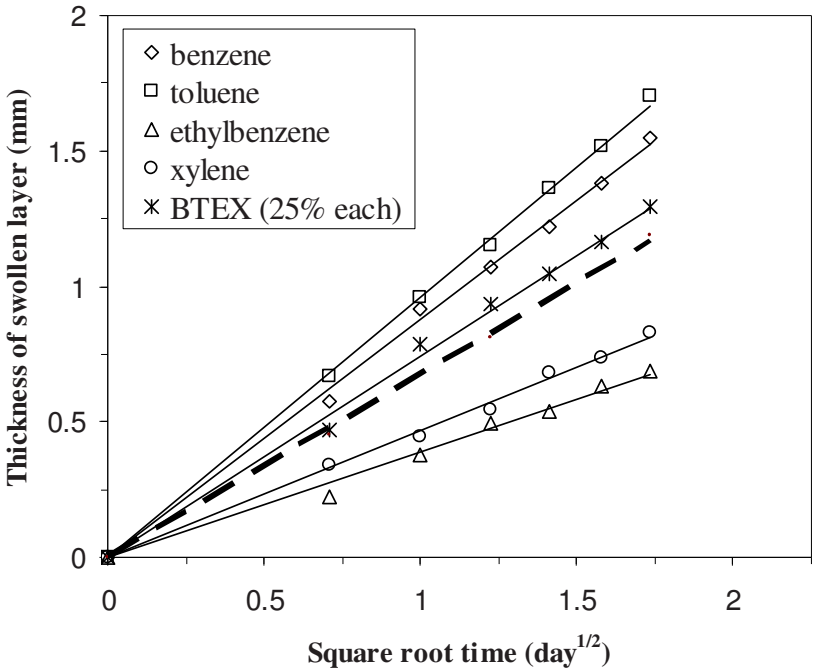

Figure 3.8 Thickness of swollen layer with time for PVC samples exposed to benzene, toluene, ethylbenzene, xylene, and mixture BTEX (BTEX: mixture of 25 percent by volume of benzene, toluene, ethylbenzene and xylene; Dashed line estimated by: $0.25 \times M_{b,t}+0.25\times M_{t,t}+0.25\times M_{e,t}+0.25\times M_{x,t}$, where $M_{b,t}$, $M_{t,t}$, $M_{e,t}$ and $M_{x,t}$ were the moving front data at a specific time t for benzene, toluene, ethylbenzene and xylene, respectively)

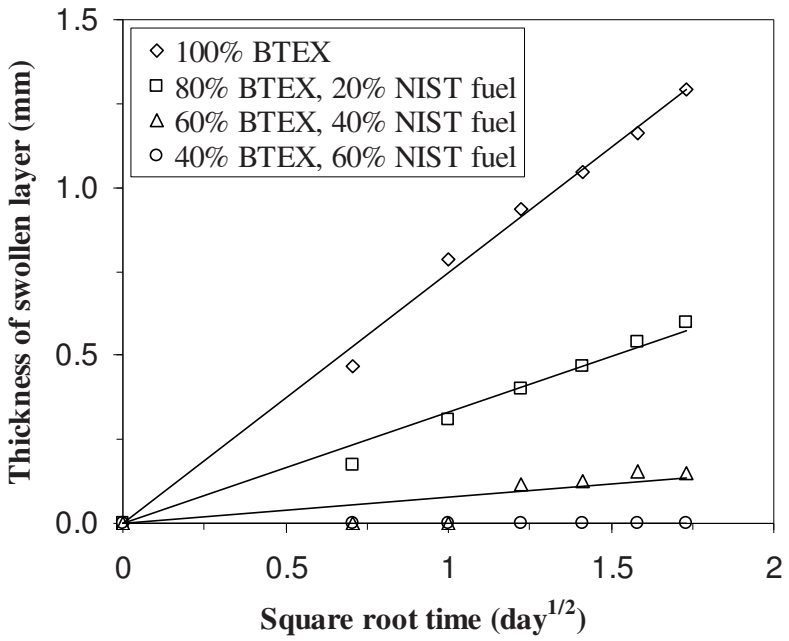

Figure 3.9 Thickness of swollen layer with time for PVC samples exposed to BTEX mixtures in NIST reference fuel (BTEX 100%: 25 % (v/v) of each BTEX compound; BTEX 80%: 20% (v/v) of each BTEX compound; BTEX 60%: 15% (v/v) of each BTEX compound; BTEX 40%: 10% (v/v) of each BTEX compound)

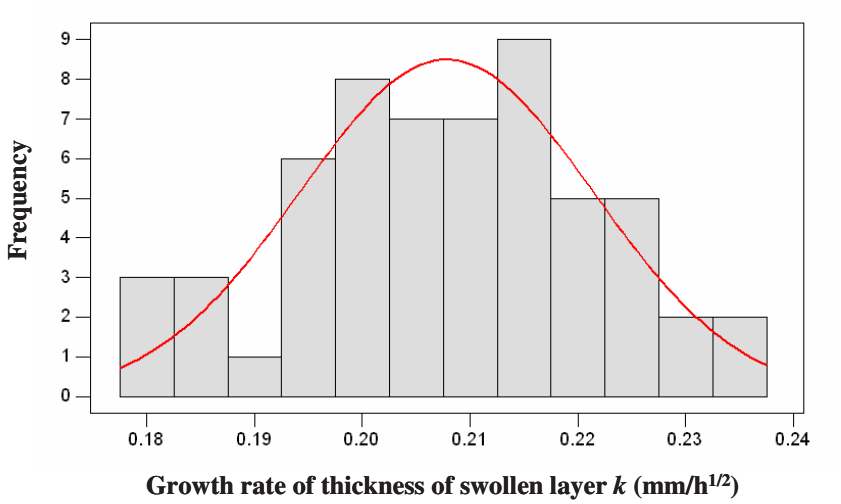

Figure 3.10 Growth rates of thickness of swollen layer (k) obtained from exposure to toluene for 58 PVC samples

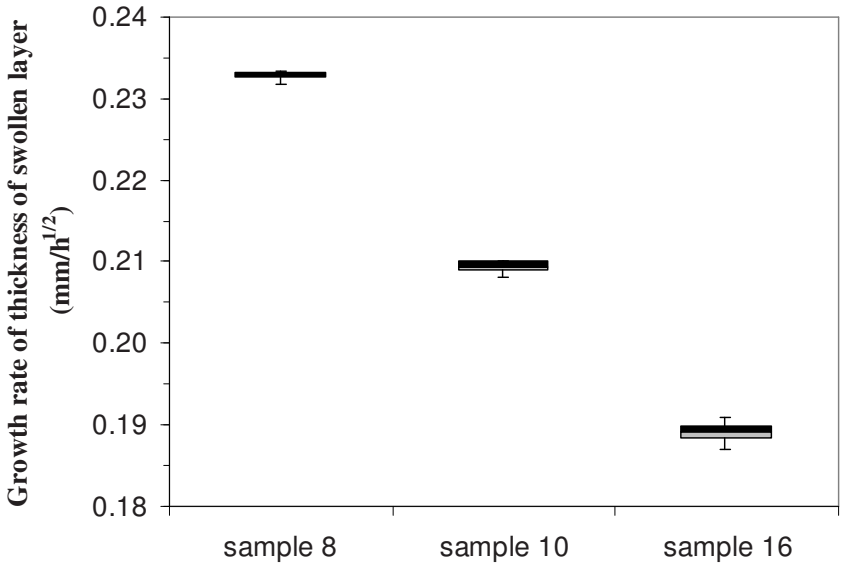

Figure 3.11 Comparison of growth rates of thickness of swollen layer (*k*) obtained from exposure to toluene for Samples 8, 10 and 16

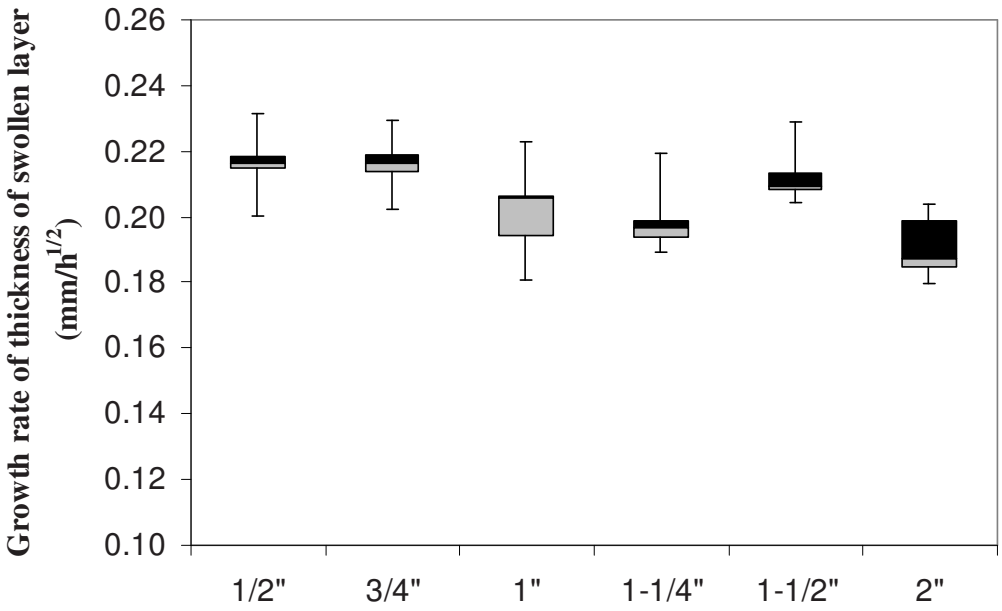

Figure 3.12 Comparison of growth rates of thickness of swollen layer (*k*) obtained from exposure to toluene for different pipe sizes

CHAPTER 4. PERMEATION OF ORGANIC CONTAMINANTS THROUGH PVC PIPES FROM VAPOR AND AQUEOUS PHASES

A paper to be submitted to *Journal of American Water Works Association*

Feng Mao, James A. Gaunt, Say Kee Ong

Abstract

This study investigated the permeation of benzene, toluene and trichloroethylene (TCE) through PVC pipes from vapor and aqueous phases by using a combination of pipe-bottle tests, gravimetric sorption tests and microscopic visualization tests. Saturated organic vapors of target compounds rapidly penetrated through 1-inch PVC pipes within 30 days. Organic compounds in saturated aqueous solutions also permeated through 1-inch PVC pipes but the breakthrough times were significantly delayed. The breakthrough times of TCE and benzene were found to range from 60 days to 240 days, depending on the experimental mixing conditions. Insignificant sorption and no moving front were detected when exposed to the organic vapors that were in equilibrium with ≤ 40% (v/v) benzene or toluene in NIST reference fuel. Insignificant sorption and no moving front were detected when exposed to water that is ≤ 60% of the aqueous solubility of benzene and toluene. The test results suggest that new PVC pipe materials are an effective barrier against the permeation of BTEX in either gasoline vapors or gasoline-contaminated groundwater.

Keywords: PVC; Permeation; Vapor; Aqueous; Gasoline

4.1 Introduction

It has long been known that organic contaminants can permeate through plastic pipes and adversely affect the quality of drinking water in a water distribution system (Vonk, 1985; Thompson and Jenkins, 1987). The plastic pipe materials involved include polybutylene (PB), polyethylene (PE) and polyvinyl chloride (PVC) and the contaminants of interest include highly volatile hydrocarbons and organic chlorinated solvents (Holsen et al., 1991).

To ascertain the susceptibility of PVC pipes to permeation by organic chemicals, some efforts such as the gravimetric sorption test (Berens, 1985; Vonk, 1985) and the pipe-bottle exposure test (Vonk, 1985) have been conducted. The results of these studies indicated that PVC pipe is essentially impermeable to environmental organic contaminants but permeation cannot be excluded in heavily contaminated situations. A recent study developed a microscopic visualization technique to examine the formation and propagation of organic fronts in the PVC matrix and concluded that PVC pipe is an effective barrier to resist the permeation of free product gasoline (Ong et al., 2007).

However, previous studies generally focused on the sorption of organic solvents by pipe material or penetration of organic solvents in pipe material and the results may not be sufficient to reflect the comprehensive permeation behavior of pipes in the subsurface environment, as permeation can also occur either from the vapor phase or aqueous phase. Organic solvents or fuels may release volatized organic vapors in the vadose zone, or may migrate downward to the water table, resulting in dissolution of organic compounds into the aqueous phase. Pipes in a site contaminated by spills would more commonly be exposed to organic vapors or organic aqueous solutions rather than to organic solvents.

According to Vonk (1985), no significant permeation would occur if the concentration of organic compound is less than 0.25 times the maximal concentration in water or in the vapor phases. However, this value was based on sorption experiments involving exposure of thin films of pure PVC polymer to solvents and has not be confirmed by any aqueous or vapor experiment. It remains unknown whether this threshold value determined from solvent experiments is applicable for the permeation of organic compounds from the water and vapor phases. In Berens's study (1985), sorption by pure PVC polymer in toluene vapor and toluene liquid at the same activity of 0.75 exhibited identical kinetics at the initial stage. Based on this finding, Berens concluded that the sorption rate of the penetrant was dependent on the activity of the penetrant rather than the penentrant concentration or physical state, although he did not explain why the two sorption curves of toluene deviated from each other after the initial stage. Using the data on PVC powers or thin films to predict the permeation behavior of thick PVC pipes may also be inappropriate since the sample thickness significantly affects the sorption or penetration kinetics of penetrants (Hopfenberg, 1978). There are significant uncertainties associated with the performance of PVC pipes exposed to organic aqueous solutions as well as organic vapors.

The aim of the present study was to investigate the permeation of organic contaminants through PVC pipes from vapor phase and aqueous phase using the pipe-bottle test, the gravimetric sorption test and the microscopic visualization test. The results serve as a base for predicting the threshold contamination level at which PVC pipes would be susceptible to permeation under organic vapor or aqueous solution exposure conditions. Combining the results from the current study with the previous study (Ong et al., 2007), we

further examined the similarities and differences of the permeation behavior of organic contaminants observed in the aqueous, vapor and solvent experiments.

4.2 Materials and Method

4.2.1 Materials

One-inch diameter PVC pipes (SCH 40 450 psi@73F ASTMD NSF-PW) were purchased new from local stores. Tests were not conducted on old, used, or compromised pipes since the age, exposure history, and conditions are typically not known. Three organic compounds, benzene, toluene and trichloroethylene (TCE) were selected on the basis of their occurrence in contaminated soil and groundwater. Reagent-graded solvents were purchased from Fisher Scientific (Chicago, IL). To dilute benzene and toluene to a certain concentration level, the National Institute of Standards & Technology's (NIST) formula for "reference fuel" was used to simulate the conditions of free product gasoline. The NIST reference fuel consists of 91% (v/v) (91.09% w/w) 2,2,4-trimethylpentane (iso-octane) and 9% (v/v)(8.91 w/w) n-heptane. As a Standard Reference Material (SRM), reference fuel has been used for calibrating instruments and determining lead (NIST, 1988) and alcohols contents (National Bureau of Standards, 1986) in gasoline. This reference fuel is a good surrogate for the alkanes in gasoline which are inert to pipe materials. Reagent-grade solvents of iso-octane and n-heptane were purchased from Fisher Scientific (Chicago, IL).

4.2.2 Pipe-bottle test

The experiments were conducted in a pipe-bottle apparatus, which has been previously described in detail (Ong et al., 2007). It consisted of a 1-L glass bottle with one PVC pipe mounted horizontally through holes drilled in the glass. The connection between

the glass bottle and the pipe was sealed by a chemically resistant sealant and the ends of the pipes were sealed with Teflon® plugs. The Teflon® plug had a small hole that was plugged with a threaded brass plug to allow filling and draining of the water inside the pipe with a glass syringe. The bottle was capped with a Teflon®-lined cap.

Three pipe-bottle apparatuses were set up with a PVC pipe directly exposed to the vapor of benzene, toluene and TCE, respectively. In this test, the pipe segment was first filled with deionized water and 100 mL solvent was then transferred to the bottom of the bottle. The visible liquid level of the solvent was around 3 cm below the lowest edge of the pipe segment. Preliminary experiments found that organic vapor condensed on the pipe surface. To avoid the effect of condensation and to simulate the conditions closer to field conditions with humidity close to saturation, an opened glass vial containing 10 ml of deionized water was mounted between the pipe segment and the inner wall of the bottle. Pipe water samples were taken each day and analyzed for the presence of the target compounds. After each sampling event, the pipe was immediately flushed three times with deionized water before fresh deionized water was added and the pipes sealed.

At a typical contaminated site, aqueous solvent-saturated solutions would represent extreme field conditions encountered by PVC pipes in contaminated groundwater. To simulate such conditions, three pipe-bottle apparatuses were set up with a PVC pipe exposed to aqueous saturated solutions of benzene, toluene and TCE, respectively. To prepare the benzene and toluene-saturated solutions, a mixture of 200 mL solvent and 3.5 L deionized water was moderately stirred with a magnetic stirrer in a glass bottle for 48 hours and then allowed to sit undisturbed for 2 hours. To prepare the TCE-saturated solution, a mixture of 50 mL TCE with deionized water was vigorously stirred with a magnetic stirrer under zero

head-space conditions for 48 hours in a 2-L volumetric flask with a Teflon® stopper, and then allowed to sit undisturbed for 2 hours. Preliminary experiments indicated that the above procedures produced reproducible saturated solutions. The measured concentrations of benzene, toluene and TCE were 1,767 mg/L, 501 mg/L and 1,093 mg/L, respectively, and were close to the solubilities reported in the literature.

To start the exposure experiments, aqueous saturated solution was transferred into the pipe-bottle apparatus using a Masterflex pump with Teflon® tubing. In attempt to maintain the benzene or toluene concentrations at saturation, 50 mL corresponding solvent was added to provide a thin layer of the solvent on the water surface. The water was gently stirred by a magnetic stirrer at regular intervals. The concentration of the TCE-saturated solution was maintained at saturation by keeping approximately 10 mL of TCE solvent at the bottom of the bottle with regular gentle stirring. Two additional pipe-bottle apparatuses were used to replicate the benzene and TCE exposure experiments under the conditions of continuous stirring. The mixing condition (periodic or continuous) has a strong effect on both the dissolution of solvents from NAPL phase to aqueous phase and the mass transfer of contaminants in aqueous solutions, and thus potentially determine the availability of contaminants for permeation through PVC pipes. Headspace was minimized in all pipe-bottle apparatuses. Pipe water was sampled at regular intervals (twice each month) and analyzed for the presence of the target compounds. After the breakthrough was detected, pipe water was sampled each day.

Benzene, toluene and TCE in water samples were determined using a gas chromatograph (Tracor 540, Tracor Instruments Austin, Inc., Austin TX) equipped with a packed column (1.8 m × 2 mm; 1% SP1000 on 60/80 mesh Carbopack B), a photoionization

detector, and an automated purge and trap concentrator (Tekmar LSC2/ALS). The detection limits for benzene, toluene and TCE were 0.24 µg/L, 0.24 µg/L, and 1.2 µg/L, respectively.

4.2.3 Gravimetric sorption test

Pipes to be tested were cut across the longitudinal axis of the pipe, so as to form ring-like specimens that were 1.5 cm in length. The specimens were washed with detergent, rinsed with tap water and distilled water, placed on a paper towel to air-dry, and weighed using an analytical balance.

In vapor sorption experiments, pipes specimens were exposed to benzene/toluene vapors which were in equilibrium with pure solvent, 80%, 60%, 40%, 20% (v/v) in NIST reference fuel, respectively. As mentioned earlier, organic vapor condensed on the pipe surface. To avoid the effect of condensation and to simulate the conditions closer to field conditions, a pipe specimen was mounted on the top of a 20-mL open glass vial containing 10 mL of deionized water. The glass vial with the pipe specimen was then placed in a 1-L glass jar containing 100 mL of benzene/toluene solvent or mixtures of benzene/toluene and NIST reference fuel. The 1-L glass jar was closed with a Teflon®-lined cap. Under these conditions, the pipe specimens were exposed to organic solvent vapor with humidity close to saturation. At various times, the specimens were removed from the glass jar, placed on paper towels, wiped, and allowed to air dry for thirty seconds before weighing.

In aqueous sorption experiments, three organic compounds (TCE, benzene and toluene) at five concentrations (saturated aqueous solution [100%], 80%, 60%, 40%, and 20% saturated aqueous solutions of the solvents) were tested. Detailed procedures to prepare the aqueous saturated solutions were previously described. In benzene and toluene experiments, the saturated aqueous solution was transferred into a 120-mL glass jar and the

pipe specimen was then immersed in the solution. This was followed by adding 3-mL solvent into the jar so the aqueous solution was covered with the solvent. The headspace above the solution was minimized as much as possible. Prior to measuring the weight of pipe specimens during the experimental period, the glass jar was opened in a fume hood and the solvent film on the surface was allowed to evaporate. After weighing, the samples were re-immersed in freshly prepared saturated aqueous solution and 3 mL benzene or toluene added to the solution, creating a film of benzene or toluene on the surface of the water. The concentration of the TCE-saturated aqueous solution was maintained at saturation by keeping 3-mL of TCE solvent at the bottom of the jar with regular stirring. In this case, pipe specimens were placed on a glass stand in the jar as to avoid contact with the TCE. For experiments with 80%, 60%, 40% and 20% aqueous solutions of the solvents, the solutions were replaced each week to maintain a relatively constant concentration. A control experiment using deionized water as exposure media was also conducted.

4.2.4 Microscopic visualization test

This approach has been previously described in details (Ong et al., 2007) and so is only briefly summarized here. Swelling of PVC pipe by an organic solvent may result in the formation of a moving (diffusion) front, a sharp interface separating the inner glassy core from the outer swollen layer. With a series of solvent experiments, Ong et al. (2007) demonstrated that drinking water could be contaminated only if the moving front propagates in the pipe matrix and reaches the inner wall of pipes. This conclusion, on the basis of the observations from solvent experiments, was assumed in the present study to be valid for the cases of PVC pipes exposed to organic vapors or organic aqueous solutions.

The test conditions were identical to those described in the gravimetric sorption experiments. At different exposure times, a pipe specimen was removed from the exposure media (vapors or aqueous solutions) and wiped dry. Each dried specimen was firstly cut parallel the longitudinal axis and then cut across the longitudinal axis of the pipe specimen, so as to form an approximately 1/5 ring-like sample with a length of 0.5 cm. The sample cross section was observed under a reflected light microscope (Olympus BHM) and its precise image was captured by a camera mounted on the microscope. With PC-Image (version 5.0) software package, the penetration distance of the moving front was precisely measured.

All experiments were conducted at room temperature (23 ± 1.5°C).

4.3 Results and Discussion

4.3.1 Pipe-bottle test

Significant permeation through PVC pipes occurred when pipes were exposed to saturated organic vapors of TCE, toluene and benzene and their corresponding breakthrough times were estimated to be 13 days, 28 days and 31 days, respectively (Figure 4.1). No detectable permeation occurred through PVC pipes until a breakthrough point was reached. At that point, permeation occurred at a constant rate. As shown in Figure 4.1, the permeation curves obtained in the vapor experiments were very similar to those obtained in the liquid solvent experiments. TCE permeated first, followed by toluene and benzene. For a specific organic compound, once breakthrough occurred, the permeation rate in the organic vapor was nearly identical to that in the neat solvent, as demonstrated by an identical slope of the cumulative mass permeated per unit area versus the exposure time. However, there was a

delay in breakthrough when exposed to organic vapors. The delay is probably due to the effect of mass transfer, which will be discussed later when comparing the data obtained from solvent, vapor and aqueous experiments.

The permeation of TCE and benzene through PVC pipe in saturated aqueous solutions is shown in Figure 4.2. To the authors' knowledge, this is the first experimental study to demonstrate that organic contaminants can permeate through PVC pipes from aqueous phase. Under regular stirring conditions, the breakthrough times for TCE and benzene were estimated to be 168 days (around five and a half months) and 250 days (around eight and a half months), respectively. Breakthrough of toluene did not occur during the ten-month duration of the experiment, after which it was terminated due to a leak in the apparatus. In comparing with regular stirring, continuous stirring significantly shortened the breakthrough times of benzene and TCE, as demonstrated by 60 days of breakthrough time for TCE and 80 days for benzene (Figure 4.2). The much longer breakthrough times in the regular stirring experiments was due to the mass transfer limitation. Such limitation occurred when organic contaminant absorption by the pipe wall is fast enough to decrease the external concentration of organic contaminant immediately adjacent to the pipe wall, while the release of contaminants from NAPL phase to aqueous phase and the diffusion of contaminant in water solutions were not sufficiently rapid to compensate for the loss of contaminant due to the absorption by pipe materials. In other words, it was very likely that the pipe segments were not continuously exposed to the saturated solutions under regular stirring. Under field conditions where PVC pipes were exposed to contaminated groundwater in close proximity to a benzene or TCE NAPL, it is expected that the breakthrough of the contaminant would be not occur within 60 days for TCE and 80 days for benzene because of the lack of sufficient

mixing conditions in the field.

It is known that organic compound permeation of polymer is directly dependent on the activity of the organic compound in the exposure media. However, the permeation behavior in pure solvents, saturated organic vapors and saturated aqueous solutions showed significant differences in breakthrough times even though the activity for each phase was equal to 1.0 as defined by Berens (1985) and Vonk (1986). They defined activity in the context of permeation theory as:

$$a = \frac{C_w}{C_{w,m}} \qquad \text{(Eq. 4.1)}$$

$$a = \frac{C_v}{C_{v,m}} \qquad \text{(Eq. 4.2)}$$

Where a is the activity ($0 \leq a \leq 1$); C_w is concentration in water (mg/L); $C_{w,m}$ is the maximal (saturated) solubility in water (mg/L); C_v is the concentration in the vapor phase (mg/L); and $C_{v,m}$ is the maximal (saturated) solubility in the vapor phase (mg/L). To explain the mechanisms involved when a PVC pipe is exposed to a saturated aqueous solution or a saturated vapor, a key question is whether a constant activity of 1.0 for organic compounds in the organic vapor or the aqueous solution was maintained immediately adjacent to the pipe wall. In aqueous solution, the impacts of contaminants on PVC pipes are not only dependent on the interaction between organic chemicals and polymer materials but also on the effective availability of the compounds for permeation. It is probable that there is a thin film of stagnant water immediately adjacent to the pipe wall for the experiments using saturated aqueous solutions. Organic chemicals must diffuse from the bulk solution through this thin film of stagnant water to the pipe for sorption to occur, even under well-mixed conditions.

With pure solvent experiments there is direct contact between the pipe and the solvent. In the case of the solvent vapor experiments, the thin film of water may not exist unless the relative humidity is high. Diffusion coefficients through stagnant water are on the order of 10^{-5} cm^2/s, while diffusion coefficients through stagnant air are on the order of 10^{-2} cm^2/s (Schwarzenbach et al., 1993). The difference in the order of magnitudes of diffusion coefficients in air and water may help to explain why the breakthrough of contaminants in saturated organic vapors occurred slightly behind that in pure solvents while significant delay of breakthrough was found in saturated aqueous solutions.

Significant swelling of pipe materials occurred as a result of the permeation process. In the present study, all pipe specimens showed signs of softening and localized swelling. To assess whether the PVC pipe would be restored to its original properties when the external contaminant source was removed, the chemicals in the bottle was emptied and the pipes allowed to stand in the fume hood for about half a year. During this time, the pipe segments were filled with deionized water and drained regularly. On examination after 6 months, the rubberization of the PVC pipes continued to persist and relatively high concentrations of organic compounds were detected in the pipe-water. These results indicated that once PVC pipes have been permeated, the permeation cannot be readily corrected by removing the contaminated soil and flushing the pipelines with clean water for a protracted period of time.

4.3.2 Gravimetric sorption test

As previously described, PVC pipes samples were exposed to organic vapors that were in equilibrium with neat benzene/toluene solvent and their mixtures with NIST reference fuel. Theoretically, the vapor pressure of benzene (or toluene) equilibrated with the liquid mixtures can be estimated based on Raoult's Law:

$$V_i = \alpha_i x_i P_i^o \qquad \text{(Eq. 4.3)}$$

where V_i is the vapor pressure of *i* equilibrated with a liquid mixture (atm); α_i is theactivity coefficient; x_i is the mole fraction of *i* in the mixture; and P_i^0 is the saturated vapor pressure of *i* in the pure organic liquid (atm).

The activity coefficient α_i can be assumed to be 1.0 since the liquid phase was comprised of a mixture of similar types of organic chemicals, i.e., benzene/toluene, iso-octane and n-heptane.

If the saturated vapor of benzene (or toluene) in equilibrium with the pure liquid is assigned an activity of 1 (Berens, 1985; Vonk, 1985), the activity of benzene/toluene in a vapor mixture can be expressed below:

$$a = \frac{V_i}{P_i^0} = x_i \qquad \text{(Eq. 4.4)}$$

where a is the activity of the compound in a vapor mixture.

As indicted in Eq. 4.4, in a vapor-liquid equilibrium system the activity of benzene/ toluene in a vapor mixture is equal to its mole fraction in the corresponding liquid mixture. According to Eq. 4.4, the activities of benzene in organic vapors that were in equilibrium with pure solvent, and 80%, 60%, 40% and 20% (v/v) in the reference fuel were estimated as 1.0, 0.88, 0.73, 0.55 and 0.32, respectively. The corresponding activities of toluene were 1.0, 0.86, 0.70, 0.51, and 0.28, respectively. Figure 4.3 shows weight gains versus time for pipe samples exposed to benzene and toluene vapor with different activities.

As shown in Figure 4.3, the sorption data of benzene and toluene followed apparent Fickian kinetics sorption (linear with square root of time) but there was a time lag at the initial period. The phenomenon of the initial time lag was also found in the sorption or

diffusion process for some penetrant–polymer pairs (Morrissey and Vesely, 2000; Billovits and Durning, 1988; Grinsted et al., 1992). It was suggested that the initial time lag diffusion resulted from the plasticization of the polymer by the penetrant, after which the sorption or the diffusion of penetrant is no longer inhibited by the relaxation rate of the polymer. Figure 4.3 also demonstrated that the weight gain decreased dramatically as the benzene/toluene activity was reduced. When the activity was less than 0.55 for benzene and 0.51 for toluene (the corresponding volumetric percent in the reference fuel was around 40%), sorption of benzene/toluene vapors by pipe materials was insignificant within a 2.5-day exposure.

TableCurve3D 4.0 (Systat Software Inc) was used to find optimal equations that can ideally describe the three dimensional data above, i.e., weight gain, time, and activity. Two empirical equations were obtained with an excellent fit of R^2>0.999:

$$\ln(WG) = 6.30 + 0.71\ln(t) - 4.55/a \quad \text{for benzene} \qquad \text{(Eq. 4.5)}$$

$$\ln(WG) = 5.52 + 0.79\ln(t) - 4.07/a \quad \text{for toluene} \qquad \text{(Eq. 4.6)}$$

where WG is the weigh gain percent (%); t is the exposure time (day); and a is the activity of the target compound in organic vapors.

For commercial gasoline, the total mole fraction of aromatic compounds was approximately 0.25 or lower. Based on Eq. 4.4, the total activity of aromatic compounds in gasoline vapors should be around 0.25 or lower. With a=0.25, both Eq. 4.5 and Eq. 4.6 predict that thousands of years are needed to achieve 1% weight gain. Obviously, sorption of gasoline vapors by PVC pipe is extremely low and thus the impact of gasoline vapors on pipe material can be safely neglected, even in a long-term exposure.

Weight gains versus time for PVC samples immersed in benzene and toluene at five saturation levels (100%, 80%, 60%, 40% and 20% saturated aqueous solutions) are presented

in Figure 4.4. In comparison with the square-root-of-time relationship in pure solvents or in saturated organic vapor, the percent weight gain was linear with time in aqueous solutions. This does not mean, however, that the sorption process in aqueous solutions belonged to Case II sorption because such process was extremely slow and the exact sorption kinetics could not be resolved with the data collected in a large sampling interval (1 week). As shown in Figure 4.4, none of these sorption experiments had reached equilibrium during the 8 months of exposure, although sorption in the 100% benzene-saturated aqueous solution asymptotically approached equilibrium uptake. The sorption rate decreased dramatically as the percent of saturation (contaminant strength) was reduced. For benzene and toluene, significant sorption was found for the 100% and 80% aqueous saturation levels while the percent weight gains for 60%, 40%, and 20% saturated aqueous solutions were below 2% after 8 months of exposure. Sorption at the 20% aqueous saturated level was found to be statistically similar to that of the control experiment (deionized water sorption). This implies that sorption can be neglected for contaminant levels below 20% aqueous saturation for both toluene and benzene. Solutions at 20% aqueous saturation (toluene, benzene and TCE at 100 mg/L, 340 mg/L and 220 mg/L respectively) are considered to be a high level of environmental pollution. These concentrations are seldom encountered in the field except in close proximity to a NAPL. For water saturated with gasoline, sorption of BTEX by pipe materials should be negligible since the concentration of the dissolved BTEX is generally less than 150 mg/L (Ong et al., 2007; Cline et al., 1991).

4.3.3 Microscopic visualization test

Figure 4.5 presents the results of the moving front test for pipe samples exposed to organic vapors that were in equilibrium with neat benzene/toluene solvent and their mixtures

with NIST reference fuel. The activities of benzene/toluene in organic vapors were identical to those calculated in the gravimetric tests. Similar to the observations from the gravimetric tests, the penetration data followed apparent Fickian kinetics (linear with square root of time) with a time lag at the initial period. The growth rates of the thickness of swollen layer decreased sharply with decreasing benzene/toluene activity. No moving front was detected for benzene at an activity of 0.55 and for toluene at an activity of 0.51 (the corresponding volumetric percent in the reference fuel was 40%) within a 2.5-day exposure. These findings were consistent with those observed in liquid solvent direct exposure experiments (Ong et al., 2007), which proved that 40% volumetric percent in NIST reference fuel was insufficiently aggressive to initiate a moving front.

To predict whether a moving front would be formed after a long-term cumulative exposure to gasoline vapors, TableCurve3D 4.0 was used to fit the data obtained from the moving front testing and two empirical equations were developed:

$$\ln(TSL) = 3.08 + 0.79\ln(t) - 4.08/a \quad \text{for benzene } (R^2=0.989) \quad \text{(Eq. 4.7)}$$

$$\ln(TSL) = 3.27 + 0.84\ln(t) - 4.05/a \quad \text{for toluene } (R^2=0.989) \quad \text{(Eq. 4.8)}$$

where TSL is the thickness of swollen layer (mm) while a and t have been previously defined. Assuming the total activity of BTEX in the vapor mixture saturated with gasoline is 0.25, both Eq. 4.7 and Eq. 4.8 predict that thousands of years' exposure is needed to produce a 0.01 mm swollen layer. As demonstrated in Ong's study (2007), the formation and propagation of a moving front in the pipe matrix are the essential conditions for the occurrence of a permeation incident. Therefore, it is concluded that PVC pipe is an effective barrier to resist the permeation of gasoline vapors.

The thickness of the swollen layer versus time for aqueous saturated solutions of benzene and toluene are shown in Figure 4.6. The formation of a moving front was found to be strongly dependent on the weight gain from aqueous solution. In this study, the critical weight gain which would result in the formation of an observable moving front was estimated to be roughly 2-3%. In the 100% saturated aqueous solutions of benzene, a moving front appeared during the first two weeks of exposure. In contrast, there was an induction period for the formation of the moving front in the 100% saturated aqueous solution of toluene, mainly due to relatively low uptake of toluene. The moving front was also detected in the 80% saturated aqueous solutions once the weight gain exceeded 2%. No moving front was found in the other three solutions (60%, 40% and 20% saturated aqueous solutions) after 12 months of exposure. Since the concentration of total BTEX in gasoline-saturated water was far below those in 60% saturated solutions, PVC pipes should resist the permeation of BTEX when they are exposed to gasoline-contaminated groundwater.

As discussed above, the same conclusions were made on the basis of the data obtained from the gravimetric sorption tests and the microscopic visualization tests. It is not surprising, since sorption leads to an increase in the contaminant concentration at the polymer surface and, thus to the formation of a moving front. An increase in the contaminant sorbed would result in an increase in swelling and would promote advancement of the moving front. Figure 4.7 demonstrates the strong correlation between the two techniques by combining the data of the thickness of the swollen layer versus the corresponding weight gain as shown in Figure 4.3 and Figure 4.5. The gravimetric sorption is generally believed to be relatively simple but not obvious since it yields no direct permeation related information. If the correlation between the sorption data and the penetration data can be pre-

established, however, a simple sorption experiment can be used to approximately predict the penetration of contaminant in the pipe matrix.

4.4 Conclusion

A combination of pipe-bottle tests, gravimetric sorption tests and microscopic visualization tests were conducted to investigate the permeation of organic contaminants through PVC pipes from vapor and aqueous phases. Based on the experimental results, the following conclusions can be drawn:

(i) PVC pipes can be rapidly penetrated when exposed to saturated organic vapors of chlorinated solvents and monoaromatic compounds. The breakthrough times of TCE, benzene and toluene were found to be less than 30 days for 1-inch PVC pipes.

(ii) Chlorinated solvents and monoaromatic compounds in saturated aqueous solutions can also permeate through 1-inch PVC pipes. However, the breakthrough times in saturated aqueous solutions were much longer than those observed in pure solvents or in saturated organic vapors, mainly due to the mass transfer limitation in water solution. The breakthrough times of TCE and benzene were found to range from 60 days to 240 days, depending on the experimental mixing conditions.

(iii) Gravimetric sorption and moving front tests showed that PVC pipe was not permeated by exposure to the benzene/toluene vapors that were in equilibrium with ≤ 40% (v/v) benzene/toluene in NIST reference fuel. These tests also showed that PVC pipe was not permeated by exposure to water that is ≤ 60% of the aqueous solubility of benzene and toluene. All the evidences suggest that new PVC pipe materials are an effective barrier

against the permeation of BTEX in either gasoline-saturated vapors or gasoline-saturated water.

Acknowledgment

The authors thank the Awwa Research Fundation for its financial, technical and administrative assistance in funding and managing the project through which this information was discovered. The comments and views detailed herein may not necessarily reflect the views of the Awwa Research Fiundation, its officers, directors, affiliates, or agents.

Reference

Berens, A.R. 1985. Prediction of organic chemical permeation through PVC pipe. *Journal AWWA*, 77 (11): 57-64.

Cline, P.V., J.J. Delfino, and P.S.C. Rao. 1991. Partitioning of aromatic constituents into water from gasoline and other complex mixtures. *Environmental Science and Technology*, 25(5): 914-920.

Holsen, T.M., J.K. Park, D. Jenkins, and R.E. Selleck. 1991. Contamination of potable water by permeation of plastic pipe. *Journal AWWA*, 83(8): 53-56.

Hopfenberg, H.B.1978. The effect of film thickness and sample history on the parameters describing transport in glassy polymers. *Journal of membrane science*, 3(2):215-230.

Morrissey, P. and D.Vesely. 2000. Accurate measurement of diffusion rates of small molecules through polymers. *Polymer*, 41(5):1865-1872.

National Bureau of Standards, 1986. *Alcohols in Reference Fuel*. Standard Reference Material 1829. NBS (now NIST), Gaitbersburg, MD.

National Institute of Standards & Technology, 1988. *Lead in Reference Fuel*. Standard Reference Matherial 2712. NIST, Gaitbersburg, MD.

Ong, S.K., J.A. Gaunt, F. Mao, C.L Cheng, L.E. Agelet and C.R. Hurburgh. 2007. Impact of petroleum-based hydrocarbons on PE/PVC pipes and pipe gaskets. AwwaRF, Denver, CO.

Thompson, C. and D. Jenkins. 1987. Review of Water Industry Plastic Pipe Practices. AwwaRF, Denver, CO.

Vonk, M.W. 1985. Permeation of organic compounds through pipe materials. Publication No. 85. KIWA, Neuwegein, Netherlands.

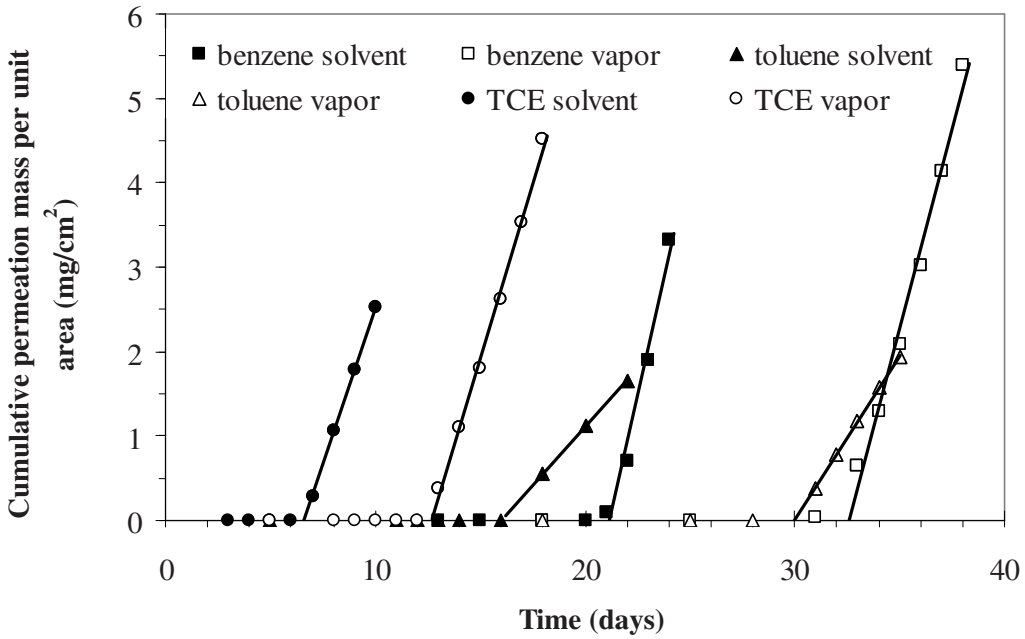

Figure 4.1 Cumulative mass permeated per unit area for 1-inch PVC pipes exposed to saturated vapor of benzene, toluene, and trichloroethylene (solvent data from Ong et al., 2007)

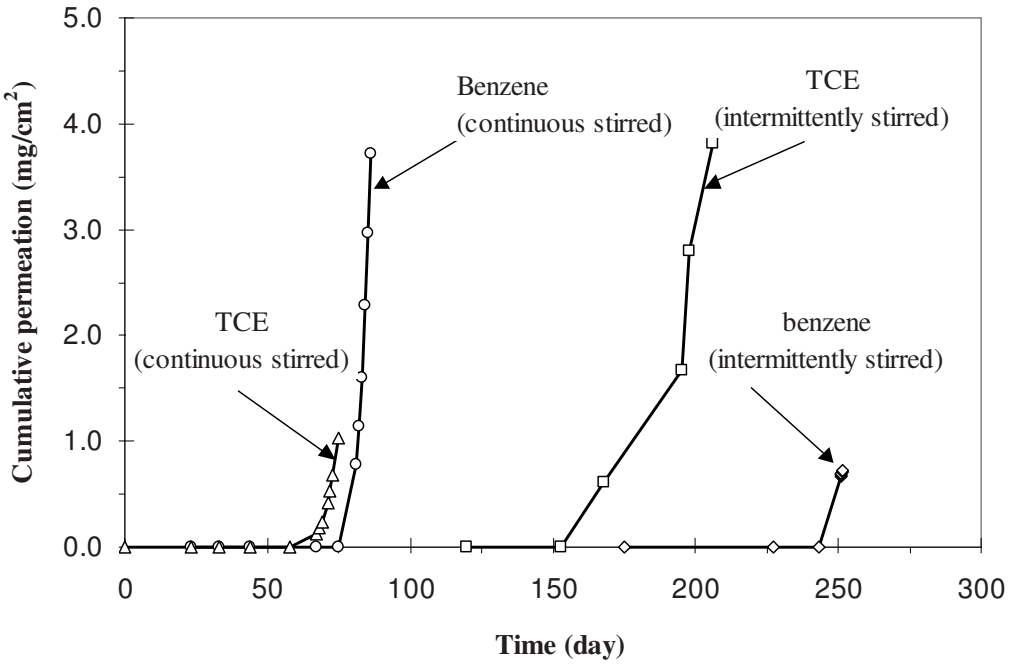

Figure 4.2 Cumulative mass of benzene and trichloroethylene permeated per unit area for 1-inch PVC pipe exposed to benzene and TCE-saturated aqueous solution

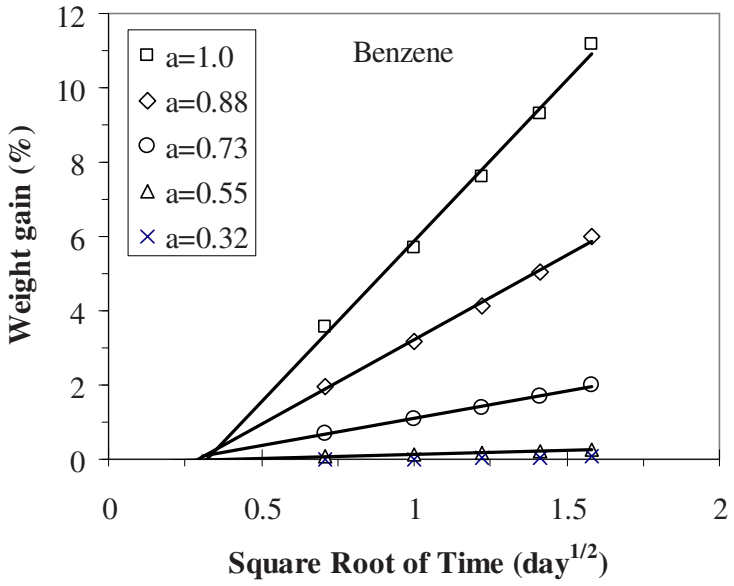

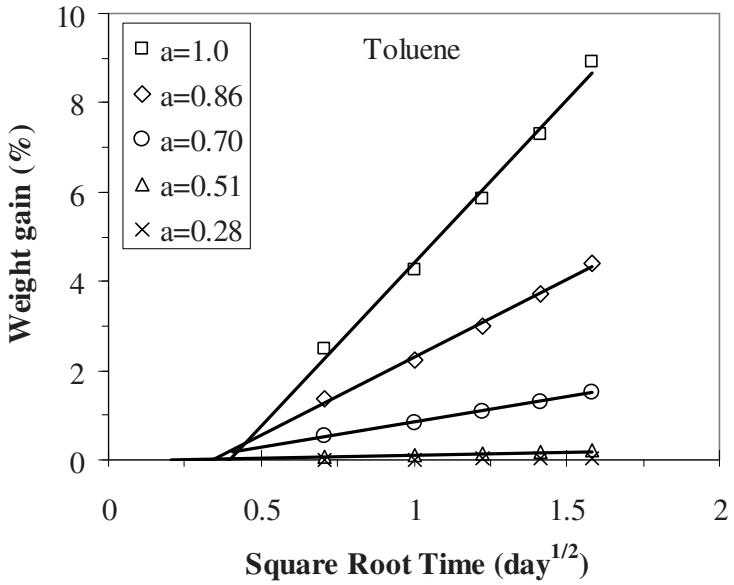

Figure 4.3 Weight gains for 1-inch PVC pipe exposed to benzene and toluene vapor (a is the activity of compound in vapor mixture, calculated from Eq. 4.4)

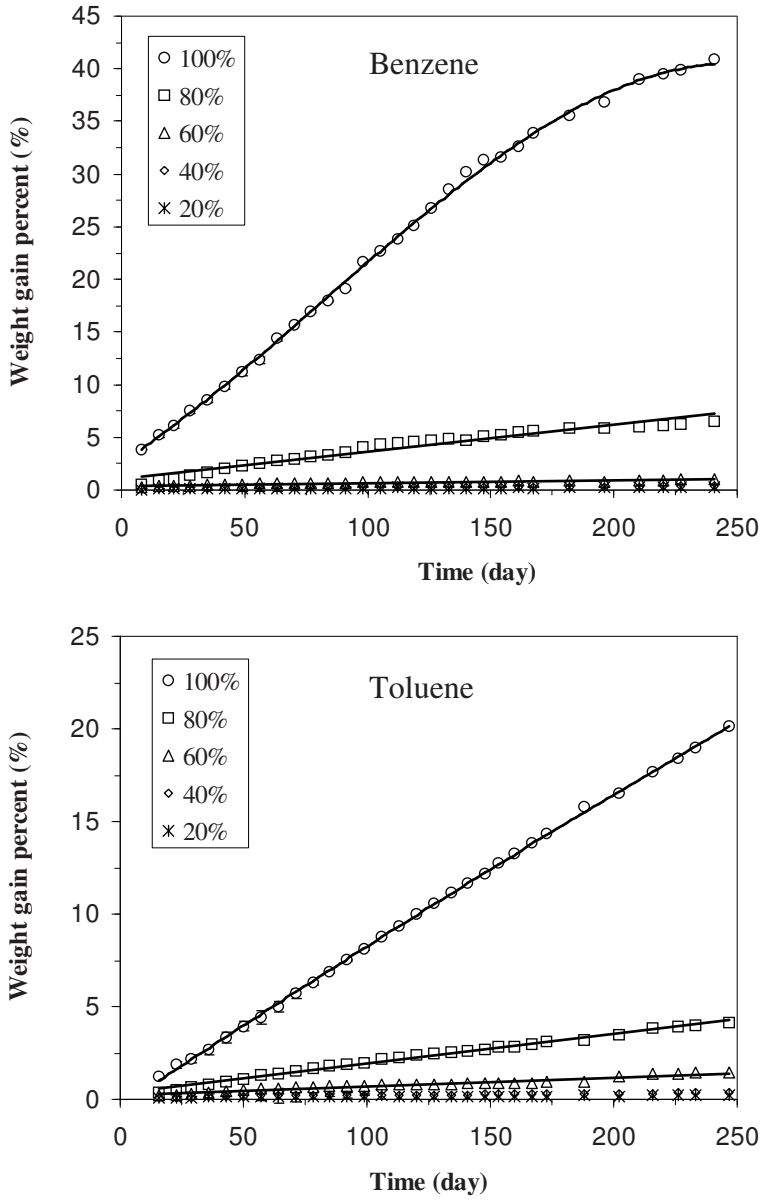

Figure 4.4 Weight gains for 1-inch PVC pipe exposed to various percent of aqueous saturated solutions of benzene and toluene

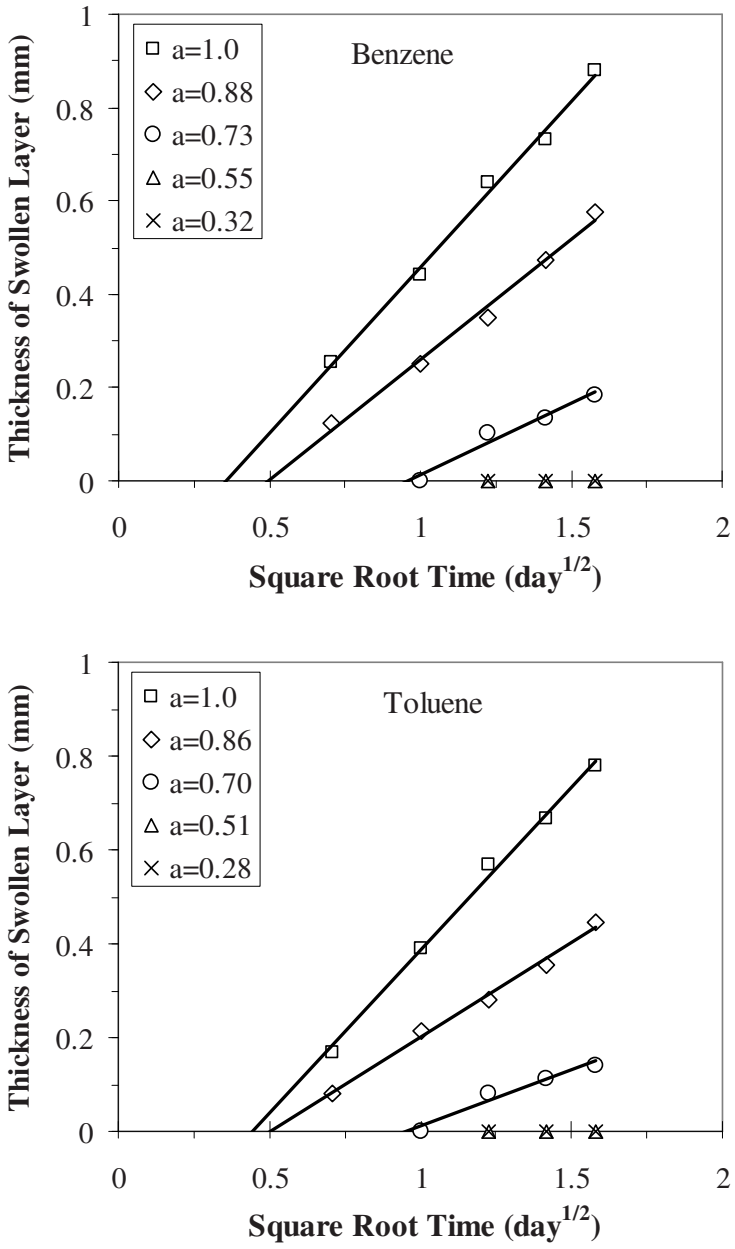

Figure 4.5 Growth of thickness of swollen layer in 1-inch PVC pipe exposed to benzene and toluene vapor (a is the activity of compound in vapor mixture, calculated from Eq. 4.4)

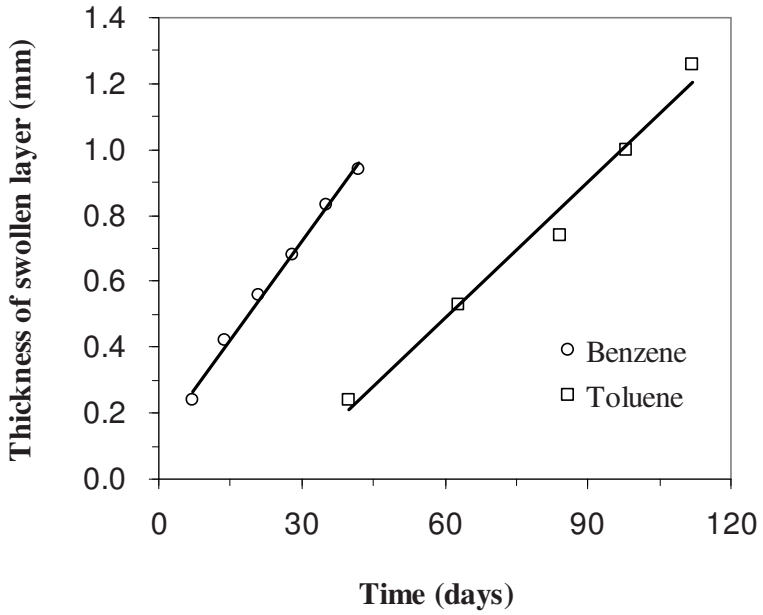

Figure 4.6 Growth of thickness of swollen layer in 1-inch PVC pipe exposed to saturated aqueous solutions of benzene and toluene

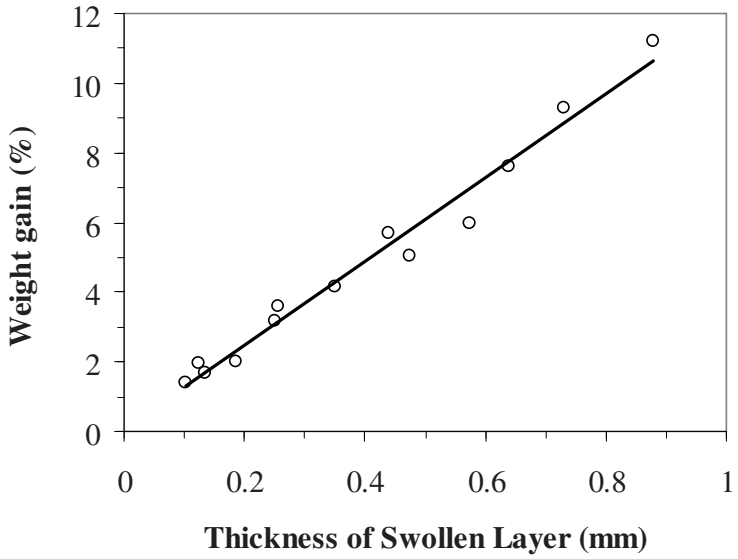

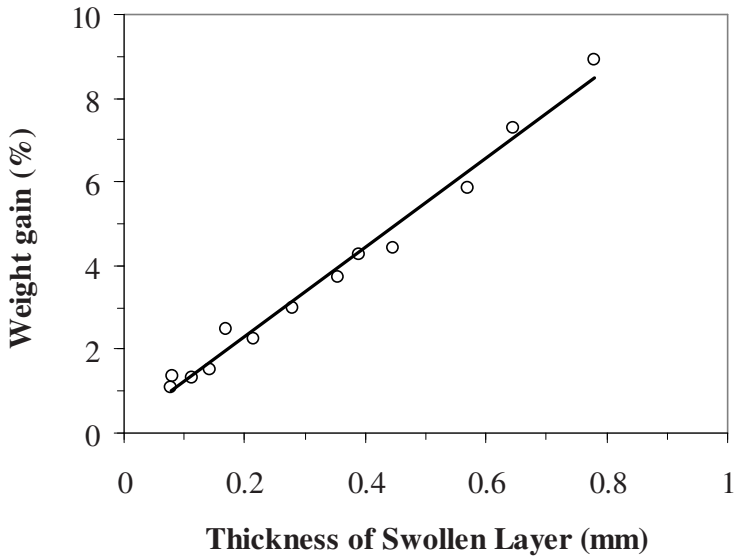

Figure 4.7 Correlation of weight gains with thickness of swollen layer for 1-inch PVC pipe exposed to benzene and toluene vapor

CHAPTER 5. PERMEATION OF PETROLEUM-BASED HYDROCARBONS THROUGH GASKETED PVC PIPES

A paper to be submitted to *Journal of American Water Works Association*

Feng Mao, James A. Gaunt, Say Kee Ong

Abstract

This study investigated the permeation of petroleum-based hydrocarbons (BTEX) through PVC pipes equipped with Rieber gasket systems by conducting pipe-drum tests as well as model simulation. Under premium gasoline-exposure conditions, benzene was the first compound detected with a breakthrough time of approximately 21 days for 2-inch PVC pipe joints. The steady-state permeation rates of benzene were found to be 0.73±0.29 mg/joint/day and 0.19±0.18 mg/joint/day for 2-inch SBR and NBR gaskets, respectively. The corresponding diffusion coefficients of benzene in SBR and NBR gaskets were determined to be 1.1×10^{-7} cm^2/s and 6.0×10^{-8} cm^2/s, respectively. No significant amounts of BTEX compounds were detected in the pipe-water for pipes using either SBR or NBR Rieber gaskets after 9 months of exposure to any level of gasoline contamination in water, even at 100% saturated. The results of model simulations demonstrated that small size pipes with gaskets were more vulnerable to permeation than large size gasketed pipes, and pressurized pipes joint systems potentially pose much higher permeation risk (two orders of magnitude) than non-pressurized joint systems.

Keywords: Rieber gasket; PVC pipe; SBR; NBR; Permeation; BTEX

5.1 Introduction

According to a national survey by Thompson and Jenkins (1987), a very large majority of the drinking water permeation incidents in U.S. were related to petroleum products in contact with plastic pipes such as polyethylene (PE), polybutylene (PB), and polyvinyl chloride (PVC). As a result, many studies have been conducted to understand the permeation of petroleum-based hydrocarbons in contaminated soils through plastic pipes (Berens 1985; Vonk 1986; Park et al. 1991; Holsen et al. 1991a, 1991b; Ong et al., 2007). Results showed that PE and PB pipes are highly permeable to gasoline while PVC pipes are essentially impermeable to typical commercial gasoline.

One percent of the reported permeation incidents were due to permeation through gasket materials as reported by Holsen et al. (1991a). Styrene-butadiene rubber (SBR) is the most common synthetic rubber used for pipe gaskets (more than 90%) due to its low cost. Nitrile (NBR), ethylene propylene diene monomer (EPDM), neoprene (CR), and fluoroelastomer rubber (FKM) are used for specific environmental applications. To ascertain the susceptibility of gaskets to permeation by gasoline, some lab studies have been conducted to investigate the permeation of benzene, toluene, ethylbenzene and xylene (BTEX) compounds through the Tyton® gaskets of ductile-iron pipes with (Glaza and Park, 1992; Ong et al, 2007). EPDM, CR and SBR gaskets were found to be susceptible to BTEX compounds when exposed to gasoline while NBR and FKM gaskets were more resistant than other types of gaskets (Glaza and Park, 1992; Ong et al, 2007). Permeation of BTEX compounds were also observed for SBR gaskets when exposed to gasoline-contaminated aqueous solutions but the breakthrough times were significantly delayed in comparison to exposure to free product gasoline (Ong et al, 2007). Based on the steady-state permeation

rates of benzene obtained from the free product gasoline exposure experiments, Ong et al. (2007) concluded that minimal flow in water mains would dilute benzene concentrations in drinking water to below the 5 µg/L MCL, even when SBR gaskets are used. This may help explain the low numbers of permeation incidents involving gaskets in comparsion to plastic pipes because gaskets are primarily used in water mains with high flows and little stagnation as compared to service connections.

In comparison to ductile iron pipes, PVC pipes are easy to install and immune to corrosion. Therefore, PVC pipes have been used increasingly as water mains (Uni-Bell, 2001). As in ductile-iron pipes, buried PVC pipelines are commonly joined through the use of an elastomeric gasket. The most widely used method for joining PVC pipes is the Rieber joint system in which the gasket is integrated into the pipe bell during the manufacturing and belling process. This Rieber joint system has been fully adopted by the PVC pipe industry in the U.S. and Canada as it offers many advantages such as high resistance to water infiltration and exfiltration, withstanding high internal pressure and vacuum, and preventing leakage when axial joint deflection takes place within allowable limits (Rahman and Alchin, 2005).

There has been scant research, however, aimed at determining the susceptibility of PVC pipes with gaskets to permeation of organic contaminants. As previously discussed above, the elastomeric gasket materials such as SBR and NBR are quite susceptible to permeation by gasoline. Therefore, from the perspective of pipe resistance to permeation, the gasket is the weak link in gasketed PVC pipes. Olson et al. (1987) reported that the PVC pipes with gaskets exhibited faster permeation compared to the unjointed (straight) pipes when exposed to pure solvents of toluene and 1,1,1-trichloroethane. However, it remains

unknown that the performance of the Rieber joint system to resist permeation of organic contaminants under typical field conditions.

The present study examined the impact of petroleum-based hydrocarbons (benzene, toluene, ethylbenzene and xylene) on PVC pipes with gaskets equipped with the Reiber gasket system. Both simulated field experimental studies as well as model simulation studies were conducted. Simulated field conditions include simulating subsurface gasoline spills and gasoline-contaminated groundwater of various levels of contamination. The results obtained from this study can be used as guidance to utilities regarding conditions under which PVC pipes with gaskets can be applied in gasoline-contaminated areas.

5.2 Materials and Methods

5.2.1 Materials

Two-inch diameter pipe systems were tested. The pipes tested were: (i) PVC pipes (SDR 21, 200 psi, Hultec S&B Technical Products) with styrene-butadiene rubber (SBR) gaskets; (ii) straight PVC pipes (SDR 21, 200 psi, Hultec S&B Technical Products); (iii) PVC pipes (IPS 1120, 200 psi, Specified Fittings) with nitrile (NBR) gaskets; and (iv) straight PVC pipes (IPS 1120, 200 psi, Specified Fittings). Two-inch diameter pipes were used as they allow for easy installation and manipulation in the experimental apparatus. Two-inch diameter SBR and NBR gaskets (both of which were not integrated into pipe joints) were also obtained from the pipe manufacturers.

Premium gasoline was purchased from a local store and the concentrations of benzene, toluene, ethylbenzene, m-xylene, and o+p-xylene (BTEX) were determined using gas chromatography to be 26.7 g/L, 106.4 g/L, 13.7 g/L, 39.4 g/L, and 38.4 g/L, respectively.

BTEX compounds were roughly about 28% by volume of the gasoline. Silica sand (Granusil 4030) was purchased from UNIMIN Corporation, Portage, WI. The sand contained very low organic matter and had a uniform particle size diameter of 0.25 mm.

5.2.2 Experimental apparatus

To simulate a buried pipe in contaminated soils, a pipe-drum apparatus was developed as shown in Figure 5.1. The apparatus consists of a 20-L drum with the gasketed PVC pipe mounted vertically through holes drilled in the lid and bottom of the drum. The ends of the pipes were capped with PVC caps and equipped with brass needle valve assemblies for filling and draining of the water in the pipes. Pipes were filled with deionized water from bottom to top and drained under gravitational force. Two holes were drilled through the drum lid and two copper tubes (influent and effluent) installed to allow aqueous gasoline-saturated solutions to be pumped with a Masterflex pump into the drum to renew the solution in the drum. All connections were sealed with Loctite® epoxy putty (Henkel Technologies, Rocky Hill, CT). Experiments were conducted at room temperature at 23 ± 1.5° C.

5.2.3 Straight PVC pipes and pipes with gaskets exposed to gasoline

Eight pipe-drum apparatuses were constructed for this test, three PVC pipes with SBR gaskets (triplicate experiment), three PVC pipes with NBR gaskets (triplicate experiment), and two straight PVC pipes as controls. To prepare a pipe-drum apparatus, silica sand was placed into the apparatus until the drum was nearly full. Premium gasoline was then added until a visible liquid level of gasoline appeared above the surface of the sand. The lid was secured to the pail with the lever-locks, minimizing the volatilization of gasoline.

The PVC pipes were filled with deionized water with zero headspace. Pipe-water was removed each week to analyze the BTEX compounds by gas chromatography. After each sampling event, the pipe was flushed with deionized water three times immediately before fresh deionized water was added and the needle valves closed.

5.2.4 PVC pipes with gaskets exposed to gasoline-contaminated water

To prepare gasoline-saturated water, a mixture of 1 L premium gasoline and 10 L deionized water was moderately stirred with a magnetic stirrer in a glass bottle for 48 hours. Several preliminary experiments indicated that a mixing time of 48 hours was sufficient to produce a saturated gasoline solution. The concentration of the dissolved BTEX was around 150 mg/L which was slightly higher than the average concentration of 135 mg/L reported by Cline et al. (1991) for water saturated with various grades of gasoline. Benzene and toluene were the major aromatic compounds in the aqueous phase, accounting for nearly 90% of total BTEX. Three aqueous solutions of varying concentrations (75%, 50%, and 10% saturated aqueous solutions of gasoline) were prepared by diluting the stock solution with deionized water at appropriate ratios. In the experiments, a prepared gasoline solution was introduced into the drum through the copper tubes from bottom to top, using a Masterflex pump, until the drum was full. The aqueous solutions in the drum were replaced with fresh aqueous gasoline solutions each month to maintain relatively constant exposure concentrations. BTEX concentrations in the drum were periodically analyzed.

5.2.5 Analysis for BTEX water samples.

BTEX in water samples were determined using a gas chromatograph (Tracor 540, Tracor Instruments Austin, Inc., Austin TX) equipped with a packed column (1.8 m × 2 mm;

1% SP1000 on 60/80 mesh Carbopack B), a photoionization detector, and an automated purge and trap concentrator (Tekmar LSC2/ALS). The detection limits for benzene, toluene, ethylbenzene, m-xylene and o+p-xylene were 0.24µg/L, 0.24µg/L, 0.26µg/L, 0.29µg/L and 0.53µg/L, respectively.

5.2.6 Equilibrium sorption testing for gaskets

As a supplement test for the pipe-drum tests, sorption experiments were conducted for 2-inch SBR gaskets and NBR gaskets by exposure to free product gasoline and gasoline-saturated aqueous solution. In gasoline sorption experiments, gaskets were immersed in 500 mL of the premium gasoline in a 1-L glass jar with a Teflon-lined lid. The gaskets were removed at hourly intervals, wiped dry with paper towels, and weighed using an analytical balance with an accuracy of 0.001 g. The specimens were returned to the jars immediately after weighing. The samples were weighed until constant weight was reached. In aqueous sorption experiments, the gasoline-saturated aqueous solution was transferred into a 1-L glass jar and the tested gaskets were then immersed in the solution. In attempt to maintain the saturation condition, the aqueous solution was covered by 50 mL premium gasoline and continuously stirred by a magnetic stirrer. Prior to measuring the weight of gaskets during the experimental period, the glass jar was opened in a fume hood and the gasoline film on the surface was allowed to evaporate. After weighing, the samples were re-immersed in freshly prepared gasoline-saturated aqueous solution and covered by 50 mL premium gasoline. All sorption experiments were conducted in triplicate at room temperature at 23 ± 1.5^{o} C.

5.3 Results and Discussion

5.3.1 Equilibrium sorption tests for gaskets

The results of sorption tests for 2-inch SBR and NBR gaskets in gasoline and gasoline-saturated aqueous solution are presented in Figure 5.2. In gasoline, sorption equilibrium was rapidly achieved within 24 hours for both types of gaskets. The equilibrium weight gains for SBR and NBR gaskets were 102.3±5.6% and 77.6±1.1% of their original mass, respectively. It is interesting to note that the NBR materials used in the present study differed from the NBR rubber of Tyton® gaskets used in ductile iron pipe, as the weight gain found for Tyton® NBR gaskets was only 24% (Ong et al., 2007). In comparison to sorption in gasoline, the sorption in gasoline-saturated aqueous solution was extremely slow. None of the sorption experiments using gasoline-saturated aqueous solution had reached equilibrium during the experimental period of nearly 80 days. The difference in sorption rates under the two exposure conditions may be due to the mass transfer limitations occurred in aqueous experiments. In aqueous solution, the sorption of BTEX by gaskets is not only dependent on the interaction between organic chemicals and polymer materials but also on the effective availability of the compounds for sorption. It is likely that BTEX sorption by the elastomeric materials is faster than either the dissolution of gasoline into aqueous phase or the movement of the organic chemical through the "stagnant water film" surrounding the outer surface of gaskets.

5.3.2 PVC pipes with SBR gaskets exposed to gasoline

The cumulative permeated masses of BTEX compounds over time are plotted in Figure 5.3. The triplicate experiments (SBR1, SBR2 and SBR3) demonstrated that the

permeation of BTEX through PVC pipes with SBR gaskets was rapid when exposed to premium gasoline. Of the five compounds of interest, benzene was the first compound detected with a breakthrough time of about 21 days. When breakthrough occurred, the level of benzene in the pipe-water immediately exceeded the maximum contaminant level (MCL) of 5 μg/L. Toluene breakthrough lagged slightly behind that of benzene, while ethylbenzene and xylene were detected later at about 50 days and at much lower concentrations. Benzene and toluene accounted for 85 - 90% of the entire total BTEX that permeated into the pipe-water. This is mainly due to the higher solubility of benzene in water and the higher mass fraction of toluene in gasoline. Similar permeation behavior for BTEX (i.e., the order of breakthrough time and the relative permeation rate) was found for the permeation of premium gasoline in PE pipes (Ong et al., 2007) and ductile iron pipe joints (Glaza and Park, 1992; Ong et al, 2007).

The results of the triplicate tests indicated that the cumulative mass of BTEX permeated varied for the three pipes with gaskets under the same exposure conditions. The steady state permeation rates for benzene for SBR1, SBR2 and SBR3 were estimated to be 0.43, 0.76, and 1.0 mg/joint/day, respectively. The corresponding permeation rates for toluene were 0.45 mg/joint/day, 1.1 mg/joint/day and 1.3 mg/joint/day, respectively. Overall, the estimated permeation rates for SBR2 and SBR3 were similar to each other but the permeation rate for SBR1 was relatively lower. Factors resulting in the variability of permeated mass will be discussed later.

5.3.3 PVC pipes with NBR gaskets exposed to gasoline

The cumulative permeated masses of BTEX permeated through NBR gaskets versus time are plotted in Figure 5.4. The triplicate experiments (NBR1, NBR2 and NBR3)

demonstrated that permeation of BTEX through pipes with NBR gaskets was rapid when exposed to premium gasoline. The breakthrough time for benzene was 21 days. These results were different from the results for ductile iron pipes with NBR gaskets which showed NBR gaskets were more resistant to gasoline permeation than SBR gaskets (Ong et al, 2007). This may be due to the fact that NBR materials for PVC pipes and ductile iron pipes were not identical in their compounding or their permeation properties, as shown in the previous equilibrium sorption tests.

The results of the triplicate tests for NBR gaskets also indicated that the mass permeated varied for the three pipes with NBR gaskets under the same exposure conditions. The steady state permeation rates for benzene for NBR1, NBR2 and NBR3 were estimated to be 0.22, 0.0008, and 0.34 mg/joint/day, respectively. The corresponding permeation rates for toluene were 0.56, 0.0008 and 0.56 mg/joint/day, respectively. Overall, the estimated permeation rates for NBR1 and NBR3 were similar to each other. The mass permeated for NBR2 was characterized by a constant but extremely low permeation rate.

5.3.4 Straight PVC pipes exposed to gasoline

As expected, no BTEX compounds were detected in the pipe water of the PVC pipe control experiments after 9 months of exposure.

5.3.5 PVC pipes with gaskets exposed to gasoline-contaminated water

No significant amounts of BTEX compounds were detected in the pipe-water for pipes using either SBR or NBR Rieber gaskets after 9 months of exposure to any level of gasoline contamination in water, even at 100% saturated. The concentrations of BTEX in many pipe water-samples were below the detection limits. In some pipe water samples,

benzene and toluene were detected but the concentrations were extremely low (less than the MCL of benzene, 5 μg/L) and no permeation rate could be determined. It is concluded that the MCL for benzene will not be exceeded for any level of gasoline contamination in groundwater for at least 9 months of exposure.

5.3.6 Discussion of permeation process in PVC pipes with gaskets

Figure 5.5 shows the cross section of a pipe joint with a Rieber gasket. Permeation of contaminants through the PVC pipe joint may be perceived as involving three processes: (i) contaminants in the environmental media diffuse/move through the gap between the bell and the spigot of the pipe joints to reach the gasket; (ii) contaminants then diffuse through the gasket material; and (iii) the contaminants diffuse/move through the gap between the bell and the spigot of the pressure pipe joints to the pipe water. Therefore, the permeation of contaminants through pipe joints is not only dependent on the properties of gasket materials but also on the size of gap between the bell and the spigot. Generally, the gap size varies from joint to joint, mainly due to the axial joint deflection within allowable limits. Moreover, during the assembly of pipe joints, lubricant is applied to the spigot and the lubricated spigot is then pushed past the gasket into the bell. For the pipe joint shown in Figure 5.5, significant amounts of lubricant were found to occupy the empty space between the gasket and the spigot. The lubricant may affect the permeation of contaminants through the pipe joints by either covering the exposure area of gasket or providing another pathway for diffusion or a medium for sorption of the petroleum hydrocarbons. The effect of gap size and the amount of lubricant may account for the discrepancy detected in the testing of triplicate samples reported above.

5.4 Model Simulation

The experimental studies described above estimated permeation rates of benzene and toluene through 2-inch diameter SBR and NBR Rieber joint systems by exposure to free product gasoline. However, some critical issues related to gasket permeation have remained unknown. First, the traditional time-lag method is unable to estimate the diffusion coefficients of benzene and toluene under the experimental conditions because the geometry of gaskets is irregular and the uncertainty with respect to the length of the pathway. Another issue is the scale-up of permeation in PVC pipes with Rieber gaskets, i.e., using available 2-inch permeation data to estimate and evaluate the permeation risks for gaskets with varied dimensions (sizes). Furthermore, the experimental studies were conducted for Rieber joints in nonpressurized systems, and it is likely the data obtained may not accurately reflect the permeation behavior of contaminants in pressurized systems, where Rieber joints are exposed to internal hydrostatic pressure when they are in operation.

To gain the insights into the permeation process of organic contaminants through Rieber joints, model simulation studies were performed using FEMLAB 3.1 (COMSOL), a modeling software package for simulation of a multi-physics process. More specifically, these studies were aimed (i) to fit the measured permeation data to the diffusion model to determine the diffusion coefficients of contamiants; (ii) to estimate the steady-state permeation flux of contaminants into larger size gaskets; and (iii) to predict the permeation behavior of contaminants in pressurized Rieber joint systems.

To simplify the complexity of the permeation process in pipe joints, the model simulations focused on the permeation of contaminants through elastomeric materials and neglect the impact of lubricants and the size of gap between bell and spigot on contaminant

transport. The experimental data for SBR 3 and NBR 3 were selected as the data to be modeled since they exhibited the maximum permeation rates of benzene and toluene detected in triplicate experiments.

5.4.1 Geometry and boundary conditions

Figure 5.6 shows the geometry of the cross section of a nonpressurized Riebert joint. The elastomer (SD1-see Figure 5.6) is compressed between the bell and the spigot so that several sealing zones are formed (B2, B4, B6, B8 and B9). The elastomer is also reinforced with an internal steel ring, producing an impermeable boundary B7 and subdomain SD2. Moreover, there is an air zone (SD3) that fills the space between the elastomer and the spigot. The external contaminants permeate through the elastomer from B1 (the surface exposed to external contaminants) to B5 (the surface in contact with pipe water) and subsequently enter the drinking water.

The diffusion process of organic contaminants through elastomeric materials can be described by the classic Fickian diffusion equation:

$$\frac{\partial C}{\partial t} + \nabla(-D_e \nabla C) = 0 \qquad \text{(Eq. 5.1)}$$

where D_e is the diffusion coefficient of contaminants in the elastomer. In the present study, this is an unknown parameters to be determined later.

In the experimental studies, the total quantity of benzene and toluene diffusing into a 2-inch PVC pipes with gaskets as a function of time, Q_t, were measured under relatively strict conditions: (i) the outer concentrations of contaminants remained relatively constant (C_0); (ii) the initial concentrations of contaminants in the elastomer were zero; and (iii) the

inner concentrations of contaminants were kept at nearly zero. Therefore, the initial and boundary conditions of the diffusive model were:

$$\begin{aligned} &t < 0,\ \text{elastomer area}, C = 0; \\ &t \geq 0, \text{boundary B1}, C = C_0; \\ &t \geq 0, \text{boundary B5}, C = 0; \\ &t \geq 0, \text{boundary B3}, D_e \nabla C = D_a \nabla C; \\ &t \geq 0, \text{boundary B2, B4, B6, B7, B8 and B9}, \nabla C = 0. \end{aligned} \qquad \text{(Eq. 5.2)}$$

where D_a were the diffusion coefficients of contaminants in the air zone (SD3). Here, D_a for benzene and toluene were set to 0.096 cm^2/s and 0.088 cm^2/s, respectively (Schwarzenbach et al. 1993).

The constant outer concentrations of benzene and toluene (C_0) were calculated on the basis of the results of equilibrium sorption tests. Assuming B5 was instantaneously saturated with gasoline when the surface was exposed to gasoline, C_0 can be assumed to be the concentration of benzene or toluene in a whole elastomer which is equilibrated with gasoline. For a SBR gasket with a volume of 13 cm^3 and a NBR gasket with a volume of 11.2 cm^3, the corresponding equilibrium weight gain was 13.6 mg and 11.6 mg, respectively. Assuming the weight gains were due to the sorption of BTEX by elastometric materials and the fractions of BTEX in the elastomer were equal to those in gasoline, the equilibrium concentrations of benzene and toluene in a SBR gasket were estimated to be 120 mg/cm^3 and 500 mg/cm^3, respectively. The corresponding concentrations in a NBR gasket were 114 mg/cm^3 and 474 mg/cm^3, respectively.

5.4.2 Determination of diffusion coefficients of benzene and toluene in gaskets

The diffusion coefficients of benzene and toluene were initially given a value and then adjusted through several trials until the observed data points matched the theoretical

permeation curve. These relatively rough adjustments generally yielded a small range of diffusion coefficients. Within this range, fine adjustments were made and the least-square method was applied to determine the diffusion coefficient of benzene and toluene that led to the "best fit".

As shown in Figure 5.7, the measured data were well fitted by the Fickian diffusion model. The predicted curve captured the main characteristics of experimental data, showing that there was a transient state from contaminants first entered the pipes until the steady state of flux was established. Moreover, with an appropriate diffusion coefficient, the amount of permeated contaminant as a function of time can be well estimated. The diffusion coefficients of benzene and toluene in SBR gaskets were estimated to be 1.1×10^{-7} cm^2/s and 6×10^{-8} cm^2/s, respectively (SSEs were 244 mg^2 and 42 mg^2, respectively). The corresponding diffusion coefficients in NBR gaskets were 6×10^{-8} cm^2/s and 4×10^{-8} cm^2/s, respectively (SSEs were 33 mg^2 and 89 mg^2, respectively). These diffusion coefficients were 4~10 times higher than those found for PE pipes exposed to gasoline (Ong et al., 2007). It appeared that SBR or NBR gaskets are more permeable than PE pipes under identical exposure conditions.

5.4.3 Scale-up of permeation in PVC pipes with Rieber gaskets

The permeation of organic molecules through polymer materials is dependent on the chemical characteristics and concentration (activity) of the contaminant, the chemical characteristics of the polymer, and the interactions between the contaminant and the polymer. Given the same gasket materials and the same exposure conditions, therefore, the diffusion coefficients obtained from 2-inch gaskets are valid for other gasket sizes. The problem is then reduced to that of the effects of the gasket size on permeation. Increasing the gasket

size will enlarge the interface area of gasket-pipe water but reduce the permeation flux (mass per unit area per time) due to the increase in the length of the diffusion path. Therefore, the net impacts of the gasket size on the total permeation mass after a certain exposure time will depend on which effect is the dominating factor.

Table 5.1 lists the scale-up parameters and the modeled steady-state permeation fluxes (mass per unit area per time) and permeation rates (mass per joint per time) of benzene for different diameter SBR gaskets. As shown in Table 5.1, the ratio of the height of the gasket cross section to its width are essentially identical for all gaskets, indicating that all cross sections are congruent. The scale-up factors for varied-size gaskets were calculated using the width (or height) of the cross section of 2-inch gasket as the reference length. These scale-up factors were then applied to the diffusion model and the corresponding steady-state permeation fluxes for varied-size SBR gaskets were estimated under the identical diffusion coefficient and boundary conditions that have previously described. With the known surface area of the interface of gasket-pipe water, the permeation rates were further estimated.

As shown in Table 5.1, the permeation rate can be estimated for any size gasket by using permeation data experimentally determined from 2-inch gaskets and the ratio of pipe outer diameters. It is not surprising, since theoretically the permeation rate for any size gasket can be calculated by:

$$P = -D_e \frac{\Delta c}{l_d} \{\pi (OD) l_e\} \qquad \text{(Eq. 5.3)}$$

where P is the steady-state permeation rate of benzene (mg/joint/day); l_d is the length of the diffusion pathway (cm); OD is the outer diameter of pipe (cm); and l_e is the short interface

length of gasket-pipe water (cm), referring to the length of B5 as shown in Figure 5.6. Defining l_d and l_e for 2-inch gasket as $l_{d,1}$ and $l_{e,1}$, respectively, and assuming l_d and l_e for a certain size gasket were directly proportional to the scaling factor (SF) of the gasket, the equation becomes:

$$P = -D_e \frac{\Delta C}{l_{d,1} SF}\{\pi(OD) l_{e,1} SF\} = -D_e \frac{\Delta C}{l_{d,1}}\{\pi(OD) l_{e,1}\} \qquad \text{(Eq. 5.4)}$$

Defining P and OD for 2-inch gasket as P_1 and OD_1, respectively, and rearranging:

$$P = -D_e \frac{\Delta C}{l_{d,1}}\{\pi(OD_1) l_{e,1}\}\frac{OD}{OD_1} = P_1 \frac{OD}{OD_1} \qquad \text{(Eq 5.5)}$$

The steady-state permeation rates of benzene presented above can be used to predict the concentration of benzene in the pipe water after a period of stagnation:

$$C_{pw} = \frac{M}{V} = \frac{nPt}{\frac{1}{4}\pi(ID)^2 L} \qquad \text{(Eq. 5.6)}$$

where C_{pw} is the benzene concentration in pipe water (mg/cm^3); M is the total mass of permeated contaminant (µg); V is the volume of water in the pipe (L); n is the number of pipe joints; t is the period of stagnation (days); L is length of contaminated pipelines (cm); and ID is inside diameter of pipe (cm). Assuming a scenario of 100 ft of PVC pipeline with 5 gasketed joints that is exposed to free product gasoline, the concentrations of benzene that might result from 8 hours of water stagnation are presented in Figure 5.8. As shown in Figure 5.8, the benzene MCL of 5 µg/L would be exceeded in the pipe water for all size pipes with SBR gaskets. Same approach was used to scale up the permeation rate of benzene for NBR gaskets. It was found that the benzene MCL would be exceeded for a 10-inch or smaller size PVC pipe with NBR Rieber gaskets under the identical stagnation and exposure conditions.

Under normal conditions, water flows in the pipes and the benzene concentration depends on the flow rate. In this case, assuming a continuous, full-pipe flow and complete mixing of permeated benzene in the pipe water, the concentration of the benzene in the pipe water (C_{pw}) can be estimated by:

$$C_{pw} = \frac{M}{V} = \frac{nPt}{qt} = \frac{nP}{q} \qquad \text{(Eq. 5.7)}$$

where q is the water flow (cm^3/day). Typically, the average water flow velocity for pressure PVC pipes ranges from 0.6 m/s to 3.1 m/s (Uni-Bell 2001). This corresponds to a flow rate of 7.9×10^7 to 4.0×10^8 cm^3/day for 2 inch pipe. Under the worst-case scenario (the smallest flow rate), the calculated C_{pw} would be 0.07 μg/L for 100 ft of 2-inch PVC pipeline with 5 SBR gasketed joints. It is expected that C_{pw} will be lower than 0.07 μg/L for larger size pipes because of the increase of flow rates. Due to the effect of dilution, therefore, the concentration of benzene in PVC pipes with gaskets with a minimal water flow would not exceed the MCL.

5.4.4 Permeation of organic contaminants in pressurized Rieber joint systems

As shown in Figure 5.9, hydrostatic pressure in pressurized Rieber joint systems pushes the gasket forward/out within the gasket groove, forming new sealing zones (Rahman, 2007). Model simulation studies were conducted for pressurized Rieber joint systems under the following initial and boundary conditions:

$$\begin{aligned}
&t < 0,\ \text{elastomer area}, C = 0;\\
&t \geq 0, \text{boundary B1}, C = C_0;\\
&t \geq 0, \text{boundary B5, B7, B8}, C = 0;\\
&t \geq 0, \text{boundary B6}, D_e \nabla C = D_a \nabla C;\\
&t \geq 0, \text{boundary B2, B3, B4, B9 and B10}, \nabla C = 0
\end{aligned} \qquad \text{(Eq. 5.8)}$$

The selected values of C_0, D_e and D_a were identical to those in non-pressurized SBR systems. Figure 5.10 sketches the diffusion pathways of benzene in both non-pressurized and pressurized Rieber joint systems. In the non-pressurized system, benzene diffuse into pipe water through an extremely narrow gasket-water interface area since most of the outer surface of the gasket is directly in contact with the internal wall of the pipe bell. In the pressurized system, however, hydraulic pressure "opens" several insulation boundaries. This significantly expands the gasket-water interface area as well as shortens the diffusion pathway of benzene, promoting the permeation of benzene into pipe water. Therefore, it is of great interest to quantitively compare the permeation rate of benzene for two types of SBR Rieber joint systems under the identical gasoline exposure conditions.

Theoretically, the permeation fluxes of benzene (mass per unit area per time) through the interface of gasket-pipe water are different from location to location because of the difference in the length of the diffusion pathway. To estimate the permeation flux of benzene, the boundaries of B5, B7 and B8 were divided into 19 short segments by 20 points, PM 1 to PM 20 as shown in Figure 5.11. It was found that the steady-state permeation flux of benzene ranged from 0 to 3.4×10^{-6} mg/(cm^2·s), from 0 to 7.8×10^{-6} mg/(cm^2·s), and from 7.8×10^{-6} to 2.5×10^{-5} mg/(cm^2·s) through B5 (PM 17-20), B7 (PM 7-17) and B8 (PM 1-7), respectively. As indicated, benzene molecules "prefer" to move along the pathways from B1 to B8 because these pathways have a relatively short diffusion distance. On the contrary, insignificant permeation flux was detected through PM16-17 and PM17-18, mainly due to the fact that benzene molecules need to diffuse along the longest pathways until reach such boundaries.

The total cumulative permeation mass of benzene through a 2-inch pressurized SBR gasket was estimated based on the following assumptions: (i) the permeation flux of benzene was uniform within any segment; (ii) the interface area of gasket-pipe water for any segment can be approximately estimated by the length of the segment and the pipe perimeter, and (iii) the cumulative permeation mass for the 19 segments was additive. Figure 5.12 shows the modeled permeation curves for the pressurized joint system versus the non-pressurized joint system. The steady-state permeate rate of benzene in the pressurized system was around 100 mg/joint/day, nearly two orders of magnitude higher than that of the non-pressurized system. Using the approach previously described, the benzene concentration in pipe water resulting from 8 hours of water stagnation would be as high as 3.8 mg/L. Under a continuous full pipe flow with a flow velocity of 0.6 m/s, the calculated benzene concentration in pipe water would be 7 μg/L, slightly higher than the benzene MCL of 5 μg/L. The results of the model simulation indicated that pressurized joint systems potentially pose much higher permeation risk (about two orders of magnitude higher) to threaten the safety of drinking water than non-pressurized joint systems.

A significant concern is whether the MCL of 5 μg/L for benzene would be exceeded when a pressurized pipe joint system is exposed to gasoline-contaminated water solutions. Due to the lack of the permeation data, modeling the diffusion process of benzene from the aqueous phase through gaskets becomes impossible. However, the relative magnitude (R_{PM}) of the permeation rate for pressurized and non-pressurized pipe joint systems under an identical exposure condition still can be evaluated by:

$$R_{PM} = \frac{P_p}{P_{np}} = \frac{-D_e \frac{\Delta c}{l_{d,p}} S_p}{-D_e \frac{\Delta c}{l_{d,np}} S_{np}} = \frac{\frac{S_p}{l_{d,p}}}{\frac{S_{np}}{l_{d,np}}} \qquad \text{(Eq. 5.9)}$$

where P_p and P_{np} are the steady-state permeation rate of benzene for a pressurized pipe joint and a non-pressurized pipe joint, respectively; $l_{d,p}$ and $l_{d,np}$ are corresponding length of the diffusion pathway, respectively; and S_p and S_{np} are corresponding surface area of the gasket-water interface, respectively. As indicated in Eq. 5.9, the value of R_{PM} is independent of the exposure condition, assuming the exposure condition would not change the geometry of gaskets (this assumption is very likely since the gaskets are confined in the gap between the bell and the spigot of pipe joints). In other words, R_{PM} under the exposure of gasoline-contaminated water solutions is equal to that under the exposure of free-product gasoline. Therefore, under an identical aqueous exposure condition, the permeation rate of benzene in a pressurized pipe joint system would be two orders of magnitude higher than a non-pressurized system.

As previously described, no significant amounts of BTEX compounds were detected in the pipe-water for non-pressurized 2-inch pipe joints after 9 months of exposure to any level of gasoline contamination in water, even at 100% saturated. In some pipe-water samples collected at a 14-day interval, benzene and toluene were detected but the concentrations of benzene were less than the MCL of 5 µg/L. It indicates that, under the exposure of gasoline-contaminated water solutions, the permeation rate of benzene for a 2-inch non-pressurized pipe joint system would not exceed 0.44 µg/day/joint. Thus, the

corresponding permeation rate would not exceed 44 μg/day/joint if the pipe joint were pressurized. Assuming a scenario of 100 ft of PVC pipeline with 5 gasketed pressurized pipe joints that is exposed to gasoline-contaminated water solutions, the concentrations of benzene that might result from 8 hours of water stagnation would be less than 1.7 μg/L. This suggests that the no level of gasoline contamination in groundwater will cause the benzene MCL to be exceeded in pressurized PVC pipes with SBR or NBR gaskets.

5.5 Conclusion

Pipe-drum tests were conducted to investigate the permeation of BTEX compounds through 2-inch PVC pipes with Reiber gaskets under simulated field conditions. Model simulation studies were further conducted to estimate the diffusion coefficients of benzene and toluene in gaskets under experimental conditions, to estimate the permeation rates of benzene for larger size gaskets, and to predict the permeation behavior of benzene in pressurized Rieber joint systems. Based on the analysis of the results of experiments and simulations, the following conclusions can be drawn:

(i) In comparison with straight PVC pipes, PVC pipes with gaskets are much more vulnerable to permeation.

(ii) Under premium gasoline-exposure conditions, the steady-state permeation rates of benzene were found to be 0.73±0.29 mg/joint/day and 0.19±0.18 mg/joint/day for 2-inch SBR and NBR gaskets, respectively. The corresponding diffusion coefficients of benzene in SBR and NBR gaskets were determined to be 1.1×10^{-7}cm^2/s and 6.0×10^{-8}cm^2/s, respectively.

(iii) For non-pressurized pipe joint systems, the benzene MCL will likely be exceeded during an 8 hour stagnation period for a 12-inch or smaller size PVC pipe with SBR Rieber

gaskets in contact with premium gasoline. The benzene MCL would be exceeded for a 10-inch or smaller size PVC pipe with NBR Rieber gaskets under the identical stagnation and exposure conditions. Under conditions of continuous full pipe flow, the MCL will not be exceeded, provided that there is at least a minimal flow of water in the main.

(iv) Pressurized joint systems potentially pose much higher permeation risk (about two orders of magnitude higher) to threaten the safety of drinking water than non-pressurized joint systems. However, no level of gasoline contamination in groundwater will cause the benzene MCL to be exceeded in pressurized PVC pipes with SBR or NBR gaskets.

Acknowledgment

The authors thank the Awwa Research Fundation for its financial, technical and administrative assistance in funding and managing the project through which this information was discovered. The comments and views detailed herein may not necessarily reflect the views of the Awwa Research Fiundation, its officers, directors, affiliates, or agents.

Reference

Cline, P.V., J.J. Delfino, and P.S.C. Rao. 1991. Partitioning of aromatic constituents into water from gasoline and other complex mixtures. *Environmental Science and Technology*, 25(5): 914-920.

Glaza, E.C. and J.K. Park. 1992. Permeation of organic contaminants through gasketed pipe joints. *Journal AWWA*, 84(7): 92-100.

Holsen, T. M., J. K. Park, D. Jenkins, and R.E. Selleck. 1991. Contamination of potable water by permeation of plastic pipe. *Journal AWWA*, 83(8): 53-56.

Olson, A.J., D.Goodman and J.P. Pfau. 1987. Evaluation of permeation of organic solvents through PVC, asbestos/cement, and ductile iron pipes. *Journal of Vinyl and Additive Technology*, 9(3): 114-118.

Ong, S.K., J.A. Gaunt, F. Mao , C.L Cheng, L.E. Agelet and C.R. Hurburgh. 2007. Impact of petroleum-based hydrocarbons on PE/PVC pipes and pipe gaskets. AwwaRF, Denver, CO.

Rahman, S. and N. Alchin. 2005. Riebert joint system for PVC Pipe: synopsis of a locked-In elastomeric gasket. In *Proc. Pipe 2005 Conference*. Wagga, NSW, Australia.

Rahman, S. 2007. Sealing our buried lifelines [Opflow Online]. www.awwa.org/communications/opflow

Schwarzenbach, R.P., P.M. Gschwend, and D.M. Imboden. 1993. Environmental Organic Chemistry. Wiley and Sons, New York.

Thompson, C. and D. Jenkins. 1987. Review of water industry plastic pipe practices. AwwaRF, Denver, CO.

Uni-Bell. 2001. Handbook of PVC Pipe Design and Construction. Uni-Bell PVC Pipe Association, Dallas, TX.

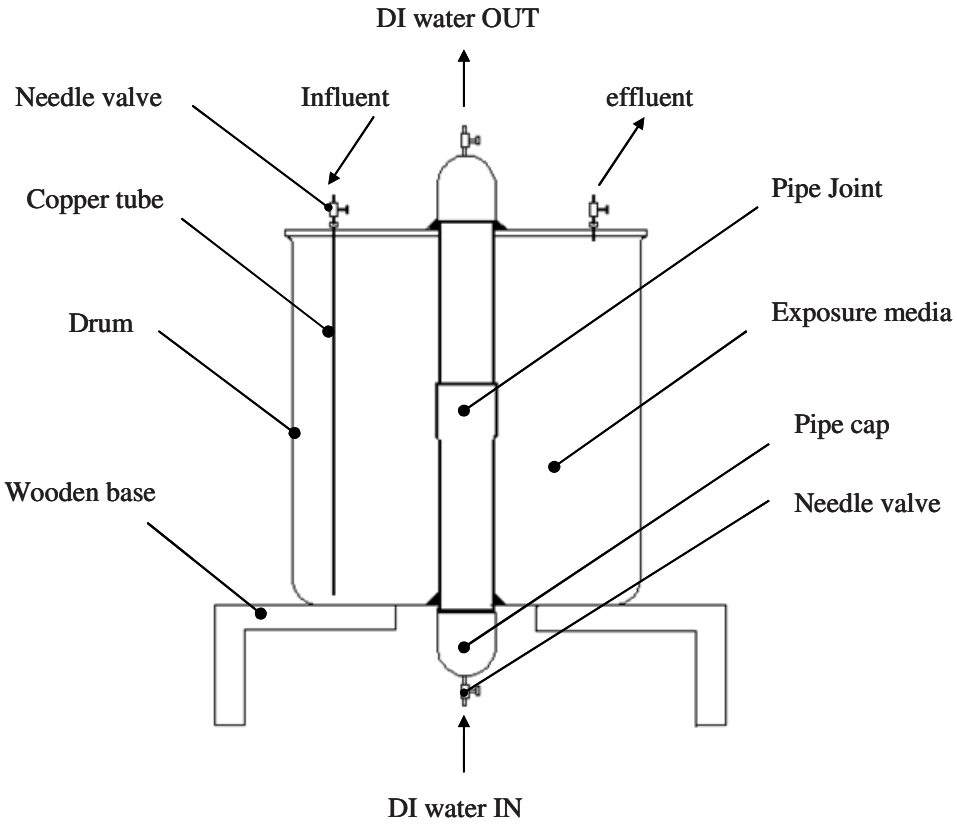

Figure 5.1 Pipe-drum apparatus

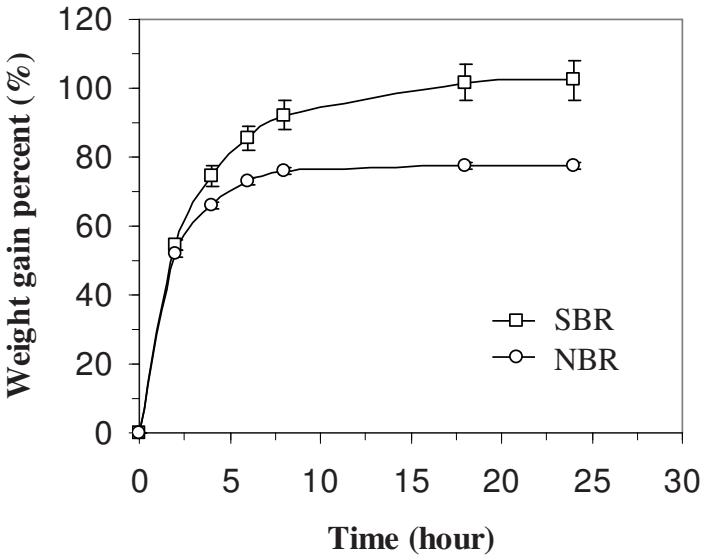

(a) Free product gasoline

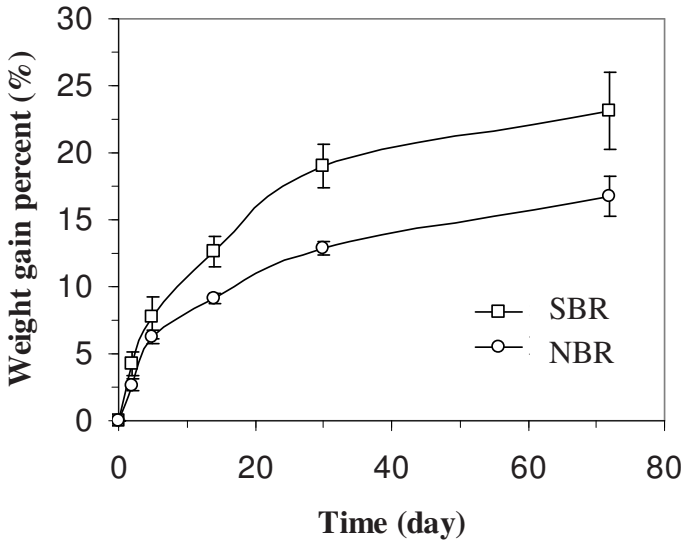

(b) Water saturated with gasoline

Figure 5.2 Equilibrium sorption test for 2-inch SBR and NBR gaskets exposed to free product gasoline and gasoline-saturated water

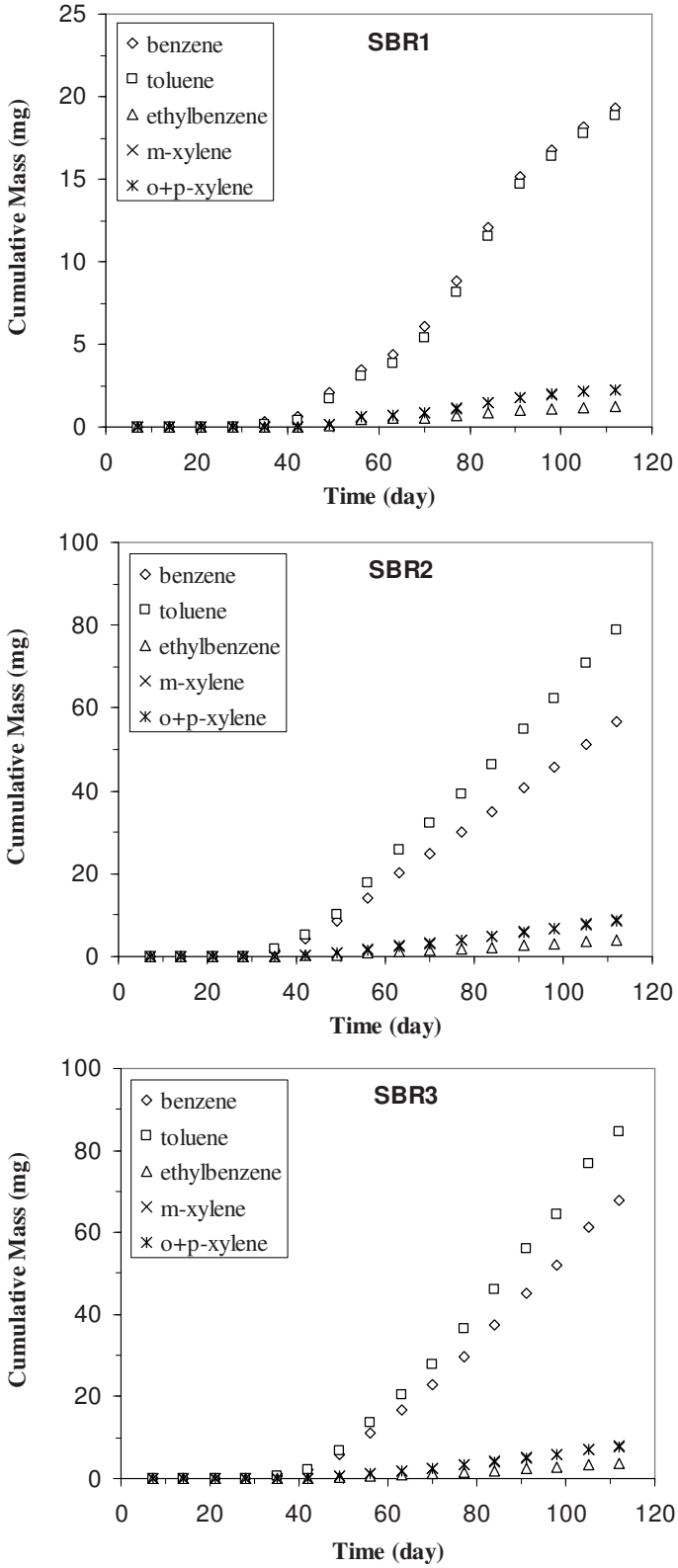

Figure 5.3 Cumulative mass of BTEX compounds permeated per joint in PVC pipes with SBR gaskets exposed to premium gasoline

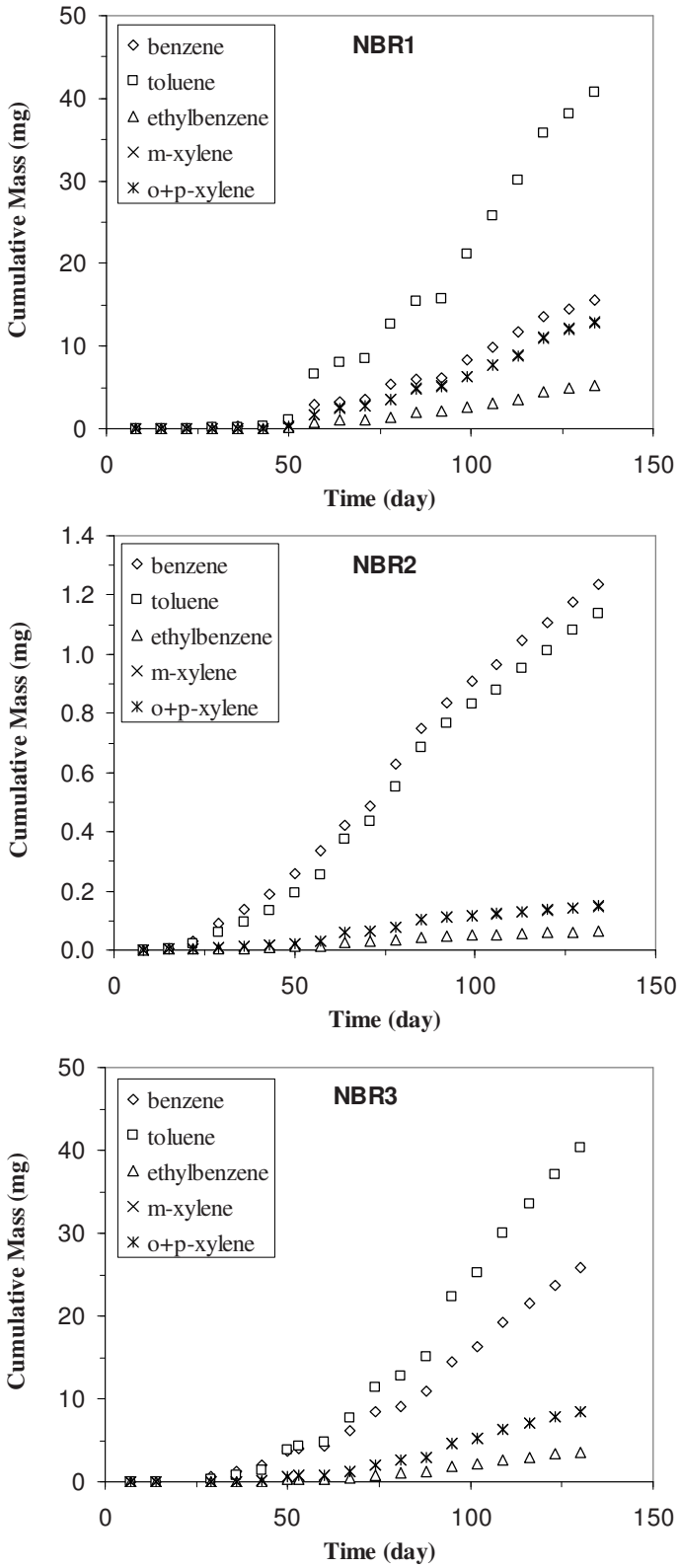

Figure 5.4 Cumulative mass of BTEX compounds permeated per joint in PVC pipes with NBR gaskets exposed to premium gasoline

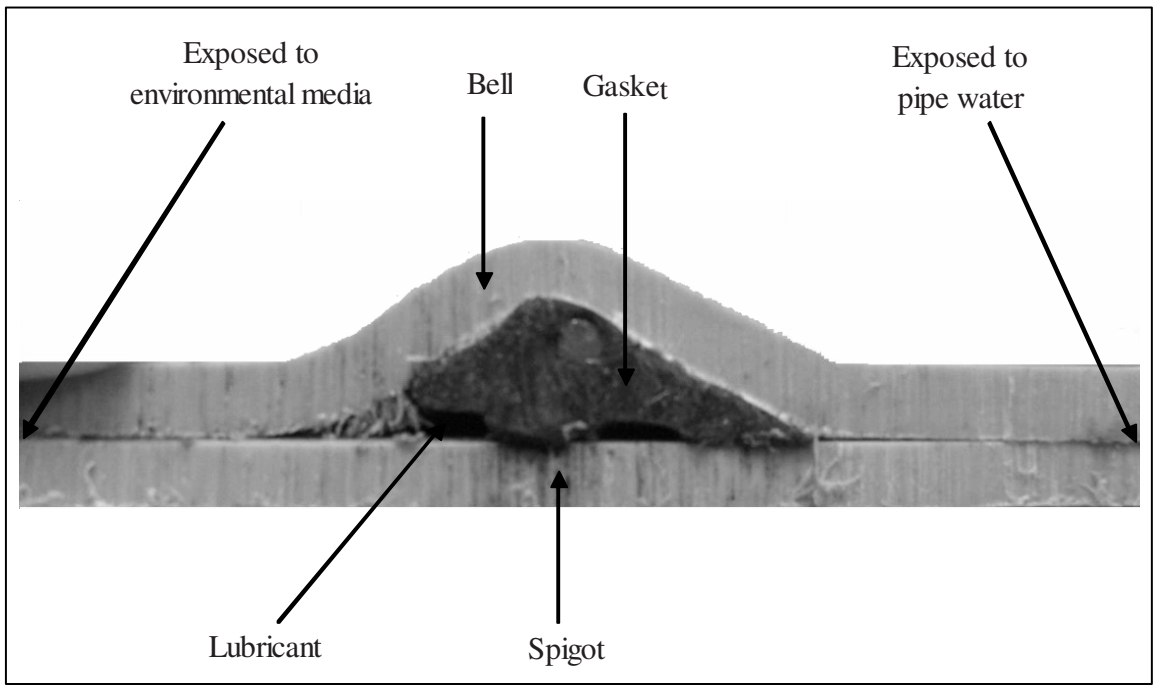

Figure 5.5 Cross section of PVC pipe joint with SBR Rieber gasket

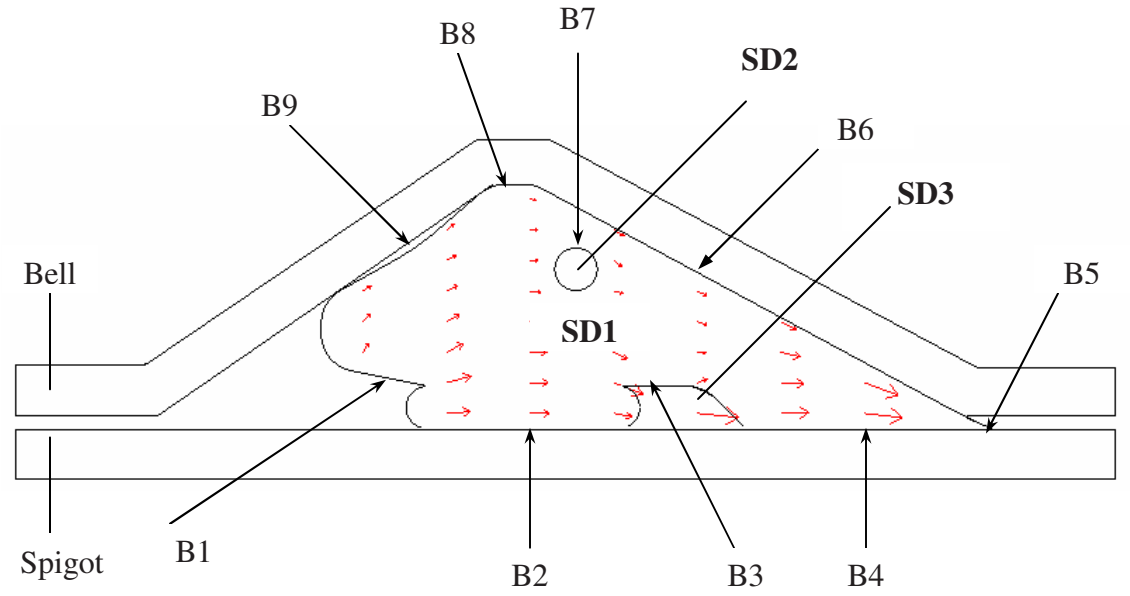

Figure 5.6 Geometry and boundaries of the cross section of non-pressurized Rieber joints (reduced scale for bell and spigot) (B- Boundary, SD1-subdomain elastomer, SD2-subdomain steel ring, SD3-subdomain air zone)

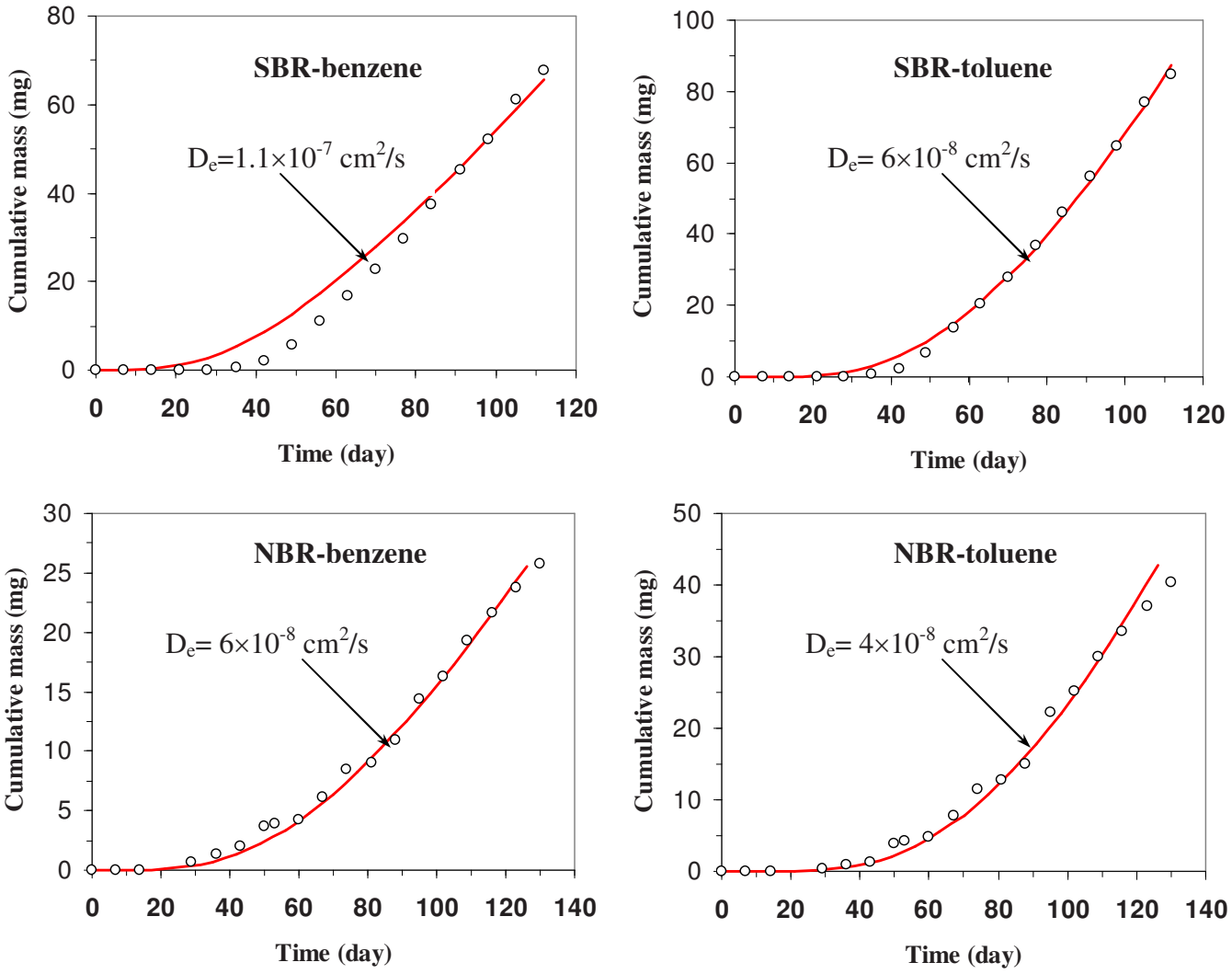

Figure 5.7 Fit the measured permeation data to the diffusion model to determine the diffusion coefficients of benzene and toluene in 2-inch SBR and NBR gaskets exposed to free product gasoline (o measured data; ——— model)

Table 5.1 Scale-up parameters and modeled steady-state permeation rates of benzene for varied-size gaskets exposed to free product gasoline

Gasket dimension (inch)	2	2-1/2	3	4	5	6	8	10	12
W[1](cm)	1.71	2.36	2.57	2.73	3.00	3.21	3.64	4.29	4.71
H[2](cm)	0.80	1.10	1.20	1.30	1.40	1.50	1.70	2.00	2.20
W/H	0.47	0.47	0.47	0.48	0.47	0.47	0.47	0.47	0.47
Scale Factor	1.00	1.38	1.50	1.60	1.75	1.88	2.13	2.51	2.75
Pipe O.D.(cm)	6.03	7.30	8.89	11.43	14.13	16.83	21.91	27.31	32.39
Exposure length[3] (cm)	0.05	0.069	0.075	0.080	0.088	0.094	0.106	0.125	0.138
Exposure area[4] (cm^2)	0.95	1.58	2.10	2.86	3.89	4.96	7.32	10.76	14.00
Steady-state permeation flux ($mg/cm^2/day$)	1.10	0.80	0.73	0.69	0.63	0.59	0.52	0.44	0.40
Steady-state Permeation rate (mg/joint/day)	1.05	1.27	1.54	1.96	2.45	2.92	3.78	4.74	5.64

[1] width of gasket cross section
[2] height of gasket cross section
[3] refers to the length of B5 shown in Figure 5.6
[4] calculated by: $\pi \times$pipe O.D$\times$exposure length

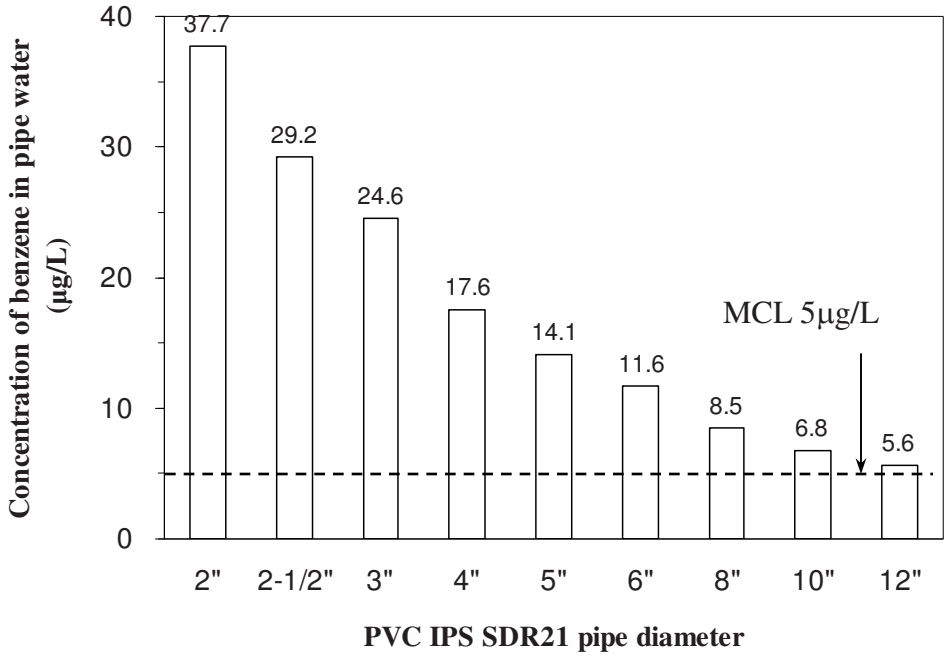

Figure 5.8 Benzene concentrations after 8 hours of stagnation in 100 feet of 2-inch to 12-inch PVC IPS SDR21 pipes with SBR Rieber gaskets in contact with gasoline.

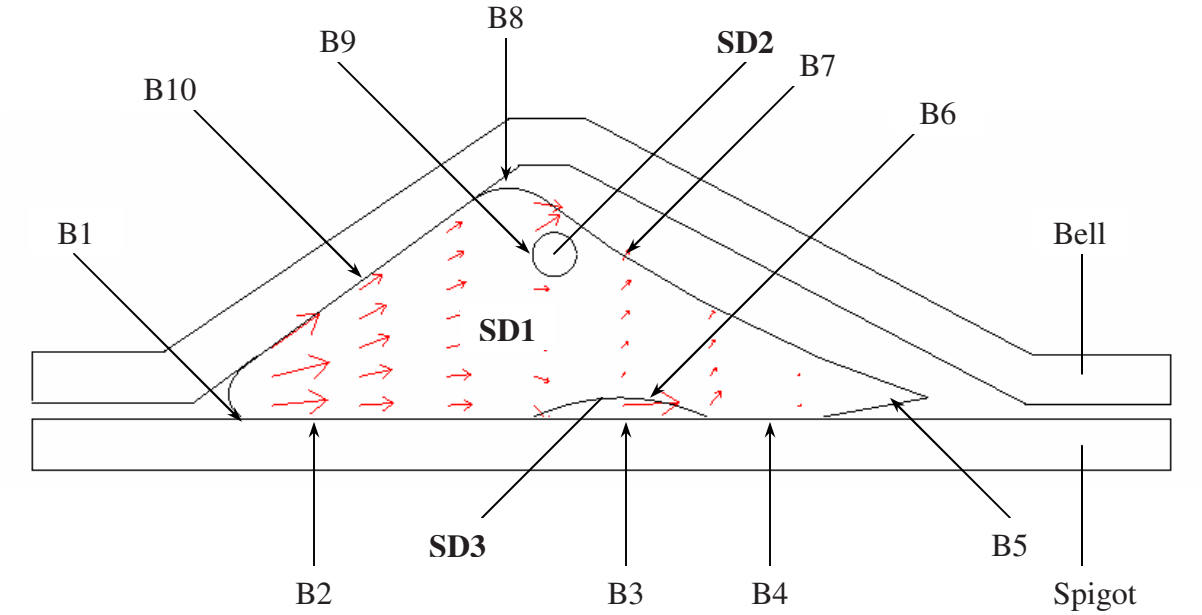

Figure 5.9 Geometry and boundaries of the cross section of pressurized Rieber joints (reduced scale for bell and spigot) (B- Boundary, SD1-subdomain elastomer, SD2-subdomain steel ring, SD3-subdomain air zone)

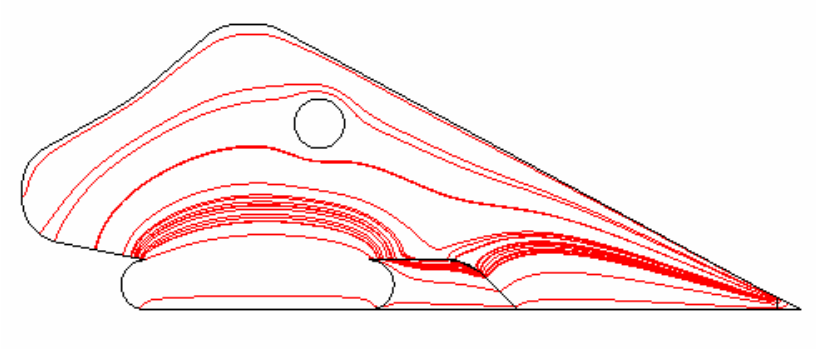

Non-pressurized system

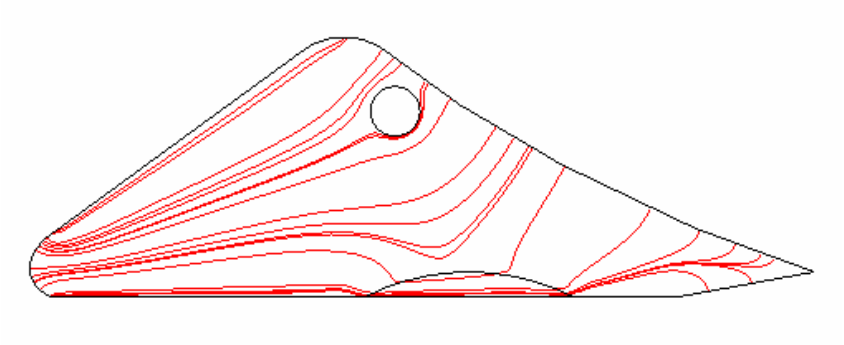

Pressurized system

Figure 5.10 Streamlines showing significant differences in the benzene diffusion pathways for non-pressurized and pressurized Rieber joint systems

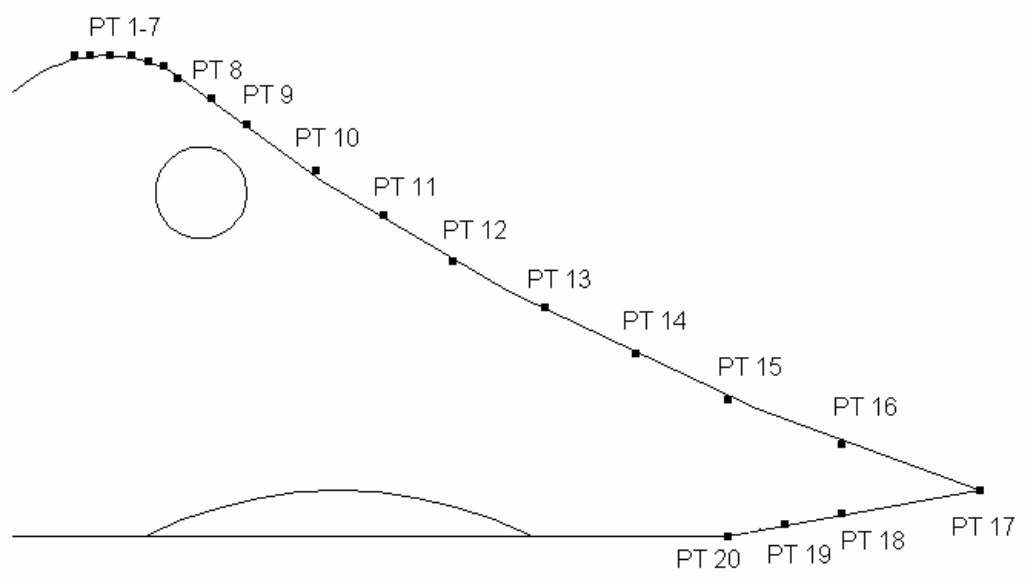

Figure 5.11 Interface of Rieber gasket-pipe water, divided into 19 segments to estimate the steady-state permeation flux of benzene in pressurized 2-inch SBR gaskets exposed to free product gasoline

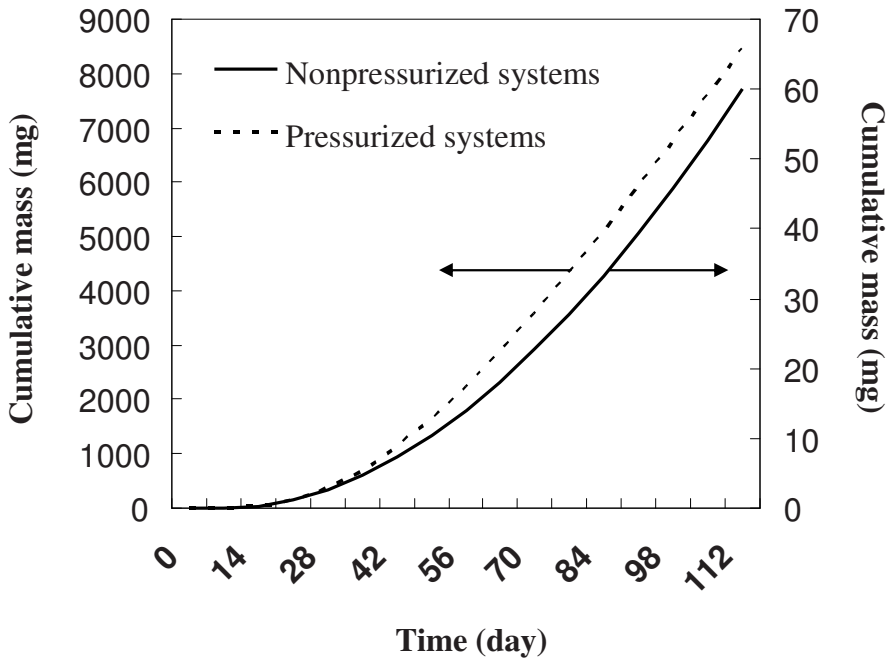

Figure 5.12 Modeled permeation curves of benzene for non-pressurized and pressurized 2-inch SBR gaskets exposed to free product gasoline (D_e=1.1×10^{-7} cm^2/s)

CHAPTER 6. PERMEATION OF PETROLEUM-BASED AROMATIC COMPOUNDS THROUGH POLYETHYLENE PIPES UNDER SIMULATED FIELD CONDITIONS

A paper to be submitted to *Journal of American Water Works Association*

Feng Mao, James A. Gaunt, Say Kee Ong

Abstract

This study conducted pipe-bottle tests to investigate the permeation of BTEX compounds through 1-inch diameter SIDR 9 high density polyethylene (PE) pipe under simulated field conditions of subsurface gasoline spills, gasoline-contaminated groundwater and unsaturated soil with varied levels of contamination. For all testing conditions, benzene was the first compound detected. Using the time-lag method, the concentration-dependent diffusion coefficients of BTEX compounds in PE pipe were estimated to be in the order of 10^{-8} cm^2/s when exposed to free product gasoline and in the order of 10^{-9} cm^2/s when exposed to gasoline-contaminated water solutions or unsaturated contaminated soil. This study also demonstrated that small size pipes were more vulnerable to permeation than large size pipes, and pipes with water stagnation periods posed a much higher risk of exceeding the MCL of benzene than pipes with continuous water flow. Under otherwise identical conditions, a PE pipe buried in soil of high organic matter was found to permeate to a lesser extent than a pipe buried in a soil of low organic matter.

Keywords: Polyethylene; Permeation; BTEX; Soil

6.1 Introduction

Polyethylene (PE) pipes have excellent abrasive, impact and corrosion resistance properties and are widely used in water service line connections and in some cases, water mains (Chevron Phillips Chemical Company LP, 2003). However, there is strong evidence in the literature and from field studies to suggest that organic contaminants permeate PE pipes of water distribution systems and adversely affect the quality of drinking water in water distribution systems. According to a survey completed in the 1980s (Thompson and Jenkins, 1987), PE pipes were involved in 39% of total incidents of drinking water contamination resulting from organic contaminant permeation. Holsen et al. (1991a) reported that contamination by aromatics and chlorinated solvents in drinking water as a result of permeation through PE pipes were more noticeable especially after a period of water stagnation in the pipe.

The permeability of organic compounds through PE pipes is attributed to the structural characteristics of PE. PE is characterized as a semi-crystalline polymer, having both crystalline and amorphous regions. The crystalline zones act as impermeable barriers for diffusion, while the non-crystalline matrix (amorphous regions) is readily permeable since the polymeric chains in the amorphous areas are relatively "mobile" (Naylor, 1989).

Although it is well known that organic compounds permeate PE pipes readily (Vonk, 1985; Thompson and Jenkins, 1987), significantly less effort has been devoted to simulate field contamination conditions and thus there are few data which can be applied to predict the permeation behavior in the real world (Holsen et al., 1991). Field contamination conditions are generally characterized by complex mixtures of organic chemicals distributed among aqueous, solid, and gas phases and non-aqueous phase liquids (NAPL), which implicitly

determine the effective availability of these compounds for permeation through pipe materials. For example, gasoline released into the environment are trapped by capillary force in the soil of the vadose zone as NAPL (Zhou and Crawford, 1995), volatilize and form hydrocarbon vapors in the vadose zone (Jutras et al., 1997), or migrate downward to the water table, resulting in the pooling of gasoline and dissolution of hydrocarbons into aqueous phase (Cline et al., 1991). Therefore, permeation can occur either from the vapor, aqueous, or NAPL phases and plastic pipes buried in both the vadose and saturated zones are susceptible to permeation.

According to Vonk's study (1985), lipophilic organic compounds in aqueous solutions rapidly permeated through PE pipes while PE pipes showed excellent resistance to the permeation by strongly polar compounds. Vonk's study, however, was focused on the permeation of one single compound through PE pipes exposed to aqueous solutions. Aqueous exposure experiments were insufficient to simulate a comprehensive permeation behavior of pipes in subsurface environment. Permeation characteristics of organic vapors through PE pipes remain unknown. Moreover, most chemical spills and contamination events in the field involve organic mixtures and the permeation characteristics of organic mixtures may differ widely from those of single organic chemicals studies due to the synergistic effects (Park et al., 1991). In addition, soil type and characteristics may implicitly determine the effective availability for permeation of organic compounds through pipe materials. Holsen et al. (1991b), in experiments with PB pipes, found that pipes buried in high organic soils were permeated more slowly than those buried in low organic soils. None of research has been done to investigate the effect of soil type and soil organic matter on the permeation of organic compounds through PE pipes.

The aim of this study was to investigate the permeation of petroleum-based aromatic compounds (benzene, toluene, ethylbenzene, m-xylene, and o+p-xylene (BTEX)) through PE pipes under simulated field conditions including subsurface gasoline spills, gasoline-contaminated groundwater, and gasoline-contaminated soil with varied levels of contamination. For each specific testing condition, the permeation fluxes of BTEX compounds through PE pipe were quantified and the diffusion coefficients of BTEX compounds in PE pipe were estimated. Correlations between the steady state permeation rates and the bulk concentrations were established and empirical equations developed. The results served as a basis for predicting the permeation behavior of BTEX through PE pipe at contaminant levels typically encountered in the environment.

6.2 Materials and Methods

6.2.1 Materials

One-inch diameter PE pipe (high density, SIDR 9 IPS NSF PW PE3408 ASTM-D2239-81) was obtained from a PE pipe manufacturer. Premium gasoline was purchased from a local store and the concentrations of benzene, toluene, ethylbenzene, m-xylene, and o+p-xylene in the gasoline were determined by gas chromatography to be 19.8 g/L, 75.9 g/L, 14.7 g/L, 33.7 g/L, and 32.5 g/L, respectively. Three types of soils, silica sand, organic topsoil, and a mixture of sand and topsoil were used in the experiments. Silica sand (Granusil 4030) was purchased from UNIMIN Corporation, Portage WI. Organic topsoil, purchased from a local store, was air dried and sieved to pass a 2 mm sieve. Another soil was prepared by mixing approximately equal parts of silica sand and dried, sieved, organic topsoil with a Hobart mixer. Triplicate samples were taken randomly from each prepared

soil and analyzed for their important physical and chemical properties according to the Methods of Soil Analysis (Klute, 1986; Page, 1986). The results are summarized in Table 6.1.

6.2.2 Experimental apparatus

Experiments were conducted in a pipe-bottle apparatus (Figure 6.1), consisting of a 1-L glass bottle with the PE pipe mounted horizontally through holes drilled in the glass. The connections between pipe and bottle were sealed with Loctite® plastic epoxy and further covered by Loctite® epoxy putty (Henkel Technologies, Rocky Hill, CT). The ends of the pipes were sealed with Teflon® plugs. One of the Teflon® plugs had a small hole that was plugged with a threaded brass plug to allow filling and draining of the water inside the pipe with a glass syringe. The bottle was capped with a Teflon® -lined cap. The total surface area of PE pipe exposed to the bulk solution was approximately 81.9 cm^2. To simplify the experimental system and facilitate ease in handling the pipe-bottle apparatus, all experiments were conducted at room temperature (23 ± 1.5°C).

6.2.3 Exposure of PE pipes to free product gasoline

In this test, the pipe segment was first filled with deionized water and the bottle filled with silica sand and premium gasoline until the bottle was nearly full and a visible liquid level of gasoline appeared above the surface of the sand. The level of liquid gasoline in the bottle was monitored visually and there was no significant drop in the level during the experimental period of four weeks. Pipe-water samples were taken at regular intervals (about three times a week) and analyzed for the presence of BTEX. The pipe was flushed with deionized water three times immediately after each sampling before fresh deionized water

was added and the Teflon® plug of the pipe sealed with the threaded brass plug.

6.2.4 Exposure of PE pipes to gasoline-contaminated groundwater

Aqueous gasoline-saturated solution was prepared by mixing 350 mL premium gasoline and 3.5 L deionized water in a 4-L glass bottle for 48 hours using a magnetic stirrer. Several preliminary experiments indicated that a mixing time of 48 hours was sufficient to produce an aqueous gasoline-saturated solution. Fresh gasoline saturated solution was prepared once every week throughout this study. The concentration of the dissolved BTEX was around 150 mg/L, which was slightly higher than the average value of 135 mg/L reported by Cline et al. (1991) for water saturated with gasoline of different grades. Benzene and toluene were the major aromatic compounds in the aqueous phase, accounting for nearly 90% of total BTEX. Three diluted aqueous solutions of varying concentrations, 50%, 10%, and 1% of aqueous gasoline-saturated solutions, were obtained by diluting the gasoline-saturated solution with deionized water at a ratio of 1:1, 1:9, 1:99, respectively. The BTEX concentrations in the four aqueous solutions (≈150 mg/L, ≈75 mg/L, ≈15 mg/L and ≈1.5 mg/L for 100%, 50%, 10% and 1% of aqueous gasoline-saturated solutions, respectively) typically reflect the concentration range of BTEX found in groundwater associated with gasoline release.

For each experiment, the mini pipe-bottle apparatuses were filled with silica sand until the bottle was nearly full. Sodium azide (1.5 g) was added to inhibit potential biodegradation of BTEX and was thoroughly mixed with the sand by rotating the bottle in order. The bottle was loosely capped with a Teflon®-lined cap which had a small hole drilled and a Teflon® tube installed, reaching to the bottom of bottle. Aqueous gasoline

solution was then introduced into the sand through the Teflon® tubing, from bottom to top, using a Masterflex pump, until the bottle was full. The Teflon® tube was removed along with the cap and the bottle was then tightly capped with a Teflon®-lined cap with no hole. The final water level was approximately 2 cm above the surface of the soil, with minimum headspace. The apparatuses were wrapped with aluminum foil to minimize photodegradation.

The silica sand and the aqueous solution were replaced each week with new sand and fresh aqueous gasoline solution to maintain relatively constant aqueous concentrations of BTEX in the bottle. BTEX concentrations in the soil pore water were periodically measured. To collect samples, the pipe-bottles were gently rotated several times and then allowed to sit undisturbed for 10 minutes. Liquids above the soils were collected in vials using a glass syringe and then centrifuged at 5,000 rpm for 10 minutes. These supernatant liquids were analyzed in the same manner as the pipe-water samples.

6.2.5 Exposure of PE pipes to unsaturated gasoline-contaminated soil

Four levels of gasoline-contaminated soil were prepared by spiking 1 kg sand-topsoil mixture with known amounts of premium gasoline and mixing the soil by rotating the soil container for one week. The volumetric moisture content of the soil was adjusted to approximately 10% - which was above the water content of soils equilibrated at a relative humidity > 98 % (Holsen et al., 1991b). The amounts of BTEX sorbed onto the four soils were determined using methanol extraction and analyzed by gas chromatography. The total BTEX in the four soils were found to be 32, 89, 388 and 1,216 mg/kg dry soil. Toluene and xylene were the major aromatic compounds in the soil accounting for approximately 90% of the total BTEX.

In these experiments, gasoline-contaminated soils were packed into the pipe-bottle apparatus. Under those conditions, mass transfer limitations in the soil might have occurred when organic compounds were absorbed rapidly by the pipe wall, decreasing the concentration of organic compounds in the soil immediately adjacent to the pipe wall. Due to volatilization and diffusion, the concentration of BTEX in the soil and surrounding the pipes may not have remained constant over the experimental period. Through the experiments, water inside the pipes was drained for BTEX analysis and replenished with fresh deionized water. At the end of the experiments, soil samples were collected from the top layer (around 4 cm above the pipe), middle layer (surrounding the pipe) and bottom layer (around 4 cm below the pipe), and the residual BTEX in the soil was extracted by methanol and analyzed by gas chromatography.

6.2.6 Impact of soil organic matter on permeation

In these experiments, pipes were buried in the three types of soils, silica sand, organic topsoil, and a sand-topsoil mixture. The soils were initially soaked with aqueous gasoline-saturated solutions. The experimental procedures were the same as described in simulated groundwater experiments except that the soil and aqueous solution were not replenished. During the experiment, soil pore water and pipe-water were collected over the experimental period and the BTEX concentrations measured. To compensate for the liquid loss (around 4 mL) from sampling and to maintain zero headspace, additional fresh gasoline-saturated water was rapidly added to each bottle following sampling. The additions did not affect the concentration of BTEX in soil pore water since the total capacity of soil pore water (around 400 mL) was greater than the volume of fresh gasoline-saturated water added.

6.2.7 Gas chromatographic determination of BTEX

BTEX in the samples was determined using a gas chromatograph (Tracor 540, Tracor Instruments Austin, Inc., Austin TX) equipped with a packed column (1.8 m (6 ft) × 2 mm; 1% SP1000 on 60/80 mesh Carbopack B), a photoionization detector, and an automated purge & trap concentrator (Tekmar LSC2/ALS). The method detection limits for benzene, toluene, ethylbenzene, m-xylene and o+p-xylene were 0.24 µg/L, 0.24 µg/L, 0.26 µg/L, 0.29 µg/L, and 0.53 µg/L, respectively.

6.2.8 Determination of diffusion coefficient

The total mass of contaminant permeating the PE pipe (mass/surface area) between sampling periods was estimated based on the contaminant concentration in the pipe water, the volume of water in the pipe and the pipe surface area. Using a plot of cumulative mass permeated per unit area, Q (µg/cm^2), versus time, the time lag, T_L, defined as the intersect with the time (t) axis of the straight line drawn through the $Q(t)$ data at steady state conditions was determined. If diffusion takes place in a hollow cylinder with inner and outer radii of a and b respectively, the diffusion coefficients (D) can be estimated by (Crank, 1975):

$$D = \frac{b^2 - a^2 + (a^2 + b^2)\ln(a/b)}{4T_L \ln(a/b)} \qquad \text{(Eq. 6.1)}$$

where a is the inner radius (cm); b is the outer radius (cm) ; D is the diffusion coefficient (cm^2/s).

6.3 Results and Discussion

6.3.1 Exposure of PE pipes to gasoline

The cumulative masses permeated per unit area for BTEX compounds are plotted in

Figure 6.2. The permeation of BTEX through PE pipe exposed to gasoline was extremely rapid. Of the five compounds of interest, benzene was the first compound detected with a breakthrough time of approximately one week. When breakthrough was detected, the concentration of benzene measured in the pipe-water exceeded the maximum contaminant level (MCL) of 5 μg/L. Toluene breakthrough lagged just slightly behind that of benzene, while ethylbenzene and xylene were detected later (approximately 15 days) and at much lower concentrations. Benzene and toluene accounted for nearly 90% of the entire total BTEX permeated into the pipe-water. This is mainly due to the higher solubility of benzene in water and the higher mass fraction of toluene in gasoline. Similar permeation behavior of BTEX (i.e., the order of breakthrough time and the relative permeation concentrations) was found in ductile iron (DI) pipe joints with styrene butyl rubber (SBR) gaskets exposed to gasoline (Glaza and Park, 1992; Ong et al., 2007).

The T_L for benzene and toluene were estimated to be 14.1 days and 15.2 days, respectively. Based on the time lag method (Eq. 6.1), the corresponding diffusion coefficients were estimated to be 1.3×10^{-8} cm^2/s and 1.1×10^{-8} cm^2/s, respectively. Under steady state permeation conditions, the concentrations of BTEX in the pipe water at the end of the 3-day sampling intervals were found to be very close to the BTEX concentrations in aqueous gasoline-saturated solution. Apparently, the pipe material was saturated with gasoline, resulting in BTEX concentrations in the pipe-water to be close to the ssolubility limit of gasoline in water.

6.3.2 Exposure of PE pipes to gasoline-contaminated groundwater

The cumulative mass permeated per unit area for BTEX compounds at four levels of contamination are plotted in Figure 6.3. The measured concentrations of BTEX in soil pore

water at four levels of contamination were slightly lower than the expected concentrations (100%, 50%, 10% and 1%), mainly due to sorption by the pipe and volatilization loss.

As shown in Figure 6.3, benzene and toluene rapidly permeated through PE pipe, even from the most dilute solution. As in the pure gasoline exposure experiments, benzene was the first compound to be detected in the pipe-water, probably due to the high concentration of benzene in the simulated ground water and its smaller molecular diameter. Once breakthrough occurred, the level of benzene in the pipe-water quickly exceeded its MCL. The breakthrough of toluene was slightly behind that of benzene, while ethylbenzene and xylene were detected later (approx. 41 days for both compounds for gasoline-saturated water) and at much lower concentrations (breakthrough data not shown). Figure 6.3 also demonstrated that the breakthrough time and the lag time increased with lower BTEX groundwater contamination, which implied that higher bulk groundwater hydrocarbon concentrations would lead to earlier breakthrough.

Diffusion coefficients (D) of benzene and toluene at four levels of contamination were estimated using the time lag method (Eq. 6.1). Diffusion coefficients for benzene and toluene ranged from 1.8×10^{-9} to 3.6×10^{-9} and 1.8×10^{-9} to 3.3×10^{-9} cm^2/s, respectively and are summarized in Table 6.2 for the different bulk exposure concentrations. Included in Table 6.2 for comparison purposes are diffusion coefficients from other studies.

As shown in Table 6.2, diffusion coefficients from this study and other studies were of the same order of 10^{-9} cm^2/s, despite the different polymer composition and crystallinity, different concentration of contaminants, and different experimental conditions used. Diffusion coefficients for toluene obtained from this study using PE pipes (high density) were similar to those of Vonk's study (1985) using low density polyethylene (LDPE) pipes.

Table 6.2 also indicates that diffusion coefficients were concentration-dependent and increased with an increase in bulk exposure concentration. This concentration effect may be attributed to increased mobility of polymer segments resulting from increases in the average free volume in the polymer caused by the presence of the diffusing contaminant. For each contamination level (approximately gasoline-saturated (100%), 50%, 10%, or 1% aqueous gasoline-saturated solutions), insignificant differences between the diffusion coefficients of benzene and toluene were found, which agreed with the results of Sangam and Rowe (2001) for HDPE geomembrane but conflicted with those of Joo et al. (2004) for HDPE geomembrane. In Joo's study, diffusion coefficients of benzene were found to be 1.5 times higher than that of toluene for a bulk concentration of 30 mg/L. One possible explanation for the nearly identical permeation of benzene and toluene detected in this study might be the synergistic effect of organic compounds on permeation. Most studies reported in Table 6.2 were based on the permeation of a single organic compound in aqueous solution through the polymeric material while this study used gasoline-contaminated water which is a mixture of organic compounds and, therefore, the presence of benzene with toluene may enhance the diffusion of toluene through the HDPE pipes. Synergistic effects were also observed in the study by Park et al. (1991) where toluene permeation through PB pipe was considerably enhanced by the presence of TCE.

The steady state permeation rates P_m [µg/cm^2/day]] versus the bulk (external) concentrations C_{bulk} (mg/L) are plotted as shown in Figure 6.4. It indicates that the permeation rates were strongly dependent on the bulk concentrations of contaminants in the soil pore water. Two empirical correlation equations were obtained:

$$P_m = 0.0079 C_{bulk}^{1.1323} \quad \text{for benzene} \qquad \text{(Eq. 6.2)}$$

$$P_m = 0.0087 C_{bulk}^{1.1444} \quad \text{for toluene} \qquad \text{(Eq. 6.3)}$$

6.3.3 Exposure of PE pipes to unsaturated gasoline-contaminated soil

The cumulative mass permeated per unit area for BTEX compounds at four levels of contamination are plotted in Figure 6.5. Toluene and xylenes were the major compounds detected in the pipe-water while the permeation of benzene through pipes was insignificant. These observations were consistent with the results found in the permeation incidents (Holsen et al., 1991a). In three reported incidents involving gasoline, toluene permeated to the greatest degree, followed by xylenes, ethylbenzne, and benzene (in the same order as shown in Figure 6.5-a) while in the other cases associated with gasoline, xylenes permeated more readily, followed by toluene and ethylbenzene (in the same order shown in Figure 6.5-b and 6.5-c). Holsen et al. (1991a) attributed the low permeation of benzene to its relatively higher polarity. The properties of polarity, however, cannot explain the higher and faster permeation of benzene than the other BTEX compounds when pipes were exposed to free gasoline or gasoline-contaminated water. One possible reason, as indicated in this study, is the relatively low benzene concentration remaining in the soils. The low concentration in the soils is due to the high volatility of benzene and therefore has the lowest soil sorption affinity among the BTEX compounds (Zytner, 1994). In the gasoline-contaminated groundwater, however, a relatively high concentration of benzene is generally detected because of its high solubility in water (Cline et al., 1991). From the perspective of permeation risk, therefore, the plastic pipes buried in the water-saturated zone will be more easily permeated by benzene than in the vadose zone. The case of benzene indicates that knowledge of environmental fate and transport is critical to evaluate the potential permeation risk of contaminants since the

distribution of chemicals among environmental media determines the contaminant levels plastic pipes might encounter in the field.

In the unsaturated soil, plastic pipe permeation was believed to occur from vapor phase (Holsen et al., 1991b; Park et al., 1991). This study did not collect the vapor samples for BTEX analysis and thus the exact concentration of BTEX in soil gas was unknown over the experimental period. At the end of the experiments, soil samples were taken from different positions (top, middle and bottom) of the glass bottle and the BTEX concentrations in the soils were found to be relatively uniform. However, for each of the four contamination levels, more than 90 percent of total BTEX in soils was lost over the entire experimental period of 3 months. The loss of toluene was relatively higher than that of xylene. The losses were mainly due to the sorption/diffusion into the pipe and volatilization. Generally, the diffusion coefficients of organic compounds in the vapor phase through soil pores are several orders of magnitude larger than the diffusion coefficients through plastic pipes (Holsen et al., 1991b). Therefore, the mass transfer in soils may be rapid enough to hinder the development of a concentration gradient in the soils. The drop of BTEX concentration in soils indicated that the pipes were exposed to variable contaminant levels, which resulted in somewhat less than ideal permeation curves for constant exposure concentration. As shown in Figures 6.5-a and 6.5-b (initial BTEX concentrations of 1,216 and 388 mg/kg), the permeation curves, especially for toluene, flattened out at later time periods. However, Figures 6.5-c and 6.5-d still showed a linear increase of cumulative mass permeated per unit area with time after steady state permeation was reached – a typical curve predicted by permeation theory.

The time lag method approach cannot be used to estimate the diffusion coefficients of BTEX for this case since the experimental conditions did not meet the requirement of

"constant exposure concentration." However, it may be reasonable to assume that the exposure concentrations did not significantly decrease at the early time period and thus it is still possible to apply the time lag method to calculate the diffusion coefficients based on the early breakthrough data. The first 50 days of data were used to estimate the diffusion coefficients for the individual BTEX compounds as shown in Figures 6.5-a and 6.5-b. The permeation parameters of toluene, ethylbenzene and xylene under the test conditions are summarized in Table 6.3.

Generally, the diffusion coefficients (D) in Table 6.3 were of the same order of magnitude as those found in the aqueous experiments (10^{-9} cm^2/s), were concentration-dependent, and showed signs of synergistic effects. The synergistic effect was demonstrated by the diffusion coefficients of the three xylene isomers. In a previous study on HDPE geomembrane (Saleem et al., 1989), significant differences in the diffusion coefficients were detected for the three xylene isomers due to the effect of molecule structure (shape) on diffusion. In this study, however, the three compounds shared identical permeation characteristics when they coexisted in the soils. There are no means of comparing the results of diffusion coefficients found in this study as none of previous experimental studies have specifically investigated the permeation of organic contaminants through PE pipe buried in the unsaturated soil. In addition, comparing the diffusion coefficients obtained from the three permeation tests (free product gasoline, gasoline-contaminated water, and gasoline-contaminated unsaturated soil) based on the values of activity is a challenge due to the lack of consistent definitions of activity (Park et al., 1991).

6.3.4 Impact of soil organic matter on permeation

Sorption of BTEX into the soil organic matter is rapid, as shown in Figure 6.6.

BTEX in the soil pore water for the organic topsoil and sand-topsoil mixture dropped dramatically within the first week (mainly due to sorption to the soil) and then decreased slowly (mainly due to sorption/diffusion into to the pipe and volatilization losses). Under otherwise identical initial conditions, the BTEX concentrations in soil pore water after 55 days were lowest in the organic topsoil (approx. 30 mg/L as compared to an initial concentration of approximately 128 mg/L) which had the highest organic carbon content (5.1%). The BTEX concentrations in the soil pore water of the sand-topsoil mixture with an organic carbon content of 1.9 % were approximately 50 mg/L. The BTEX concentrations in soil pore water for the silica sand with insignificant organic carbon content were approximately 65 mg/L.

The different BTEX concentrations were attributed to different BTEX sorption capacities for different types of soil. The higher organic matter in the organic topsoil resulted in greater soil uptake of BTEX and a significant decrease of BTEX concentrations in the soil pore water (Chiou and Peters, 1981).

As demonstrated earlier, the permeation rates of BTEX through PE pipes were strongly dependent on the external bulk concentration. The sorption of BTEX by soils decreased the BTEX concentration in the soil pore water and, thereby, decreased the permeation rate of BTEX through PE pipes (see Figure 6.7). The breakthrough times of benzene for silica sand, sand-topsoil mixture, and organic topsoil were 13 days, 16 days, and 19 days, respectively. Since the external bulk concentration varied with exposure time, steady state permeation was not reached and, therefore, the diffusion coefficients of BTEX for the three different types of soils could not be estimated. The relative permeation rates, however, can be compared with each other. For example, after two months of exposure, the

cumulative mass of BTEX permeated per unit area through the pipe buried in silica sand was nearly twice that of the sand-topsoil mixture, and four times that of organic topsoil. However, high soil organic matter can not be relied upon to protect pipes from permeation because such soils will eventually reach their maximum adsorption capacities under field conditions. The effects of soil organic matter on permeation found in this study were consistent with the results of the study on the permeation of organic contaminants through polybutylene (PB) pipes (Holsen et al., 1991b).

6.3.5 Prediction of contaminant concentration in pipe-water under stagnation and continuous flow conditions

Using the permeation rates of Eq. 6.2 and Eq. 6.3, the concentrations of benzene and toluene in the pipe-water were estimated respectively for a given bulk contaminant concentration after a period of stagnation. Water stagnation, representing the worst-case scenario, is typically found during the night in service lines of residences and office buildings. The concentration of contaminant in pipe-water (C_{pw}) can be estimated by the following equation:

$$C_{pw} = \frac{M}{V} = \frac{P_m \times \pi \times O.D \times L_C \times t}{\frac{1}{4} \times \pi \times I.D.^2 \times L_T} = \frac{4 \times f(C_{bulk}) \times O.D. \times L_C \times t}{I.D.^2 \times L_T} \qquad \text{(Eq. 6.4)}$$

where M is the total mass of permeated contaminant (µg); V is the volume of water in the pipe (L); P_m is the steady permeation rate of the contaminant [µg/cm^2/day]], a function of the bulk concentration of contaminant in the soil pore water, $f(C_{bulk})$ (Eq. 6.2 and Eq. 6.3); C_{bulk} is the bulk concentration of contaminant in the soil pore water, C_{bulk} (µg/L); t is the period of stagnation (days); L_C is the length of contaminated pipe (cm); L_T is total length of

pipe (cm); *I.D* is the inside diameter of pipe (cm); and *O.D.* is the outside diameter of the pipe (cm).

Eq. 6.4 assumes that the contaminants instantaneously diffused across the entire pipe once they had permeated the pipe. Therefore, the estimated values using Eq. 6.4 are essentially the average pipe water concentration over the period of stagnation. To further simplify the calculation, the ratio of L_C to L_T was arbitrarily set to four values (1:1, 1:5, 1:10 and 1:20), and the period of stagnation, *t,* was set to 8 hours. With these simplifying conditions, the concentrations of benzene and toluene in pipe water were estimated for bulk concentrations or soil pore water concentrations ranging from 0.1 to 100 mg/L (see Figure 6.8).

As shown in Figure 6.8, the estimated bulk concentrations, C_{bulk}, (at steady state permeation) that would result in exceeding the benzene MCL (5 µg/L) in a 1-inch SIDR 9 IPS PE pipe for a stagnation period of 8 hours were approximately 1 mg/L, 4 mg/L, 8 mg/L and 15 mg/L, corresponding to the ratios (L_C/L_T) of 1:1, 1:5, 1:10 and 1:20, respectively. For identical bulk concentrations, however, the concentration of toluene in pipe-water would not exceed its MCL (1,000 µg/L) except at a high bulk concentration of 100 mg/L, which is not usually encountered in the field. Therefore, prevention of potential risk of benzene in drinking water should be a priority if PE pipes are exposed to gasoline-contaminated groundwater. Conservatively, if the bulk concentration of benzene is 1 mg/L or above, PE pipes must be rapidly replaced by other pipe materials (such as copper pipe) since the MCL in pipe-water will be exceeded within several hours. It should also be emphasized that Figure 6.8 was based on an 8-hour stagnation period. Under long-term stagnation (such as weeks), much lower bulk concentration will result in the MCL being exceeded. For example,

the concentration of benzene in pipe water was estimated to be 7 µg/L when the pipe was exposed to a bulk concentration of 50 µg/L for a stagnation period of 2 weeks at a ratio of 1:1.

Under normal conditions, the contaminant concentration will be impacted by the water flow rate in the pipe. Assuming a full pipe flow and complete mixing of permeated contaminant in the pipe-water, the concentration of contaminant in pipe-water (C_{pw}) can be estimated by:

$$C_{pw} = \frac{M}{V} = \frac{P_m \times \pi \times O.D \times L_C \times t}{q \times t} = \frac{4 \times f(C_{bulk}) \times O.D. \times L_C}{I.D.^2 \times v} \qquad \text{(Eq. 6.5)}$$

where q is the water flow rate (cm^3/day); v is the average water flow velocity (cm/day). Other nomenclatures were defined previously. Typically, the average water flow velocity for plastic pipes, v, ranges from 0.06 m/s to 3.7 m/s (Chevron Phillips Chemical Company, 2003; Uni-Bell, 2001). By setting the average water flow velocities at six values (0.06, 0.30, 0.61, 1.52, 2.44, and 3.7 m/s), the length of contaminated pipelines, L_C, required (at steady state permeation) to exceed the MCL of benzene was estimated for a specific bulk concentration. The results are shown in Figure 6.9.

Figure 6.9 indicates that only very low water flow velocities (< 1 ft/s or 0.3 m/s) will pose a risk of exceeding the MCL for benzene under the conditions of full pipe flow. Given a water flow velocity of 0.3 m/s or above, a long contaminated pipeline (> 100 m) and a high bulk concentration (> 40 mg/L), which is not usually encountered in the real permeation incidents, would be needed to exceed the MCL. When the bulk concentration is below 10 mg/L and the length of contaminated pipe was less than 150 m, it is expected that the concentration of benzene in pipe-water would be below its MCL for any typical water flow

velocity. Due to the effect of dilution, the hydrocarbon concentrations in PE pipes with water flow would be less than those for conditions of stagnation.

6.3.6 Prediction of contaminant concentration in pipe-water for pipes with varied sizes

The discussion above has been focused on 1-inch SIDR 9 IPS PE pipe. A key issue is to apply the data to predict the permeation behavior of contaminants for pipes with other dimensions. In Eq. 6.4, the inside diameter (I.D.) and outside diameter (O.D.) are known for a specific pipe size, but the steady state permeation rate (P_m) needs to be corrected for the effects of dimension. Based on the physicochemical theory of permeation (Crank and Park, 1968), P_m can be expressed as:

$$P_m = C_0 \times \frac{P_C}{l} = C_0 \times \frac{D \times S}{l} \qquad \text{(Eq. 6.6)}$$

where C_0 is the bulk concentration of contaminant surrounding the pipe (μg/L); P_C is the permeation coefficient (cm^2/s); D is the diffusion coefficient, (cm^2/s); S is the solubility (dimensionless); and l is the wall thickness of pipe (cm).

S describes the partition of contaminant between bulk solution and polymeric material and in principle is a constant for a given contaminant-polymer pair. There are disagreements with respect to whether D is dependent on the polymer thickness. Generally, it is believed that D is independent of polymer thickness since D is only determined by the chemical characteristics of the polymer, the concentration (activity) of the contaminant compound, and the interactions between the contaminant and the polymer. However, Park et al. (1996) investigated the effects of thickness on diffusion coefficients for HDPE geomembrane exposed to four organic compounds (methylene chloride, toluene, trichloroethylene and m-xylene), and found that the diffusion coefficients decreased by 28 to 36% when the thickness

increased from 0.76 mm to 2.54 mm at an initial concentration of 100 mg/L. Here, D was assumed to be a constant for various pipe sizes since this assumption would be conservative, but safe, to predict the permeation risk for large pipe dimensions. For different pipe sizes, therefore, P_m [µg/cm^2/day] is only a function of wall thickness of pipe (l). The steady state permeation rate for a specific pipe dimension can be deduced:

$$P_{mp} = P_{ms}\frac{l_s}{l_p} = \gamma P_{ms} \qquad \text{(Eq. 6.7)}$$

where P_{mp} is the predicted steady state permeation rate for the wall thickness of l_p; P_{ms} is the known steady state permeation rate for the wall thickness of l_s; γ is the correction factor. With the known wall thickness, inside diameter, and outside diameter, the corresponding concentration of benzene in pipe-water was estimated after 8-hour stagnation for two standard types of PE pipes (SIDR 9 and DIPS DR 17.0 PSI 100 series) under various bulk concentrations using Eq. 6.7. The results are shown in Figure 6.10.

Figure 6.10 indicates that small size pipes are more vulnerable to permeation than large size pipes. For example, approximately 400 µg/L of benzene in soil pore water would result in the exceedance of the benzene MCL for ½ inch SIDR 9 series pipe while the bulk concentration required to exceed the MCL for 2 inch SIDR 9 pipe would be 3.5 mg/L or higher. The higher susceptibility of small size pipes to permeation is supported by the findings of real permeation incidents, as reported in the study by Holsen et al. (1991a), where all permeation incidents for service lines were associated with 1 inch or less diameter pipes. For the same bulk concentration, the concentration of contaminant in pipe-water decreased with an increase in pipe size, mainly due to the increase of wall thickness and consequently the decrease of permeation rate.

In comparison with PE service lines, PE water mains have much lower susceptibility to permeation, particularly under a heavy contamination conditions. As shown in Figure 6.10, a bulk concentration of 10 mg/L would result in the exceedance of the benzene MCL in SIDR 9 series of PE service lines for a stagnation period of 8 hours, while that would not be expected to occur in DIPS DR 17.0 100PSI series of PE water mains. For water mains with a size of 14 inch or larger, the concentration of benzene in pipe-water would not exceed its MCL for a stagnation period of 8 hours even at an extremely high bulk concentration of 100 mg/L.

6.4 Conclusions

Pipe-bottle tests were conducted to investigate the permeation of petroleum-based aromatic compounds (BTEX) through 1-inch SIDR 9 PE pipe under simulated field conditions of gasoline leaks and spills, gasoline-contaminated groundwater, and gasoline-contaminated soil with various levels of contamination. Based on the analysis of experimental results, the following conclusions can be drawn:

(i) PE pipe was rapidly permeated when exposed to either free product gasoline, gasoline-contaminated water solutions, or gasoline-contaminated unsaturated soils. Benzene and toluene accounted for nearly all the total BTEX that permeated into the pipe-water when pipes were buried in the silica sand saturated with free product gasoline or gasoline-contaminated water solutions. Toluene and xylenes were the major compounds detected in the pipe-water when pipes were buried in the gasoline-contaminated unsaturated soils, while permeation of benzene and ethylbenzene was insignificant.

(ii) Using the time-lag method, the diffusion coefficients of BTEX compounds were estimated to be in the order of 10^{-8} cm^2/s when exposed to free product gasoline and in the order of 10^{-9} cm^2/s when exposed to gasoline-contaminated water solutions or unsaturated contaminated soils. The diffusion coefficients were concentration-dependent and might be influenced by the synergistic effect of organic mixtures.

(iii) The steady state permeation rates of BTEX compounds were strongly dependent on the bulk concentration. Empirical correlation equations (Eq. 6.2 and Eq. 6.3) were derived for the permeation rates and bulk concentrations. The equations can be used in conjunction with Eq. 6.4, Eq. 6.5 and Eq. 6.7 to predict the concentration of contaminants in pipe-water for different size PE pipes exposed to various bulk concentrations after a period of stagnation or under continuous flow conditions. Predictions using the empirical equations indicated that small size pipes were more vulnerable to permeation than large size pipes, and pipes with water stagnation periods posed a much higher risk of exceeding the MCL of benzene relative to pipes with continuous water flow.

(iv) PE pipes buried in soils of high organic matter were permeated to a lesser extent than a pipe buried in a soil of low organic matter. This is due to the sorption of organic compounds by the organic matter resulting in a lower soil pore water concentration than soils with low organic matter.

Acknowledgement

The authors thank the Awwa Research Fundation for its financial, technical and administrative assistance in funding and managing the project through which this information was discovered. The comments and views detailed herein may not necessarily reflect the

views of the Awwa Research Fiundation, its officers, directors, affiliates, or agents.

Reference

Chevron Phillips Chemical Company, 2003. The Performance Pipe: Engineering Manual. Chevron Phillips Chemical Company LP, Plano, TX.

Chiou, C.T. and L.J. Peters. 1981. Soil-Water equilibria for nonionic organic compounds. *Science*, 213(4508): 683-684.

Cline, P.V., J.J. Delfino, and P.S.C. Rao. 1991. Partitioning of aromatic constituents into water from gasoline and other complex mixtures. *Environmental Science and Technology*, 25(5): 914-920.

Crank, J. and G.S. Park, 1968. Diffusion in Polymers. Academic Press, London, UK.

Crank, J. 1975. The Mathematics of Diffusion. Clarendon Press, Oxford, UK.

Glaza, E.C. and J.K. Park. 1992. Permeation of organic contaminants through gasketed pipe joints. *Journal AWWA*, 84(7): 92-100.

Holsen, T.M., J.K. Park, L. Bontoux, D. Jenkins, and R.E. Selleck. 1991a. The effect of soils on the permeation of plastic pipes by organic chemicals. *Journal AWWA*, 83(11): 85-91.

Holsen, T. M., J.K. Park, D. Jenkins, and R.E. Selleck. 1991b. Contamination of potable water by permeation of plastic pipe. *Journal AWWA*, 83(8): 53-56.

Joo, J.C., J.Y. Kim, and K. Nam. 2004. Mass transfer of organic compounds in dilute aqueous solutions into high density polyethylene geomembranes. *Journal of Environmental Engineering*, 130(2):175-183.

Jutras, E.M., C.M. Smart, R. Rupert, I.L. Pepper, and R.M. Miller. 1997. Field-scale biofiltration of gasoline vapors extracted from beneath a leaking underground storage tank. *Biodegradation*, 8(1): 31-42.

Klute, A. 1986. Methods of soil analysis: part I: physical and mineralogical methods. Monograph Number 9. American Society of Agronomy, Madison, WI.

Nalylor, T.deV. 1989. *Permeation properties*. In: Comprehensive Polymer Science. Edited by Colin B. and Colin P. Pergamon Press, Oxford, UK.

Ong, S.K., J.A. Gaunt, F. Mao, C.L Cheng, L.E. Agelet, and C.R. Hurburgh. 2007. Impact of petroleum-based hydrocarbons on PE/PVC pipes and pipe gaskets. AwwaRF, Denver, CO.

Page, A.L. 1986. Methods of soil analysis: Part II: chemical and microbiological properties. Monograph Number 9. American Society of Agronomy, Madison, WI.

Park, J.K., L. Bontoux, D. Jenkins, and R.E. Selleck. 1991. Permeation of polybutylene pipe and gasket material by organic chemicals. *Journal AWWA*, 83(10): 71-78.

Park, J.K., J.P. Sakti, and J.A. Hoopes. 1996. Transport of aqueous organic compounds in thermoplastic geomembranes. II: Mass Flux Estimates and Practical Implications. *Journal of Environmental Engineering*, 130(2):807-813.

Saleem, M., A.A. Asfour, D. De Kee, and B. Harison. 1989. Diffusion of organic penetrant through lowdensity polyethylene (LDPE) films: effect of size and shape of the penetrant molecules. *Journal of Applied Polymer Science*, 37(3): 617- 625.

Sangam, H.P. and R.K. Rowe. 2001. Migration of dilute aqueous organic pollutants through HDPE geomembranes. *Geotextiles and Geomembranes*, 19(6): 329-357.

Thompson, C. and D.Jenkins. 1987. Review of water industry plastic pipe practices. AwwaRF, Denver, CO.

Uni-Bell. 2001. Handbook of PVC pipe design and construction. Uni-Bell PVC Pipe Association, Dallas, TX.

Vonk, M.W. 1985. Permeation of Organic Compounds through Pipe Materials. Publication No. 85. KIWA, Neuwegein, Netherlands.

Zhou, E. and R.L. Crawford, 1995. Effects of oxygen, nitrogen, and temperature on gasoline biodegradation in Soil. *Biodegradation*, 6(2):127.

Zytner, R.G. 1994. Sorption of benzene, toluene, ethylbenzene and xylenes to various media. *Journal of Hazardous Materials*, 38(11): 113-126.

Table 6.1 Physiochemical characteristics of soils used for testing

Soil	Silica sand	Organic topsoil	Sand-topsoil mixture
Soil pH	6.6	6.2	6.3
Organic carbon content (%)	Below detection limit	5.1	1.9
Specific surface area (m^2/g)	0.6	115	36
Particle size distribution			
Sand (%)	99.7	93.9	97.2
Silt (%)	0.3	5.1	2.5
Clay (%)	0	1.0	0.4

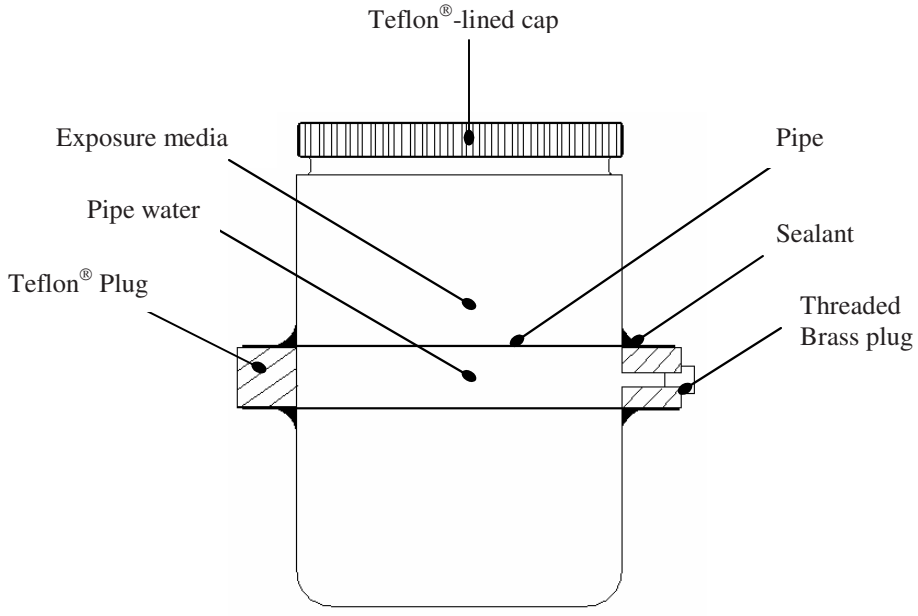

Figure 6.1 Pipe-bottle apparatus

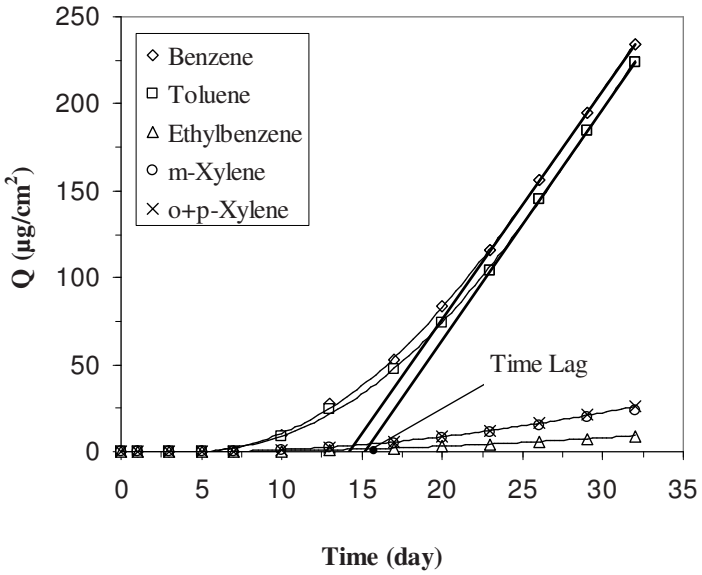

Figure 6.2 Cumulative mass permeated per unit area for BTEX compounds in PE pipe exposed to premium gasoline (Benzene, 19.8 g/L; toluene, 75.9 g/L; ethylbenzene, 14.7 g/L; m-xylene, 33.7 g/L; o+p xylene, 32.5 g/L)

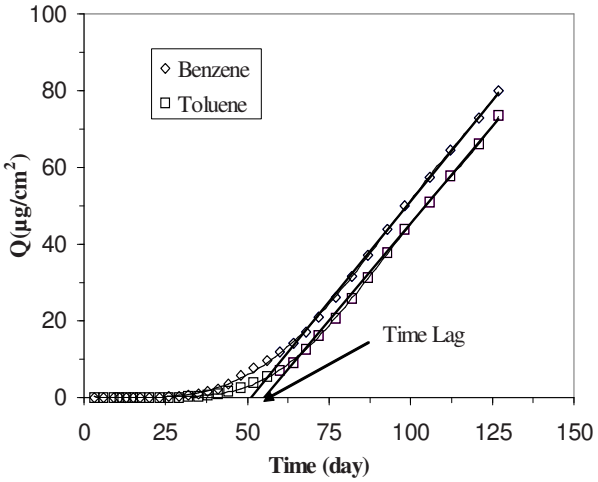

≈ 100% Saturated with gasoline: Total BTEX, 136.6±13.0 mg/L; benzene, 67.5±4.9 mg/L; toluene, 56.2 ± 4.9 mg/L

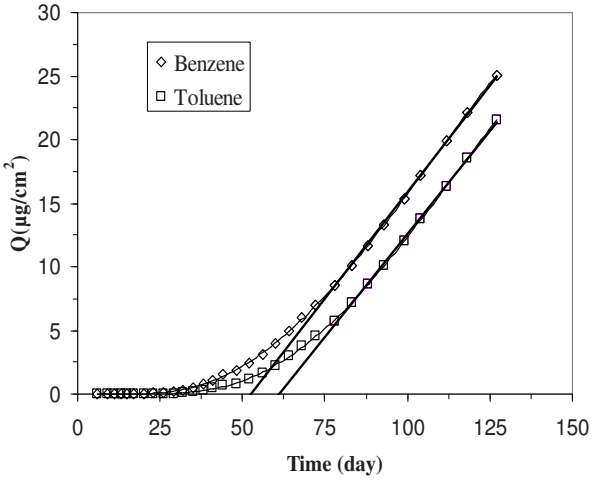

≈ 50% Saturated with gasoline: Total BTEX, 63.9±5.7 mg/L; benzene, 31.2±2.9 mg/L; toluene, 26.3±2.4 mg/L

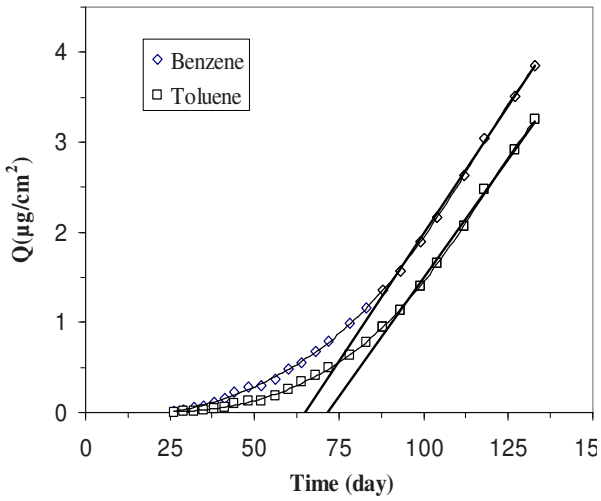

≈ 10% Saturated with gasoline: Total BTEX, 12.6±1.1 mg/L; benzene, 6.0±0.6 mg/L; toluene, 5.2±0.4 mg/L

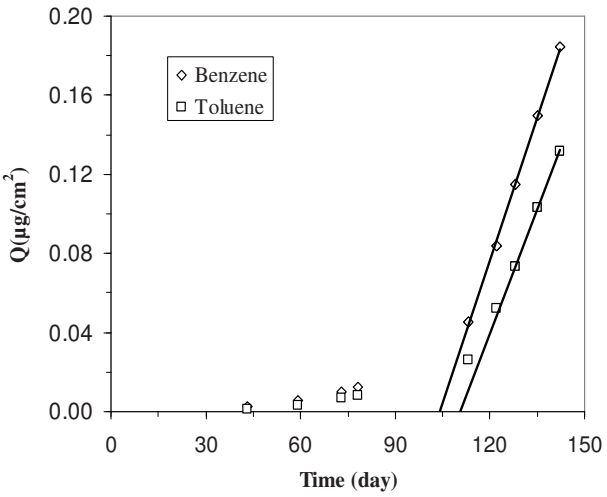

≈ 1% Saturated with gasoline: Total BTEX, 1.2±0.6 mg/L; benzene, 0.6±0.3 mg/L; toluene, 0.5±0.3 mg/L

Figure 6.3 Cumulative mass permeated per unit area for benzene and toluene in PE pipes exposed to gasoline-contaminated water solutions

Table 6.2 Comparison of diffusion coefficients obtained from this study with previous studies

Organic chemical	Materials	Exposure concentration (mg/L)	Diffusion coefficient ($\times 10^{-9}$ cm^2/s)	References
Toluene	HDPE pipe Wall thickness: 3.1 mm	56.2±4.9 26.3±2.4 5.2±0.4 0.5±0.3	3.4 3.0 2.6 1.8	This study
Toluene	LDPE pipe Wall thickness: 3.5 mm	91±16 49±11 31±5 2.9±1.3	4.7* 3.9* 3.9* 3.5*	Vonk (1985)
Toluene	HDPE geomembrane Thickness: 2.0 mm	30	3.3	Joo et al. (2004)
Toluene	HDPE geomembrane Thickness: 0.76 mm	100 50 10	5.3 3.6 3.2	Park et al. (1996)
Toluene	HDPE geomembrane Thickness: 2.0 mm	2	3.0	Sangam and Rowe (2001)
Benzene	HDPE pipe Wall thickness: 3.1 mm	67.5±4.9 31.2±2.9 6.0±0.6 0.6±0.3	3.6 3.5 2.9 1.8	This study
Benzene	HDPE geomembrane Thickness: 2.0 mm	30	8.5	Joo et al. (2004)
Benzene	HDPE geomembrane Thickness: 2.0 mm	2	3.5	Sangam and Rowe (2001)

** Calculated on the basis of the permeation data in the reference.*

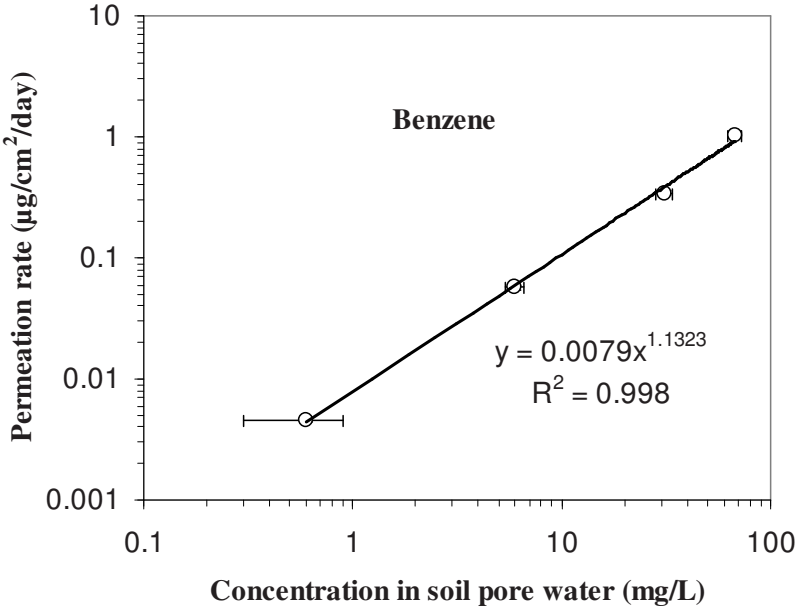

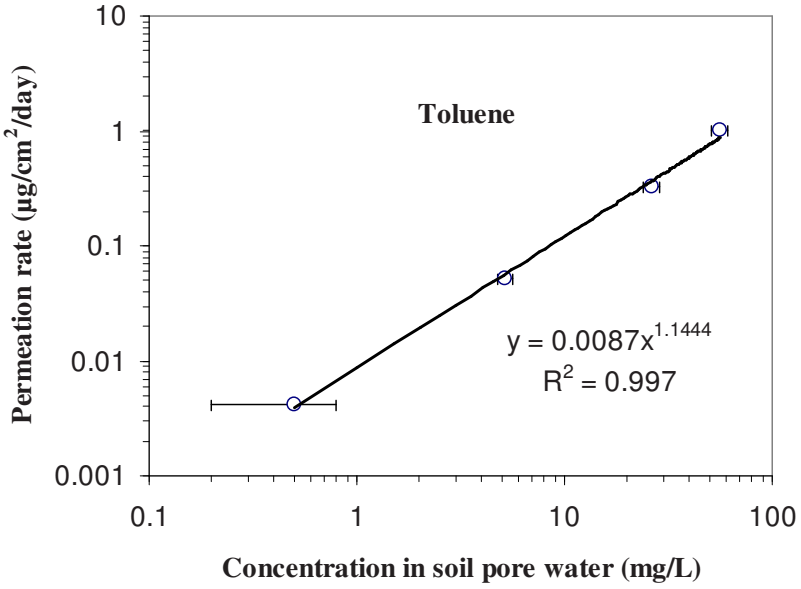

Figure 6.4 Correlation between the steady state permeation rates and the external bulk concentrations in soil pore water for benzene and toluene

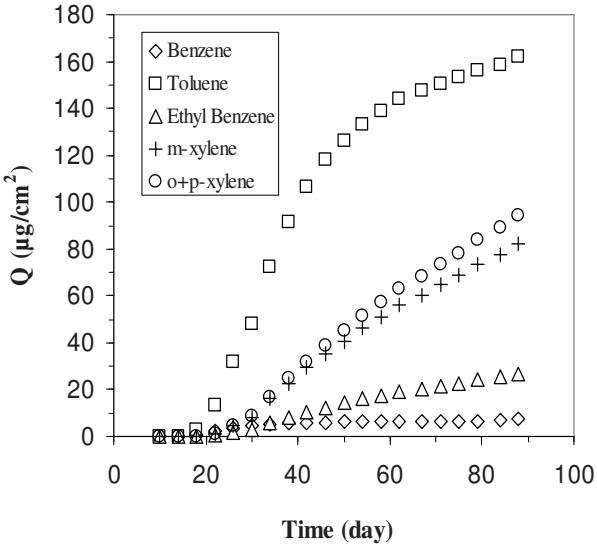

(a) Initial BTEX concentration (mg/kg dry soil): total BTEX, 1216; benzene, 72; toluene, 531; ethylbenzene, 85; m-xylene, 267; o+p-xylene, 261.

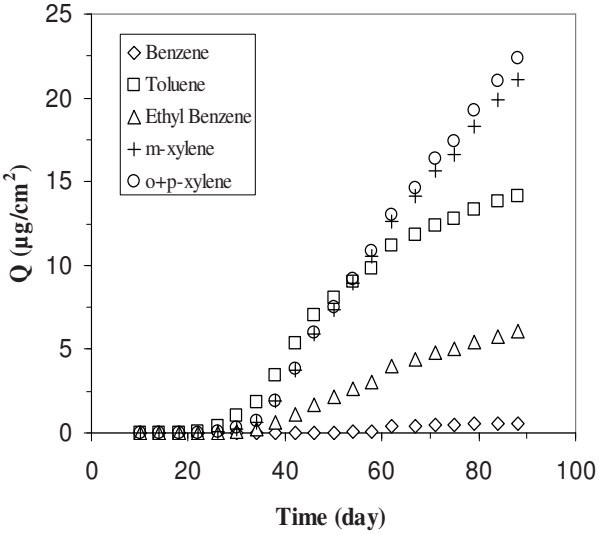

(b) Initial BTEX concentration (mg/kg dry soil): total BTEX, 388; benzene, 3; toluene, 119; ethylbenzene, 36; m-xylene, 115; o+p-xylene, 115.

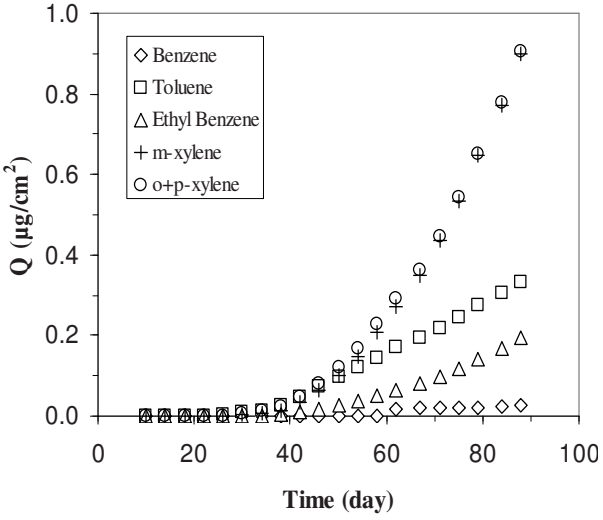

(c) Initial BTEX concentration (mg/kg dry soil): total BTEX, 89; benzene, <1; toluene, 9; ethylbenzene, 9; m-xylene, 34; o+p-xylene, 37.

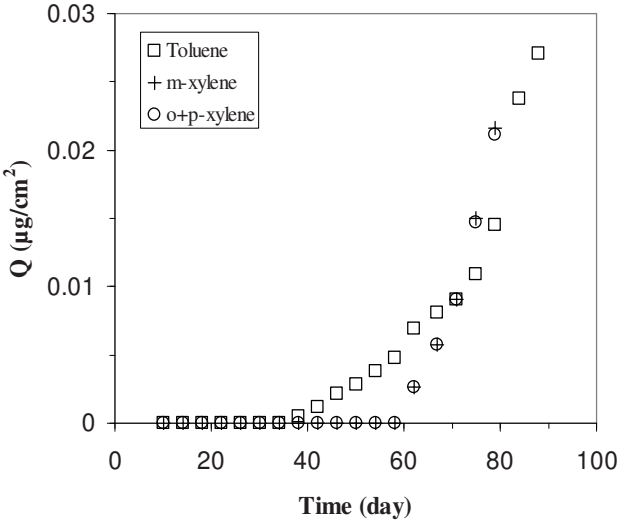

(d) Initial BTEX concentration (mg/kg dry soil): total BTEX, 32; benzene, <1; toluene, 3; ethylbenzene, 3; m-xylene, 12; o+p-xylene, 14.

Figure 6.5 Cumulative mass permeated per unit area for BTEX compounds in PE pipes exposed to gasoline-contaminated soils

Table 6.3 Permeation parameters for toluene, ethylbenzene and xylenes in PE pipes exposed to gasoline-contaminated soils

Chemical	External bulk concentration (mg/kg dry soil)	Breakthrough time (day)	Time lag (day)	Steady state permeation rate (µg/cm^2/day)	Diffusion coefficient (×10^{-9} cm^2/day)
Toluene	531	10	20	5.1	9.3
	119	14	30	0.43	6.1
	9	26	34	0.0061	5.4
	3	42	69	0.0014	2.7
ethylbenzene	85	18	22	0.5	8.4
	36	22	32	0.12	5.8
	9	38	53	0.0054	3.5
	3	-	-	-	-
m-xylene	267	14	23	1.5	8.1
	115	18	33	0.43	5.7
	34	30	55	0.027	3.4
	12	62	65	0.0016	2.9
o+p-xylene	261	14	23	1.7	8.1
	115	18	33	0.43	5.7
	37	30	55	0.027	3.4
	14	62	66	0.0016	2.8

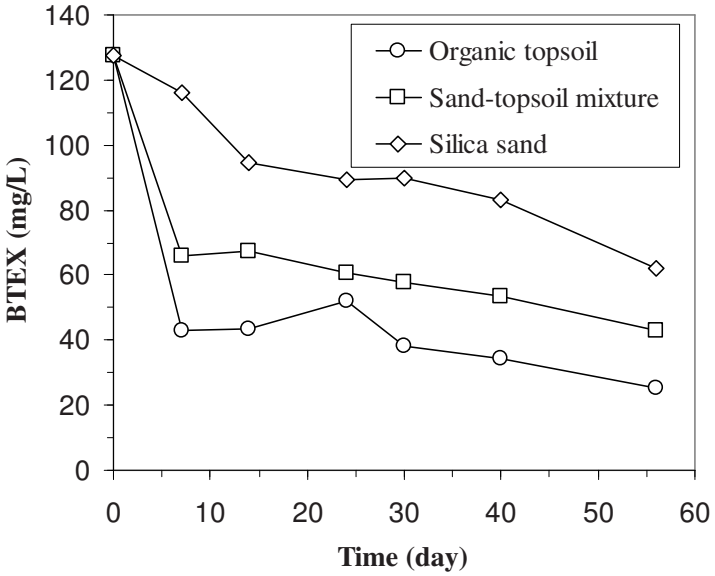

Figure 6.6 Change of total BTEX concentrations in soil pore water with exposure time

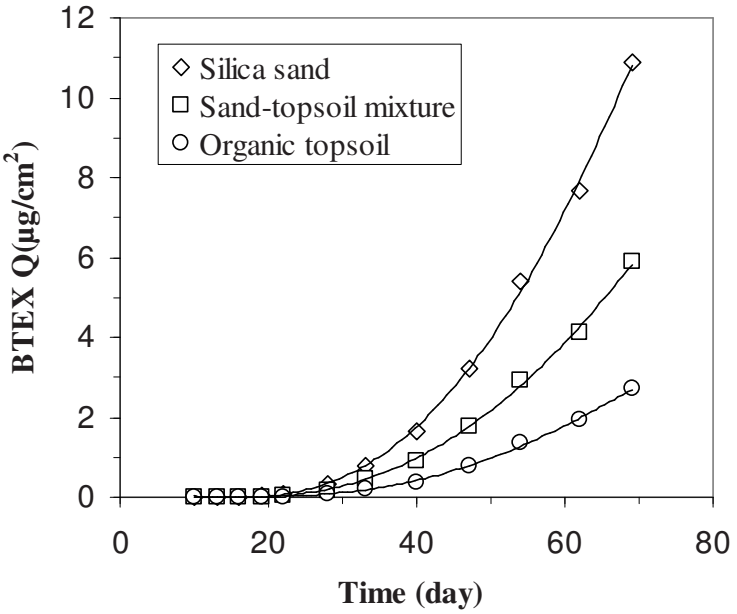

Figure 6.7 Cumulative mass of total BTEX permeated per unit area in PE pipes

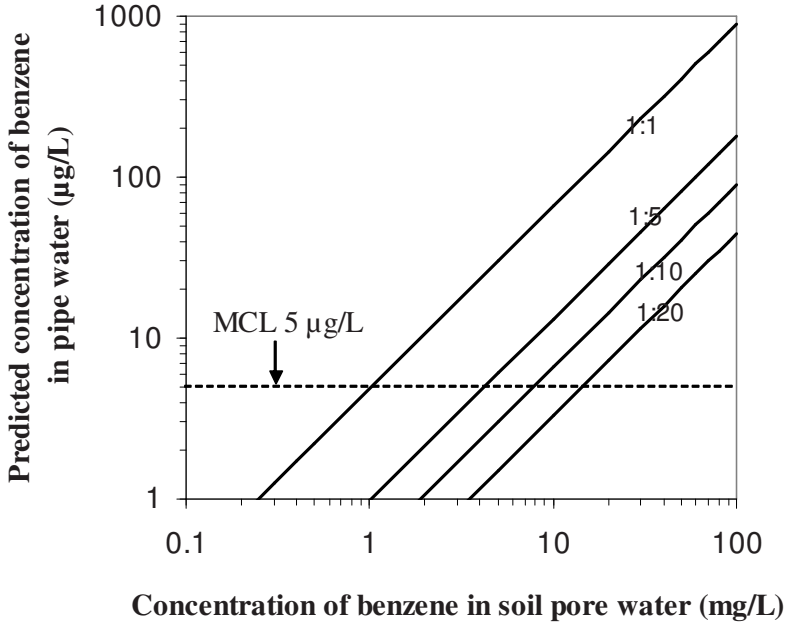

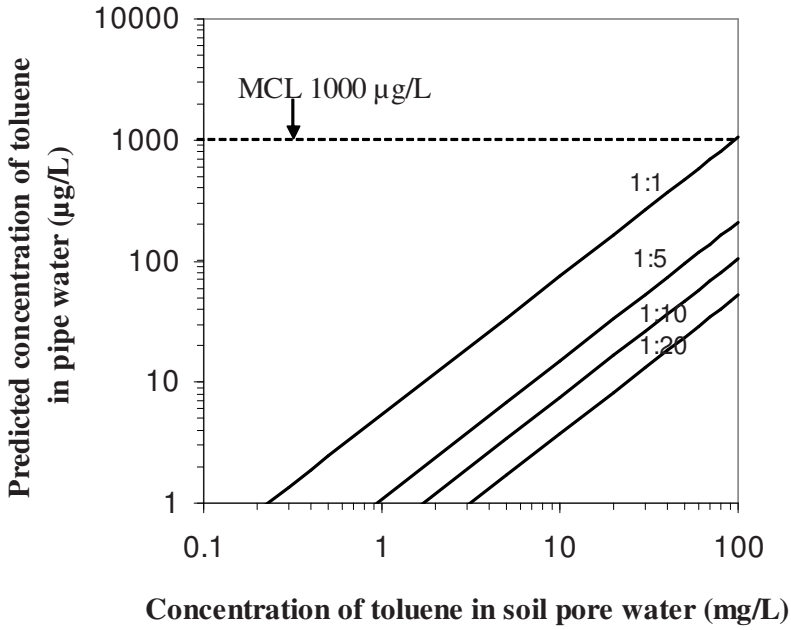

Figure 6.8 Concentrations of benzene and toluene in pipe water for various water bulk concentrations after 8-hour stagnation for 1-inch SIDR 9 PE pipe (ratios L_C/L_T = length of contaminated pipe/total length of pipe)

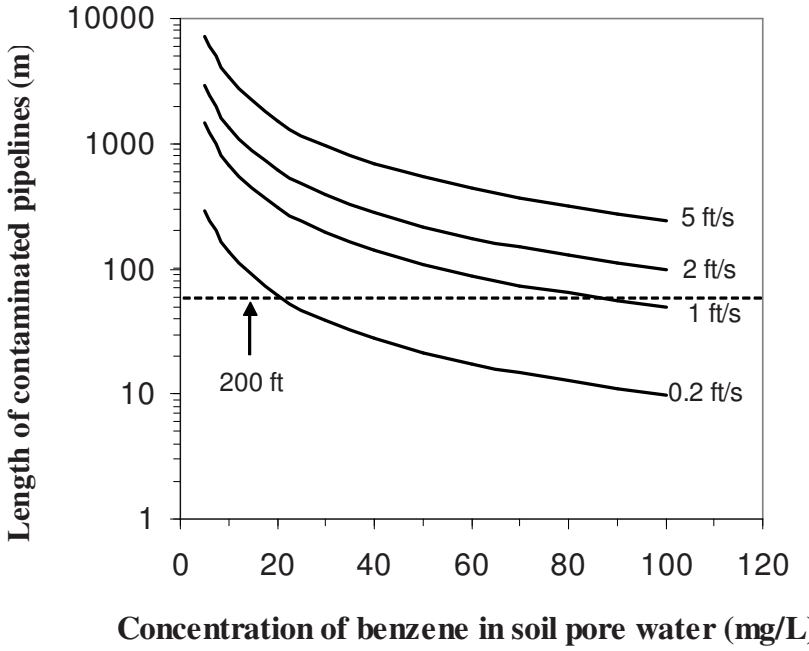

Figure 6.9 Length of contaminated pipe required to exceed the MCL of benzene (5 µg/L) in pipe water for various bulk concentrations and water flow velocities for 1-inch SIDR 9 PE pipe (L_C/L_T = 1:1)

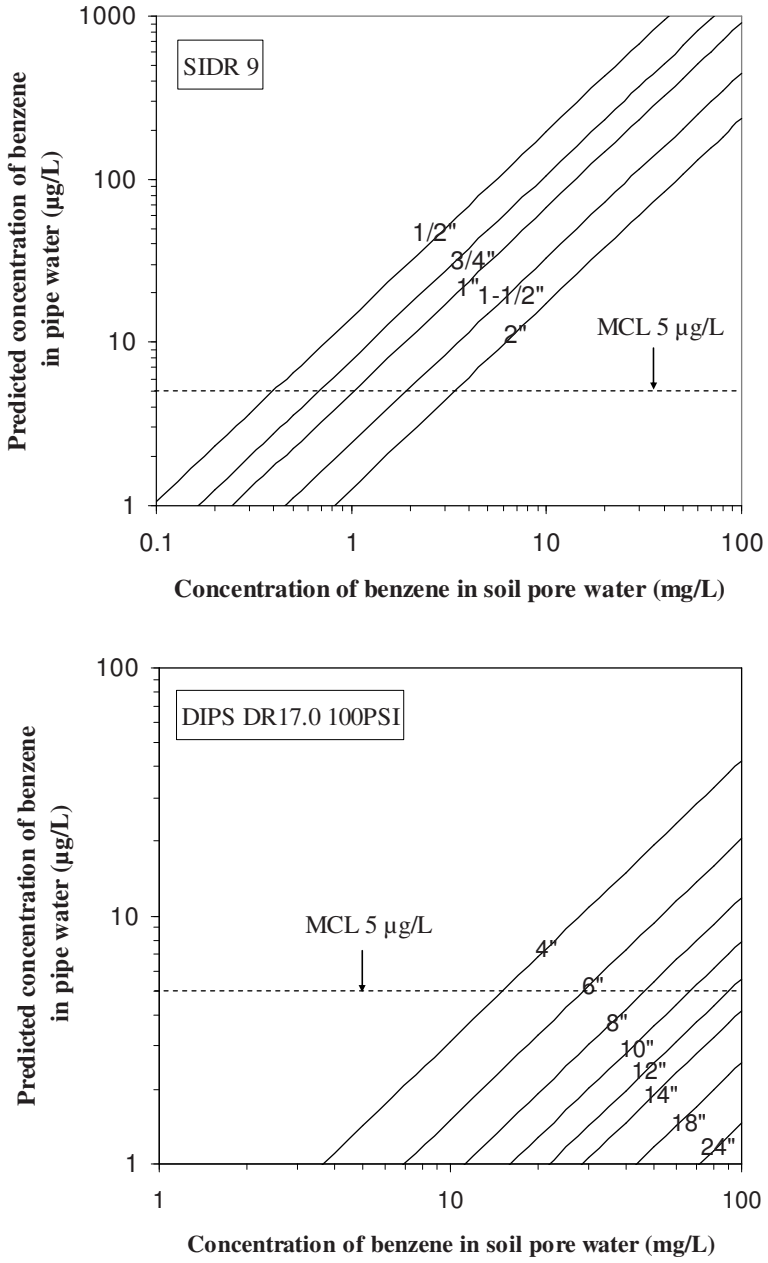

Figure 6.10 Predicted concentrations of benzene in pipe water for various bulk concentrations after 8-h stagnation for SIDR 9 and DIPS DR 17.0 PSI 100 series of PE pipe (L_C/L_T = 1:1)

CHAPTER 7. NUMERICAL MODELING OF PERMEATION OF BENZENE THROUGH POLYETHYLENE (PE) PIPES

A paper to be submitted to *Journal of American Water Works Association*

Feng Mao, James A. Gaunt, Say Kee Ong

Abstract

Permeation parameters of benzene in 1-inch SIDR 9 PE pipes were estimated by fitting the measured data to a permeation model based on a combination of equilibrium partitioning and Fick's diffusion. For bulk concentrations between 6.0 to 67.5 mg/L in soil pore water, the concentration-dependent diffusion coefficients of benzene were found to range from 2.0×10^{-9} cm^2/s to 2.8×10^{-9} cm^2/s while the solubility parameter was determined to be 23.7. The simulated permeation curves of benzene for SIDR 9 and SIDR 7 series of PE pipes indicated that small diameter pipes are more vulnerable to permeation than large diameter pipes and the breakthrough of organic contaminants is retarded and the corresponding permeation flux decreases with the increase of the pipe thickness. PE pipes exposed to an instantaneous plume exhibit distinguishable permeation characteristics from those exposed to a continuous source with a constant input. The properties of aquifer such as dispersion coefficients (D_L) also influence the permeation behavior of organic contaminants through PE pipes.

Keyword: Permeation; Benzene; PE pipes; Fick's diffusion.

7.1 Introduction

In many urban areas, plastic pipes used for the conveyance of drinking water in water distribution systems may come into contact with contaminated soils as a result of leaks from underground storage tanks, chemical spills, and improper disposal of used chemicals. These pollutants from leaking storage tanks and contaminated soils may permeate through the plastic materials, resulting in drinking water contamination (Thompson 1987; Ong et al., 2007).

The majority of the reported permeation incidents were associated with petroleum products, mainly due to gasoline spills or leaks (Thompson 1987; Ong et al., 2007). The aromatic compounds in gasoline, benzene, toluene, ethyl benzene and o-, m-, and p-xylene (BTEX), permeated polybutylene (PB) and polyethylene (PE) pipes readily and were the compounds of concern in permeation incidents (Holsen et al., 1991). Among BTEX compounds, benzene is of the most concern because it is highly toxic and is a known carcinogen, and therefore it is a U.S. Environmental Protection Agency "priority pollutant." A concentration range of 13 to 1300 μg/L for benzene in drinking water after a period of stagnation of the water has been recorded as a result of permeation through PB and PE pipes (Holsen et al., 1991). In a recent study by Ong et al. (2007), permeation by benzene through 1-inch diameter high density polyethylene (PE) pipe was found to be rapid. Breakthrough times were in the order of 5 days for exposure to free product gasoline and 15 days for gasoline-saturated groundwater.

To improve the level of understanding of permeation mechanisms and risks related to PE pipes, however, it is necessary to model the permeation process of organic compounds, even though permeation is rapid and obvious. Fick's law is commonly used to predict

permeation but requires the permeation characters such as diffusion coefficients a prior. Conventionally, the diffusion coefficient for a penetrate-polymer pair was determined by permeation experiments with the time-lag method (Crank, 1975), which is based on the fact that the permeation rate of a penetrant that is brought into contact with a polymer sample becomes constant with time if the exposure concentration is kept a constant. Using the time-lag method, the concentration-dependent diffusion coefficients of benzene in PE pipes were estimated as on the order of 10^{-8} cm^2/s under the exposure of free product gasoline and on the order of 10^{-9} cm^2/s under the exposure of gasoline-contaminated water solutions (Ong et al., 2007).

With the estimated diffusion coefficients, permeation risks for different diameter size PE pipes can be evaluated assuming that the data obtained from small diameter pipe experiments can be scaled up for other diameters based on the permeation theory (Ong et al., 2007). Water utilities are interested in the early stage of the permeation process, particularly the breakthrough time for a certain size pipe under a given contaminant level so that necessary activities can be taken within appropriate time.

However, the constant exposure conditions for the lab experiments to simulate field conditions may not reflect the actual permeation incidents in the real world where the concentration may change with time when a groundwater plume travels through the area where pipes are buried. More specifically, it would be of interest to study the permeation characteristics if the contaminant plume is due to an instantaneous source or due to a continuous source with a constant input.

The objective of this study was to model the permeation process of benzene through PE pipes using a numerical modeling method based on the Fick's diffusion and experimental

results of the pipe-bottle tests (Ong et al., 2007). More specifically, this study aimed to i) fit the measured permeation data to a Fick's permeation model to determine permeation parameters such as diffusion coefficients of benzene for pipe-bottle experiments; ii) to estimate the breakthrough time of benzene and their steady permeation flux into PE pipes of different diameters (sizes) under different exposure contamination levels; and iii) to examine how time-dependent boundary conditions affect the permeation characteristics of benzene in PE pipes.

7.2 Methods

7.2.1 Permeation theory and modeling scheme

Figure 7.1 shows the schematic of the permeation process of organic contaminants from the exterior environment (groundwater) to the water in the pipe. Permeation occurs by a three-step process: (i) partitioning of the contaminant between the ground water and the outer wall of the pipe; (ii) diffusion of the contaminant through the pipe; and (iii) partitioning of the contaminant between the inner wall of the pipe and water in the pipe. Both partitioning steps proceed according to Henry's law

$$C_p^1 = SC_a^1 \qquad \text{(Eq. 7.1)}$$

$$C_p^2 = SC_a^2 \qquad \text{(Eq. 7.2)}$$

where C_p^1 is the concentration of the contaminant on the outer wall of pipe in contact with the exterior environment (M/L^3); C_a^1 is the concentration of the contaminant in the exterior environment such as groundwater (M/L^3); C_p^2 is the concentration of the contaminant on the inner wall of pipe in contact with the water in the pipe (M/L^3); C_a^2 is the concentration of the

contaminant in the water in the pipe (M/L^3); and S is the partitioning coefficient (solubility parameter, dimensionless) and is a constant for given contaminant and temperature of interest.

Fick's diffusion was proposed as the dominant mechanism for the diffusion of organic contaminants through PE pipes (Vonk, 1985). For diffusion in a cylinder (such as PE pipes), the governing equation of Fick's law is

$$\frac{\partial C_p}{\partial t} = \frac{1}{r}\frac{\partial}{\partial r}(rD\frac{\partial C_p}{\partial r}) \qquad \text{(Eq. 7.3)}$$

where C_p is the concentration of the contaminant in the PE material (M/L^3); and D is the diffusion coefficient (L^2/T); and r is the cylindrical coordinate (L). The AWWA standard dimension ratio DR (the ratio of the inside pipe diameter to the wall thickness) for the tested 1-inch SIDR 9 PE pipes is 9. At this dimension ratio, the effect of pipe curvature on permeation can be safely ignored and the problem is reduced to that of a thin shell (Selleck and Marinas, 1991). Therefore, the governing equation of Fick's law becomes

$$\frac{\partial C_p}{\partial t} = D\frac{\partial^2 C_p}{\partial x^2} \qquad \text{(Eq. 7.4)}$$

For laboratory pipe-bottle experiments, the total quantity of contaminants diffusing into PE pipes as a function of time, $Q_t(M/L^2)$, was measured under relatively strict conditions with (i) the concentration of the contaminant in the bulk solution (C_a^1) remained relatively constant; (ii) the initial concentration of the contaminant in the PE material was zero; and (iii) the inner concentration of the contaminant in the pipe water (C_a^2) was kept as low as possible by changing water frequently and assumed zero for the convenience of modeling. The initial and boundary conditions for modeling can be assumed to be

$$
\begin{aligned}
&t < 0, \quad 0 \le x \le l, \; C_p = 0 \quad \text{(inital condition)} \\
&t \ge 0, \quad x = 0, \; C_p = SC_a^1 \quad \text{(boundary condition for outer wall)} \\
&t \ge 0, \quad x = l, \; C_p = 0 \quad \text{(boundary condition for inner wall)}
\end{aligned}
\qquad \text{(Eq. 7.5)}
$$

where l is the wall thickness (L). Given a sufficient exposure time, the steady-state permeation flux [$M/(L^2/T)$] is

$$F = DS\frac{(C_a^1 - C_a^2)}{l} = DS\frac{C_a^1}{l} \qquad \text{(Eq. 7.6)}$$

In the permeation experiments, F is directly measured and D estimated using the time-lag method. Therefore, S can be determined using Eq. 7.6.

7.2.2 Determination of diffusion coefficient and solubility parameter

The diffusion coefficient and solubility parameter of benzene under three exposure conditions (C_a^1= 67.5±4.9 mg/L, 31.2±2.9 mg/L, and 6.0±0.6 mg/L, respectively) were determined by fitting the measured permeation data for 1-inch SIDR 9 PE pipes to the permeation model. Explicit method was applied to estimate the cumulative permeation flux with time. The scheme is briefly described as follows:

(i) Consider $0 \le x \le l$ and subdivide [$0,l$] into m equal subintervals (dx), i.e., $dx = l/m$ and ($x_1, x_2, \ldots, x_m, x_{m+1}$) = ($0, dx, 2dx, \ldots, l - dx, l$);

(ii) Similarly, consider $0 \le t \le T$ and subdivide [$0, T$] into k equal subintervals (dt), i.e., $dt = T/k$ and ($t_1, t_2, \ldots, t_k, t_{k+1}$) = ($0, dt, 2dt, \ldots, T - dt, T$);

(iii) Explicit method

$$\frac{\partial c_p}{\partial t} \approx \frac{c_{i,j+1} - c_{i,j}}{dt} \qquad \text{(Eq. 7.7)}$$

$$\frac{\partial^2 c_p}{\partial x} \approx \frac{c_{i-1,j} - 2c_{i,j} + c_{i+1,j}}{(dx)^2} \quad \text{(Eq. 7.8)}$$

$$\frac{c_{i,j+1} - c_{i,j}}{dt} \approx D\frac{c_{i-1,j} - 2c_{i,j} + c_{i=1,j}}{(dx)^2} \quad \text{(Eq. 7.9)}$$

$$Define: r_p = \frac{D \times dt}{(dx)^2} \quad \text{(Eq. 7.10)}$$

$$c_{i,j+1} = r_p c_{i-1,j} + (1 - 2r_p)c_{i,j} + r_p c_{i+1,j} \quad \text{(Eq. 7.11)}$$

The formula was used to calculate all the values of *c* at step *j +1* using the values at step *j*. The permeation flux into the pipe at step *j* can be estimated by:

$$F_j = D \times \frac{c_{m,j} - c_{m-1,j}}{dx} \times dt \quad \text{(Eq. 7.12)}$$

For the curve fitting process, the diffusion coefficients and the solubility parameters were determined by the time-lag method and used as the starting values. The cumulative permeation flux was then estimated following the steps described above. The two parameters were adjusted through several trials until the observed data points matched the theoretical permeation curve. The least-square method was used to test whether the "best fit" was achieved. A special consideration was that the solubility parameters determined for the three exposure conditions should be identical since this parameter is assumed to be independent of the exposure concentration.

7.2.3 Estimation of breakthrough times and permeation fluxes for pipes with varied different diameters

Based on the thermodynamic view of the permeation process, the permeation of organic molecules through polymer materials is dependent on the chemical characteristics

and concentration (activity) of the contaminant, the chemical characteristics of the polymer, and the interactions between the contaminant and the polymer. For the same pipe materials and the same exposure conditions, the diffusion coefficient (D) and the solubility parameter (S) obtained from 1-inch pipe SIDR 9 PE pipe experiments would remain valid for other pipe sizes. Permeation is then reduced to the effects of wall thickness of the pipe.

Model simulation was conducted for SIDR 9 and SIDR 7 series of commercial HDPE pipes (Table 7.1). Based on manufacturer's specification, SIDR 7 series pipes are of similar material to that of SIDR 9 series. The breakthrough times of organic contaminants were obtained by returning the simulation time once the arbitrary requirement (permeation flux <= 0.001 $\mu g/cm^2$) was not met. The slopes of simulated permeation curves in later time (steady-state) periods were calculated to estimate the steady permeation flux for each size of pipe.

7.2.4 Predication of permeation behavior under time-dependent boundary conditions

The surface concentration at the outer wall generally varies with time in the field conditions, such as a groundwater plume traveling through the area where the pipes are buried, or decay of environmental contaminants due to biodegradation. For these cases, the boundary conditions for the outer wall (Equation 7.5) can be modified to

$$t \geq 0, x = 0, \ C_p = SC_a^1(t) \qquad \text{(Eq. 7.13)}$$

where $C_a^1(t)$ is the concentration of the contaminant in the bulk solution at time (t). This study simulated three time-dependent boundary conditions: (i) degradation of organic contaminants with the first-order kinetics; (ii) a continuous source with a constant input of contaminants; and (iii) a pulse source or a spill.

Case I: Degradation with the first-order kinetics

The first-order degradation kinetics can be described by:

$$C_a^1 = C_0 e^{-kt} \qquad \text{(Eq. 7.14)}$$

where C_0 is the initial concentration (M/L^3) and k is the first order degradation constant (T^{-1}) of specific organic compound in an aquifer. For a specific compound, there is a large variation in degradation rate constant among different studies, mainly due to the difference in experimental conditions and aquifer characteristics. Here, 0.005~ 0.02 day^{-1} for benzene was selected on the basis of the in-situ data reported by Nielsen (1996). C_0 was arbitrary set as 31.2 mg/L, an exposure concentration used in Ong's study (2007).

Case II: Continuous source with a constant input

The concentration, C, at some distance, L, from the source at concentration, C_0, at time t, is given by the following expression (Fetter, 2000), where *erfc* is the complementary error function:

$$C_a^1 = \frac{C_0}{2}\left[erfc\left(\frac{L - v_x t}{2\sqrt{D_L t}}\right) + \exp\left(\frac{v_x}{D_L}\right) erfc\left(\frac{L + v_x t}{2\sqrt{D_L t}}\right)\right] \qquad \text{(Eq. 7.15)}$$

where L is the flow path length (L), v_x is the average linear groundwater velocity(L/T), t is the times since release of the contaminant (T), and D_L is the longitudinal dispersion coefficient(L^2/T). This simulation assumed: L = 10 m (a drinking water pipe about 10 m from a leaking storage tank); v_x = 0.05 m/day (a typical value for groundwater movement in a sandy aquifer); D_L=0.001~0.05 m^2/day. C_0 was set as 31.2 mg/L, being identical to that of Case I.

Case III: Instantaneous Source

The concentration of an instantaneous source of contaminant is best described using a Gaussian distribution curve. This variation of the advection-dispersion equation assumes a homogeneous, isotropic, and saturated porous medium; steady state flow; and conditions where Darcy's Law applies (Fetter, 1990). The change of concentration in a pulse source with time in one dimension can be predicted by:

$$C_a^1 = \frac{M}{(4\pi D_L t)^{1/2}} \exp\left[\frac{-(L - v_x t)^2}{4 D_L t}\right] \qquad \text{(Eq. 7.16)}$$

where M is mass of contaminant per unit cross-sectional area (M/L^2). This simulation used the same values for parameters of L, v_x, and D_L, which were previously described in Case II. M was arbitrary set as 38 mg/L.

As indicated above, the concentration at the outer wall varies with time were given in the form of algebraic formula (Equation 7.16, 7.17 and 7.18). The data was substituted directly at each time step into the explicit scheme, i.e., at each time step the boundary condition for the outer wall was updated on the basis of the given algebraic formulas.

Scilab, a numerical computational package developed by INRIA and ENPC in Paris, France, was used to do all numerical analysis. Distributed with open source freely via the internet since 1994, *Scilab* is widely used as a powerful open computing environment for engineering and scientific applications (Bunks et al., 1999).

7.3 Results and Discussion

7.3.1 Determination of diffusion coefficient and solubility parameter

As shown in Figure 7.2, the measured data were well fitted by the permeation model

(SSEs were 41 $(\mu g/cm^2)^2$, 5 $(\mu g/cm^2)^2$, 4 $(\mu g/cm^2)^2$, respectively). The predicted curve captured the main characteristics of experimental data, i.e., there was a transient state from the time the organic contaminant first entered the pipe until the steady state conditions was established. This simulation study confirmed the previous assumption that the Fickian diffusion is the main mechanism for organic compounds to diffuse through PE pipe (Vonk, 1985).

Table 7.2 summarizes the permeation parameters (diffusion coefficients, solubility parameters, and steady-state permeation rates) of benzene determined by the numerical modeling method for the different bulk exposure concentrations. It indicates that diffusion coefficients (D) as shown in Table 7.2 were concentration-dependent and increased with an increase in bulk exposure concentration (C_a^1). This concentration effect may be attributed to increased mobility of polymer segments resulting from increases in the average free volume in the polymer caused by the presence of the diffusing contaminant (Crank and Park 1968). The relationship between D and C_a^1 can be described by

$$D = D_0 e^{\alpha C_a^1} = 1.94 \times 10^{-9} e^{0.0055 C_a^1} \quad (R^2=1) \qquad \text{(Eq. 7.17)}$$

where D_0 is the diffusion coefficient in the limit as $C_a^1 \rightarrow 0$ (L^2/T), the characteristic diffusion coefficient for a specific polymer-penetrant pair; and α is the concentration-dependent constant. The exponential relationship between D and the bulk concentration have been found in the permeation of 1,2-dichloropropane through polybutylene pipes (Park et al., 1991) and the permeation of *m*-xylene through HDPE geomembranes (Park et al., 1996).

Using a constant solubility parameter (S) of benzene led to a good fitting for all observed data. The value of S determined in the present study (23.7) was very close to those

obtained from two previous studies, 25.0 (Henri and Rowe, 2001), and 28.2 (Joo et al., 2004) on the permeation of benzene through HDPE geomembranes.

Included in Table 7.2 for comparison purposes are the permeation parameters obtained from the time lag method. Although the two methods used the same initial and boundaries, the results of the permeation parameters were different. Under a given exposure concentration, the diffusion coefficient of benzene determined by the numerical modeling method was approximately 30% lower than that of the time lag method while the steady-state permeation rate of benzene was 15%~25% higher. The solubility parameters estimated from the time-lag method were much lower and seemed to vary with the bulk concentrations, deviating from the predictions that the solubility parameter is a characteristic parameter for a specific polymer-penetrant pair and should be independent of the bulk concentration. To avoid the intensive mathematical treatment required by other numerical techniques, the time lag method, an analytical method, only utilizes the steady-state permeation data and the diffusion coefficient estimated from the lag time. The accuracy of the estimates of the method is strongly dependent on the accuracy of the steady-state permeation data. For experiments using dilute aqueous solutions, it is difficult to ascertain whether the steady-state permeation is achieved, mainly due to the slight change of the permeation flux with time and the random errors occurred in the measurements. Therefore, the time lag method may mistakenly treat the transient or near-steady state data as the steady-state data, resulting in the underestimation of the steady-state permeation rate and the overestimation of the diffusion coefficient. To estimate the permeation parameters of organic contaminants in plastic pipes with the time lag method, this study suggests that the “steady-state” permeation data must be

carefully examined and the effectiveness of the time lag method need to be tested by other techniques such as by numerical modeling.

7.3.2 Estimation of breakthrough times and permeation fluxes for pipes with different diameters

Simulated permeation curves were obtained for SIDR 9 and SIDR 7 series of HDPE pipes using the diffusion coefficients and solubility parameter of benzene determined by the numerical modeling method (Figure 7.3). It is evident from Figure 7.3 that small size pipes are more vulnerable to permeation than large diameter pipes. Under identical exposure conditions, benzene breakthrough is longer and its permeation flux decreased with the increase in pipe diameters. For an identical pipe dimension, SIDR 7 series pipe is less permeable than SIDR 9 series pipe. This is due to the fact that, SIDR 7 series (200 psi pressure rated) generally has a thicker wall than SIDR 9 pipe (160 psi pressure rated). Figure 7.3 also reveals that it takes a longer time for larger diameter pipes to reach the steady-state permeation and thus it is experimentally more difficult infeasible to use the time-lag method to determine the permeation parameters for 2-inch or larger diameter pipes.

Table 7.3 summarizes the breakthrough times and the steady-state permeation rates of benzene for various pipe diameters under three exposure conditions. As shown in Table 7.3, benzene rapidly permeates across 1/2-inch HDPE pipe lines within several days, while the breakthrough for 2-inch HDPE pipe lines occurs in one to a few months. The steady-state permeation rate of benzene for 1/2-inch pipe is more than three times higher than that for 2-inch diameter pipe. The permeation rates determined by the numerical modeling method were identical to those directly calculated from Equation 7.6.

7.3.3 Prediction of permeation behavior under time-dependent boundary conditions

Case I: degradation with the first-order kinetics

As shown in Figure 7.4, the permeation flux of benzene decreased with an increase of in the first-order rate constant. That is not surprising, since large degradation rate constant indicates rapid degradation of organic compound surrounding pipes and the permeation flux is strongly dependent upon the external bulk concentration. For the three degradation conditions, the obtained permeation curves deviated from that of no decay condition at later time period and the rising slope became gentle with an increase in the first order constant. However, the breakthrough of benzene occurs at the same time for the four conditions simulated, which implies that the degradation process is unable to prevent or retard the occurrence of permeation once the outer wall of pipes is contaminated and that breakthrough is only a function of the wall thickness. .

Case II: continuous source with a constant input

If the flow length (the distance between the contaminant source and the target pipe) and the average linear groundwater velocity are constant, the concentrations of the contaminant in the groundwater for a given time are strongly dependent upon the hydrodynamic dispersion coefficients (D_L) as seeing in Figure 7.5 (a). The benzene plume in the aquifer with the highest D_L first reaches the target pipe, resulting in the rapid breakthrough of benzene at the pipe. On the contrary, the breakthrough time for lower D_L is retarded. Due to the continuous and constant release of benzene, the external concentration of benzene surrounding pipes finally reach a constant value and consequently the four permeation curves with different dispersion coefficients will be of the same magnitude, showing a linear increase with time, a characteristic of permeation curve for constant

boundary conditions.

Case III: instantaneous source

An instantaneous source (such as a spill) yields a slug that grows with time as it moves down the groundwater flow path. In this case, D_L also significantly influences the contaminant concentration in groundwater and therefore the permeation behavior of contaminant through pipes, since it determines when the target pipe will be affected by contaminants and the time duration. As shown in Figure 7.5, the highest D_L leads to the fastest breakthrough of benzene while the breakthrough is significantly retarded for lower D_L. Corresponding to the increase and decrease in the external concentration profile, the permeation curve at lower D_L is characterized by a dramatic increase in permeation flux, followed by a rapid transition to stationary phase. At higher D_L, the contrary trend is observed.

7.4. Conclusion

Numerical modeling of the permeation of benzene through HDPE pipes using the Scilab language was conducted. Based on the results of the numerical computation and analysis, the following conclusion can be drawn:

(i) The measured data obtained from the pipe-bottle tests were well fitted using the permeation model based on a combination of equilibrium partition and classic Fick's diffusion. The results indicate that Fick's diffusion is the main mechanism for organic compounds to diffuse through PE pipe.

(ii) The numerical modeling method provided a better estimation for permeation parameters than the time lag method since it evaluates both the transient and steady-state

permeation data. For the bulk concentrations between 6.0 and 67.5 mg/L in soil pore water, the concentration-dependent diffusion coefficients of benzene were found to range from $2.0\times10^{-9}cm^2/s$ to $2.8\times10^{-9}cm^2/s$ while the solubility parameter was determined to be 23.7.

(iii) Small diameter pipes are more vulnerable to permeation than large diameter pipes. Under identical exposure conditions, the breakthrough of organic contaminants will be retarded and the corresponding permeation flux will decrease with the increase of the pipe thickness.

(iv) Under field conditions, the permeation behavior of a specific organic compound is strongly dependent on the characteristics of contaminant source (instantaneous source or continuous source) and the properties of aquifer such as dispersion coefficients (D_L), which implicitly determine the effective contaminant concentration in soil water that are available for permeation of the compound through pipe materials.

Acknowledgment

The authors thank the Awwa Research Fundation for its financial, technical and administrative assistance in funding and managing the project through which this information was discovered. The comments and views detailed herein may not necessarily reflect the views of the Awwa Research Fiundation, its officers, directors, affiliates, or agents.

Reference

Berens, A.R. 1985. Prediction of organic chemical permeation through PVC pipe. *Journal AWWA*, 77(11): 57-64.

Bunks, C., J.P. Chancelier, F. Delebecque, and M. Goursat. Engineering and Scientific Computing with Scilab. 1999. Birkhäuser, Boston.

Crank J. and G.S. Park 1968. Diffusion in Polymers. Academic Press, London, UK.

Crank J. 1975. The Mathematics of Diffusion. Clarendon Press, Oxford, UK.

Fetter, C.W. 1999. Contaminant Hydrogeology. Prentice-Hall, Inc, New Jersey.

Fetter, C.W. 2000. Applied Hydrogeology (4th edition). Prentice-Hall, Inc, New Jersey.

Holsen, T. M., J. K Park, D. Jenkins, and R.E. Selleck. 1991. Contamination of potable water by permeation of plastic pipe. *Journal AWWA*, 83(8): 53-56.

Joo, J.C., J. Y. Kim, and K.Nam.2004. Mass transfer of organic compounds in dilute aqueous solutions into high density polyethylene geomembranes. *Journal of Environmental Engineering*, 130 (2):175-183.

Nielsen, P.H., P.L.Bjerg, P.Nielsen, P.Smith, and T.H.Christensen. 1996. In situ and laboratory determined first-order degradation constants of specific organic compounds in an aerobic aquifer. *Environmental Science and Technology*, 30(1): 31-37.

Ong, S.K., J.A.Gaunt, F. Mao, C.L. Cheng , L.E. Agelet, and C.R.Hurburgh. 2007. Impact of petroleum-based hydrocarbons on PE/PVC pipes and pipe gaskets. AwwaRF, Denver, CO.

Selleck, R.E. and Marinas B.J. 1991. Analyzing the permeation of organic chemicals through plastic pipes. *Journal AWWA*, 83(8): 92-97.

Thompson, C. and D. Jenkins. 1987. Review of water industry plastic pipe practices. AwwaRF, Denver, CO.

Vonk, M.W. 1985. Permeation of organic compounds through pipe materials, Pub. No. 85. KIWA, Neuwegein, Netherlands.

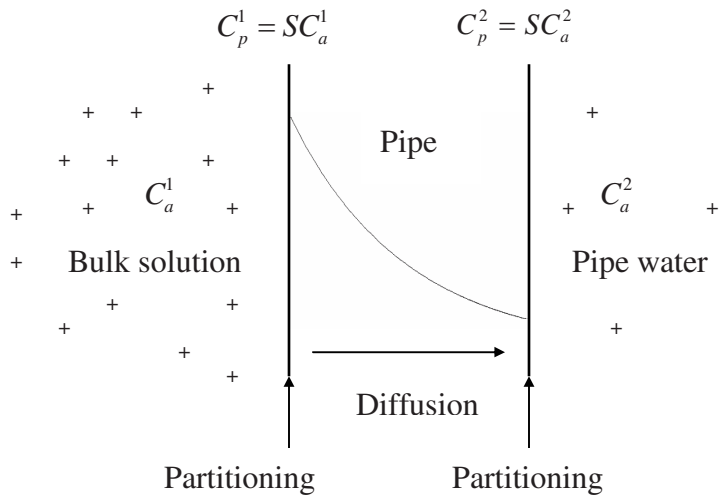

Figure 7.1 Schematic of permeation of organic contaminants through PE pipes

Table 7.1 Dimension of SIDR 7 and SIDR 9 series of HDPE pipes

Pipe type	Nominal O.D. (inch)	O.D. (inch)	I.D. (inch)	Average wall thickness (inch)	O.D. (cm)	I.D. (cm)	Average wall thickness (cm)
SIDR 7	¾	1.070	0.824	0.123	2.718	2.093	0.312
	1	1.359	1.049	0.155	3.452	2.664	0.394
	1¼	1.785	1.380	0.202	4.534	3.505	0.514
	1½	2.086	1.610	0.238	5.298	4.089	0.604
	2	2.675	2.067	0.304	6.795	5.250	0.772
SIDR 9	½	0.760	0.622	0.069	1.930	1.580	0.175
	¾	1.018	0.824	0.097	2.586	2.093	0.246
	1	1.293	1.049	0.122	3.284	2.664	0.310
	1½	1.918	1.610	0.154	4.872	4.089	0.391
	2	2.537	2.067	0.235	6.444	5.250	0.597

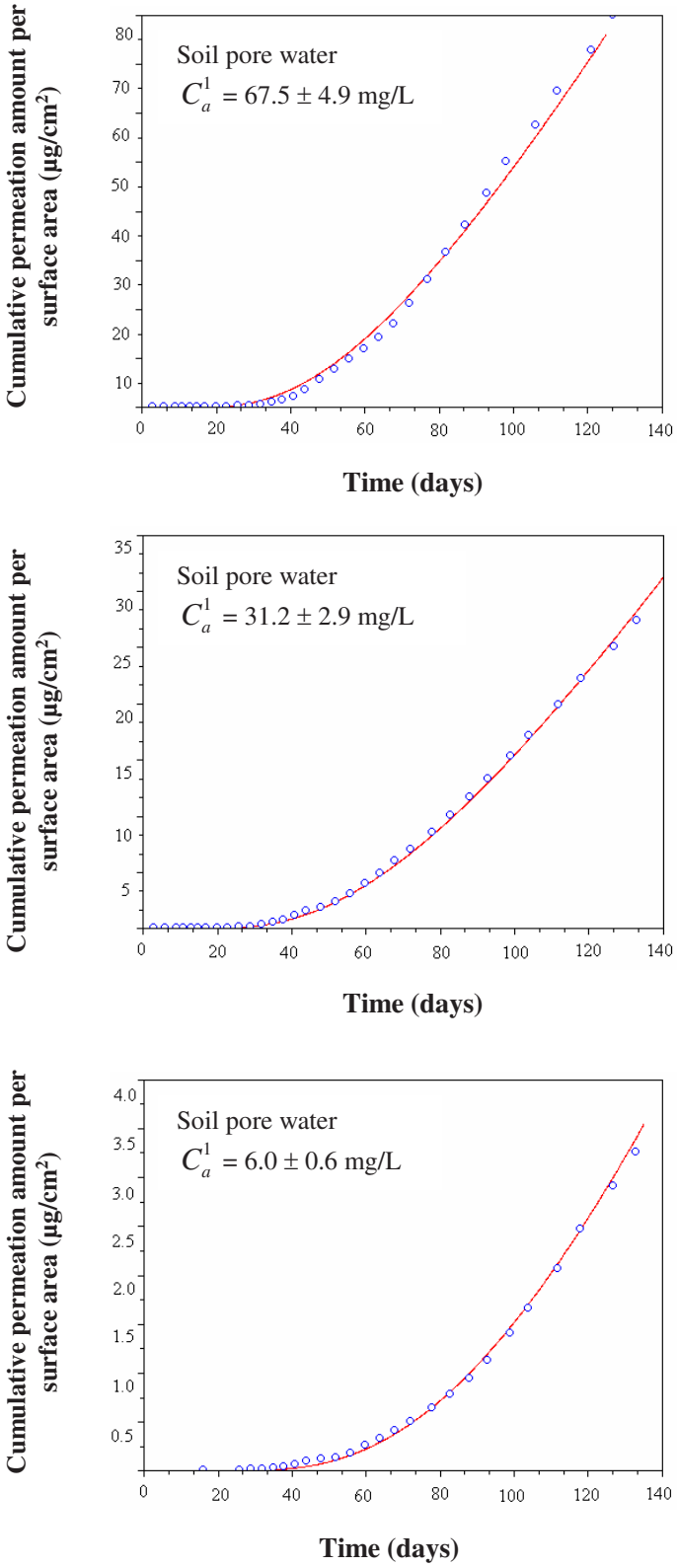

Figure 7.2 Measured permeation data of benzene and curve fit data of permeation model
o measured data —— modeled curve

Table 7.2 Permeation parameters of benzene determined by the numerical modeling method and the time lag method

C_a^1 (mg/L)	Numerical modeling method			Time lag method		
	Diffusion coefficient ($\times 10^{-9}$ cm^2/s)	Solubility parameter	Steady-state permeation rate [μg/(cm^2·day)]	Diffusion coefficient ($\times 10^{-9}$ cm^2/s)	Solubility parameter	Steady-state permeation rate [μg/(cm^2·day)]
67.5±4.9	2.8	23.7	1.22	3.6	15.7	1.04
31.2±2.9	2.3	23.7	0.47	3.5	11.2	0.34
6.0±0.6	2.0	23.7	0.08	2.9	11.9	0.06

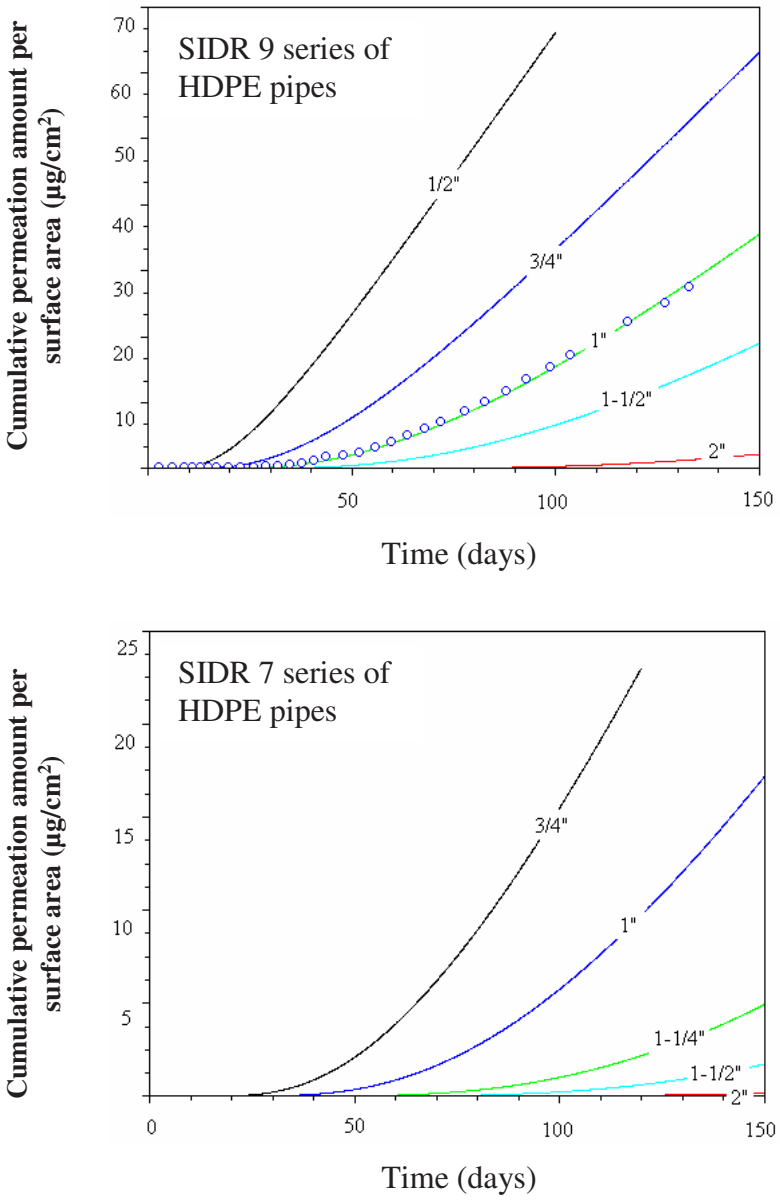

Figure 7.3 Simulated permeation curves of benzene for SIDR 9 and SIDR 7 series HDPE pipes (concentration of benzene in soil pore water: 31.2±2.9 mg/L)

Table 7.3 Estimated breakthrough times and steady-state permeation rates of benzene for SIDR 7 and SIDR 9 series of HDPE pipes

Pipe	Concentration in soil pore water: 67.5±4.9 mg/L		Concentration in soil pore water: 31.2±2.9 mg/L		Concentration in soil pore water: 6.0±0.6 mg/L	
	Breakthrough time* (days)	Steady-state permeation rate (µg/(cm^2·day)	Breakthrough time* (days)	Steady-state permeation rate (µg/(cm^2·day)	Breakthrough time* (days)	Steady-state permeation rate (µg/(cm^2·day)
SIDR 9						
1/2”	3.6	2.19	4.7	0.85	6.6	0.11
3/4”	6.7	1.56	8.9	0.60	12.5	0.08
1”	10.8	1.22	14.4	0.47	20.2	0.06
1-1/2”	14.8	0.98	20.0	0.38	28.5	0.05
2”	34	0.64	46.0	0.25	64.5	0.03
SIDR 7						
3/4”	10.8	1.23	14.4	0.47	20.2	0.06
1”	16.6	0.97	22.2	0.38	31.0	0.05
1-1/4”	27.5	0.75	36.8	0.29	51.5	0.04
1-1/2”	36.5	0.64	49.0	0.25	69.0	0.03
2”	58	0.50	78.0	0.19	108.0	0.02

* defined as the exposure time when permeation flux <= 0.001 µg/cm^2 was not met.

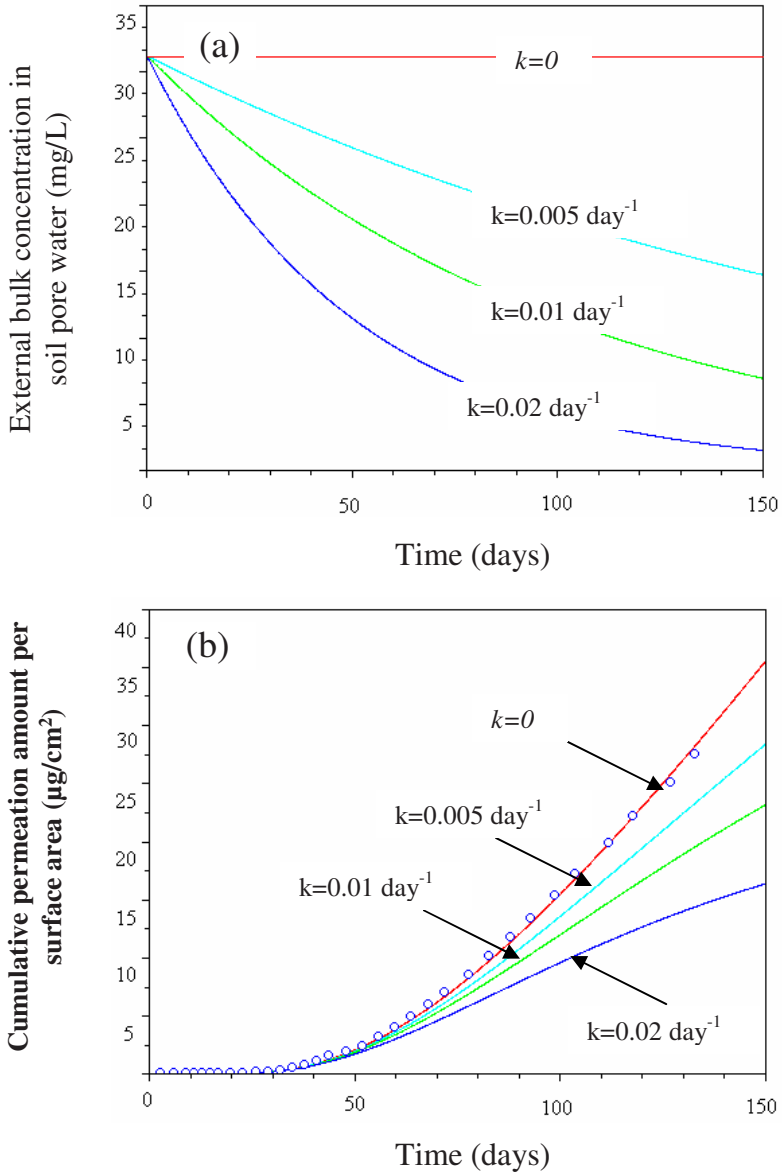

Figure 7.4 (a) Change in external concentration with first-order degradation; (b) Simulated permeation curves of benzene for 1-inch SIDR 9 HDPE pipe when the first-order degradation occurs

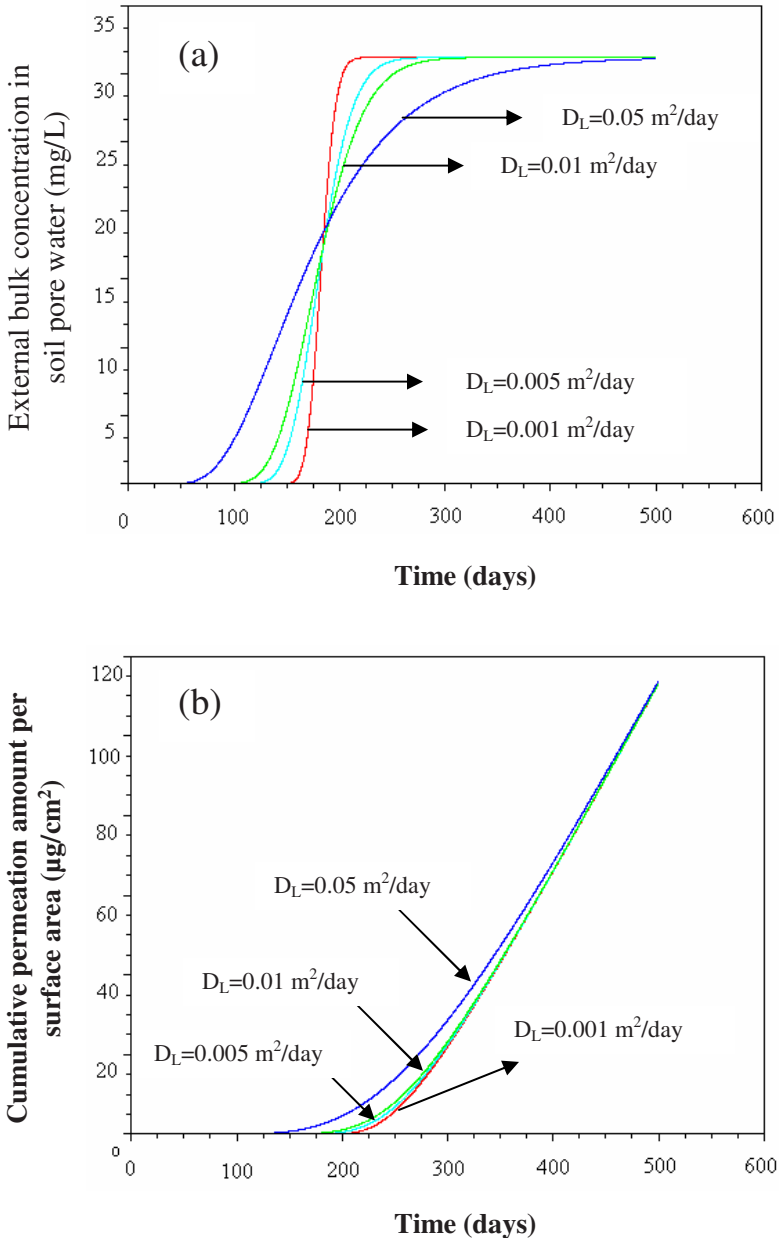

Figure 7.5 (a) Concentration profile for a continuous source with a constant input; (b) Simulated permeation curves of benzene for 1-inch SIDR 9 HDPE pipe that is buried in an aquifer with a continuous source releases benzene at 10 m away (average linear groundwater velocity v_x = 0.056 m/day)

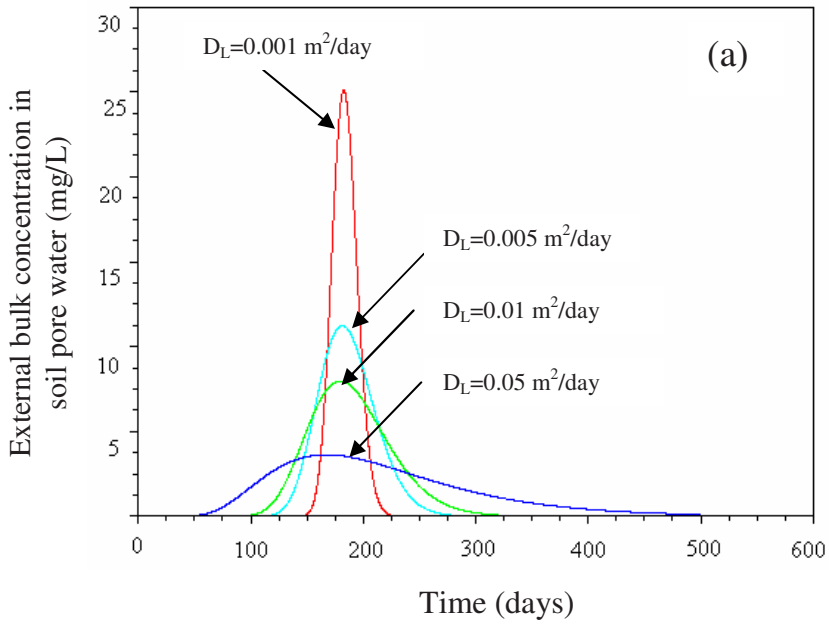

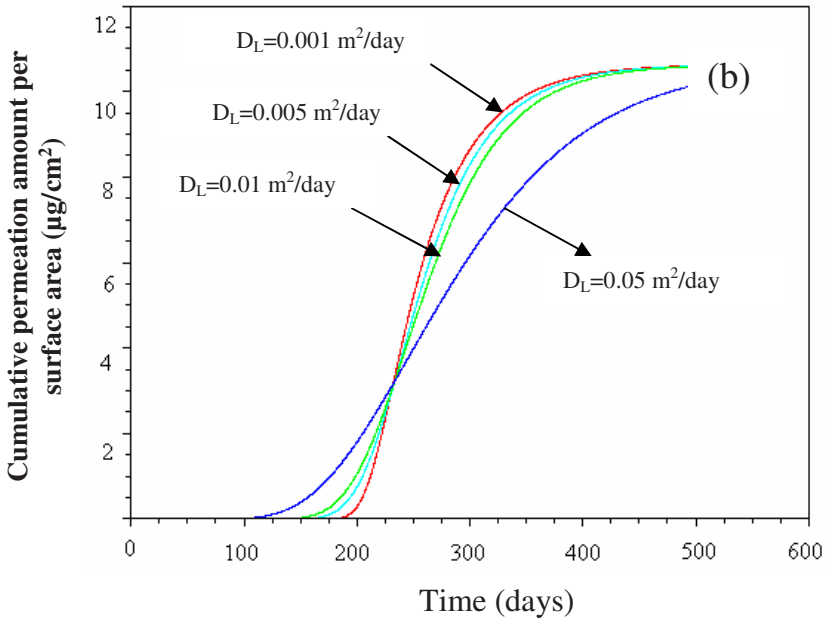

Figure 7.6 (a) Concentration profile for a pulse source; (b) Simulated permeation curves of benzene for 1-inch SIDR 9 HDPE pipe that is buried in an aquifer where a pulse source releases benzene at 10 m away (average linear groundwater velocity v_x = 0.056 m/day; mass of benzene released: 38 mg/m^2)

CHAPTER 8. CONCLUSION

This study was motivated by the aim to advance the water industry's understanding of the impact of organic contaminants on PE and PVC pipes. The major tasks included: (i) conducting hydrocarbon permeation experiments using the pipe-drum or pipe-bottle apparatus for PE and PVC pipes under simulated environmental conditions; (ii) developing predictive laboratory tests to predict and assess susceptibility of PVC pipes to permeation by hydrocarbons; and (iii) investigating the mechanisms and modeling of permeation of organic molecules through PE and PVC pipes. A summary of the major findings is described below.

8.1 Permeation of Hydrocarbons through PVC Pipes

8.1.1 Pipe-bottle test

One-inch diameter new PVC pipes were used in all pipe-bottle experiments. Pipe-bottle experiments showed that (i) PVC pipe was rapidly permeated by pure benzene (20 days), toluene (16 days), and TCE (6.5 days); (ii) PVC pipe was rapidly permeated by saturated benzene vapor (31 days), toluene (28 days), and TCE vapor (13 days); and (iii) chlorinated solvents and monoaromatic compounds in saturated aqueous solutions can also permeate through PVC pipes. However, the breakthrough times in saturated aqueous solutions were much longer than those observed in pure solvents or in saturated organic vapors, mainly due to the mass transfer limitation in water solution. The breakthrough times of saturated aqueous solution of TCE and benzene were found to range from 60 days to 240 days, depending on the experimental mixing conditions.

Pipe-bottle experiments indicated that PVC pipes were impervious to gasoline and gasoline-saturated water over two years of exposure and, therefore, can be used in soils

contaminated with gasoline, regardless of the level of contamination. An explanation for this resistance to permeation is that the premium gasoline did not have sufficient swelling compounds such as benzene, toluene, ethylbenzene and xylene (BTEX) to soften the PVC material.

Experiments indicated that permeation of PVC pipe can not be readily reversed by soil remediation and flushing of the pipe. PVC pipes permeated by benzene, toluene and TCE continued to leach contaminants into the pipe-water for six months after external contamination was removed (at which time the experiment was terminated). Since permeation of organic solvents results in a rubbery phase and therefore loss in material strength, it is possible that the pipe may bust under pressure before the permeation is completely through the pipe wall thickness.

8.1.2 Microscopic visualization test

The moving front test directly measures the progression of permeation caused by swelling in a PVC pipe. Reflected light microscopy was used to visualize and measure the rate of advance of the moving front.

Moving front rates for 58 specimens of PVC pipes of differing lot codes from six different manufacturers and diameters (0.5 inch to 2 inch) in a 48-hour toluene test were found to range from 0.185 to 0.234 mm/hour$^{1/2}$. The results demonstrated that the microscopic visualization technique was rapid, accurate, and was able to detect the differences among PVC pipes in their susceptibility to organic permeation.

In experiments with PVC pipes exposed to various percent volume of toluene in PEG, no moving front was found when the percent volume of toluene was less than 25%. In experiments with PVC pipes exposed to various concentrations of toluene in the NIST

reference fuel, no moving front was found when the percent volume of toluene was 40% (v/v) or below. For organic vapors of benzene or toluene, no moving front was found for PVC pipes by exposure to the vapors that were in equilibrium with ≤ 40% (v/v) benzene or toluene in NIST reference fuel. For aqueous solutions of benzene, toluene or TCE, moving fronts were observed at 100% and 80% of saturation, but no moving fronts at 60%, 40%, of 20% of saturation after 12 months of exposure.

Experiments with equal-volume-mixtures of benzene, toluene, ethylbenzene, and xylene in reference fuel showed that the contribution of BTEX compounds in initiating a moving front in PVC pipe was additive. A 40% (v/v) solution of the mixture (i.e., 10% (v/v) of each of the four compounds) or lower did not initiate a moving front, but a 60% (v/v) solution (i.e., 15% (v/v) of each compound) or greater did initiate a moving front. As the sum of the volumetric fractions of BTEX compounds in free product gasoline is generally lower than 30%, PVC pipe should be an effective barrier against gasoline permeation.

8.1.3 Gravimetric sorption test

The gravimetric sorption test is an indirect measure of permeation in a PVC pipe by measuring the weight gain of the test specimen when exposed to gasoline or solvents.

There was significant sorption of toluene or benzene by PVC pipe materials when exposed to the vapors that were in equilibrium with ≥ 60% (v/v) benzene or toluene in NIST reference fuel and no significant sorption was detected when exposed to the vapors that were in equilibrium with ≤ 40% (v/v). With aqueous saturated solutions of benzene, toluene, or TCE, the weight gain for aqueous solutions of ≤ 60% saturation was less than 2% after 8 months of exposure. Sorption from the 20% aqueous solutions of toluene and benzene was found to be statistically similar to that of the control experiment - implying that sorption was

negligible for contaminant levels below 20% of aqueous saturation for both toluene and benzene. Solutions at 20% aqueous saturation are considered to be high levels of environmental pollution which are seldom encountered in the field except in close proximity to a NAPL.

The gravimetric sorption test results showed that the rates of sorption of solvents parallel the progress of the moving front test described earlier.

8.2 Permeation of Hydrocarbons through PVC Pipes with Gaskets

8.2.1 Gravimetric sorption test

Two-inch diameter Rieber SBR and NBR gaskets in gasoline and gasoline-saturated aqueous solution were tested. In gasoline, sorption equilibrium was rapidly achieved within 24 hours for both types of gaskets. The equilibrium weight gains for SBR and NBR gaskets were 102.3±5.6% and 77.6±1.1% of their original mass, respectively. In comparison to sorption in gasoline, sorption in gasoline-saturated aqueous solution was extremely slow. None of the sorption experiments using gasoline-saturated aqueous solution had reached equilibrium during the experimental period of nearly 80 days.

8.2.2 Pipe-drum test

Permeation of premium gasoline through 2-inch diameter PVC pipes with SBR and NBR Rieber gaskets was rapid with breakthrough times for benzene of about 21 days. When breakthrough occurred, the level of benzene in the pipe-water immediately exceeded the maximum contaminant level (MCL) of 5 μg/L. The results were different from the results for ductile iron pipe joints which showed NBR gaskets to be more resistant to gasoline permeation than SBR gaskets. The steady-state permeation rates of benzene were found to

be 0.73±0.29 mg/joint/day and 0.19±0.18 mg/joint/day for 2-inch SBR and NBR gaskets, respectively.

No significant amounts of BTEX compounds were detected in the pipe-water for pipes using either SBR or NBR Rieber gaskets after 9 months of exposure to any level of gasoline contamination in water, even at 100% saturated.

8.2.3 Model simulation

Model simulation studies were performed to fit the measured permeation data to the diffusion model to determine the diffusion coefficients of contamiants. The diffusion coefficients of benzene and toluene in SBR gaskets were estimated to be 1.1×10^{-7} cm^2/s and 6×10^{-8} cm^2/s, respectively. The corresponding diffusion coefficients in NBR gaskets were 6×10^{-8} cm^2/s and 4×10^{-8} cm^2/s, respectively.

Model simulation was used to scale up the steady-state permeation rate of benzene for larger size pipes with SBR and NBR gaskets. The results indicated that the steady-state permeation rate of benzene can be estimated for any size gasket by using permeation data experimentally determined from 2-inch gaskets and the ratio of pipe outer diameters. The benzene MCL of 5 μg/L would be exceeded in the pipe water for all size pipes with SBR gaskets. The benzene MCL would be exceeded for a 10-inch or smaller size PVC pipe with NBR Rieber gaskets under the identical stagnation and exposure conditions. Due to the effect of dilution, therefore, the concentration of benzene in PVC pipes with gaskets with a minimal water flow would not exceed the MCL.

Model simulation studies also estimated that the steady-state permeate rate of benzene in the pressurized system was around 100 mg/joint/day when exposed to premium gasoline, nearly two order higher than that of the non-pressurized system. This was mainly

due to the fact that hydraulic pressure in the pressurized system significantly expands the gasket-water interface area as well as shortens the diffusion pathway of benzene, promoting the permeation of benzene into pipe water. Pressurized joint systems potentially pose much higher permeation risk to threaten the safety of drinking water than non-pressurized joint systems. However, no level of gasoline contamination in groundwater will cause the benzene MCL to be exceeded in pressurized PVC pipes with SBR or NBR gaskets.

8.3 Permeation of Hydrocarbons through PE Pipes

8.3.1 Pipe-bottle test

Laboratory experiments indicated that HDPE pipe is rapidly permeated by gasoline and solvents, whether in groundwater, in soil pore vapor, or as the free product. Benzene was the first of the BTEX compounds to permeate HDPE pipe from water contaminated with gasoline, with the first detectable concentrations exceeding the 5 μg/L MCL for all experiments. The rates of diffusion of the BTEX compounds in gasoline through HDPE pipe are logarithmically dependent on the external bulk concentration and are an order of magnitude faster for free product gasoline than for saturated groundwater or soil pore vapor (diffusion coefficients are 10^{-8} cm^2/s and 10^{-9} cm^2/s, respectively).

Equations were derived to predict the concentration of contaminants in PE pipes for various external contaminant concentrations during continuous flow and after periods of stagnation. For a given contaminant in soil water, smaller pipes are more vulnerable than larger pipes and the risk of exceeding EPA MCLs is much higher during periods of stagnation than during continuous flow.

Laboratory experiments showed that for a given mass of contaminants in soil, organic matter in the soil strongly sorbed the contaminants, decreasing the contaminant concentrations in soil water or soil vapor, thereby decreasing the permeation of contaminants into HDPE pipe. While the organic content of soils can effectively lower the concentration of hydrocarbon contaminants in the soil pore water, once the organic adsorption capacity of the soil is exceeded, the organic content of the soil makes no difference. This indicates that the steady state permeation rates in HDPE pipes are dependent on the external bulk concentrations regardless of the soil types. While organic content might reduce permeation incidents in the case of transient hydrocarbon contamination, it would be irrelevant for continuous contamination.

8.3.2 Model simulation

Permeation parameters of benzene in 1-inch SIDR 9 PE pipes were estimated by fitting the measured data to a permeation model based on a combination of equilibrium partitioning and Fick's diffusion. For bulk concentrations between 6.0 to 67.5 mg/L in soil pore water, the concentration-dependent diffusion coefficients of benzene were found to range from 2.0×10^{-9} cm^2/s to 2.8×10^{-9} cm^2/s while the solubility parameter was determined to be 23.7.

The simulated permeation curves of benzene for SIDR 9 and SIDR 7 series of PE pipes indicated that small diameter pipes are more vulnerable to permeation than large diameter pipes and the breakthrough of organic contaminants is retarded and the corresponding permeation flux decreases with the increase of the pipe thickness. PE pipes exposed to an instantaneous plume exhibit distinguishable permeation characteristics from those exposed to a continuous source with a constant input. The properties of aquifer such as

dispersion coefficients (D_L) also influence the permeation behavior of organic contaminants through PE pipes.

The results of model simulation studies also revealed that the permeation behavior of benzene in the field conditions was strongly dependent on the characteristics of contaminant source (continuous source or instantaneous source) and the properties of aquifer such as hydrodynamic dispersion coefficients.

8.4 Future Research

This study did not test old, used, or compromised pipes since the age, exposure history, and conditions are typically not known. Under actual field conditions, pipe materials may suffer degradation or deterioration due to UV exposure, temperatures extremes, abrasion, stress variation, and even biological attack. Such degradation or deterioration may result in the loss in structural integrity and the pipes may become more susceptible to the process of permeation. The microscopic visualization test can be easily used to test aged PVC pipes and to study whether aging increases susceptibility. Since it is difficult to obtain aged pipes and their history, a deliberate attempt should be made to age the pipes in the laboratory. These pipes could then be tested using the microscopic visualization test and the progression of the moving front would provide information on the susceptibility of the pipe under different aging conditions.

The research has focused on some of the major hydrocarbons encountered in the field such as BTEX in gasoline, and chlorinated solvents such as TCE. Testing should continue by using the microscopic visualization tests and pipe-bottle apparatuses to assess the permeation of similar light aromatic compounds such as ethylbenzene, xylenes, and

chlorinated solvents such as tetrachloroethylene (PCE), dichloroethylene (DCE), tetrachloroethane (PCA), and trichloroethane (TCA) to determine whether these chemicals behave in a manner similar to benzene, toluene and TCE. Methyl tert-butyl ether (MTBE) is another compound of interest since it is a widely used gasoline additive and found in numerous groundwater and surface water reservoirs across the United States, imposing a serious risk to public health and to the environment. While the impact of permeation of mixtures of BTEX compounds was studied in this study, future research should investigate permeation by mixtures of chlorinated solvents and by mixtures of chlorinated solvents and BTEX compounds.

Of interest is a further understanding of the pathway of contamination or the permeation process through the Rieber gaskets. This study neglected the impact of lubricants and the size of the gap between the bell and the spigot on contaminant transport. It is possible to develop a model combining the permeation process in elastomeric materials and the diffusion/advection process through the gap between the bell and the spigot. Moreover, the results of the model simulation in this research indicated that pressurized joint systems potentially posed much higher permeation risk that threaten the safety of drinking water than non-pressurized joint systems. This conclusion needs to be tested more rigorously with future experimental studies.

APPENDIX

A.1 Prediction of Moving Front and Experimental Data for Chapter 3

Prediction of moving front

To address whether Fickian diffusion with two different diffusion coefficients can predict the concentration profile of toluene in PVC, a software tool, COMSOL Multiphysics® (COMSOL group, Stockholm, Sweden), was used to simulate the diffusion process.

The permeation of toluene in the PVC pipe can be represented as shown in Figure A.1-a. The thickness of pipe wall is equal to X_0. The penetration takes place from the outer wall (left) to the inner wall (right) with surface $x=0$ maintained at a constant concentration C_0. Assume that at time t the moving boundary (front) reaches $0.5X_0$, and the concentration at the boundary is C_x. Also, the diffusion coefficient in the region $0<x<0.5X_0$ is denoted by D_1 respectively, and in the region $x>0.5X_0$ by D_2. At the discontinuity, the flux before and after the moving front must be same:

$$C = C_X, \quad x = 0.5X_0 \tag{Eq.A.1}$$

$$D_1 \frac{\partial C\big|_{0.5X_0-\Delta x}}{\partial x} = D_2 \frac{\partial C\big|_{0.5X_0+\Delta x}}{\partial x}, \quad x = 0.5X_0 \tag{Eq. A.2}$$

In the region $0<x<0.5X_0$:

$$\frac{\partial C}{\partial t} = D_1 \frac{\partial^2 C}{\partial x^2} \quad 0 < x < 0.5X_0 \tag{Eq. A.3}$$

$$C = C_0 \quad x = 0 \tag{Eq. A.4}$$

In the region $x>0.5X_0$:

$$\frac{\partial C}{\partial t} = D_2 \frac{\partial^2 C}{\partial x^2} \quad x > 0.5X_0 \qquad \text{(Eq. A.5)}$$

$$C = 0 \quad x = X_0 \qquad \text{(Eq. A.6)}$$

The simulated concentration profile of toluene in PVC polymer is shown in Figure A.1-b. As indicated in Figure A.1-b, the concentration of toluene decreased dramatically to 0 within a very narrow region ahead of the boundary of the glassy and rubbery portions.

As shown by the modeling, Fickian diffusion with two different diffusion coefficients can predict the shape concentration profile of toluene in the PVC matrix.

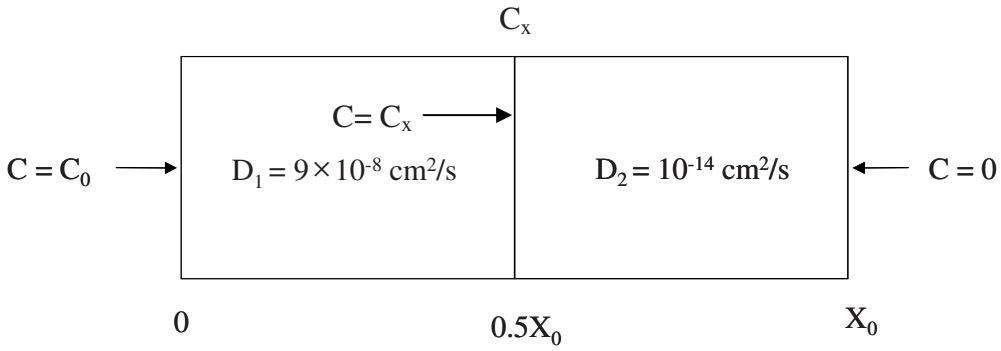

(a)

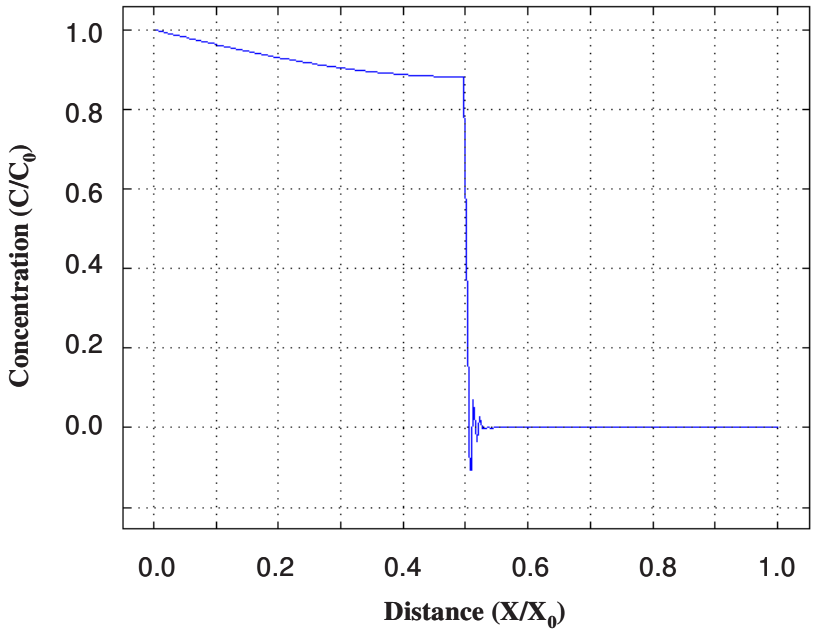

(b)

Figure A.1 Modelling concentration profile of toluene in PVC based on Fickian equation with discontinuous diffusion coefficients

Data for Figure 3.3

Benzene

Exposure time (day)	Sample concentration (ug/L)	Pipe water concentration (ug/L)	Pipe water volume (mL)	Permeation mass ug	Exposure surface area (cm^2)	Permeation per unit area (ug/cm^2)	Cumulative permation (ug/cm^2)	Cumulative permeation (mg/cm^2)
13	ND	0	84.9	0	87	0	0	0
15	ND	0	84.9	0	87	0	0	0
18	2.1	9.0	84.9	0.8	87	0	0	0
20	791.9	3405	84.9	289	87	3	3	0.003
21	23193	99730	84.9	8467	87	97	101	0.101
22	141530	608579	84.9	51668	87	594	695	0.695
23	286740	1232982	84.9	104680	87	1203	1898	1.898
24	339040	1457872	84.9	123773	87	1423	3320	3.320

Toluene

Exposure time (day)	Sample concentration (ug/L)	Pipe water concentration (ug/L)	Pipe water volume (mL)	Permeation mass ug	Exposure surface area (cm^2)	Permeation per unit area (ug/cm^2)	Cumulative permation (ug/cm^2)	Cumulative permeation (mg/cm^2)
5	ND	0	84.9	0	87	0	0	0
11	ND	0	84.9	0	87	0	0	0
12	ND	0	84.9	0	87	0	0	0
13	ND	0	84.9	0	87	0	0	0
14	1.7	7	84.9	1	87	0	0.0	0
15	1	4	84.9	0	87	0	0.0	0
16	26.5	114	84.9	10	87	0	0.1	0
18	129492	556816	84.9	47274	87	543	543	0.543
20	137264	590235	84.9	50111	87	576	1119	1.119
22	128088	550778	84.9	46761	87	537	1657	1.657

TCE

Exposure time (day)	Sample concentration (ug/L)	Pipe water concentration (ug/L)	Pipe water volume (mL)	Permeation mass ug	Exposure surface area (cm^2)	Permeation per unit area (ug/cm^2)	Cumulative permation (ug/cm^2)	Cumulative permeation (mg/cm^2)
3	ND	0	84.9	0	87	0	0	0
4	ND	0	84.9	0	87	0	0	0
5	ND	0	84.9	0	87	0	0	0
6	2.2	9	84.9	1	87	0	0	0
7	67800	291540	84.9	24752	87	285	285	0.285
8	185000	795500	84.9	67538	87	776	1061	1.061
9	171000	735300	84.9	62427	87	718	1778	1.778
10	176000	756800	84.9	64252	87	739	2517	2.517

Note: Pipe water concentration = Sample concentration × 4.3
Taking 10-mL pipe water into 43-mL vials for BTEX analysis

Data for Figure 3.5

Time (hour)	Time (day)	Square root time (day $^{1/2}$)	Penetration distance (mm)		
			TCE	Benzene	Toluene
2	0.08	0.29	0.060 ±0.002		
6	0.25	0.50	0.387 ±0.011		
12	0.50	0.71	0.723 ±0.018		
18	0.75	0.87	0.990 ±0.030		
24	1	1.00	1.113 ±0.041	0.656 ±0.031	0.670 ±0.010
48	2	1.41		1.070 ±0.025	1.094 ±0.010
72	3	1.73		1.314 ±0.032	1.391 ±0.000
96	4	2.00		1.497 ±0.070	1.817 ±0.042
120	5	2.24		1.697 ±0.029	1.970 ±0.029
144	6	2.45		1.975 ±0.022	2.247 ±0.041
168	7	2.65		2.132 ±0.026	2.357 ±0.034
192	8	2.83			2.504 ±0.017

Data for Figure 3.6

Time (day)	Square root time (day$^{1/2}$)	Thickness of swollen layer (mm)							
		100% toluene 0%PEG	80% toluene 20%PEG	60% toluene 40%PEG	40% toluene 60%PEG	35%toluene 65% PEG	30% toluene 70%PEG	25% toluene 75%PEG	20% toluene 80%PEG
0	0.00	0	0	0	0	0	0	0	0
1	1.00	0.982 ± 0.027	0.883 ± 0.012	0.737 ± 0.015	0.331 ± 0.020	0.185 ± 0.016			
2	1.41	1.319± 0.035	1.168 ± 0.024	0.952 ± 0.015	0.424 ± 0.019	0.292 ± 0.015	0.136 ± 0.012	ND	ND
3	1.73	1.702 ± 0.031	1.404 ± 0.021	1.173 ± 0.021	0.471 ± 0.023				
4	2.00	1.943 ± 0.059	1.672 ± 0.033	1.400 ± 0.026	0.532 ± 0.016				
6	2.45					0.584 ± 0.026	0.332 ± 0.011	ND	ND
9	3.00					0.639 ± 0.021	0.430 ± 0.017	ND	ND

Data for Figure 3.7

Time (day)	Square root time ($day^{1/2}$)	Thickness of swollen layer (mm)				
		100% toluene 0% NIST fuel	80% toluene 20% NIST fuel	60% toluene 40% NIST fuel	40% toluene 60% NIST fuel	20% toluene 80% NIST fuel
0	0	0	0	0	0	0
0.5	0.71	0.653 ± 0.001	0.260 ± 0.012	ND	ND	ND
1.0	1.00	0.897 ± 0.012	0.383 ± 0.021	ND	ND	ND
1.5	1.22	1.140 ± 0.016	0.500 ± 0.027	0.133 ± 0.010	ND	ND
2.0	1.41	1.330 ± 0.015	0.613 ± 0.020	0.149 ± 0.017	ND	ND
2.5	1.58	1.520 ± 0.034	0.717 ± 0.032	0.210 ± 0.014	ND	ND
3.0	1.73	1.677 ± 0.031	0.810 ± 0.043	0.228 ± 0.013	ND	ND
3.5	1.87	1.837 ± 0.034	0.877 ± 0.030	0.258 ± 0.032	ND	ND

Data for Figure 3.8

Time (day)	Square root time ($day^{1/2}$)	Thickness of swollen layer (mm)					
		Benzene 100%	Toluene 100%	Ethylbenzene 100%	Xylene 100%	BTEX 25% each	Modeled results
0	0	0	0	0	0	0	0
0.5	0.71	0.577 ±0.021	0.667 ±0.015	0.190 ±0.026	0.340 ±0.000	0.470 ±0.020	0.469
1.0	1.00	0.917 ±0.012	0.958 ±0.015	0.380 ±0.010	0.446 ±0.021	0.787 ±0.011	0.694
1.5	1.22	1.070 ±0.044	1.150 ±0.017	0.493 ±0.006	0.543 ±0.006	0.937 ±0015	0.839
2.0	1.41	1.220 ±0.010	1.360 ±0.021	0.537 ±0.021	0.683 ±0.006	1.047 ±0.006	0.979
2.5	1.58	1.380 ±0.046	1.520 ±0.011	0.630 ±0.020	0.737 ±0.025	1.163 ±0.006	1.088
3.0	1.73	1.547 ±0.012	1.700 ±0.032	0.690 ±0.026	0.827 ±0.035	1.293 ±0.023	1.212

Data for Figure 3.9

Time (day)	Square root time ($day^{1/2}$)	Thickness of swollen layer (mm)			
		100% BTEX, 25 % each % NIST fuel	80% BTEX, 20% each 20% NIST fuel	60% BTEX, 15% each 40% NIST fuel	40% BTEX, 10% each 60% NIST fuel
0	0	0	0	0	0
0.5	0.71	0.470 ±0.020	0.173 ±0.030	ND	ND
1.0	1.00	0.787 ±0.011	0.310 ±0.020	ND	ND
1.5	1.22	0.937 ±0015	0.400 ±0.012	0.115 ±0.000	ND
2.0	1.41	1.047 ±0.006	0.467 ±0.011	0.123 ±0.005	ND
2.5	1.58	1.163 ±0.006	0.540 ±0.010	0.152 ±0.003	ND
3.0	1.73	1.293 ±0.023	0.597 ±0.012	0.149 ±0.005	ND

Data for Figure 3.10

	Thickness of Swollen Layer (mm)							Slope (k)	R^2
Time (h)	0	6	12	24	30	36	48		
Square root time ($h^{1/2}$)	0.000	2.449	3.464	4.899	5.477	6.000	6.928		
sample 1	0	0.49	0.72	1.07	1.17	1.29	1.54	0.216	0.997
sample 2	0	0.47	0.72	1.05	1.18	1.30	1.51	0.215	0.997
sample 3	0	0.43	0.66	0.97	1.07	1.17	1.43	0.198	0.995
sample 4	0	0.51	0.76	1.09	1.19	1.30	1.54	0.219	0.999
sample 5	0	0.49	0.73	1.08	1.18	1.32	1.54	0.218	0.998
sample 6	0	0.49	0.73	1.03	1.12	1.31	1.52	0.214	0.996
sample 7	0	0.51	0.74	1.04	1.17	1.27	1.54	0.215	0.998
sample 8	0	0.56	0.84	1.13	1.29	1.39	1.61	0.233	0.999
sample 9	0	0.50	0.76	1.07	1.18	1.31	1.52	0.218	0.999
sample 10	0	0.47	0.72	1.00	1.17	1.27	1.45	0.209	0.999
sample 11	0	0.52	0.78	1.08	1.18	1.30	1.54	0.219	0.999
sample 14	0	0.46	0.70	1.04	1.17	1.27	1.46	0.210	0.997
sample 15	0	0.47	0.70	1.01	1.14	1.25	1.43	0.206	0.999
sample 16	0	0.42	0.67	0.89	1.04	1.15	1.32	0.189	0.996
sample 17	0	0.45	0.70	1.01	1.11	1.26	1.44	0.206	0.997
sample 18	0	0.44	0.68	0.96	1.06	1.18	1.34	0.194	0.999
sample 19	0	0.48	0.63	0.95	1.06	1.18	1.35	0.194	0.998
sample 20	0	0.47	0.70	1.01	1.13	1.23	1.42	0.205	0.999
sample 21	0	0.47	0.68	0.98	1.10	1.21	1.36	0.199	0.999
sample 22	0	0.45	0.65	0.90	1.05	1.16	1.32	0.190	0.999
sample 23	0	0.45	0.66	0.93	1.10	1.21		0.197	0.996
sample 24	0	0.54	0.78	1.16	1.26	1.32	1.53	0.225	0.997
sample 25	0	0.45	0.70	1.00	1.16	1.26	1.41	0.206	0.997
sample 26	0	0.47	0.70	1.04	1.17	1.26	1.44	0.209	0.998
sample 27	0	0.51	0.70	1.04	1.18	1.26	1.43	0.210	0.998
sample 28	0	0.45	0.65	0.89	0.98	1.08	1.28	0.182	0.999
sample 29	0	0.44	0.70	1.01	1.16	1.27	1.49	0.210	0.995
sample 30	0	0.43	0.62	0.93	1.07	1.11	1.29	0.187	0.997
sample 31	0	0.43	0.69	1.00		1.29	1.52	0.211	0.992
sample 32	0	0.42	0.63	0.96		1.21	1.43	0.200	0.992
sample 33	0	0.52	0.74	1.13		1.39	1.63	0.230	0.997
sample 34	0	0.52	0.79	1.15		1.41	1.68	0.236	0.997
sample 35	0	0.48	0.72	1.11		1.33	1.60	0.224	0.994
sample 36	0	0.48	0.75	1.09		1.38	1.61	0.227	0.995
sample 37	0	0.48	0.69	1.03		1.27	1.51	0.212	0.997
sample 38	0	0.40	0.62	0.95		1.22	1.47	0.201	0.985
sample 39	0	0.44	0.69	1.06		1.30	1.51	0.214	0.993
sample 40	0	0.56	0.74	1.12		1.40	1.61	0.230	0.998
sample 41	0	0.48	0.70	1.05		1.25	1.47	0.210	0.998
sample 42	0	0.47	0.70	1.05		1.33	1.52	0.216	0.995
sample 43	0	0.53	0.78	1.10		1.38	1.59	0.227	0.999
sample 44	0	0.36	0.57	0.86		1.11	1.31	0.181	0.987
sample 45	0	0.43	0.61	1.12		1.40	1.61	0.224	0.975
sample 46	0	0.43	0.64	0.94		1.16	1.39	0.194	0.995
sample 47	0	0.48	0.68	1.00				0.200	0.999
sample 48	0	0.49	0.77	1.06		1.30	1.53	0.218	0.999
sample 49	0	0.39	0.62	0.95		1.20	1.45	0.199	0.987
sample 51	0	0.45	0.64	0.97		1.19	1.41	0.199	0.997
sample 52	0	0.51	0.71	0.99		1.20	1.36	0.200	0.999
sample 53	0	0.44	0.59	0.95		1.17	1.41	0.195	0.990
sample 54	0	0.44	0.65	0.90		1.21	1.37	0.195	0.995
sample 55	0	0.50	0.68	1.08		1.32	1.51	0.217	0.996
sample 56	0	0.48	0.67	1.03		1.26	1.40	0.205	0.997
sample 57	0	0.51	0.73	1.05		1.30	1.50	0.216	0.999
sample 58	0	0.50	0.67	1.01		1.21	1.46	0.206	0.997
sample 59	0	0.40	0.58	0.88		1.14	1.34	0.186	0.989
sample 60	0	0.39	0.59	0.87		1.10	1.30	0.182	0.994
sample 61	0	0.47	0.68	1.02		1.27	1.56	0.214	0.992

Note: Sample 12 and Sample 13 are C-PVC pipes. Their data are not reported here.

Data for Figure 3.11

Time	Square root time	Thickness of Swollen Layer (mm)									
		Sample 8					Sample 10				
(hours)	($h^{1/2}$)	1	2	3	4	5	1	2	3	4	5
0	0	0	0	0	0	0	0	0	0	0	0
6	2.45	0.57	0.56	0.55	0.55	0.56	0.44	0.48	0.47	0.48	0.48
12	3.46	0.86	0.82	0.84	0.82	0.84	0.73	0.73	0.72	0.74	0.73
24	4.90	1.13	1.10	1.13	1.14	1.13	1.00	1.03	1.00	1.01	1.02
30	5.48	1.28	1.29	1.30	1.30	1.29	1.15	1.16	1.17	1.14	1.18
36	6.00	1.38	1.40	1.38	1.39	1.39	1.28	1.27	1.27	1.28	1.26
48	6.93	1.60	1.60	1.60	1.61	1.61	1.44	1.47	1.45	1.45	1.45
	Slope (k)	0.2326	0.2317	0.233	0.2333	0.2332	0.2081	0.2101	0.209	0.2093	0.2101
	R^2	0.998	0.999	0.999	0.999	0.999	0.996	0.999	0.999	0.999	0.999

Time	Square root time	Thickness of Swollen Layer (mm)				
		Sample 16				
(hours)	($h^{1/2}$)	1	2	3	4	5
0	0.000	0	0	0	0	0
6	2.449	0.42	0.43	0.42	0.43	0.44
12	3.464	0.64	0.65	0.67	0.68	0.69
24	4.899	0.88	0.88	0.89	0.89	0.89
30	5.477	1.05	1.05	1.04	1.07	1.07
36	6.000	1.13	1.15	1.15	1.13	1.15
48	6.928	1.31	1.32	1.33	1.33	1.33
	Slope (k)	0.1869	0.1885	0.189	0.1899	0.191
	R^2	0.997	0.997	0.996	0.996	0.997

	Sample 8	Sample 10	Sample 16
MEAN	0.233	0.209	0.189
STDEV	0.0006	0.0008	0.0015
MEDIAN	0.233	0.209	0.189
Q1	0.233	0.209	0.189
Q3	0.233	0.210	0.190
Minimum	0.232	0.208	0.187
Maximum	0.233	0.210	0.191

Data for Figure 3.12

	Pipe Size					
	1/2"	3/4"	1"	1-1/4"	1-1/2"	2"
Slope (k)	0.216	0.214	0.210	0.194	0.225	0.182
	0.215	0.215	0.206	0.205	0.206	0.210
	0.198	0.234	0.185	0.199	0.209	0.187
	0.219	0.218	0.206	0.190	0.210	0.205
	0.218	0.204	0.194	0.197	0.199	0.216
	0.211	0.219	0.210	0.224	0.200	0.206
	0.200	0.227	0.216	0.194	0.195	0.186
	0.230	0.212	0.227	0.200	0.195	0.214
	0.236	0.201	0.189	0.218	0.217	
	0.224	0.214		0.199		
		0.232				
MEAN	0.217	0.217	0.204	0.202	0.206	0.201
STDEV	0.012	0.010	0.015	0.011	0.010	0.014
MEDIAN	0.217	0.215	0.206	0.199	0.206	0.206
Q1	0.212	0.213	0.194	0.195	0.199	0.187
Q3	0.223	0.223	0.210	0.203	0.210	0.211
Minimum	0.198	0.201	0.181	0.190	0.195	0.182
Maximum	0.236	0.2336	0.227	0.224	0.2252	0.216

A.2 Experimental Data for Chapter 4

Data for Figure 4.1

Benzene Vapor

Exposure time (day)	Sample concentration (ug/L)	Pipe water concentration (ug/L)	Pipe water volume (mL)	Permeation mass ug	Exposure surface area (cm^2)	Permeation per unit area (ug/cm^2)	Cumulative permation (ug/cm^2)	Cumulative permeation (mg/cm^2)
18	ND	0	84.9	0	87	0	0	0
25	ND	0	84.9	0	87	0	0	0
31	9115	39194.5	84.9	3327.6	87	38	38	0
33	143573	617364	84.9	52414	87	602	641	0.641
34	155686	669450	84.9	56836	87	653	1294	1.294
35	190508	819184	84.9	69549	87	799	2093	2.093
36	219224	942663	84.9	80032	87	920	3013	3.013
37	267221	1149050	84.9	97554	87	1121	4135	4.135
38	297718	1280187	84.9	108688	87	1249	5384	5.384

Toluene Vapor

Exposure time (day)	Sample concentration (ug/L)	Pipe water concentration (ug/L)	Pipe water volume (mL)	Permeation mass ug	Exposure surface area (cm^2)	Permeation per unit area (ug/cm^2)	Cumulative permation (ug/cm^2)	Cumulative permeation (mg/cm^2)
18	ND	0	84.9	0	87	0	0	0
25	ND	0	84.9	0	87	0	0	0
28	306.5	1318.0	84.9	111.9	87	1	1	0
31	89092	383096	84.9	32525	87	374	375	0.375
32	98181	422178	84.9	35843	87	412	787	0.787
33	94902	408079	84.9	34646	87	398	1185	1.185
34	95161	409192	84.9	34740	87	399	1585	1.585
35	85713	368566	84.9	31291	87	360	1944	1.944

TCE Vapor

Exposure time (day)	Sample concentration (ug/L)	Pipe water concentration (ug/L)	Pipe water volume (mL)	Permeation mass ug	Exposure surface area (cm^2)	Permeation per unit area (ug/cm^2)	Cumulative permation (ug/cm^2)	Cumulative permeation (mg/cm^2)
5	ND	0	84.9	0	87	0	0	0
8	ND	0	84.9	0	87	0	0	0
9	ND	0	84.9	0	87	0	0	0
10	ND	0	84.9	0	87	0	0	0
11	ND	0	84.9	0	87	0	0	0
12	516	2219	84.9	188	87	2	2	0.002
13	88640	381152	84.9	32360	87	372	374	0.374
14	173150	744545	84.9	63212	87	727	1101	1.101
15	167810	721583	84.9	61262	87	704	1805	1.805
16	193310	831233	84.9	70572	87	811	2616	2.616
17	219620	944366	84.9	80177	87	922	3538	3.538
18	235880	1014284	84.9	86113	87	990	4527	4.527

Data for Figure 4.2

Benzene-Saturated Aqueous Solution (intermittently stirred)								
Exposure time (day)	Sample concentration (ug/L)	Pipe water concentration (ug/L)	Pipe water volume (mL)	Permeation mass ug	Exposure surface area (cm^2)	Permeation per unit area (ug/cm^2)	Cumulative permation (ug/cm^2)	Cumulative permeation (mg/cm^2)
175	ND	0	84.9	0	87	0	0	0
227	ND	0	84.9	0	87	0	0	0
243	ND	0	84.9	0.0	87	0	0	0
251	160220	688946	84.9	58492	87	672	672	0.672
251.083	2095	9009	84.9	765	87	9	681	0.681
251.167	2156	9271	84.9	787	87	9	690	0.690
251.250	4085	17566	84.9	1491	87	17	707	0.707
251.333	2431	10453	84.9	887	87	10	717	0.717

Benzene-Saturated Aqueous Solution (continuous stirred)								
Exposure time (day)	Sample concentration (ug/L)	Pipe water concentration (ug/L)	Pipe water volume (mL)	Permeation mass ug	Exposure surface area (cm^2)	Permeation per unit area (ug/cm^2)	Cumulative permation (ug/cm^2)	Cumulative permeation (mg/cm^2)
23	ND	0	84.9	0	87	0	0	0
33	ND	0	84.9	0	87	0	0	0
44	ND	0	84.9	0.0	87	0	0	0
67	ND	0	84.9	0	87	0	0	0.000
75	ND	0	84.9	0	87	0	0	0.000
81	186984	804031	84.9	68262	87	785	785	0.785
82	85212	366412	84.9	31108	87	358	1142	1.142
83	108000	464400	84.9	39428	87	453	1595	1.595
84	162748	699816	84.9	59414	87	683	2278	2.278
85	164916	709139	84.9	60206	87	692	2970	2.970
86	177266	762244	84.9	64714	87	744	3714	3.714
87	222602	957189	84.9	81265	87	934	4648	4.648

Data for Figure 4.2 (continued)

TCE-Saturated Aqueous Solution (intermittently stirred)								
Exposure time (day)	Sample concentration (ug/L)	Pipe water concentration (ug/L)	Pipe water volume (mL)	Permeation mass ug	Exposure surface area (cm^2)	Permeation per unit area (ug/cm^2)	Cumulative permation (ug/cm^2)	Cumulative permeation (mg/cm^2)
120	0	0	84.9	0	87	0	0	0
153	299.05	1286	84.9	109	87	1	1	0
168	146200	628660	84.9	53373	87	613	615	1
195	253200	1088760	84.9	92436	87	1062	1677	1.677
198	266900	1147670	84.9	97437	87	1120	2797	2.797
206	242700	1043610	84.9	88602	87	1018	3816	3.816
207	214900	924070	84.9	78454	87	902	4717	4.717
208	177800	764540	84.9	64909	87	746	5463	5.463
209	135100	580930	84.9	49321	87	567	6030	6.030
210	103200	443760	84.9	37675	87	433	6463	6.463
211	83500	359050	84.9	30483	87	350	6814	6.814

TCE-Saturated Aqueous Solution (continuous stirred)								
Exposure time (day)	Sample concentration (ug/L)	Pipe water concentration (ug/L)	Pipe water volume (mL)	Permeation mass ug	Exposure surface area (cm^2)	Permeation per unit area (ug/cm^2)	Cumulative permation (ug/cm^2)	Cumulative permeation (mg/cm^2)
0	0	0	84.9	0	87	0	0	0
23	9.8	42	84.9	4	87	0	0	0
33	5.5	24	84.9	2.0	87	0	0	0
44	2.3	10	84.9	1	87	0	0	0
58	2	9	84.9	1	87	0	0	0
67	30900	132870	84.9	11281	87	130	130	0.130
68	12500	53750	84.9	4563	87	52	182	0.182
69	13900	59770	84.9	5074	87	58	241	0.241
71	42200	181460	84.9	15406	87	177	418	0.418
72	28200	121260	84.9	10295	87	118	536	0.536
73	34900	150070	84.9	12741	87	146	682	0.682
75	83100	357330	84.9	30337	87	349	1031	1.031

Data for Figure 4.3

Benzene Vapor

Time (h)	Weight (g)					Weight gain (%)				
	a=1	a=0.88	a=0.73	a=0.55	a=0.32	a=1	a=0.88	a=0.73	a=0.55	a=0.32
0	7.135	6.827	6.976	7.073	7.010	0.000	0.000	0.000	0.000	0.000
12	7.390	6.961	7.025	7.078	7.015	3.574	1.961	0.702	0.071	0.071
24	7.540	7.043	7.053	7.082	7.017	5.684	3.165	1.099	0.130	0.100
36	7.678	7.110	7.074	7.086	7.018	7.622	4.136	1.406	0.188	0.114
48	7.798	7.172	7.094	7.090	7.021	9.300	5.047	1.689	0.238	0.157
60	7.933	7.236	7.115	7.093	7.021	11.191	5.985	1.993	0.281	0.157

Toluene Vapor

Time (h)	Weight (g)					Weight gain (%)				
	a=1	a=0.86	a=0.70	a=0.51	a=0.28	a=1	a=0.86	a=0.70	a=0.51	a=0.28
0	7.033	7.037	7.124	6.969	7.108	0.000	0.000	0.000	0.000	0.000
12	7.207	7.132	7.162	6.974	7.110	2.474	1.360	0.529	0.076	0.028
24	7.332	7.194	7.183	6.977	7.111	4.251	2.241	0.824	0.112	0.042
36	7.444	7.248	7.202	6.979	7.109	5.841	2.999	1.092	0.142	0.014
48	7.547	7.298	7.218	6.981	7.110	7.306	3.708	1.314	0.175	0.028
60	7.660	7.348	7.233	6.983	7.113	8.921	4.421	1.526	0.201	0.070

Data for Figure 4.4

Benzene-saturated aqueous solution

Time	Weight (g)					Weight gain (%)				
(day)	100%	80%	60%	40%	20%	100%	80%	60%	40%	20%
0	6.4359	6.4547	6.5391	6.7531	6.4153	0	0	0	0	0
8	6.6818	6.4837	6.5542	6.7587	6.4183	3.821	0.449	0.231	0.083	0.047
15	6.7696	6.5083	6.5611	6.7613	6.4201	5.185	0.830	0.336	0.121	0.075
21	6.8293	6.5240	6.5640	6.7630	6.4206	6.113	1.074	0.381	0.147	0.083
28	6.9212	6.5460	6.5681	6.7650	6.4224	7.541	1.414	0.443	0.176	0.111
35	6.9864	6.5648	6.5707	6.7658	6.4234	8.554	1.706	0.483	0.188	0.126
42	7.0690	6.5850	6.5734	6.7661	6.4238	9.837	2.019	0.525	0.193	0.132
49	7.1564	6.6001	6.5750	6.7679	6.4255	11.195	2.253	0.549	0.219	0.159
56	7.2294	6.6164	6.5785	6.7697	6.4251	12.329	2.505	0.603	0.246	0.153
63	7.3593	6.6321	6.5785	6.7697	6.4251	14.348	2.748	0.603	0.246	0.153
70	7.4472	6.6454	6.5793	6.7696	6.4260	15.713	2.954	0.615	0.244	0.167
77	7.5291	6.6575	6.5802	6.7690	6.4260	16.986	3.142	0.629	0.235	0.167
84	7.5905	6.6707	6.5816	6.7703	6.4262	17.940	3.346	0.650	0.255	0.170
91	7.6642	6.6865	6.5833	6.7707	6.4266	19.085	3.591	0.676	0.261	0.176
98	7.8266	6.7158	6.5852	6.7708	6.4268	21.608	4.045	0.705	0.262	0.179
105	7.8991	6.7381	6.5867	6.7713	6.4274	22.735	4.391	0.728	0.270	0.189
112	7.9691	6.7434	6.5876	6.7728	6.4281	23.823	4.473	0.742	0.292	0.200
119	8.0553	6.7518	6.5874	6.7713	6.4272	25.162	4.603	0.739	0.270	0.185
126	8.1561	6.7597	6.5876	6.7705	6.4262	26.728	4.725	0.742	0.258	0.170
133	8.2727	6.7704	6.5894	6.7717	6.4270	28.540	4.891	0.769	0.275	0.182
140	8.3799	6.7601	6.5915	6.7719	6.4267	30.206	4.731	0.801	0.278	0.178
147	8.4557	6.7830	6.5914	6.7720	6.4262	31.383	5.086	0.800	0.280	0.170
154	8.4681	6.7958	6.5913	6.7720	6.4263	31.576	5.285	0.798	0.280	0.171
161	8.5373	6.8102	6.5938	6.7726	6.4279	32.651	5.508	0.837	0.289	0.196
167	8.6145	6.8176	6.5926	6.7715	6.4248	33.851	5.622	0.818	0.272	0.148
182	8.7273	6.8334	6.5973	6.7743	6.4287	35.603	5.867	0.890	0.314	0.209
196	8.8041	6.8350	6.5915	6.7740	6.4285	36.800	5.892	0.801	0.310	0.206
210	8.9439	6.8374	6.5984	6.7743	6.4285	38.969	5.929	0.907	0.314	0.206
220	8.9765	6.8499	6.5999	6.7758	6.4308	39.475	6.123	0.930	0.336	0.242
227	9.0022	6.8607	6.6055	6.7756	6.4293	39.875	6.290	1.015	0.333	0.218
241	9.0688	6.8750	6.6024	6.7771	6.4308	40.910	6.512	0.968	0.355	0.242

Data for Figure 4.4 (continued)

Toluene-saturated aqueous solution

Time	Weight (g)					Weight gain (%)				
(day)	100%	80%	60%	40%	20%	100%	80%	60%	40%	20%
0	7.4566	7.5888	7.3919	7.5027	7.7103	0	0	0	0	0
16	7.5510	7.6165	7.4058	7.5089	7.7159	1.266	0.365	0.188	0.083	0.073
23	7.5951	7.6270	7.4095	7.5108	7.7163	1.857	0.503	0.238	0.108	0.078
29	7.6103	7.6370	7.4148	7.5107	7.7177	2.160	0.635	0.310	0.107	0.096
36	7.6550	7.6489	7.4187	7.5136	7.7195	2.661	0.792	0.363	0.145	0.119
43	7.7068	7.6626	7.4248	7.5155	7.7196	3.355	0.972	0.445	0.171	0.121
50	7.7503	7.6737	7.4293	7.5161	7.7211	3.939	1.119	0.506	0.179	0.140
57	7.7871	7.6899	7.4366	7.5174	7.7214	4.432	1.332	0.605	0.196	0.144
64	7.8272	7.6952	7.4360	7.5180	7.7208	4.970	1.402	0.597	0.204	0.136
71	7.8815	7.7061	7.4403	7.5184	7.7235	5.698	1.546	0.655	0.209	0.171
78	7.9251	7.7157	7.4419	7.5199	7.7234	6.283	1.672	0.676	0.229	0.170
85	7.9702	7.7256	7.4443	7.5200	7.7235	6.888	1.803	0.709	0.231	0.171
92	8.0174	7.7310	7.4449	7.5201	7.7224	7.521	1.874	0.717	0.232	0.157
99	8.0629	7.7371	7.4466	7.5216	7.7234	8.131	1.954	0.740	0.252	0.170
106	8.1095	7.7519	7.4489	7.5216	7.7253	8.756	2.149	0.771	0.252	0.195
113	8.1548	7.7603	7.4510	7.5217	7.7238	9.364	2.260	0.800	0.253	0.175
120	8.2035	7.7678	7.4519	7.5217	7.7240	10.017	2.359	0.812	0.253	0.178
127	8.2448	7.7740	7.4533	7.5212	7.7223	10.571	2.440	0.831	0.247	0.156
134	8.2876	7.7788	7.4530	7.5208	7.7228	11.144	2.504	0.827	0.241	0.162
141	8.3253	7.7879	7.4535	7.5213	7.7215	11.650	2.624	0.833	0.248	0.145
148	8.3643	7.7934	7.4554	7.5224	7.7229	12.173	2.696	0.859	0.263	0.163
153	8.4074	7.8017	7.4565	7.5237	7.7240	12.751	2.805	0.874	0.280	0.178
160	8.4477	7.8054	7.4542	7.5236	7.7228	13.292	2.854	0.843	0.279	0.162
167	8.4905	7.8166	7.4585	7.5225	7.7231	13.866	3.002	0.901	0.264	0.166
173	8.5244	7.8241	7.4621	7.5232	7.7242	14.320	3.101	0.950	0.273	0.180
188	8.6347	7.8314	7.4642	7.5249	7.7246	15.800	3.197	0.978	0.296	0.185
202	8.6869	7.8543	7.4807	7.5251	7.7242	16.500	3.498	1.201	0.298	0.180
216	8.7766	7.8780	7.4915	7.5253	7.7244	17.702	3.811	1.347	0.301	0.183
226	8.8308	7.8870	7.4962	7.5294	7.7278	18.429	3.929	1.411	0.356	0.227
233	8.8698	7.8939	7.4975	7.5288	7.7270	18.952	4.020	1.429	0.348	0.217
247	8.9605	7.8997	7.4986	7.5294	7.7286	20.169	4.097	1.443	0.356	0.237

Data for Figure 4.5

Benzene Vapor

Time (day)	Thickness of Swollen Layer (mm)									
	a=1		a=0.88		a=0.73		a=0.55		a=0.32	
0	0	0	0	0	0	0	0	0	0	0
0.5	0.25	0.26	0.12	0.13	ND	ND	ND	ND	ND	ND
1	0.44	0.44	0.24	0.26	ND	ND	ND	ND	ND	ND
1.5	0.63	0.65	0.34	0.36	0.102	0.105	ND	ND	ND	ND
2	0.75	0.71	0.47	0.48	0.139	0.130	ND	ND	ND	ND
2.5	0.87	0.89	0.59	0.56	0.184	0.187	ND	ND	ND	ND

Square root time ($day^{1/2}$)	Thickness of Swollen Layer (mm)				
	a=1	a=0.88	a=0.73	a=0.55	a=0.32
0.000	0	0	0	0	0
0.707	0.255	0.125	ND	ND	ND
1.000	0.440	0.250	ND	ND	ND
1.225	0.640	0.350	0.104	ND	ND
1.414	0.730	0.475	0.135	ND	ND
1.581	0.880	0.575	0.186	ND	ND

Toluene Vapor

Time (day)	Thickness of Swollen Layer (mm)									
	a=1		a=0.86		a=0.70		a=0.51		a=0.28	
0	0	0	0	0	0	0	0	0	0	0
0.5	0.16	0.18	0.08	0.08	ND	ND	ND	ND	ND	ND
1	0.40	0.38	0.21	0.22	ND	ND	ND	ND	ND	ND
1.5	0.59	0.55	0.28	0.28	0.082	0.076	ND	ND	ND	ND
2	0.66	0.67	0.36	0.35	0.113	0.113	ND	ND	ND	ND
2.5	0.77	0.79	0.44	0.45	0.144	0.139	ND	ND	ND	ND

Square root time ($day^{1/2}$)	Thickness of Swollen Layer (mm)				
	a=1	a=0.86	a=0.70	a=0.51	a=0.28
0.000	0	0	0	0	0
0.707	0.170	0.080	ND	ND	ND
1.000	0.390	0.215	ND	ND	ND
1.225	0.570	0.280	0.079	ND	ND
1.414	0.665	0.355	0.113	ND	ND
1.581	0.780	0.445	0.142	ND	ND

Data for Figure 4.6

Benzene-saturated aqueous solution

Time (day)	Thickness of Swollen Layer (mm)		
	Sample 1	Sample 2	Average
7	0.26	0.22	0.24
14	0.48	0.36	0.42
21	0.60	0.52	0.56
28	0.73	0.63	0.68
35	0.88	0.78	0.83
42	0.98	0.90	0.94

Toluene-saturated aqueous solution

Time (days)	Thickness of Swollen Layer (mm)		
	Sample 1	Sample 2	Average
40	0.21	0.27	0.24
63	0.65	0.41	0.53
84	0.80	0.68	0.74
98	1.12	0.88	1.00
112	1.39	1.13	1.26

A.3 Experimental Data and Modeled Results for Chapter 5

Data for Figure 5.2

Free Product Gasoline

Time	Weight (g)						Weight gain(%)					
(hour)	SBR1	SBR2	SBR3	NBR1	NBR2	NBR3	SBR1	SBR2	SBR3	NBR1	NBR2	NBR3
0	19.273	19.090	19.192	17.197	17.198	17.163	0	0	0	0	0	0
2	26.88	26.62	26.41	23.24	23.18	23.35	55.43	55.61	52.91	51.89	51.36	53.27
4	29.62	29.48	28.92	24.86	24.80	24.97	75.40	76.74	71.31	65.80	65.27	67.22
6	31.16	31.02	30.30	25.68	25.58	25.75	86.62	88.11	81.43	72.84	71.97	73.94
8	32.13	32.01	31.11	26.05	25.97	26.13	93.69	95.42	87.37	76.01	75.32	77.21
18	33.51	33.37	32.23	26.20	26.10	26.30	103.75	105.47	95.58	77.30	76.43	78.67
24	33.63	33.48	32.28	26.23	26.11	26.3	104.62	106.28	95.94	77.56	76.52	78.67

Time	SBR		NBR	
(hour)	AVE.	STDEV	AVE.	STDEV
0	0	0	0	0
2	54.65	1.51	52.17	0.99
4	74.48	2.83	66.10	1.01
6	85.39	3.51	72.91	0.99
8	92.16	4.24	76.18	0.96
18	101.60	5.28	77.47	1.13
24	102.28	5.55	77.58	1.08

Weight of Rod

Sample 1	5.61 g
Sample 2	5.48 g
Sample 3	5.55 g
Sample 4	5.54 g
Average	5.55 g

Water Saturated with Gasoline

Time	Weight (g)						Weight gain(%)					
(day)	SBR1	SBR2	SBR3	NBR1	NBR2	NBR3	SBR1	SBR2	SBR3	NBR1	NBR2	NBR3
0	19.070	19.250	19.150	17.150	17.190	17.120	0	0	0	0	0	0
2	19.51	19.90	19.80	17.51	17.61	17.42	3.25	4.81	4.81	2.66	3.11	2.22
5	19.90	20.50	20.20	17.99	18.10	17.90	6.14	9.25	7.77	6.21	6.73	5.77
14	20.80	20.80	21.00	18.37	18.48	18.32	12.80	11.46	13.68	9.02	9.54	8.88
30	21.40	22.00	21.80	18.82	18.96	18.92	17.23	20.34	19.60	12.35	13.09	13.31
72	21.85	22.80	22.20	19.38	19.28	19.60	20.54	26.26	22.56	16.48	15.44	18.34

Time	SBR		NBR	
(day)	AVE.	STDEV	AVE.	STDEV
0	0	0	0	0
2	4.29	0.90	2.66	0.44
5	7.72	1.55	6.24	0.48
14	12.65	1.12	9.15	0.35
30	19.06	1.62	12.92	0.50
72	23.12	2.90	16.76	1.47

Note: Initial weight of SBR/NBR material
= Weight of gasket – Weight of rod

Data for Figure 5.3

SBR 1

	Concentration of BTEX in water samples (ug/L)															
Time (days)	7	14	21	28	35	42	49	56	63	70	77	84	91	98	105	112
Benzene	1.8	<0.3	1.3	12	253.8	235.1	1176	1154	738	1377	2219	2646	2483	1357	1123	910
Toluene	3.2	<0.3	0.6	5	146.5	145.6	1065	1164	603	1231	2277	2770	2553	1384	1103	882
Ethylbenzene	2.4	<0.2	<0.2	<0.1	4.1	5.7	50	326	28	55	101	120	110	58	72	40
m-Xylene	2.5	<0.2	<0.2	0.2	7.6	10.7	112	373	69	120	224	279	255	138	135	95
o+p-Xylene	2.4	<0.2	<0.2	0.2	7.2	10	112	352	71	127	224	292	265	144	138	100

SBR 2

	Concentration of BTEX in water samples (ug/L)															
Time (days)	7	14	21	28	35	42	49	56	63	70	77	84	91	98	105	112
Benzene	<0.3	0.4	7.3	72.6	1246	2329	3413	4632	4997	3893	4410	4037	4776	4126	4621	4615
Toluene	0.3	<0.3	3.8	54.5	1435	2775	4242	6247	6659	5319	5957	5749	7211	5971	7127	6605
Ethylbenzene	<0.1	<0.2	<0.2	1.5	45.1	128	205	310	348	265	228	305	418	317	377	351
m-Xylene	0.2	<0.2	0.2	2.6	86.2	261	424	664	726	592	660	682	916	706	869	792
o+p-Xylene	0.2	<0.2	<0.2	2.5	81.4	243	402	641	707	572	654	663	910	697	863	794

SBR 3

	Concentration of BTEX in water samples (ug/L)															
Time (days)	7	14	21	28	35	42	49	56	63	70	77	84	91	98	105	112
Benzene	<0.3	1.3	6.9	48.9	458.1	1307	2928	4437	4643	4836	5714	6284	6351	5620	7583	5303
Toluene	0.4	0.7	4.3	37.4	485.6	1352	3754	5644	5380	6104	7283	7842	8027	6970	10044	6406
Ethylbenzene	<0.1	<0.2	<0.2	0.9	13.9	42.3	170	250	223	262	335	330	342	290	442	289
m-Xylene	0.2	0.3	0.4	1.8	26.6	79.9	351	534	477	568	717	742	762	630	978	628
o+p-Xylene	<0.2	0.2	0.2	1.8	25.7	79	338	511	464	556	694	729	744	619	957	642

Volume of Water in Pipe Joint	
SBR 1	1.230 L
SBR 2	1.205 L
SBR 3	1.220 L

Data for Figure 5.3 (continued)

SBR 1

	Mass of BTEX permeated (ug)															
Time (days)	7	14	21	28	35	42	49	56	63	70	77	84	91	98	105	112
Benzene	0	0	2	15	312	289	1446	1419	908	1694	2729	3255	3054	1669	1381	1119
Toluene	0	0	1	6	180	179	1310	1432	742	1514	2801	3407	3140	1702	1357	1085
Ethylbenzene	0	0	0	0	5	7	62	401	34	68	124	148	135	71	89	49
m-Xylene	0	0	0	0	9	13	138	459	85	148	276	343	314	170	166	117
o+p-Xylene	0	0	0	0	9	12	138	433	87	156	276	359	326	177	170	123
	Cumulative mass of BTEX permeated (mg)															
Time (days)	7	14	21	28	35	42	49	56	63	70	77	84	91	98	105	112
Benzene	0	0	0	0	0.3	0.6	2.1	3.5	4.4	6.1	8.8	12.1	15.1	16.8	18.2	19.3
Toluene	0	0	0	0	0.2	0.4	1.7	3.1	3.8	5.4	8.2	11.6	14.7	16.4	17.8	18.9
Ethylbenzene	0	0	0	0	0	0	0.1	0.5	0.5	0.6	0.7	0.8	1.0	1.1	1.1	1.2
m-Xylene	0	0	0	0	0	0	0.2	0.6	0.7	0.9	1.1	1.5	1.8	2.0	2.1	2.2
o+p-Xylene	0	0	0	0	0	0	0.2	0.6	0.7	0.8	1.1	1.5	1.8	2.0	2.1	2.3

SBR 2

	Mass of BTEX permeated (ug)															
Time (days)	7	14	21	28	35	42	49	56	63	70	77	84	91	98	105	112
Benzene	0	0	9	96	1598	4404	8517	14098	20120	24811	30125	34989	40745	45716	51285	56846
Toluene	0	0	5	70	1799	5143	10255	17782	25806	32216	39394	46322	55011	62206	70794	78753
Ethylbenzene	0	0	0	2	56	210	457	831	1250	1570	1844	2212	2716	3098	3552	3975
m-Xylene	0	0	0	3	107	422	932	1733	2607	3321	4116	4938	6042	6892	7940	8894
o+p-Xylene	0	0	0	3	101	394	878	1651	2503	3192	3980	4779	5875	6715	7755	8712
	Cumulative mass of BTEX permeated (mg)															
Time (days)	7	14	21	28	35	42	49	56	63	70	77	84	91	98	105	112
Benzene	0	0	0	0.1	1.6	4.4	8.5	14.1	20.1	24.8	30.1	35.0	40.7	45.7	51.3	56.8
Toluene	0	0	0	0.1	1.8	5.1	10.3	17.8	25.8	32.2	39.4	46.3	55.0	62.2	70.8	78.8
Ethylbenzene	0	0	0	0	0.1	0.2	0.5	0.8	1.3	1.6	1.8	2.2	2.7	3.1	3.6	4.0
m-Xylene	0	0	0	0	0.1	0.4	0.9	1.7	2.6	3.3	4.1	4.9	6.0	6.9	7.9	8.9
o+p-Xylene	0	0	0	0	0.1	0.4	0.9	1.7	2.5	3.2	4.0	4.8	5.9	6.7	7.8	8.7

SBR 3

	Mass of BTEX permeated (ug)															
Time (days)	7	14	21	28	35	42	49	56	63	70	77	84	91	98	105	112
Benzene	0	0	8	68	627	2222	5794	11207	16872	22772	29743	37409	45157	52014	61265	67735
Toluene	0	0	5	51	643	2292	6872	13758	20322	27768	36654	46221	56014	64517	76771	84586
Ethylbenzene	0	0	0	1	18	70	277	582	854	1174	1582	1985	2402	2756	3295	3648
m-Xylene	0	0	0	2	35	132	560	1212	1794	2487	3361	4267	5196	5965	7158	7924
o+p-Xylene	0	0	0	2	34	130	542	1166	1732	2410	3257	4146	5054	5809	6977	7760
	Cumulative mass of BTEX permeated (mg)															
Time (days)	7	14	21	28	35	42	49	56	63	70	77	84	91	98	105	112
Benzene	0	0	0	0.1	0.6	2.2	5.8	11.2	16.9	22.8	29.7	37.4	45.2	52.0	61.3	67.7
Toluene	0	0	0	0.1	0.6	2.3	6.9	13.8	20.3	27.8	36.7	46.2	56.0	64.5	76.8	84.6
Ethylbenzene	0	0	0	0	0	0.1	0.3	0.6	0.9	1.2	1.6	2.0	2.4	2.8	3.3	3.6
m-Xylene	0	0	0	0	0	0.1	0.6	1.2	1.8	2.5	3.4	4.3	5.2	6.0	7.2	7.9
o+p-Xylene	0	0	0	0	0	0.1	0.5	1.2	1.7	2.4	3.3	4.1	5.1	5.8	7.0	7.8

Data for Figure 5.4

NBR 1

	Concentration of BTEX in water samples (ug/L)															
Time (days)	8	15	22	29	36	43	50	57	64	71	78	85	92	99	106	113
Benzene	0.3	5.8	53	72	80	78	291	1814	231	223	1480	461	182	1747	1228	1506
Toluene	0.7	3.9	38	52	58	60	672	4449	1156	359	3283	2204	352	4304	3691	3453
Ethylbenzene	<0.1	0.8	2	2	3	3	92	476	260	55	266	420	112	391	447	361
m-Xylene	0.3	1	4	5	6	6	231	1152	665	163	604	1070	280	940	1115	904
o+p-Xylene	0.2	1	4	6	7	7	224	1163	633	150	627	1024	254	953	1111	901

NBR 2

	Concentration of BTEX in water samples (ug/L)															
Time (days)	8	15	22	29	36	43	50	57	64	71	78	85	92	99	106	113
Benzene	0.3	1.9	22.3	43.7	38.2	40.4	52.4	58.5	66.8	51.2	107.6	92.1	66.7	58.5	41.8	61.2
Toluene	0.8	2.5	13.6	31	26.5	29.4	45.3	45.3	95.2	45.8	89.6	101.9	61.3	51.5	36.2	56.1
Ethylbenzene	0.1	2.1	<0.2	1.7	1	1.2	2.3	1.7	9.4	2.3	4	7.9	2.9	2	1.5	2.4
m-Xylene	0.4	2	1.2	3.5	2.5	2.8	5.4	4.2	23	5.4	9.1	19.1	6.7	4.8	3.4	5.4
o+p-Xylene	0.4	1.9	1.2	3.5	2.6	2.9	5.5	4.4	22.6	5.5	9.4	19.1	6.9	5.1	3.5	5.6

NBR 3

	Concentration of BTEX in water samples (ug/L)															
Time (days)	7	14	29	36	43	50	53	60	67	74	81	88	95	102	109	116
Benzene	<0.3	4.1	495	541	548	1364	198	256	1486	1846	526	1461	2806	1494	2399	1846
Toluene	<0.3	1.7	296	374	417	1998	340	394	2330	3010	1081	1803	5753	2364	3886	2836
Ethylbenzene	<0.2	<0.2	11.9	12.3	14.3	170	36	33	120	274	178	105	568	222	354	235
m-Xylene	<0.2	<0.2	22	26.4	31	400	102	82	282	642	453	257	1389	541	853	579
o+p-Xylene	<0.2	<0.2	23	28	33	401	96	82	293	650	427	265	1405	531	858	580

Volume of Water in Pipe Joint	
NBR 1	1.245 L
NBR 2	1.300 L
NBR 3	1.250 L

Data for Figure 5.4 (continued)

NBR 1

	Mass of BTEX permeated (ug)															
Time (days)	8	15	22	29	36	43	50	57	64	71	78	85	92	99	106	113
Benzene	0	8	74	164	263	359	722	2980	3268	3545	5388	5962	6188	8363	9892	11767
Toluene	1	6	52	117	189	263	1100	6639	8078	8525	12613	15357	15795	21153	25749	30048
Ethylbenzene	0	1	3	6	9	13	127	720	1044	1112	1443	1966	2106	2592	3149	3598
m-Xylene	0	2	6	13	21	29	316	1751	2579	2781	3533	4865	5214	6384	7772	8898
o+p-Xylene	0	1	6	13	21	30	309	1757	2545	2731	3512	4787	5103	6289	7672	8794
	Cumulative mass of BTEX permeated (mg)															
Time (days)	8	15	22	29	36	43	50	57	64	71	78	85	92	99	106	113
Benzene	0	0	0	0	0.3	0.4	0.7	3.0	3.3	3.5	5.4	6.0	6.2	8.4	9.9	11.8
Toluene	0	0	0	0	0.2	0.3	1.1	6.6	8.1	8.5	12.6	15.4	15.8	21.2	25.7	30.0
Ethylbenzene	0	0	0	0	0	0	0.1	0.7	1.0	1.1	1.4	2.0	2.1	2.6	3.1	3.6
m-Xylene	0	0	0	0	0	0	0.3	1.8	2.6	2.8	3.5	4.9	5.2	6.4	7.8	8.9
o+p-Xylene	0	0	0	0	0	0	0.3	1.8	2.5	2.7	3.5	4.8	5.1	6.3	7.7	8.8

NBR 2

	Mass of BTEX permeated (ug)															
Time (days)	8	15	22	29	36	43	50	57	64	71	78	85	92	99	106	113
Benzene	0	3	32	89	138	191	259	335	422	488	628	748	835	911	965	1045
Toluene	1	4	22	62	97	135	194	253	376	436	553	685	765	832	879	952
Ethylbenzene	0	3	3	5	6	8	11	13	25	28	34	44	48	50	52	55
m-Xylene	1	3	5	9	12	16	23	29	59	66	77	102	111	117	122	129
o+p-Xylene	1	3	5	9	12	16	23	29	59	66	78	103	112	118	123	130
	Cumulative mass of BTEX permeated (mg)															
Time (days)	8	15	22	29	36	43	50	57	64	71	78	85	92	99	106	113
Benzene	0	0	0	0.1	0.1	0.2	0.3	0.3	0.4	0.5	0.6	0.7	0.8	0.9	1.0	1.0
Toluene	0	0	0	0.1	0.1	0.1	0.2	0.3	0.4	0.4	0.6	0.7	0.8	0.8	0.9	1.0
Ethylbenzene	0	0	0	0	0.0	0.0	0.0	0.0	0.0	0.0	0.0	0.0	0.0	0.1	0.1	0.1
m-Xylene	0	0	0	0	0.0	0.0	0.0	0.0	0.1	0.1	0.1	0.1	0.1	0.1	0.1	0.1
o+p-Xylene	0	0	0	0	0.0	0.0	0.0	0.0	0.1	0.1	0.1	0.1	0.1	0.1	0.1	0.1

NBR 3

	Mass of BTEX permeated (ug)															
Time (days)	7	14	29	36	43	50	53	60	67	74	81	88	95	102	109	116
Benzene	0	5	624	1301	1985	3690	3938	4258	6115	8423	9080	10907	14414	16282	19280	21588
Toluene	0	2	372	839	1361	3858	4283	4776	7688	11451	12802	15056	22247	25202	30059	33604
Ethylbenzene	0	0	15	30	48	261	306	347	497	839	1062	1193	1903	2181	2623	2917
m-Xylene	0	0	28	61	99	599	727	829	1182	1984	2551	2872	4608	5284	6351	7074
o+p-Xylene	0	0	29	64	105	606	726	829	1195	2008	2541	2873	4629	5293	6365	7090
	Cumulative mass of BTEX permeated (mg)															
Time (days)	7	14	29	36	43	50	53	60	67	74	81	88	95	102	109	116
Benzene	0	0.0	0.6	1.3	2.0	3.7	3.9	4.3	6.1	8.4	9.1	10.9	14.4	16.3	19.3	21.6
Toluene	0	0.0	0.4	0.8	1.4	3.9	4.3	4.8	7.7	11.5	12.8	15.1	22.2	25.2	30.1	33.6
Ethylbenzene	0	0	0.0	0.0	0.0	0.3	0.3	0.3	0.5	0.8	1.1	1.2	1.9	2.2	2.6	2.9
m-Xylene	0	0	0.0	0.1	0.1	0.6	0.7	0.8	1.2	2.0	2.6	2.9	4.6	5.3	6.4	7.1
o+p-Xylene	0	0	0.0	0.1	0.1	0.6	0.7	0.8	1.2	2.0	2.5	2.9	4.6	5.3	6.4	7.1

Data for Figure 5.7

SBR-Benzene

Time	Cumulative mass (mg)	
(day)	Modeled	Measured
0	0.00	0.00
7	0.01	0.00
14	0.24	0.00
21	1.07	0.01
28	2.75	0.07
35	5.31	0.63
42	8.67	2.22
49	12.71	5.79
56	17.33	11.21
63	22.41	16.87
70	27.87	22.77
77	33.63	29.74
84	39.68	37.41
91	45.95	45.16
98	52.39	52.01
105	58.98	61.26
112	65.68	67.73

NBR-Benzene

Time	Modeled cumulative	Time	Measured cumulative
(day)	mass (mg)	(days)	mass (mg)
7	0.00	7	0.00
14	0.01	14	0.01
21	0.08	29	0.62
28	0.28	36	1.30
35	0.68	43	1.99
42	1.33	50	3.69
49	2.23	53	3.94
56	3.38	60	4.26
63	4.78	67	6.12
70	6.40	74	8.42
77	8.23	81	9.08
84	10.25	88	10.91
91	12.45	95	14.41
98	14.80	102	16.28
105	17.30	109	19.28
112	19.92	116	21.59
119	22.65	123	23.70
126	25.49	130	25.77

SBR-Toluene

Time	Cumulative mass (mg)	
(day)	Modeled	Measured
0	0.00	0.00
7	0.00	0.00
14	0.04	0.00
21	0.34	0.01
28	1.22	0.05
35	2.99	0.64
42	5.81	2.29
49	9.76	6.87
56	14.81	13.76
63	20.94	20.32
70	28.07	27.77
77	36.12	36.65
84	44.99	46.22
91	54.62	56.01
98	64.93	64.52
105	75.86	76.77
112	87.35	84.59

NBR-Toluene

Time	Modeled cumulative	Time	Measured cumulative
(day)	mass (mg)	(days)	mass (mg)
7	0.00	7	0.00
14	0.00	14	0.00
21	0.03	29	0.37
28	0.16	36	0.84
35	0.49	43	1.36
42	1.12	50	3.86
49	2.13	53	4.28
56	3.57	60	4.78
63	5.47	67	7.69
70	7.85	74	11.45
77	10.71	81	12.80
84	14.04	88	15.06
91	17.82	95	22.25
98	22.03	102	25.20
105	26.64	109	30.06
112	31.64	116	33.60
119	37.00	123	37.12
126	42.69	130	40.30

Data for Figure 5.12

Pressurized

Time (day)	Mass Permeated (mg)										
	PT 1-2	PT 2-3	PT 3-4	PT 4-5	PT 5-6	PT 6-7	PT 7-8	PT 8-9	PT 9-10	PT 10-11	PT 11-12
7	0.3	0.5	0.5	0.2	0.2	0.2	0.3	0.2	0.3	0.3	0.2
14	2.1	4.2	3.6	2.1	1.4	1.3	2.6	1.9	2.8	3.2	2.9
21	5.6	11.2	9.9	5.6	3.9	3.6	7.2	5.4	8.3	10.4	9.7
28	9.2	18.8	16.5	9.3	6.5	6.0	12.1	9.0	14.5	18.7	17.9
35	12.6	25.8	22.7	12.8	9.0	8.3	16.7	12.5	20.4	26.6	25.6
42	15.9	32.4	28.5	16.1	11.3	10.4	21.0	15.7	25.8	33.8	32.6
49	18.8	38.7	34.1	19.2	13.5	12.4	25.1	18.8	31.0	40.7	39.3
56	21.7	44.8	39.4	22.2	15.7	14.4	29.1	21.8	36.0	47.3	45.8
63	24.5	50.7	44.7	25.2	17.8	16.3	32.9	24.7	40.8	53.7	52.0
70	27.2	56.4	49.8	28.1	19.8	18.3	36.7	27.5	45.5	59.9	58.1
77	29.9	62.1	54.9	31.0	21.8	20.1	40.5	30.3	50.2	66.1	64.1
84	32.7	67.7	59.9	33.8	23.8	21.9	44.2	33.1	54.8	72.2	70.0
91	35.4	73.3	64.9	36.6	25.7	23.8	47.9	35.9	59.4	78.2	75.9
98	38.1	79.0	69.9	39.4	27.7	25.6	51.6	38.6	64.0	84.2	81.7
105	40.8	84.6	74.9	42.3	29.7	27.4	55.3	41.4	68.5	90.2	87.5
112	43.6	90.3	79.8	45.1	31.7	29.3	59.0	44.2	73.1	96.3	93.4

Time (day)	Mass Permeated (mg)									
	PT12-13	PT13-14	PT14-15	PT15-16	PT16-17	PM17-18	PT18-19	PT19-20	Total	Cumulative
7	0.2	0.2	0.1	0.0	0.0	0.0	0.0	0.0	3.6	3.6
14	2.6	2.3	1.3	0.5	0.0	0.0	0.1	0.7	35.6	39.1
21	8.8	8.0	4.6	1.8	0.1	0.1	0.3	2.4	107.0	146.2
28	16.4	15.1	8.7	3.5	0.3	0.2	0.6	4.6	187.8	334.0
35	23.7	21.8	12.6	5.0	0.4	0.3	0.9	6.7	264.4	598.4
42	30.3	27.9	16.1	6.4	0.5	0.4	1.1	8.6	335.0	933.4
49	36.6	33.6	19.4	7.7	0.6	0.4	1.3	10.4	401.8	1335.2
56	42.6	39.1	22.6	9.0	0.7	0.5	1.6	12.1	466.2	1801.4
63	48.4	44.5	25.7	10.2	0.8	0.6	1.8	13.7	529.0	2330.3
70	54.1	49.7	28.8	11.4	0.9	0.7	2.0	15.4	590.3	2920.6
77	59.7	54.8	31.7	12.6	1.0	0.7	2.2	17.0	650.7	3571.3
84	65.2	59.9	34.6	13.8	1.0	0.8	2.4	18.5	710.4	4281.6
91	70.7	64.9	37.5	14.9	1.1	0.9	2.6	20.1	769.7	5051.4
98	76.1	69.9	40.4	16.1	1.2	0.9	2.8	21.6	828.9	5880.3
105	81.5	74.9	43.3	17.2	1.3	1.0	3.0	23.1	888.2	6768.5
112	87.0	79.9	46.2	18.4	1.4	1.1	3.2	24.7	947.4	7715.8

	PT 1-2	PT 2-3	PT 3-4	PT 4-5	PT 5-6	PT 6-7	PT 7-8	PT 8-9	PT 9-10	PT 10-11	PT 11-12
Surface area (cm^2)	0.341	0.474	0.455	0.424	0.362	0.374	0.834	0.904	1.751	1.887	2.008

	PT12-13	PT13-14	PT14-15	PT15-16	PT16-17	PM17-18	PT18-19	PT19-20
Surface area (cm^2)	2.153	2.424	2.287	2.754	3.235	3.111	1.293	1.315

For non-pressurized system, see the previous appendix "SBR-Benzene Modeled"

A.4 Experimental Data for Chapter 6

Data for Figure 6.2

Concentration of BTEX in 43-mL vials (ug/L)

Time (day)	0	1	3	5	7	10	13	17	20	23	26	29	32
Benzene	0	0	0	0	23	4112	7520	10745	13086	13669	17147	16514	16844
Toluene	0	0	0	0	9	3601	6626	9840	11484	12756	17364	16726	16862
Ethylbenzene	0	0	0	0	0	145	267	400	467	523	694	670	676
m-Xylene	0	0	0	0	0	364	678	1040	1196	1376	1821	1748	1739
o+p-Xylene	0	0	0	0	0	395	737	1138	1292	1519	2012	1930	1897

Concentration of BTEX in pipe water (ug/L)

Time (day)	0	1	3	5	7	10	13	17	20	23	26	29	32
Benzene	0	0	0	0	100	17680	32338	46204	56270	58777	73734	71012	72431
Toluene	0	0	0	0	39	15485	28491	42312	49381	54851	74665	71922	72507
Ethylbenzene	0	0	0	0	1	622	1150	1720	2008	2249	2982	2882	2905
m-Xylene	0	0	0	0	1	1566	2917	4472	5143	5917	7832	7518	7479
o+p-Xylene	0	0	0	0	2	1700	3167	4893	5556	6532	8652	8299	8156

Mass of BTEX permeated (ug)

Time (day)	0	1	3	5	7	10	13	17	20	23	26	29	32
Benzene	0	0	0	0	4	792	1449	2070	2521	2633	3303	3181	3245
Toluene	0	0	0	0	2	694	1276	1896	2212	2457	3345	3222	3248
Ethylbenzene	0	0	0	0	0	28	52	77	90	101	134	129	130
m-Xylene	0	0	0	0	0	70	131	200	230	265	351	337	335
o+p-Xylene	0	0	0	0	0	76	142	219	249	293	388	372	365

Mass of BTEX permeated per unit area (ug/cm^2)

Time (day)	0	1	3	5	7	10	13	17	20	23	26	29	32
Benzene	0	0	0	0	0.05	9.7	17.7	25.3	30.8	32.2	40.3	38.8	39.6
Toluene	0	0	0	0	0.02	8.5	15.6	23.1	27.0	30.0	40.8	39.3	39.7
Ethylbenzene	0	0	0	0	0	0.3	0.6	0.9	1.1	1.2	1.6	1.6	1.6
m-Xylene	0	0	0	0	0	0.9	1.6	2.4	2.8	3.2	4.3	4.1	4.1
o+p-Xylene	0	0	0	0	0	0.9	1.7	2.7	3.0	3.6	4.7	4.5	4.5

Cumulative mass of BTEX permeated per unit area (ug/cm^2)

Time (day)	0	1	3	5	7	10	13	17	20	23	26	29	32
Benzene	0	0	0	0	0.06	9.7	27.4	52.7	83.5	115.6	156.0	194.8	234.4
Toluene	0	0	0	0	0.02	8.5	24.1	47.2	74.2	104.2	145.1	184.4	224.1
Ethylbenzene	0	0	0	0	0	0.3	1.0	1.9	3.0	4.2	5.9	7.4	9.0
m-Xylene	0	0	0	0	0	0.9	2.5	4.9	7.7	11.0	15.2	19.4	23.4
o+p-Xylene	0	0	0	0	0	0.9	2.7	5.3	8.4	12.0	16.7	21.2	25.7

Volume of pipe water

44.8 mL

Surface area

D=3.2 cm

L=8.15 cm

S=3.14*D*L 81.8912 cm^2

Data for Figure 6.3

100% SAT

Concentration of BTEX in pipe water (ug/L)

Time (day)	**3**	**6**	**9**	**11**	**13**	**15**	**17**	**20**	**23**	**26**	**29**
Benzene	0	0	0	0	2.2	6.9	14.6	43.4	92.5	148.4	255.9
Toluene	0	0	0	0	0	0	0	6.9	18.9	37.4	75.7
Ethylbenzene	0	0	0	0	0	0	0	0	0	0	0
m-Xylene	0	0	0	0	0	0	0	0	0	0	0
o+p-Xylene	0	0	0	0	0	0	0	0	0	0	0
Time (day)	**32**	**35**	**38**	**41**	**44**	**48**	**52**	**56**	**60**	**64**	**68**
Benzene	396	604	732	1117	2162	3010	3040	3277	3208	3500	4248
Toluene	137	231	323	496	1140	1668	1931	2352	2309	3010	5444
Ethylbenzene	0	0	0	2	6	8	13	4	9	9	26
m-Xylene	0	0	0	5	11	42	47	56	56	77	95
o+p-Xylene	0	0	0	6	15	252	404	340	249	116	120
Time (day)	**72**	**77**	**82**	**87**	**93**	**98**	**106**	**112**	**121**	**127**	
Benzene	6218	7542	8254	8503	10045	9671	11275	10505	12646	10879	
Toluene	5255	6734	8095	8338	9701	9460	10466	10389	12539	11292	
Ethylbenzene	69	82	90	120	189	172	172	202	245	219	
m-Xylene	138	228	250	300	374	374	417	464	581	520	
o+p-Xylene	168	237	240	300	366	361	430	469	589	520	

Cumulative mass of BTEX permeated per unit area (ug/cm^2)

Time (day)	**3**	**6**	**9**	**11**	**13**	**15**	**17**	**20**	**23**	**26**	**29**
Benzene	0	0	0	0	0.0	0.01	0.02	0.04	0.11	0.20	0.37
Toluene	0	0	0	0	0	0	0	0.00	0.02	0.04	0.09
Ethylbenzene	0	0	0	0	0	0	0	0	0	0	0
m-Xylene	0	0	0	0	0	0	0	0	0	0	0
o+p-Xylene	0	0	0	0	0	0	0	0	0	0	0
Time (day)	**32**	**35**	**38**	**41**	**44**	**48**	**52**	**56**	**60**	**64**	**68**
Benzene	0.63	1.03	1.51	2.25	3.67	5.65	7.66	9.82	11.93	14.23	17.03
Toluene	0.18	0.33	0.55	0.87	1.62	2.72	3.99	5.54	7.06	9.05	12.63
Ethylbenzene	0	0	0	0.00	0.00	0.01	0.02	0.02	0.03	0.03	0.05
m-Xylene	0	0	0	0.00	0.00	0.04	0.07	0.11	0.14	0.19	0.26
o+p-Xylene	0	0	0	0.00	0.00	0.18	0.45	0.67	0.83	0.91	0.99
Time (day)	**72**	**77**	**82**	**87**	**93**	**98**	**106**	**112**	**121**	**127**	
Benzene	21.13	26.10	31.53	37.13	43.75	50.12	57.54	64.46	72.78	79.92	
Toluene	16.09	20.53	25.86	31.35	37.74	43.97	50.87	57.71	65.97	73.40	
Ethylbenzene	0.10	0.15	0.21	0.29	0.41	0.53	0.64	0.77	0.93	1.08	
m-Xylene	0.35	0.50	0.66	0.86	1.11	1.35	1.63	1.93	2.32	2.66	
o+p-Xylene	1.10	1.26	1.41	1.61	1.85	2.09	2.37	2.68	3.07	3.41	

Volume of pipe water

53.94 mL

Surface area

D=3.2 cm

L=8.15 cm

S=3.14*D*L 81.891 cm^2

Data for Figure 6.3 (continued)

50% SAT

Concentration of BTEX in pipe water (ug/L)

Time (day)	**6**	**9**	**11**	**13**	**15**	**17**	**20**	**23**	**26**	**29**	**32**
Benzene	0	0	0	0	0.0	9.5	23.0	43.4	76.5	121.7	202.1
Toluene	0	0	0	0	0	0	0	8.6	19.8	37.0	70.09
Ethylbenzene	0	0	0	0	0	0	0	0	0	0	0
m-Xylene	0	0	0	0	0	0	0	0	0	0	0
o+p-Xylene	0	0	0	0	0	0	0	0	0	0	0
Time (day)	**35**	**38**	**41**	**44**	**48**	**52**	**56**	**60**	**64**	**68**	**72**
Benzene	288	387	515	718	359	826	1084	1229	1495	1541	1568
Toluene	111	172	235	359	189	486	723	911	1165	1114	1247
Ethylbenzene	0	0	0	0	6	3	10	7	10	12	35
m-Xylene	0	0	0	0	9	7	14	14	21	23	28
o+p-Xylene	0	0	0	0	9	8	15	16	22	24	28
Time (day)	**78**	**83**	**88**	**93**	**99**	**104**	**112**	**118**	**127**	**133**	
Benzene	2194	2378	2400	2450	3019	2657	4051	3474	4304	3586	
Toluene	1678	2150	2200	2250	2786	2593	3780	3453	4433	3831	
Ethylbenzene	26	30	40	45	47	56	82	108	73	77	
m-Xylene	39	86	90	96	116	116	189	202	185	172	
o+p-Xylene	39	112	127	112	120	120	202	202	185	163	

Cumulative mass of BTEX permeated per unit area (ug/cm^2)

Time (day)	**6**	**9**	**11**	**13**	**15**	**17**	**20**	**23**	**26**	**29**	**32**
Benzene	0	0	0	0	0.0	0.01	0.02	0.05	0.10	0.18	0.32
Toluene	0	0	0	0	0	0	0	0.01	0.02	0.04	0.09
Ethylbenzene	0	0	0	0	0	0	0	0	0	0	0
m-Xylene	0	0	0	0	0	0	0	0	0	0	0
o+p-Xylene	0	0	0	0	0	0	0	0	0	0	0
Time (day)	**35**	**38**	**41**	**44**	**48**	**52**	**56**	**60**	**64**	**68**	**72**
Benzene	0.51	0.77	1.12	1.60	1.84	2.39	3.12	3.94	4.94	5.98	7.03
Toluene	0.17	0.28	0.44	0.68	0.80	1.13	1.61	2.23	3.01	3.75	4.59
Ethylbenzene	0	0	0	0.00	0.00	0.01	0.01	0.02	0.03	0.03	0.06
m-Xylene	0	0	0	0.00	0.01	0.01	0.02	0.03	0.04	0.06	0.08
o+p-Xylene	0	0	0	0.00	0.01	0.01	0.02	0.03	0.05	0.06	0.08
Time (day)	**78**	**83**	**88**	**93**	**99**	**104**	**112**	**118**	**127**	**133**	
Benzene	8.50	10.09	11.70	13.34	15.36	17.14	19.86	22.18	25.05	27.42	
Toluene	5.71	7.15	8.63	10.13	12.00	13.74	16.27	18.58	21.55	24.12	
Ethylbenzene	0.07	0.09	0.12	0.15	0.18	0.22	0.27	0.35	0.40	0.45	
m-Xylene	0.10	0.16	0.22	0.29	0.36	0.44	0.57	0.70	0.83	0.94	
o+p-Xylene	0.11	0.18	0.27	0.34	0.42	0.51	0.64	0.78	0.90	1.01	

Volume of pipe water

54.87 mL

Surface area

D=3.2 cm

L=8.15 cm

S=3.14*D*L 81.8912 cm^2

Data for Figure 6.3 (continued)

10% SAT

Concentration of BTEX in pipe water (ug/L)

Time (day)	16	26	29	32	35	38	41	44	48	52	56	60	64
Benzene	0	21.9	23.2	31.4	38.3	46.4	64.9	117.0	74.0	21.1	109.7	163.4	199.1
Toluene	0	9.9	11.2	9.5	12.5	18.1	26.7	57.2	37.8	12.9	71.0	118.3	144.1
Ethylbenzene	0	0	0	0	0	0	0	0	0	0	0	0	0
m-Xylene	0	0	0	0	0	0	0	0	0	0	0	0	0
o+p-Xylene	0	0	0	0	0	0	0	0	0	0	0	0	0
Time (day)	**68**	**72**	**78**	**83**	**88**	**93**	**99**	**104**	**112**	**118**	**127**	**133**	
Benzene	113.5	169.9	288.5	251.6	294.7	330.3	475.6	411.5	688.9	627.8	688.0	516.0	
Toluene	82.6	132.0	215.4	206.0	246.0	281.2	415.0	372.4	609.3	609.7	658.8	520.3	
Ethylbenzene	0	0	0	0	0	0	0	0	0	0	0	0	
m-Xylene	0	0	0	0	0	0	0	0	0	0	0	0	
o+p-Xylene	0	0	0	0	0	0	0	0	0	0	0	0	

Cumulative mass of BTEX permeated per unit area (ug/cm^2)

Time (day)	16	26	29	32	35	38	41	44	48	52	56	60	64
Benzene	0	0.015	0.016	0.021	0.026	0.031	0.043	0.078	0.049	0.014	0.073	0.109	0.133
Toluene	0	0.007	0.007	0.006	0.008	0.012	0.018	0.038	0.025	0.009	0.047	0.079	0.096
Ethylbenzene	0	0	0	0	0	0	0	0	0	0	0	0	0
m-Xylene	0	0	0	0	0	0	0	0	0	0	0	0	0
o+p-Xylene	0	0	0	0	0	0	0	0	0	0	0	0	0
Time (day)	**68**	**72**	**78**	**83**	**88**	**93**	**99**	**104**	**112**	**118**	**127**	**133**	
Benzene	0.076	0.113	0.193	0.168	0.197	0.221	0.318	0.275	0.460	0.419	0.459	0.345	
Toluene	0.055	0.088	0.144	0.138	0.164	0.188	0.277	0.249	0.407	0.407	0.440	0.347	
Ethylbenzene	0	0	0	0	0	0	0	0	0	0	0	0	
m-Xylene	0	0	0	0	0	0	0	0	0	0	0	0	
o+p-Xylene	0	0	0	0	0	0	0	0	0	0	0	0	

1% SAT

Concentration of BTEX in pipe water (ug/L)

Time (day)	43	59	73	78	113	122	128	135	142
Benzene	4	4.7	6.5	3.4	49.0	58.5	46.4	52.0	51.6
Toluene	2	3.0	5.2	2.2	26.7	39.1	31.8	45.2	42.6

Cumulative mass of BTEX permeated per unit area (ug/cm^2)

Time (day)	43	59	73	78	113	122	128	135	142
Benzene	0.003	0.006	0.010	0.012	0.045	0.084	0.115	0.150	0.184
Toluene	0.001	0.003	0.007	0.008	0.026	0.052	0.073	0.103	0.132

Volume of pipe water

10%SAT 54.69 mL

1% SAT 54.69 mL

Surface area

D=3.2 cm

L=8.15 cm

S=3.14*D*L 81.8912 cm^2

Data for Figure 6.3 (continued)

100% SAT

	Concentration of BTEX in Soil Pore Water (ug/L)							Ave. (mg/L)	Std. (mg/L)
Benzene	64414	75402	71365	66086	72761	65327	57267	67.5	4.9
Toluene	53248	66756	62754	51590	61729	53669	44187	56.3	6.4
Ethylbenzene	2060	2607	2463	1864	2344	1889	1369	2.1	0.3
m-Xylene	4951	6037	5791	4239	5468	4759	3485	5.0	0.7
o+p-Xylene	5663	6844	6683	5006	6327	5423	4074	5.7	0.8
BTEX	130336	157646	149056	128785	148629	131067	110382	136.6	13.0

50% SAT

	Concentration of BTEX in Soil Pore Water (ug/L)							Ave. (mg/L)	Std. (mg/L)
Benzene	37798	28308	28689	30666	34058	31942	26810	31.2	2.9
Toluene	31056	25817	24425	27982	28599	26032	20299	26.3	2.5
Ethylbenzene	1140	919	850	1103	1045	940	714	1.0	0.1
m-Xylene	2896	2379	2149	2762	2626	2387	1826	2.4	0.3
o+p-Xylene	3319	3963	2570	3194	3066	2747	2110	3.0	0.4
BTEX	76209	61386	58683	65707	69394	64048	51759	63.9	5.7

10% SAT

	Concentration of BTEX in Soil Pore Water (ug/L)						Ave. (mg/L)	Std. (mg/L)
Benzene	6934	5643	6433	6554	5615	4834	6.0	0.6
Toluene	5977	4972	5315	5445	4578	4720	5.2	0.4
Ethylbenzene	259	215	232	218	188	204	0.2	0.0
m-Xylene	659	522	584	386	479	602	0.5	0.1
o+p-Xylene	844	867	787	547	541	680	0.7	0.1
BTEX	14673	12219	13351	13150	11401	11040	12.6	1.1

1% SAT

	Concentration of BTEX (ug/L)				Ave. (mg/L)	Std. (mg/L)
Benzene	981	634.5	472.8	367.9	0.6	0.3
Toluene	871.4	527.2	414	280	0.5	0.3
Ethylbenzene						
m-Xylene						
o+p-Xylene						
BTEX	1852.4	1161.7	886.8	647.9	1.1	0.6

Data for Figure 6.4

Benzene		Toluene	
Concentration in soil pore water X (mg/L)	Permeation rate Y Y (ug/cm^2/day)	Concentration in soil pore water X (mg/L)	Permeation rate Y (ug/cm^2/day)
67.5 ± 4.9	1.044	56.2 ± 4.9	1.011
31.2 ± 2.9	0.344	26.3 ± 2.9	0.325
6.0 ± 0.6	0.057	5.2 ± 0.4	0.052
0.6 ± 0.3	0.0046	0.5 ± 0.3	0.0042

Data for Figure 6.5

Total BTEX : 1216 mg/kg dry soil

Concentration of BTEX in pipe water (ug/L)

Time (day)	10	14	18	22	26	30	34	38	42	46	50	54
Benzene	18	66	865	2821	2580	1668	1402	757	434	280	163	155
Toluene	10	123	5286	18107	33622	29309	44484	34082	27099	21023	14895	12874
Ethylbenzene	0	0	82	912	2322	2395	4881	4257	3982	3608	3178	3165
m-Xylene	0.9	0.9	177	2077	6244	6631	13868	12272	11756	11017	9434	9856
o+p-Xylene	0.9	2.6	230	2030	6454	6966	15149	13743	13287	12685	10612	11571

Time (day)	58	62	67	71	75	79	84	88	92	96	101	130
Benzene	99	103	56	39	211	95	383	1049	65	65	60	65
Toluene	10217	8768	6257	5672	4932	5104	4764	5569	2189	1802	1582	989
Ethylbenzene	2855	2829	2197	2322	2141	2619	2348	2227	1449	1294	1200	993
m-Xylene	9138	9215	7555	7903	6902	8639	7762	7495	5117	4580	4309	3887
o+p-Xylene	10578	10724	8961	9378	8355	10483	9503	9206	6411	5719	5452	5113

Cumulative mass of BTEX permeated per unit area (ug/cm^2)

Time (day)	10	14	18	22	26	30	34	38	42	46	50	54
Benzene	0.010	0.046	0.525	2.1	3.5	4.4	5.2	5.6	5.9	6.0	6.1	6.2
Toluene	0.006	0.074	3.001	13.0	31.6	47.9	72.5	91.4	106.4	118.0	126.3	133.4
Ethylbenzene	0.000	0.000	0.046	0.6	1.8	3.2	5.9	8.2	10.4	12.4	14.2	15.9
m-Xylene	0.000	0.001	0.099	1.2	4.7	8.4	16.1	22.8	29.4	35.5	40.7	46.1
o+p-Xylene	0.000	0.002	0.129	1.3	4.8	8.7	17.1	24.7	32.0	39.1	44.9	51.3

Time (day)	58	62	67	71	75	79	84	88	92	96	101	130
Benzene	6.3	6.3	6.3	6.4	6.5	6.5	6.8	7.3	7.4	7.4	7.4	7.5
Toluene	139.0	143.9	147.4	150.5	153.2	156.0	158.7	161.8	163.0	164.0	164.9	165.4
Ethylbenzene	17.5	19.1	20.3	21.6	22.8	24.2	25.5	26.8	27.6	28.3	28.9	29.5
m-Xylene	51.2	56.3	60.5	64.9	68.7	73.5	77.8	81.9	84.7	87.3	89.7	91.8
o+p-Xylene	57.2	63.1	68.1	73.3	77.9	83.7	89.0	94.1	97.6	100.8	103.8	106.6

Volume of pipe water

49.34 mL

Surface area

D=3.2 cm

L=8.15 cm

S=3.14*D*L 81.891 cm^2

Data for Figure 6.5 (continued)

Total BTEX : 388 mg/kg dry soil

Concentration of BTEX in pipe water (ug/L)

Time (day)	10	14	18	22	26	30	34	38	42	46	50	54
Benzene	0	1	7	2	3	7	4	1	6	5	30	52
Toluene	0	2	34	181	547	1065	1540	2924	3369	3077	1836	1789
Ethylbenzene	0	1	8	6	41	145	259	633	924	1044	791	856
m-Xylene	0.0	1.3	9	13	98	362	725	2207	3429	3909	2610	2881
o+p-Xylene	0.0	1.3	9	28	135	399	734	2196	3379	3942	2713	3057

Time (day)	58	62	67	71	75	79	84	88	92	96	101	130
Benzene	39	589	26	39	120	65	52	39	495	60	409	60
Toluene	1505	2395	1101	1019	757	1002	847	576	1548	581	1135	473
Ethylbenzene	860	1737	679	658	417	761	671	568	1221	486	744	434
m-Xylene	2821	3810	2709	2829	1668	3096	2821	2193	3040	2262	2253	1969
o+p-Xylene	3023	3965	2971	3148	1849	3393	3169	2451	3388	2696	2774	2516

Cumulative mass of BTEX permeated per unit area (ug/cm^2)

Time (day)	10	14	18	22	26	30	34	38	42	46	50	54
Benzene	0.000	0.000	0.005	0.0	0.0	0.0	0.0	0.0	0.0	0.0	0.0	0.1
Toluene	0.000	0.001	0.019	0.1	0.4	1.0	1.9	3.5	5.3	7.0	8.0	9.0
Ethylbenzene	0.000	0.001	0.005	0.0	0.0	0.1	0.3	0.6	1.1	1.7	2.1	2.6
m-Xylene	0.000	0.001	0.005	0.0	0.1	0.3	0.7	1.9	3.8	5.9	7.4	9.0
o+p-Xylene	0.000	0.001	0.006	0.0	0.1	0.3	0.7	1.9	3.8	6.0	7.5	9.2

Time (day)	58	62	67	71	75	79	84	88	92	96	101	130
Benzene	0.1	0.4	0.4	0.4	0.5	0.5	0.6	0.6	0.9	0.9	1.1	1.2
Toluene	9.9	11.2	11.8	12.4	12.8	13.3	13.8	14.1	15.0	15.3	15.9	16.2
Ethylbenzene	3.1	4.0	4.4	4.8	5.0	5.4	5.8	6.1	6.8	7.0	7.5	7.7
m-Xylene	10.5	12.6	14.1	15.7	16.6	18.3	19.9	21.1	22.8	24.0	25.2	26.3
o+p-Xylene	10.8	13.0	14.7	16.4	17.4	19.3	21.0	22.4	24.3	25.7	27.3	28.7

Volume of pipe water

49.18 mL

Surface area

D=3.2 cm

L=8.15 cm

S=3.14*D*L 81.891 cm^2

Data for Figure 6.5 (continued)

Total BTEX : 89 mg/kg dry soil

Concentration of BTEX in pipe water (ug/L)

Time (day)	10	14	18	22	26	30	34	38	42	46	50	54
Benzene	0	0	0	0	0	0	0	0	0	2.6	0.0	0.0
Toluene	0	0	0	0	3.0	13.3	9.0	22.4	36.6	48.2	39.1	43.9
Ethylbenzene	0	0	0	0	0	1.3	1.3	4.3	9.5	16.3	16.8	18.9
m-Xylene	0	0	0	0	0	3.9	6.9	15.1	31.4	54.2	71.4	83.0
o+p-Xylene	0	0	0	0	1.7	8.2	12.0	21.9	39.6	61.5	74.0	84.3

Time (day)	58	62	67	71	75	79	84	88	92	96	101	130
Benzene	0.0	25.4	5.2	1.7	1.3	2.2	5.2	2.2	1.7	1.7	2.2	2.2
Toluene	45.2	44.7	43.9	43.9	47.3	50.3	53.8	52.0	46.9	46.9	46.0	55.5
Ethylbenzene	23.2	24.9	27.5	30.5	37.4	42.1	46.0	45.6	43.4	47.3	47.3	56.8
m-Xylene	105.8	117.4	136.3	154.8	175.9	201.2	226.2	226.2	221.5	242.5	243.0	305.7
o+p-Xylene	104.9	113.1	129.9	148.4	172.0	196.9	224.5	227.5	227.0	251.1	255.4	354.8

Cumulative mass of BTEX permeated per unit area (ug/cm^2)

Time (day)	10	14	18	22	26	30	34	38	42	46	50	54
Benzene	0	0	0	0	0	0	0	0	0	0.001	0.001	0.001
Toluene	0	0	0	0	0.002	0.009	0.014	0.027	0.047	0.074	0.096	0.120
Ethylbenzene	0	0	0	0	0.000	0.001	0.001	0.004	0.009	0.018	0.028	0.038
m-Xylene	0	0	0	0	0.000	0.002	0.006	0.014	0.032	0.062	0.102	0.148
o+p-Xylene	0	0	0	0	0.001	0.006	0.012	0.024	0.047	0.081	0.122	0.169

Time (day)	58	62	67	71	75	79	84	88	92	96	101	130
Benzene	0.001	0.016	0.018	0.019	0.020	0.021	0.024	0.025	0.026	0.027	0.029	0.030
Toluene	0.145	0.170	0.195	0.219	0.246	0.274	0.304	0.333	0.359	0.385	0.411	0.442
Ethylbenzene	0.051	0.065	0.080	0.097	0.118	0.142	0.168	0.193	0.217	0.244	0.270	0.302
m-Xylene	0.207	0.273	0.349	0.436	0.534	0.646	0.772	0.899	1.022	1.158	1.293	1.464
o+p-Xylene	0.228	0.291	0.363	0.446	0.542	0.652	0.778	0.905	1.031	1.172	1.314	1.512

Volume of pipe water

49.76 mL

Surface area

D=3.2 cm

L=8.15 cm

S=3.14*D*L 81.891 cm^2

Data for Figure 6.5 (continued)

Total BTEX : 32 mg/kg dry soil

Concentration of BTEX in pipe water (ug/L)

Time (day)	10	14	18	22	26	30	34	38	42	46	50	54
Benzene	0	0	0	0	0	0	0	0	0	0	0	0
Toluene	0	0	0	0	0	0	0	0.9	1.3	1.7	1.3	1.7
Ethylbenzene	0	0	0	0	0	0	0	0	0	0	0	0
m-Xylene	0	0	0	0	0	0	0	0	0	0	0	0
o+p-Xylene	0	0	0	0	0	0	0	0	0	0	0	0

Time (day)	58	62	67	71	75	79	84	88	92	96	101	130
Benzene	0	7.1	3.4	0.9	1.3	3.0	10.3	1.7	0.9	0.9	0.9	1.7
Toluene	1.7	3.9	2.2	1.7	3.4	6.5	16.8	6.0	2.6	2.2	2.2	4.3
Ethylbenzene	0	0	0	0	0	0	10.3	0.9	0.0	0.0	0.0	0.9
m-Xylene	0	4.7	5.6	6.0	10.8	12.0	20.2	10.3	9.9	10.8	11.2	18.1
o+p-Xylene	0	4.7	5.6	6.0	10.3	11.6	19.4	10.3	9.9	11.2	11.6	21.5

Cumulative mass of BTEX permeated per unit area (ug/cm^2)

Time (day)	10	14	18	22	26	30	34	38	42	46	50	54
Benzene	0	0	0	0	0	0	0	0	0	0	0	0
Toluene	0	0	0	0	0	0	0	0.0005	0.0012	0.0021	0.0029	0.0038
Ethylbenzene	0	0	0	0	0	0	0	0	0	0	0	0
m-Xylene	0	0	0	0	0	0	0	0	0	0	0	0
o+p-Xylene	0	0	0	0	0	0	0	0	0	0	0	0

Time (day)	58	62	67	71	75	79	84	88	92	96	101	130
Benzene	0	0.004	0.006	0.006	0.007	0.009	0.014	0.015	0.016	0.016	0.017	0.018
Toluene	0.005	0.007	0.008	0.009	0.011	0.015	0.024	0.027	0.029	0.030	0.031	0.033
Ethylbenzene	0	0	0	0	0	0	0.006	0.006	0.006	0.006	0.006	0.007
m-Xylene	0	0.003	0.006	0.009	0.015	0.022	0.033	0.039	0.044	0.050	0.056	0.066
o+p-Xylene	0	0.003	0.006	0.009	0.015	0.021	0.032	0.038	0.043	0.049	0.056	0.068

Volume of pipe water

49.29 mL

Surface area

D=3.2 cm

L=8.15 cm

S=3.14*D*L 81.8912 cm^2

Data for Figure 6.6

Organic top soil

	Concentration of BTEX (ug/L) in soil pore water											
Time	7 day		14 day		24 day		30 day		40 day		56 day	
	vial	soil pore	vial	soil pore	vial	soil pore	vial	soil pore	vial	soil pore	vial	soil pore
Benzene	2142	23027	2389	25682	2767	29745	2164	23263	2038	21909	1551	16673
Toluene	1571	16888	1416	15222	1756	18877	1059	11384	980	10535	714	7676
Ethylbenzene	44	473	44	473	42	452	68	731	28	301	9	97
m-Xylene	87	935	94	1011	125	1344	120	1290	62	667	37	398
o+p-Xylene	135	1451	119	1279	151	1623	131	1408	83	892	44	473
Total BTEX	3979	42774	4062	43667	4841	52041	3542	38077	3191	34303	2355	25316

Sand- topsoil mixture

	Concentration of BTEX (ug/L) in soil pore water											
Time	7 day		14 day		24 day		30 day		40 day		56 day	
	vial	soil pore	vial	soil pore	vial	soil pore	vial	soil pore	vial	soil pore	vial	soil pore
Benzene	3443	37012	3565	38324	3312	35604	3299	35464	3161	33981	2576	27692
Toluene	2263	24327	2175	23381	1970	21178	1676	18017	1565	16824	1238	13309
Ethylbenzene	77	828	75	806	70	753	82	882	37	398	24	258
m-Xylene	169	1817	143	1537	131	1408	147	1580	93	1000	67	720
o+p-Xylene	197	2118	317	3408	155	1666	160	1720	106	1140	81	871
Total BTEX	6149	66102	6275	67456	5638	60609	5364	57663	4962	53342	3986	42850

Silica sand

	Concentration of BTEX (ug/L) in soil pore water											
Time	7 day		14 day		24 day		30 day		40 day		56 day	
	vial	soil pore	vial	soil pore	vial	soil pore	vial	soil pore	vial	soil pore	vial	soil pore
Benzene	5582	60007	4811	51718	4809	51697	4726	50805	4599	49439	3716	39947
Toluene	4217	45333	3219	34604	2940	31605	2917	31358	2567	27595	1789	19232
Ethylbenzene	146	1570	104	1118	84	903	111	1193	111	1193	38	409
m-Xylene	387	4160	268	2881	216	2322	286	3075	209	2247	101	1086
o+p-Xylene	466	5010	401	4311	258	2774	312	3354	240	2580	124	1333
Total BTEX	10798	116079	8803	94632	8307	89300	8352	89784	7726	83055	5768	62006

Initial concentration (ug/L)

Benzene	60080
Toluene	53406
Ethylbenzene	2081
m-Xylene	5504
o+p-Xylene	6269
Total BTEX	127340

Note: BTEX concentration in soil pore water = BTEX concentration in vials × 10.75
Taking 4-mL soil pore water into 43-mL vials for BTEX analysis

Data for Figure 6.7

Silica sand

Concentration of BTEX in pipe water (ug/L)

Time (day)	10	13	16	19	22	28	33	40	47	54	62	69
Benzene	0	2.6	8.2	37.0	77.8	307.5	612.3	1059.1	1925.5	2522.0	2446.7	3470.1
Toluene	0	0	0	6.5	16.8	75.3	168.6	320.4	701.3	1017.0	1083.6	1724.3
Ethylbenzene	0	0	0	0	0	0	0	0	4.7	7.7	81.7	21.5
m-xylene	0	0	0	0	0	0	0	0	6.0	10.3	86.0	51.6
o+p-xylene	0	0	0	0	0	0	0	0	7.7	12.0	81.7	51.6

Cumulative mass of BTEX permeated per unit area (ug/cm^2)

Time (day)	10	13	16	19	22	28	33	40	47	54	62	69
Benzene	0	0.002	0.007	0.029	0.076	0.262	0.633	1.274	2.439	3.966	5.447	7.548
Toluene	0	0	0	0.004	0.014	0.060	0.162	0.356	0.780	1.396	2.052	3.095
Ethylbenzene	0	0	0	0	0	0	0	0	0.003	0.008	0.057	0.070
m-xylene	0	0	0	0	0	0	0	0	0.004	0.010	0.062	0.093
o+p-xylene	0	0	0	0	0	0	0	0	0.005	0.012	0.061	0.093
Total BTEX	0	0.002	0.007	0.033	0.090	0.322	0.794	1.629	3.231	5.391	7.679	10.899

Sand- topsoil mixture

Concentration of BTEX in pipe water (ug/L)

Time (day)	10	13	16	19	22	28	33	40	47	54	62	69
Benzene	0	0	3.9	21.5	44.7	169.9	351.3	559.9	1086.6	1449.5	1380.3	2055.4
Toluene	0	0	0	0.0	7.7	32.3	94.2	181.5	336.3	472.1	516.0	838.5
Ethylbenzene	0	0	0	0	0	0	0	0	0	0	0	0
m-xylene	0	0	0	0	0	0	0	0	0	0	0	0
o+p-xylene	0	0	0	0	0	0	0	0	7.7	12.0	81.7	51.6

Cumulative mass of BTEX permeated per unit area (ug/cm^2)

Time (day)	10	13	16	19	22	28	33	40	47	54	62	69
Benzene	0	0	0.002	0.016	0.043	0.147	0.362	0.705	1.371	2.259	3.105	4.365
Toluene	0	0	0	0.000	0.005	0.025	0.082	0.193	0.399	0.689	1.005	1.519
Ethylbenzene	0	0	0	0	0	0	0	0	0	0	0	0
m-xylene	0	0	0	0	0	0	0	0	0	0	0	0
o+p-xylene	0	0	0	0	0	0	0	0	0	0	0	0
Total BTEX	0	0	0.002	0.016	0.048	0.172	0.445	0.899	1.771	2.948	4.110	5.883

Organic top soil

Concentration of BTEX in pipe water (ug/L)

Time (day)	10	13	16	19	22	28	33	40	47	54	62	69
Benzene	0	0	0	9.5	19.8	83.9	179.7	221.6	501.8	731.9	726.7	946.0
Toluene	0	0	0	0	0	12.9	39.6	51.1	134.6	212.4	232.2	331.1
Ethylbenzene	0	0	0	0	0	0	0	0	0	0	0	0
m-xylene	0	0	0	0	0	0	0	0	0	0	0	0
o+p-xylene	0	0	0	0	0	0	0	0	0	0	0	0

Cumulative mass of BTEX permeated per unit area (ug/cm^2)

Time (day)	10	13	16	19	22	28	33	40	47	54	62	69
Benzene	0	0.000	0.000	0.006	0.018	0.069	0.179	0.314	0.620	1.067	1.510	2.088
Toluene	0	0	0	0.000	0.000	0.008	0.032	0.063	0.145	0.275	0.417	0.619
Ethylbenzene	0	0	0	0	0	0	0	0	0	0	0	0
m-xylene	0	0	0	0	0	0	0	0	0	0	0	0
o+p-xylene	0	0	0	0	0	0	0	0	0	0	0	0
Total BTEX	0	0	0	0.006	0.018	0.077	0.211	0.377	0.766	1.342	1.927	2.707

Data for Figure 6.8

Benzene

Bulk concentration (mg/L)	Permeation rate ($ug/cm^2/day$)	ID (cm)	OD (cm)	time (day)	Predicted concentration in pipe water (ug/L)			
					1	1/5	1/10	1/20
0.05	0.0003	2.66	3.28	0.333	0.2	0.0	0.0	0.0
0.2	0.0013	2.66	3.28	0.333	0.8	0.2	0.1	0.0
0.3	0.0020	2.66	3.28	0.333	1.2	0.2	0.1	0.1
0.4	0.0028	2.66	3.28	0.333	1.7	0.3	0.2	0.1
0.5	0.0036	2.66	3.28	0.333	2.2	0.4	0.2	0.1
5	0.0489	2.66	3.28	0.333	30.1	6.0	3.0	1.5
10	0.1071	2.66	3.28	0.333	66.1	13.2	6.6	3.3
20	0.2348	2.66	3.28	0.333	144.9	29.0	14.5	7.2
30	0.3717	2.66	3.28	0.333	229.3	45.9	22.9	11.5
40	0.5148	2.66	3.28	0.333	317.5	63.5	31.8	15.9
50	0.6628	2.66	3.28	0.333	408.8	81.8	40.9	20.4
60	0.8148	2.66	3.28	0.333	502.6	100.5	50.3	25.1
70	0.9701	2.66	3.28	0.333	598.4	119.7	59.8	29.9
80	1.1285	2.66	3.28	0.333	696.1	139.2	69.6	34.8
90	1.2895	2.66	3.28	0.333	795.4	159.1	79.5	39.8
100	1.4529	2.66	3.28	0.333	896.1	179.2	89.6	44.8

Toluene

Bulk concentration (mg/L)	Permeation rate ($ug/cm^2/day$)	ID (cm)	OD (cm)	time (day)	Predicted concentration in pipe water (ug/L)			
					1	1/5	1/10	1/20
0.1	0.0006	2.66	3.28	0.333	0.4	0.1	0.0	0.0
0.2	0.0014	2.66	3.28	0.333	0.9	0.2	0.1	0.0
0.3	0.0022	2.66	3.28	0.333	1.4	0.3	0.1	0.1
0.4	0.0030	2.66	3.28	0.333	1.9	0.4	0.2	0.1
0.5	0.0039	2.66	3.28	0.333	2.4	0.5	0.2	0.1
5	0.0549	2.66	3.28	0.333	33.9	6.8	3.4	1.7
10	0.1213	2.66	3.28	0.333	74.8	15.0	7.5	3.7
20	0.2682	2.66	3.28	0.333	165.4	33.1	16.5	8.3
30	0.4265	2.66	3.28	0.333	263.1	52.6	26.3	13.2
40	0.5928	2.66	3.28	0.333	365.7	73.1	36.6	18.3
50	0.7653	2.66	3.28	0.333	472.0	94.4	47.2	23.6
60	0.9428	2.66	3.28	0.333	581.6	116.3	58.2	29.1
70	1.1247	2.66	3.28	0.333	693.7	138.7	69.4	34.7
80	1.3104	2.66	3.28	0.333	808.3	161.7	80.8	40.4
90	1.4995	2.66	3.28	0.333	924.9	185.0	92.5	46.2
100	1.6917	2.66	3.28	0.333	1043.5	208.7	104.3	52.2

Data for Figure 6.9

Bulk concentration (mg/L)	Flow velocity (ft/s)			
	0.2	1	2	5
5	290	1450	2900	7250
10	135	675	1350	3375
20	61	305	610	1525
30	39	195	390	975
40	28	140	280	700
50	22	108	215	538
60	18	88	175	438
70	15	74	148	370
80	13	64	128	320
90	11	55	110	275
100	10	49	98	245

Sample:

Flow velocity (ft/s)	0.2	1	2	5
Flow velocity (cm/s)	6.1	30.5	61.0	152.4
Flow velocity (cm/day)	526694	2633472	5266944	13167360
I.D (cm)	2.66	2.66	2.66	2.66
Sectional area (cm^2)	5.57	5.57	5.57	5.57
Fow rate (cm^3/day)	2935261	14676306	29352613	73381532
Flow rate (L/day)	2935	14676	29353	73382
Bulk concentration (mg/L)	100	100	100	100
Permeation rate (ug/cm^2/day)	1.4529	1.4529	1.4529	1.4529
O.D.(cm)	3.28	3.28	3.28	3.28
Exposure length (m)	9.8	49	98	245
Exposure length (cm)	980	4900	9800	24500
Surface area (cm^2)	10106	50531	101062	252655
Mass permeated (ug/day)	14683	73415	146830	367075
Concentration (ug/L)	5	5	5	5

Data for Figure 6.10

SIDR 9

Bulk concentration	Predicted concentration in pipe water (ug/L)				
(mg/L)	1/2"	3/4"	1"	1-1/2"	2"
0.05	0.48	0.26	0.17	0.08	0.04
0.2	2.33	1.26	0.80	0.39	0.21
0.3	3.69	2.00	1.27	0.62	0.33
0.4	5.10	2.77	1.75	0.86	0.45
0.5	6.57	3.57	2.26	1.11	0.58
5	89.12	48.39	30.61	15.06	7.91
10	195.36	106.08	67.10	33.01	17.33
20	428.25	232.54	147.10	72.35	37.99
30	677.77	368.03	232.80	114.51	60.13
40	938.75	509.74	322.45	158.61	83.29
50	1208.59	656.27	415.14	204.20	107.23
60	1485.72	806.75	510.32	251.02	131.82
70	1769.05	960.60	607.65	298.89	156.95
80	2057.81	1117.39	706.83	347.68	182.57
90	2351.39	1276.81	807.67	397.28	208.62
100	2649.33	1438.59	910.01	447.62	235.06

DIPS DR 17.0 PSI 100

Bulk concentration	Predicted concentration in pipe water (ug/L)									
(mg/L)	4"	6"	8"	10"	12"	14"	16"	18"	20"	24"
0.05	0.01	0.00	0.00	0.00	0.00	0.00	0.00	0.00	0.00	0.00
0.2	0.04	0.02	0.01	0.01	0.00	0.00	0.00	0.00	0.00	0.00
0.3	0.06	0.03	0.02	0.01	0.01	0.01	0.00	0.00	0.00	0.00
0.4	0.08	0.04	0.02	0.02	0.01	0.01	0.01	0.00	0.00	0.00
0.5	0.10	0.05	0.03	0.02	0.01	0.01	0.01	0.01	0.01	0.00
5	1.42	0.69	0.40	0.27	0.19	0.14	0.11	0.09	0.07	0.05
10	3.12	1.51	0.88	0.58	0.41	0.31	0.24	0.19	0.15	0.11
20	6.84	3.31	1.92	1.28	0.90	0.67	0.52	0.41	0.34	0.24
30	10.82	5.24	3.04	2.02	1.43	1.06	0.82	0.66	0.53	0.37
40	14.99	7.26	4.21	2.80	1.98	1.47	1.14	0.91	0.74	0.52
50	19.29	9.35	5.42	3.60	2.55	1.90	1.47	1.17	0.95	0.67
60	23.72	11.49	6.66	4.43	3.13	2.33	1.80	1.44	1.17	0.82
70	28.24	13.68	7.93	5.27	3.73	2.78	2.15	1.71	1.39	0.98
80	32.85	15.92	9.23	6.13	4.33	3.23	2.50	1.99	1.62	1.14
90	37.54	18.19	10.54	7.00	4.95	3.69	2.85	2.27	1.85	1.30
100	42.30	20.49	11.88	7.89	5.58	4.16	3.22	2.56	2.09	1.46

A.5 Scilab Codes for Chapter 7

```
*******************************Fit measured data to the Fickian's diffusion model**********************************

Thickness = 0.315; //wall thickness, cm
simTime = 140;  //time of simulation, day
dz = 0.01;  //layer size, cm
dt = 0.1;  //time step size, day
NL = Thickness/dz; //number of layers
NT = simTime/dt; //number of time step

D = 0.00020; //Diffusion coefficient, cm2/day
r = D*dt/(dz^2);
rr = 1-2*r;

S = 23.7; //solubility, assuming there is linear relationship between the external aqueous concentration
          ///(C_AQU) and the corresponding concentration on the outer wall of pipe(C_OW), C_OW = S*
           //C_AQU
C_AQU = 31.2; //benzene concentration in aqueous solution, mg/L;
C_OW = S*C_AQU; //benzene concentration on the outer wall, mg/L;

C = zeros(NL+1, NT+1); //set up the matrix for C
C(:, 1) = 0; //assign initial conditions
C(1,:) = C_OW; //assign outer boundary conditions, mg/L
C(NL+1, :) = 0; //assign the inner boundary conditions


//calculate concentration for each layer at each time step using explicit method
time(1)=0;
for j=1:NT
  time(j+1) = time (j) + dt;
  C(2:NL, j+1) = r*C(1:NL-1,j) + rr*C(2:NL,j) + r*C(3:NL+1,j);
end


//calculate diffusion flux into the pipe
Q(1)=0;
for j=1:NT
  flux =((C(NL,j)-C(NL+1,j))/dz)*D*dt;
  Q(j+1)= Q(j)+flux;
end

clf()

plot2d(time, Q, style=5)


//measured data
TimeMeasure = [ 3, 6, 9,
11,13,15,17,20,23,26,29,32,35,38,41,44,48,52,56,60,64,68,72,78,83,88,93,99,104,112,118,12
7,133];
```

```
MassMeasure = [ 0,0,0,0,0,0,0,0.0063,0.0218,0.0509,0.1021,
0.1837,0.3191,0.5118,0.7711,1.1163,1.5972,1.8380,2.3915,3.1176,3.9407,4.9425,5.9751,7.0
255,8.4955,10.0888,11.6969,13.3385,
15.3610,17.1416,19.8556,22.1773,25.0459,27.4197];
plot(TimeMeasure, MassMeasure,'o')



**********Time-dependent boundary conditions: first order degradation**********

Thickness = 0.315; //wall thickness, cm
simTime = 150; //time of simulation, day
dz = 0.01;  //layer size, cm
dt = 0.1;  //time step size, day
NL = Thickness/dz; //number of layers
NT = simTime/dt; //number of time step

D0 = 0.00020; //Diffusion coefficient, cm2/day

ParCoeff = 23.7; //partitioning coefficient
ConAqu = 31.2; //Initial benzene concentration in aqueous solution, mg/L;

K(1) = 0;      //No degradation
K(2) = 0.005;  //first order decay constant, day-1
K(3) = 0.01;   //first order decay constant, day-1
K(4) = 0.02;   //first order decay constant, day-1

Q = zeros(4, NT+1); //set up the matrix for diffusion flux
Q(:,1)= 0; //assign initial conditions
ConWall = zeros(4, NT+1);//set up the matrix for external bulk concentration
ConWall(:,1) = ConAqu; //assign initial conditions

for n=1:4

    C = zeros(NL+1, NT+1); //set up the matrix for C
    C(:, 1) = 0;  //assign initial conditions
    C(NL+1, :) = 0;  //assign the inner boundary conditions

    time(1)= 0;

    kVar = K(n);   //assign the first order decay constant, day-1

    for j=1:NT

        time(j+1) = time (j) + dt;
        ConWall(n,j+1)= ConAqu*exp(-kVar*time(j+1)); //assign the outer boundary conditions
        C(1,:)= ParCoeff*ConWall(n,j+1);
        D = D0;
        r = D*dt/(dz^2);
        rr = 1-2*r;

        //calculate concentration for each layer at time step j using explicit method
        for i=2:NL
```

```
        C(i, j+1) = r*C(i-1,j) + rr*C(i,j) + r*C(i+1,j);
        end

        //calculate permeation  flux into pipe
        flux =((C(NL,j)-C(NL+1,j))/dz)*D*dt;
        Q(n,j+1)= Q(n,j)+flux;

      end

end

clf()

subplot(211)
plot2d(time, ConWall(1,:), style=5);
plot2d(time, ConWall(2,:), style=4);
plot2d(time, ConWall(3,:), style=3);
plot2d(time, ConWall(4,:), style=2);
xtitle('','time','external  concentration(mg/L)')

subplot(212)
plot2d(time, Q(1,:), style=5);
plot2d(time, Q(2,:), style=4);
plot2d(time, Q(3,:), style=3);
plot2d(time, Q(4,:), style=2);
xtitle('', 'time','Cumulative permeation flux(ug/cm2)')




**********Time-dependent boundary conditions: continuous source**********

C0_gw = 31.2; //initial solute concentration, mg/L
L = 10; // flow path length, m;
vx = 0.05464; //average groundwater velocity, m/day;

Thickness = 0.315; //wall thickness, cm
simTime = 500; //time of simulation, day
dz = 0.01;  //layer size, cm
dt = 0.1;  //time step size, day
NL = Thickness/dz; //number of layers
NT = simTime/dt; //number of time step

D0 = 0.00020; //Diffusion coefficient, cm2/day

ParCoeff = 23.7; //partitioning coefficient
ConAqu = 31.2; //Initial benzene concentration in aqueous solution, mg/L;


DL(1) = 0.001;  //dispersion coefficient, m2/day
DL(2) = 0.005;  //dispersion coefficient, m2/day
DL(3) = 0.01;   //dispersion coefficient, m2/day
DL(4) = 0.05;   //dispersion coefficient, m2/day
```

```
Q = zeros(4, NT+1); //set up the matrix for diffusion flux
Q(:,1)= 0; //initial condition
ConWall = zeros(4, NT+1); //set up the matrix for external bulk concentration
ConWall(:,1) = 0; //assign initial condition

for n=1:4

    C = zeros(NL+1, NT+1); //set up the matrix for C
    C(:, 1) = 0;          //assign initial conditions
    C(NL+1, :) = 0;       //assign the inner boundary conditions

    time(1)= 0;

    DLVar = DL(n);  //assign the dispersion coefficient, m2/day

    for j=1:NT

        time(j+1) = time (j) + dt;
        //assign the outer boundary conditions
        ConWall(n,j+1) = C0_gw /2 *(erfc((L - vx*time(j+1)) / (2*sqrt(DLVar*time(j+1)))) +
exp(vx*L/DLVar)* erfc((L +  vx*time(j+1)) / (2*sqrt(DLVar*time(j+1)))));
        C(1,:)= ParCoeff*ConWall(n,j+1);
        D = D0; //diffusion coefficient, cm2/day
        r = D*dt/(dz^2);
        rr = 1-2*r;

        //calculate concentration for each layer at time step j using explicit method
        for i=2:NL
        C(i, j+1) = r*C(i-1,j) + rr*C(i,j) + r*C(i+1,j);
        end
        //calculate permeation flux into pipe
        flux =((C(NL,j)-C(NL+1,j))/dz)*D*dt;
        Q(n,j+1)= Q(n,j)+flux;

      end

end



clf()

subplot(211)
plot2d(time, ConWall(1,:), style=5);
plot2d(time, ConWall(2,:), style=4);
plot2d(time, ConWall(3,:), style=3);
plot2d(time, ConWall(4,:), style=2);
xtitle('','time','external concentration(mg/L)')

subplot(212)
plot2d(time, Q(1,:), style=5);
plot2d(time, Q(2,:), style=4);
plot2d(time, Q(3,:), style=3);
```

```
plot2d(time, Q(4,:), style=2);
xtitle('', 'time','Cumulative permeation flux(ug/cm2)')



**********Time-dependent t boundary conditions: instantaneous source**********

M = 38; //mass of contaminant released, mg/m2
L = 10; // flow path length, m;
vx = 0.05464; //average groundwater velocity, m/day;

Thickness = 0.315; //wall thickness, cm
simTime = 500; //time of simulation, day
dz = 0.01;  //layer size, cm
dt = 0.1;  //time step size, day
NL = Thickness/dz; //number of layers
NT = simTime/dt; //number of time step

D0 = 0.00020; //Diffusion coefficient, cm2/day

ParCoeff = 23.7; //partitioning coefficient
ConAqu = 31.2; //Initial benzene concentration in aqueous solution, mg/L;


DL(1) = 0.001;  //dispersion coefficient, m2/day
DL(2) = 0.005;  //dispersion coefficient, m2/day
DL(3) = 0.01;   //dispersion coefficient, m2/day
DL(4) = 0.05;   //dispersion coefficient, m2/day

Q = zeros(4, NT+1); //set up the matrix for diffusion flux
Q(:,1)= 0; //initial condition
ConWall = zeros(4, NT+1); //set up the matrix for external bulk concentration
ConWall(:,1) = 0; //assign initial condition

for n=1:4

    C = zeros(NL+1, NT+1); //set up the matrix for C
    C(:, 1) = 0;          //assign initial conditions
    C(NL+1, :) = 0;       //assign the inner boundary conditions

    time(1)= 0;

    DLVar = DL(n);  //assign the dispersion coefficient, m2/day

    for j=1:NT

        time(j+1) = time (j) + dt;
        //assign the outer boundary conditions
        ConWall(n,j+1) = M* exp(-1* (L-vx*time(j+1))^2 / (4*DLVar*time(j+1))
                          )/sqrt(4*3.1415926*DLVar*time(j+1));
        C(1,:)= ParCoeff*ConWall(n,j+1);
        D = D0; //diffusion coefficient, cm2/day
        r = D*dt/(dz^2);
        rr = 1-2*r;
```

```
        //calculate concentration for each layer at time step j using explicit method
        for i=2:NL
        C(i, j+1) = r*C(i-1,j) + rr*C(i,j) + r*C(i+1,j);
        end
        //calculate permeation flux into pipe
        flux =((C(NL,j)-C(NL+1,j))/dz)*D*dt;
        Q(n,j+1)= Q(n,j)+flux;

    end

end



clf()

subplot(211)
plot2d(time, ConWall(1,:), style=5);
plot2d(time, ConWall(2,:), style=4);
plot2d(time, ConWall(3,:), style=3);
plot2d(time, ConWall(4,:), style=2);
xtitle('','time','external concentration(mg/L)')

subplot(212)
plot2d(time, Q(1,:), style=5);
plot2d(time, Q(2,:), style=4);
plot2d(time, Q(3,:), style=3);
plot2d(time, Q(4,:), style=2);
xtitle('', 'time','Cumulative permeation flux(ug/cm2)')
```